The secretome of primary human hepatocytes in an organotypic bioreactor culture for the identification of biomarkers of drug-induced hepatotoxicity

Dissertation

zur Erlangung des Grades

des Doktors der Naturwissenschaften

der Naturwissenschaftlich-Technischen Fakultät III

Chemie, Pharmazie, Bio- und Werkstoffwissenschaften

der Universität des Saarlandes

von

Georg Tascher

Saarbrücken

2012

Tag des Kolloquiums:	29.06.2012
Dekan:	Prof. Dr. Wilhelm F. Maier
Berichterstatter:	Prof. Dr. Elmar Heinzle
	Prof. Dr. Dietrich Volmer
Vorsitz:	Prof. Dr. Uli Müller
Akad. Mitarbeiter:	Dr. Gert Kohring

Danksagung

Zunächst bin ich Prof. Dr. Elmar Heinzle zu allergrößtem Dank verpflichtet ob der Möglichkeit meine Dissertation in seiner Arbeitsgruppe durchführen zu können. Ich danke ihm für die Überlassung des äußerst interessanten Themas und das entgegengebrachte Vertrauen, die fruchtbaren Diskussionen aber auch für die Kritik an der richtigen Stelle.

Ich danke Prof. Dietrich Vollmer vielmals für die Übernahme der Zweitkorrektur dieser Arbeit.

Dr. Fozia Noor möchte ich für die exzellente Führung des „Zoiga"-Labs, ihre Unterstützung und nicht zuletzt für ihre Motivation während der letzten Jahre danken.

Weiterhin danke ich Dr. Alain van Dorsselaer (LSMBO, Université de Strasbourg) und seiner Arbeitsgruppe (allen voran Magali Rompais) für die Unterstützung während der ESI-MS Analysen und dafür, dass ich in den nächsten Jahren selbst Mitglied dieser renomierten Arbeitsgruppe sein darf.

Allen Partnern des HEPATOX Projektes danke ich für die außerordentlich gute Kooperation über den gesamten Projektzeitraum hinweg: Dr. Ursula Müller-Vieira für die perfekte Koordination des Projektes, Dr. Kathrin Zeilinger und Stefan Hoffmann für die Bereitstellung der Bioreaktortechnologie und die Durchführung der serumfreien Bioreaktorkultivierung, sowie Prof. Dr. Andreas Nüssler und Dr. Daniel Knobeloch für die Versorgung mit primären humanen Hepatozyten.

Allen Mitgliedern der technischen Biochemie danke ich für die sehr gute Arbeitsatmosphäre. Ganz besonders danke ich Daniel Müller für die gute Zusammenarbeit als zweites, aktives Mitglied der „Bioreactor Group Saarbrücken", sowie Esther Hoffmann für die Durchführung des ein oder anderen Enzymassays. Auch die beiden anderen „Frischluftfanatiker" der Arbeitsgruppe, Vassilis Delis und Steffen Krauser, sollen hier namentlich erwähnt werden. Danke für die schöne Zeit!

Last but not least geht mein unendlicher Dank an meine Familie, meine Freunde und ganz besonders an Fynn, ohne deren Verständnis, Unterstützung und Hilfestellungen diese Arbeit nie zustande gekommen wäre. Danke für ALLES!!

Table of contents

Abstract

In the presented thesis, a workflow for analysis of the extracellular proteome, or “secretome”, of primary human hepatocytes by a shotgun proteomics approach was developed. The secretome analysis on hepatocytes is of special interest for the pharmaceutical industry as well as medical services because secreted proteins could serve as biomarkers for drug-induced hepatotoxicity. The avoidance of fetal calf serum, a common supplement used for *in vitro* cell culture was shown to be a prerequisite for efficient secretome analysis because supplemented proteins severely hamper the identification of secreted proteins using mass-spectrometry (MS). The removal of high abundant proteins from the sample by immunodepletion, a common strategy for proteomic analysis of human plasma, was shown to increase the number of identified proteins to almost two-fold the number of identifications obtained without prior immunodepletion, paving the way for in-depth analysis of the secretome. A prefractionation step at the level of proteins and the combination of different MS-types and ionization methods tremendously enhanced the identifications but at the cost of analysis time as well as the fraction of secreted proteins. The elaborated workflow without prior prefractionation was applied to a standard monolayer culture and a promising *in vitro* cultivation technique in a 3-dimensional bioreactor mimicking the microenvironment of a real liver. With 109 and 160 proteins identified in monolayer and bioreactor cultures, respectively, the number of proteins likely to be secreted by hepatocytes into the extracellular space was much higher than described in the current literature. Furthermore, proteome analysis on extracellular proteins in the applied culture conditions confirmed the tissue-like behavior of primary hepatocytes in the three-dimensional cultivation. Differentially expressed proteins in the bioreactor culture after application of the reference drug diclofenac were detected by label-free quantification and most of the detected differences could be traced back to the underlying mechanism of toxicity proposed for this drug. In summary, the presented work provides a basis for further in-depth analysis of the primary human hepatocytes secretome for *in vitro* drug-testing and demonstrates the valuable contributions of proteomics to toxicological research.

Zusammenfassung

In der vorliegenden Arbeit wurde eine experimentelle Strategie zur Analyse des extrazellulären Proteoms („Sekretom“) von primären humanen Hepatozyten mittels „shotgun“ proteomics entwickelt. Die Analyse des Sekretoms von Hepatozyten ist von besonderer Bedeutung für die pharmazeutische Industrie sowie das Gesundheitswesen, da sekretierte Proteine als Biomarker für arzneimittelinduzierte Lebertoxizität verwendet werden können. Es wurde gezeigt, dass die Vermeidung von foetalem Kälberserum, einem gewöhnlich in der *in vitro* Zellkultur verwendeten Zusatz, eine Grundvorraussetzung für die effiziente Analyse der sekretierten Proteine darstellt, da die zugesetzten Proteine erheblich die Identifizierung sekretierter Proteine mittels Massenspektrometrie erschweren. Desweiteren erhöhte die Entfernung hoch abundanter Proteine aus den Proben mit Hilfe einer Immunodepletion, wie sie oft in der Proteomanalyse von menschlichem Serum Verwendung findet, die Anzahl an identifizierten Proteinen fast um das Doppelte und ebnete damit den Weg für eine detailliertere Analyse des Sekretoms. Weiterhin konnte gezeigt werden, dass eine Vorfraktionierung der Proteine sowie die Kombination verschiedener Massenspektrometertypen bzw. Ionisationsmethoden die Anzahl an Identifizierungen deutlich steigert, allerdings auf Kosten der benötigten Analysezeit und des Anteils an sekretierten Proteinen. Die erarbeitete analytische Strategie ohne vorherige Fraktionierung wurde sowohl auf Standardkultivierungen in Zellkulturflaschen, als auch auf eine vielversprechende Bioreaktortechnik angewendet, wobei letztere die dreidimensionale Umgebung in einer echten Leber nachahmt. 109 bzw. 160 sekretierte Proteine konnten in Standard- bzw. Bioreaktokulturen identifiziert werden, wesentlich mehr als es derzeitig in der Literatur für primäre humane Hepatozyten beschrieben wird. Desweiteren bestätigte die Analyse des extrazellulären Proteoms in den verwendeten Kultivierungstechniken das gewebeähnliche Verhalten der primären Leberzellen in der dreidimensionalen Bioreaktorkultur. Differentiell exprimierte Proteine in mit der Referenzsubstanz Diclofenac behandelten Bioreaktorkulturen wurden mittels labelfreier Quantifizierung bestimmt und konnten auf die zugrundeliegenden Toxizitätsmechanismen zurückgeführt werden, die für dieses Medikament bekannt sind. Zusammenfassend legt die vorliegende Arbeit den Grundstein für weitere umfassende Analysen des Sekretoms von Leberzellen für *in vitro* Wirkstofftests und veranschaulicht den wertvollen Beitrag der Proteomik für die toxikologische Forschung.

Abbreviations

µg	microgram
µg/µl	microgram per microliter
µl	microliter
µm	micrometer
2D	two-dimensional
2D-DIGE	two-dimensional differntial gel electrophoresis
2-DE	two dimensional gel electrophoresis
3D	three-dimensional
ABC	ammonium bicarbonate (NH_4HCO_3)
ACN	Acetonitril
AST	Asparte-aminotransferase
CHCA	α-cyano-4-hydroxy-cinnamonic acid
DTT	Dithiothreitol
EC_{50}	effective concentration 50
ELISA	enzyme-linked immunosorbent assay
ESI	electrospray ionisation
ETD	electron transfer dissociation
FA	firmic acid
FDR	false discovery rate
HPLC	high performance liquid chromatography
IEF	isoelectric focussing
INFγ	interferon gamma
IPG	immobilized pH gradient
LC	liquid chromatography
LC-MALDI	liquid chromatography coupled to MALDI mass spectrometry
LC-MS	liquid chromatography coupled to mass-spectrometry
LDH	Lactate-dehydrogenase
m/z	mass to charge ratio
mA	milliampère
MALDI	matrix-assisted laser desorption ionisation
mg	milligram
min	minute
ml	millilitre
mM	millimol/liter
MS	mass spectrometry or mass sectrometer
MS/MS	tandem mass spectrometry (of peptide fragments)
MWCO	molecular-weight cut-off
ng	nanogram
NIH	National Institute of Health
nl	nanoliter
nm	nanometer
PAGE	polyacrylamide gelelectrophoresis
PFF	peptide fragment fingerprint
PHH	primary human hepatocytes
PMF	peptide mass fingerprint
PTM	post translational modification
QTOF	quadrupole time of flight
RP	reversed phase

RT	room temperature, retention time
SDS	sodium dodecylsulfate
TFA	trifluoroacetic acid
TOF	time of flight
UV	ultraviolet
V	volt
VEGF	vascular endothelial growth factor

Standard abbreviations for proteinogenic amino acids:

name	**3-letter code**	**1-letter code**	**name**	**3-letter code**	**1-letter code**
Alanine	Ala	A	Leucine	Leu	L
Arginine	Arg	R	Lysine	Lys	K
Asparagine	Asn	N	Methionine	Met	M
Aspartic acid	Asp	D	Phenylalanine	Phe	F
Cysteine	Cys	C	Proline	Pro	P
Glutamic acid	Glu	D	Serine	Ser	S
Glutamine	Gln	Q	Threonine	Thr	T
Glycine	Gly	G	Tryptophan	Trp	W
Histidine	His	H	Tyrosine	Tyr	Y
Isoleucine	Ile	I	Valine	Val	V

1. Introduction

1.1 Human hepatic culture-systems for *in-vitro* evaluation of hepatic toxicity

Pharmaceutical drug-development is a long and expensive process. From about 10.000 compounds entering the pipeline as possible drug candidates, only 1 approved drug exits after more than 10 years of preclinical and clinical phases. The total costs for development of one new drug are in excess of 800 million US$, with half of the costs arising already at the preclinical level during extensive *in vitro* testing of new compounds [DiMasi *et al.*, 2003]. Unexpected toxicity is the main reason why newly developed drug candidates fail to enter clinical phases and for the withdrawal of already approved drugs from the market. The latter is mainly due to the use of animal models during preclinical drug testing which are obviously not always transferable to humans [Olson *et al.*, 1998; Hartung, 2009]. Playing a central role in intermediary metabolism and detoxification of xenobiotics, the liver is one of the first sites where adverse drug effects partly take place. These adverse effects can result in severe liver injury featuring intracellular accumulation of lipids (i.e. steatosis) or bile (i.e. cholestasis), but also cytotoxic effects leading to necrosis or apoptosis [van Summeren *et al.*, 2012]. Sometimes, a drug causes toxic effects only in few patients while most others are treated successfully without negative consequences. This is called idiosyncratic toxicity and the underlying mechanisms are still elusive but polymorphisms of enzymes for hepatic drug metabolism as well as immunological processes were claimed to play an essential role [Boelsterli, 2003; Amacher, 2012]. Even though this kind of toxicity is rarely observed, very often prescribed drugs such as diclofenac provoke a concerning number of cases of severe liver failure [Aithal, 2004]. Drug-induced hepatotoxicity is often not observed until a prolonged application of a drug, thus requiring predictive and humanized *in vitro* liver models suitable for long-term toxicity studies as early as possible during drug development. Many *in vitro* studies aiming at the characterization of drug-induced hepatotoxicity use cell lines derived from hepatic tumors like HepG2, (e.g. [Thome-Kromer *et al.*, 2003; Lewis *et al.*, 2010; Van Summeren *et al.*, 2011]). While such human cell lines can easily be cultivated for longer periods, they show significantly reduced expression of many genes involved in drug metabolism. Consequently, they are not recommended as a reliable model system to estimate adverse drug reactions occurring *in vivo* [Jaeschke *et al.*, 2011]. Primary human hepatocytes (PHH) are considered as “gold standard” for *in vitro* toxicological studies because they allow detection of human-specific toxicity and exhibit *in vivo* like gene expression profiles in regard to drug metabolism. They are isolated either from human liver grafts not suitable for transplantation or from liver

resections after clinical surgeries. However, primary human hepatocytes dedifferentiate within several days in two-dimensional (2D) monolayer culture and lose drug metabolizing functions which prevents their use in long-term repeated dose experiments. 2D culture systems are widely used for *in vitro* cultivation of many different cell types but are simplified and create a rather artificial environment. *In vivo*, cells are growing in tissues and need this three-dimensional (3D) environment not only to survive but also to build-up more physiologically relevant structures *in vitro* [Cukierman *et al.*, 2001; Pampaloni *et al.*, 2007; Mazzoleni *et al.*, 2009]. One method can be considered as an intermediate step between 2D- and 3D-cultivation, the so-called "collagen-sandwich" culture. It avoids dedifferentiation by overlaying seeded primary hepatocytes with a second layer of collagen in addition to the collagen precoating of culture dishes as it is performed in standard monolayer cultures (see Fig. 1.1.). The sandwich technique ensures viability and functionality of primary hepatocytes for up to 10 days under serum-free conditions by partially providing three-dimensional stimuli to the liver cells [Godoy *et al.*, 2009; Tuschl *et al.*, 2009].

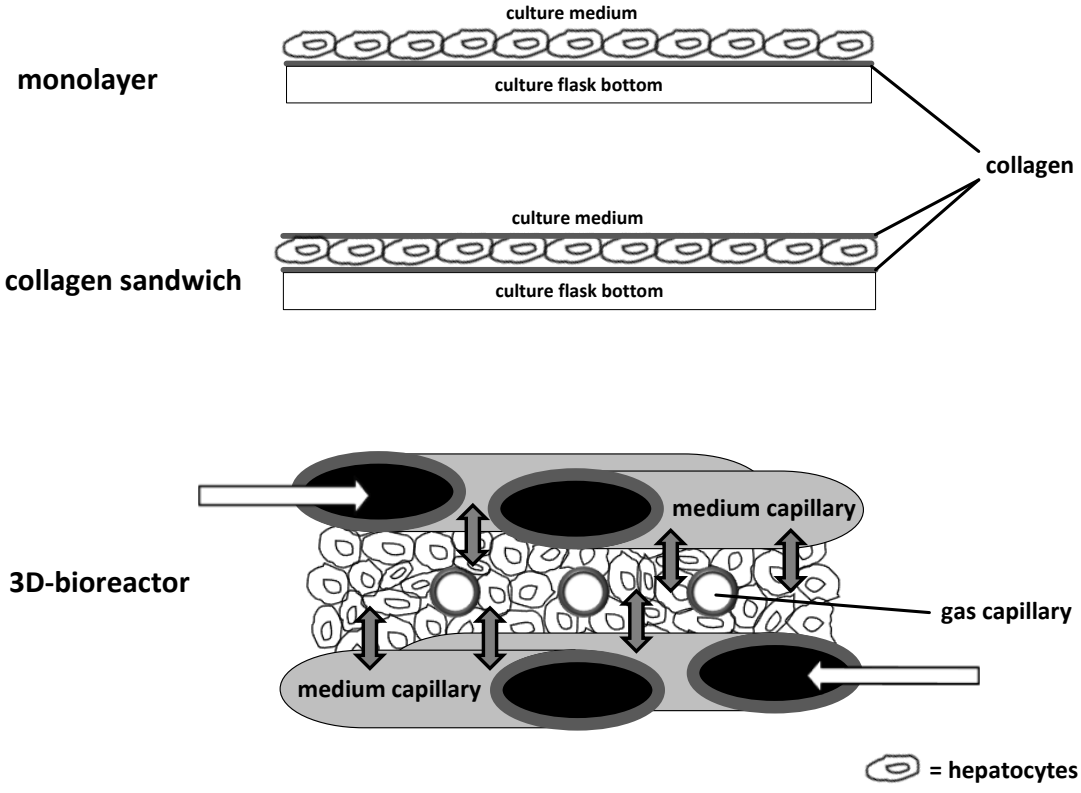

Figure 1.1. Common techniques for *in vitro* cultivation of primary human hepatocytes. The most commonly applied cultivation technique is the monolayer cultivation (top) where cells are seeded directly into a culture dish precoated with collagen. A modified form of this technique is the collagen sandwich (middle) in which cells are covered with an additional layer of collagen to increase survival and performance of the primary cells. In both techniques, the cells are covered with cultivation medium. In a perfused hollow-fiber bioreactor like the one used in this thesis (bottom), cells are maintained within a network of medium and gas capillaries which provides sufficient mass transfer for the cultivation of primary cells and allows three-dimensional organization of the cells in a tissue-like manner. White arrows indicate medium flux while grey arrows indicate exchange of nutrients and waste products.

Advances in the field of three dimensional cultivation techniques led to the development of perfused hollow-fiber bioreactors in which hepatocytes are cultivated in between a network of membrane capillaries (see Fig. 1.1). The capillaries serve as scaffold for cell adhesion and assure nutrient and oxygen supply but also elimination of waste products in the bioreactor which is essential for cultivation of larger tissue masses [Mazzoleni *et al.*, 2009]. The bioreactor system used in this thesis was originally developed for extracorporeal liver support at the Charité in Berlin [Sauer *et al.*, 2002]. Histological studies revealed that isolated primary hepatocytes reconstitute liver-like structures like bile canaliculi and can be cultivated for almost a month in this bioreactor [Gerlach *et al.*, 2003a; Gerlach *et al.*, 2003b; Zeilinger *et al.*, 2004; Schmelzer *et al.*, 2009]. Being perfectly suited for human relevant *in vitro* toxicological studies but requiring a large number of primary cells, the bioreactor was downscaled to laboratory sizes [Zeilinger *et al.*, 2011]. In these bioreactors, PHH were successfully cultivated for three weeks and in-depth physiological characterization showed that liver specific functions were maintained over the whole cultivation time [Mueller *et al.*, 2011b]. Proteomic analysis of human hepatocytes in this bioreactor is promising not only for the detection and prediction of toxic drug effects but also for general understanding of cellular processes involved in tissue reconstruction. In general, systems biological characterization in toxicology by the "-omics" technologies like (epi-)genomics, transcriptomics, proteomics and metabolomics holds great potential for the comprehensive understanding of perturbation of biological systems due to drug administration and will, on the long term, lead to predictive models for use in drug development [Bandara and Kennedy, 2002; Collins *et al.*, 2007].

1.2 Proteomics

The term PROTEOME was introduced by the Australian scientist Marc Wilkins in the mid 90`s on a symposium on two-dimensional gelelectrophoresis (2-DE) as the "PROTEin complement of a genOME". Thereof, the term proteomics emerged which, as an equivalent to genomics, aims at the analysis and characterization of all proteins in a proteome [Wasinger *et al.*, 1995; Wilkins *et al.*, 1996]. A proteome is defined as the entire set of proteins expressed by an organism, tissue or cell under specific conditions at a specific time [Lottspeich, 1999]. It is estimated that the 25.000 protein-encoding genes in the human genome are translated into up to half a million different proteins if alternative splicing and the plethora of post-translational modifications of expressed proteins is taken into account [Anderson and Anderson, 2002]. In contrast to the rather static genome, the proteome is highly dynamic both in its qualitative and quantitative composition. The proteome composition is influenced by endo- and exogenous stimuli to a cell and ultimately defines its phenotype, thus being a promising and valuable tool for many different areas of life sciences including toxicology [Bandara and Kennedy, 2002; Collins *et al.*, 2007; Gao *et al.*, 2009]. In a modern proteomic experiment, proteins are analyzed by mass spectrometry (MS) after digestion of proteins into peptides by an endoprotease (usually trypsin). The cleavage of all proteins in a given proteome can easily result in the generation of hundreds of thousands of these molecules. However, because mass spectrometers themselves cannot deal with such complex samples, a reduction of sample complexity is a prerequisite. This is accomplished by separation of the sample on the level of either intact proteins before digestion or peptides after digestion. These variants of proteomic analyses are often referred to as "top-down" or "bottom-up" approaches, respectively, with the latter also called "shotgun" proteomics in analogy to the shotgun-sequencing of genomes, in which DNA is cleaved into shorter fragments before sequencing. The most commonly applied top-down approach for sample separation is still 2-DE. For the separation on the level of peptides, i.e. bottom-up, liquid chromatography is the method of choice. Nowadays, a proteomic experiment does not only identify the proteins within a proteome, but also aims at quantification of its changes under different conditions like healthy versus diseased or treated versus untreated, for example. These changes include not only differences in expression of distinct proteins but can also be expanded to the analysis of possibly differing patterns of post-translational modifications (PTM) like proteolytic processing, phosphorylation, acetylation and glycosylation, all of them having impact on the activity and/or function of a protein. For the identification and quantification of proteins as well as characterization of their PTMs, many MS-based methods together with computational validation and interpretation tools have been developed and optimized during the last two decades.

1.2.1 Methods for sample separation

The first method capable of analyzing whole proteomes was introduced in the 1970`s as the 2-DE [Kenrick and Margolis, 1970; Klose, 1975; O'Farrell, 1975]. In the first dimension, which is called isoelectric focusing (IEF), proteins are separated based on their isoelectric point, i.e. the pH at which their net charge equals zero. The net charge of a protein is caused by its amino and carboxy termini as well as the basic and acidic side chains of the amino acids the protein is composed of. Hence, the charge distribution of a protein is influenced by the pH of the surrounding medium. For IEF, proteins are loaded onto a polyacrylamid strip containing an immobilized pH gradient (IPG) and exposed to an electric field with the cathode placed at the basic, and the anode placed at the acidic end of the IPG-strip. Due to this electric field, the charged proteins move towards the electrode of opposite charge until they reach the pH region of the strip which corresponds to their isoelectric point. Because their net charge becomes zero at this point, they stop migrating in the electric field. In the second dimension, the focused proteins are separated based on their molecular weight by polyacrylamide electrophoresis under denaturing conditions with the aid of sodium dodecylsulfate (SDS-PAGE). The anionic detergent SDS binds to a protein providing denaturation and furthermore causes a negative charge proportional to the proteins molecular mass (1.4 g SDS/ g protein). The IPG strip after focussing is therefore placed on top of a SDS polyacrylamide gel after equilibrating the strip in a buffer containing SDS. By application of an electric field to the gel, the negatively charged SDS-protein complexes migrate towards the anode and are separated by their molecular weight due to the “molecular sieve” effect of the polyacrylamide gel. After separation, proteins can be visualized within the gel using Coomassie Blue, silver staining or also fluorescent dyes. Furthermore, the intensities of stained protein spots can serve as a measure of protein abundance for semi-quantitative comparison of different proteomic samples. Proteins of interest can be cut off the gel and applied to in-gel digestion for identification using mass spectrometry [Rosenfeld *et al.*, 1992; Shevchenko *et al.*, 1996].

Even though 2-DE is relatively cheap and allows detection and quantification of up to 5000 spots within one gel [Gorg *et al.*, 2004], it has several limitations. The technique is very labor intensive and includes many steps with each of them being a possible source of errors and which can hardly be automated. Moreover, the throughput and the reproducibility are quite low and the detection of low abundant proteins is hardly feasible because of the limited sensitivity of staining techniques as well as masking effects of high abundant proteins on the gel. Finally, 2-DE fails to cover “extreme” proteins with very high or very low isoelectric points or molecular weights and also membrane

proteins cannot be separated well due to their high hydrophobicity and usually high basicity [Rabilloud, 2002].

To overcome these limitations for proteome analysis, much effort was made to elaborate gel-free proteomics approaches using liquid chromatography coupled to mass spectrometry (LC-MS) [Aebersold and Mann, 2003; Mitulovic and Mechtler, 2006]. The advantage of these shotgun approaches is the separation of the proteome on the level of peptides which overcomes many limitations of 2-DE because peptides originating from proteins having extreme physico-chemical properties can be analyzed by these methods in an automated manner. But also for these techniques, the large differences in protein abundances within a sample, the dynamic range, still remains challenging. Chromatographic separation of peptides is achieved by the use of reversed-phase high-performance liquid chromatography (RP-HPLC). In RP-HPLC, peptides are separated in respect of their hydrophobicity and the separation is based on hydrophobic interactions between the peptides and the stationary phase as well as solvophobic interactions with the mobile phase. The most common stationary phase used for RP-HPLC for the separation of peptides in proteomics is based on octadecyl carbon chain bonded silica particles (C18). The hydrophobic moieties of peptides adsorb to the non-polar alkyl chains in a polar solvent (i.e. water) and are eluted by an increasing concentration of an organic solvent (acetonitrile (ACN) or methanol) in the mobile phase. Because of their relatively large molecule size, peptides can interact with the stationary phase with more than one moiety which is called multisite adsorption [Geng and Regnier, 1984]. Hence, in order to elute a peptide from the column, the solvent strength has to be high enough to desorp all parts of the peptide interacting with the columns stationary phase. By the addition of ion-pairing reagents such as triflouroacetic acid (TFA) to the mobile phase, the elution process is changed in such a way that not only solvophobic interactions but also electrostatic interactions provide adsorption of the analyte to the stationary phase. The hydrophobic part of the modifier binds to the stationary phase and the polar moiety (i.e. carboxyl group in the case of TFA) interacts with charged groups of the peptide significantly enhancing retention and peak symmetry and thus the resolution of the chromatographic analysis [Guo *et al.*, 1987]. However, to avoid covering of large parts of the stationary phase and thus decreasing solvophobic interactions, the concentration of the ion-pairing reagent in the mobile phase is very low (0.05-0.2 %). A notable advantage of RP-HPLC for the use in MS-based proteomics is the fact that it can be operated using volatile solvents (water, ACN, TFA) in the mobile phase which permits direct coupling of the chromatographic separation to mass spectrometry.

Similar to 2-DE, in which two different gel-based methods were combined, also two-dimensional chromatographic set-ups have been developed to deal with the high complexity of proteomic

samples. For example, the combination of strong-cation exchange (SCX) chromatography and RP-HPLC or the combination of RP-HPLC at high pH (10) and low pH (2) have been successfully employed for the analysis of complex samples [Washburn *et al.*, 2001; Wolters *et al.*, 2001; Delmotte *et al.*, 2007]. Furthermore, combinations of both gel-based and gel-free approaches like SDS-PAGE and RP-HPLC can be used (GeLC-MS) and can significantly enhance the performance of a proteomic analysis regarding protein identifications and sequence coverage [Brewis and Brennan, 2010].

1.2.2 Mass spectrometry for the analysis of peptides

A mass spectrometer is a device to determine the mass-to-charge ratio (*m/z*) of an analyte of interest. In general, it consists of an ion source, a mass analyzer and a detector. First, the analytes are ionized in the ion source, separated by their *m/*z in the mass analyzer and separated ions are detected to obtain a mass spectrum, i.e. a plot of the analytes *m/z* against their abundance (intensity). Furthermore, in the case of tandem mass spectrometry (MS/MS), specific ions are selected for fragmentation (precursor ions) and the *m/z* of the resulting fragments (fragment ions) is determined. The fragmentation pattern of peptides can be used to determine the underlying amino acid sequence. In the mass spectrometers used in this thesis, the precursors are fragmented by collision with gas molecules (air, He or N_2), which is called collision induced dissociation (CID). Indeed, this is the most commonly applied technique for fragmentation of peptides besides electron transfer dissociation (ETD), which was introduced in 2004 [Syka *et al.*, 2004].

Because proteins and peptides are non-volatile substances and are labile under high temperature, the invention of “soft” ionization techniques in the late 80`s, namely matrix-assisted laser desorption ionization (MALDI) and electrospray ionization (ESI), was essential for the use of MS in the analysis of biomolecules like proteins and peptides but also oligosaccharides and nucleic acids [Karas and Hillenkamp, 1988; Tanaka *et al.*, 1988; Fenn *et al.*, 1989]. The importance of these techniques for the scientific community becomes obvious by the fact that Koichi Tanaka and John Fenn received the 2002 Novel price in chemistry for their research on these novel ionization techniques. The principles of MALDI- and ESI-MS are depicted schematically in Figure 1.2 and are explained in the following.

Prior to MALDI-MS, the sample is mixed with a matrix and this mixture is deposited on a stainless steel plate (target). The solvents evaporate resulting in co-crystallization of the matrix molecules and the analytes. The matrix is added at a high molar excess compared to the analyte, generally between 1:10,000 -1:100,000. This ensures gentle ionization and reduces aggregate formation of the analytes. The target is then brought into the high vacuum of a mass spectrometer and irradiated with a pulsed laser beam (usually in the UV). The mechanism leading to ionization of analytes is still not fully

understood but it can be divided into three general stages : i) excitation of the matrix molecules by the laser photons, ii) desorption of matrix and sample molecules into the gas phase and iii) ionization of the molecules leading to the generation of presumably singly charged ions as depicted in Fig. 1.2a [Karas *et al.*, 2000; Knochenmuss and Zenobi, 2003].

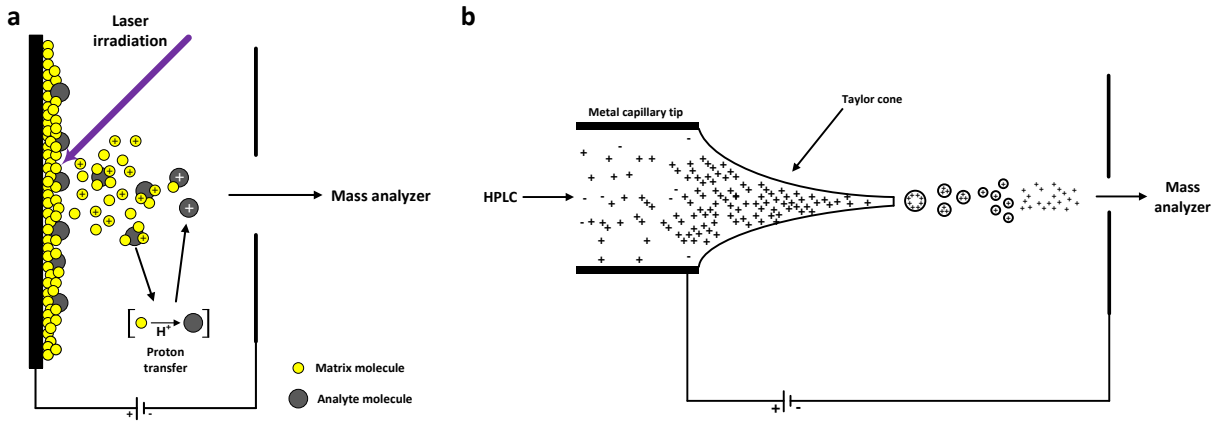

Figure 1.2. Schematic illustration of the two "soft" ionization techniques for MS analysis of proteins and peptides used in proteomics, namely MALDI (a) and ESI (b). Note that for both techniques, the operation in positive ion mode is shown as it is the most used in proteomics but it has to be noted that also negative ions can be generated by these ionization techniques.

Very recently, the Karas group proved with the aid of deuterated matrix molecules, that both gas phase protonation as well as survival of precharged analytes from solution (lucky survivors) is responsible for ionization of sample molecules during MALDI. The preference for one of these processes is depending on the analytes properties and the choice of the matrix [Jaskolla and Karas, 2011]. Because of the pulsed nature of the MALDI ionization process, this ion source is usually coupled to a time-of-flight (TOF) analyzer. In a TOF analyzer, ions are accelerated by an electric field and transferred into a field free flight tube. Because the ions are accelerated with the same kinetic energy in the source, they reach different velocities depending on their mass to charge ratio. Consequently, the time they need to pass the flight tube is depending on their mass to charge ratio and can be used to determine their molecular weight. Early TOF analyzers had only moderate mass resolution, which was significantly enhanced by the implementation of the reflector technology and the delayed extraction technique, both correcting for kinetic energy dispersion of molecules of the same mass and thus improving the resolution and mass accuracy [De Hoffmann and Stroobant, 2008]. In order to allow MS/MS measurements with such a mass spectrometer, TOF/TOF instruments were developed [Medzihradszky *et al.*, 2000]. In a TOF/TOF instrument (like the Applied Biosystems 4800 used in this thesis), the flight path is divided into two sections by a CID chamber (see Fig. 1.3). In MS mode, this chamber is evacuated and ionized peptides fly through the drifting tube until they reach

the detector to obtain a mass spectrum of all peptides in the analyzed spot. In MS/MS mode, the CID chamber is charged with an inert collision gas. The precursor meant for fragmentation is isolated by the timed ion selector (TIS), which consists of two ion gates in series. The first gate deflects low mass ions until the selected precursor reaches the gate and is turned off to let pass the precursor ion. Afterwards, the second gate is switched on and deflects ions with a higher molecular weight than the precursor. After fragmentation of the precursor in the CID chamber, the resulting fragment ions are accelerated again and separated in the second TOF analyzer to obtain the MS/MS spectrum.

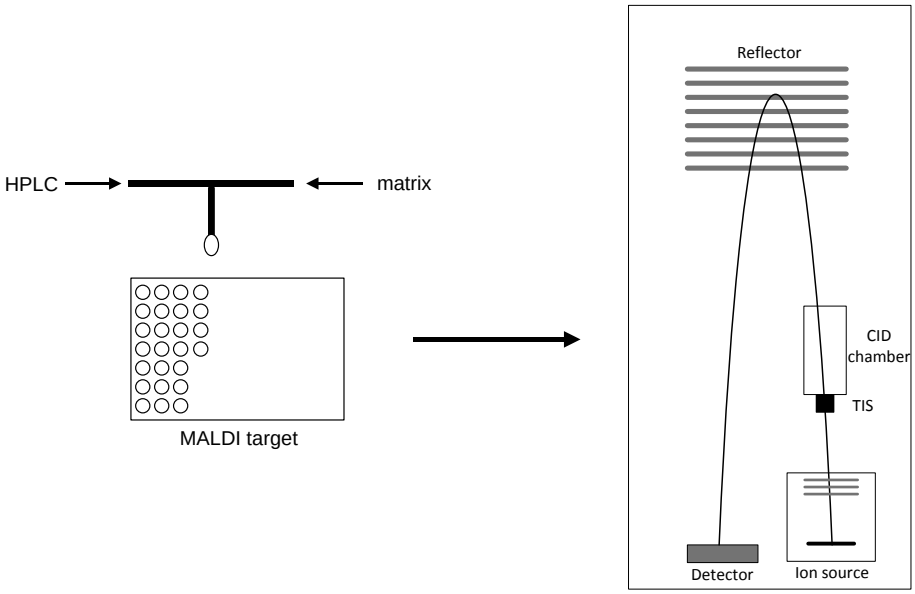

Figure 1.3. Schematic illustration of off-line LC-MALDI coupling as performed in this thesis. The effluent from the HPLC outlet is mixed automatically with matrix and fractions are collected as spots on a MALDI-target (left). Subsequently, the collected fractions are analyzed in a MALDI-TOF/TOF-MS (right).

MALDI-MS has to be coupled off-line to liquid chromatography because the peptides eluting from the HPLC have to be mixed with matrix and the solvents have to evaporate to allow the formation of crystals prior to analysis by MS (see Fig. 1.3). Commercially available fractionation devices which are capable of continuous matrix addition and automatic spot deposition have been developed. This permits automation of the process and enhances the reproducibility of sample preparation for hyphenation of liquid chromatography (LC) to MALDI-MS (LC-MALDI). For acquisition of MS/MS spectra during LC-MALDI, all fractions are first measured in MS mode to obtain an ion chromatogram for each mass. Precursors for fragmentation are then selected on the apex of their chromatographic peak, i.e. the spot in which the highest intensity of the precursor mass was detected.

While the MALDI ionization takes place in high vacuum, ESI is performed under atmospheric pressure. During ESI, the analytes pass through a small capillary tube in a volatile solvent (for example the RP-HPLCs mobile phase) and a strong voltage is applied between the capillary tip and a counter

electrode. This electric field leads to accumulation of charges at the liquid surface and to deformation of the growing droplet at the capillary tip which is resulting in a so-called “Taylor cone” (see Fig. 1.2 b) and the onset of the spray. Small, highly charged droplets break from this cone and subsequently break into smaller droplets because of occurring Coulomb explosions. After complete evaporation of solvent by the additional help of heated curtain gas (normally N_2), the analytes are released as desolvated, charged molecules. The formation of ions in ESI is a result of accumulating charges in the shrinking droplets of the spray which are retained by the desolvated molecules and electrochemical processes occurring at the probe tip [De Hoffmann and Stroobant, 2008]. In contrast to MALDI, ESI generates not only singly charged but also multiply charged ions. The ions generated at atmospheric pressure during ESI have to be transferred into the high vacuum of the mass analyzer. This is accomplished by differential pumping at the beginning of the MS progressively decreasing the pressure in several succeeding compartments. These compartments are separated from each other by hyperbolic metal plates with very small orifices, so called skimmers. The orifices are wide enough to allow introduction of as many ions as possible into the mass analyzer but, at the same time, have to be small enough to maintain the vacuum in the mass analyzer. Among the ESI-based mass spectrometers, the most often used for proteomic analyses are the ion trap and the hybrid quadropole time-of-flight (QTOF) instruments.

The QTOF is a hybrid instrument in which a quaduropole analyzer is coupled to a TOF analyzer (see Fig. 1.4 b). A quadropole analyzer consists of four parallel metal rods. Each opposing pair of rods is connected electrically and to each pair, a radio frequency (RF) voltage is applied and superimposed by a direct current voltage. This electric field influences the trajectories of axially entering ions and can be used to selectively filter ions based on their *m/z* by varying the ratios of applied voltages (i.e. RF to direct current). Only ions of a specific *m/z* exhibit stable trajectories at a given ratio and can pass the quadropole while the trajectories of other ions become instable and they hit the rods where they discharge. If the quadropole is operated in RF-only mode, i.e. no direct current voltage is applied, it can be used as an ion guide. In a QTOF, such a quadrupole is now coupled to a TOF with the two analyzers being separated by a collision cell. In MS mode, the quadrupole is operating in RF-only mode and transmitted ions are analyzed in the subsequent TOF after orthogonal acceleration using a “pusher”. In MS/MS mode, the precursor is selected in the quadrupole, subsequently fragmented in the collision cell and the fragments are analyzed in the TOF. Modern high resolution QTOF instruments like the Bruker MaXis used in this thesis have very high mass accuracies in the low (1-5) ppm range.

An ion trap consists of three electrodes: one cylindrical ring electrode and two hyperbolic end-cap electrodes. Ions generated in the source are focused by RF-only octapoles (principally a quadrupole with eight rods) and enter and leave the trap through small holes in the two end cap electrodes (see Fig. 1.4 a). The trapping mechanism is generally based on the same principles as in a quadrupole. The ions are kept on stable trajectories within the trap by application of a 3-dimensional quadrupolar field to the electrodes and can be consecutively ejected according to their *m/z* by ramping of the RF frequency. To enhance the trapping of ions, an inert damping gas (usually helium) is present at low pressures in the trap. By collisions of trapped ions with helium atoms, the kinetic energy of the ions is decreased and they are focused in the center of the trap. For the generation of MS/MS spectra, all ions except the precursor are ejected. Thereafter, the frequency of the RF-voltage at the end cap electrodes is increased resulting in excitation of the trapped ions. Consequently, strong collisions with the helium atoms lead to fragmentation of the isolated precursors. The fragments are then ejected according to their *m/z* and detected. While the ion trap mass analyzers are quite inexpensive, sensitive and robust instruments, a disadvantage is their low mass accuracy (80-100 ppm).

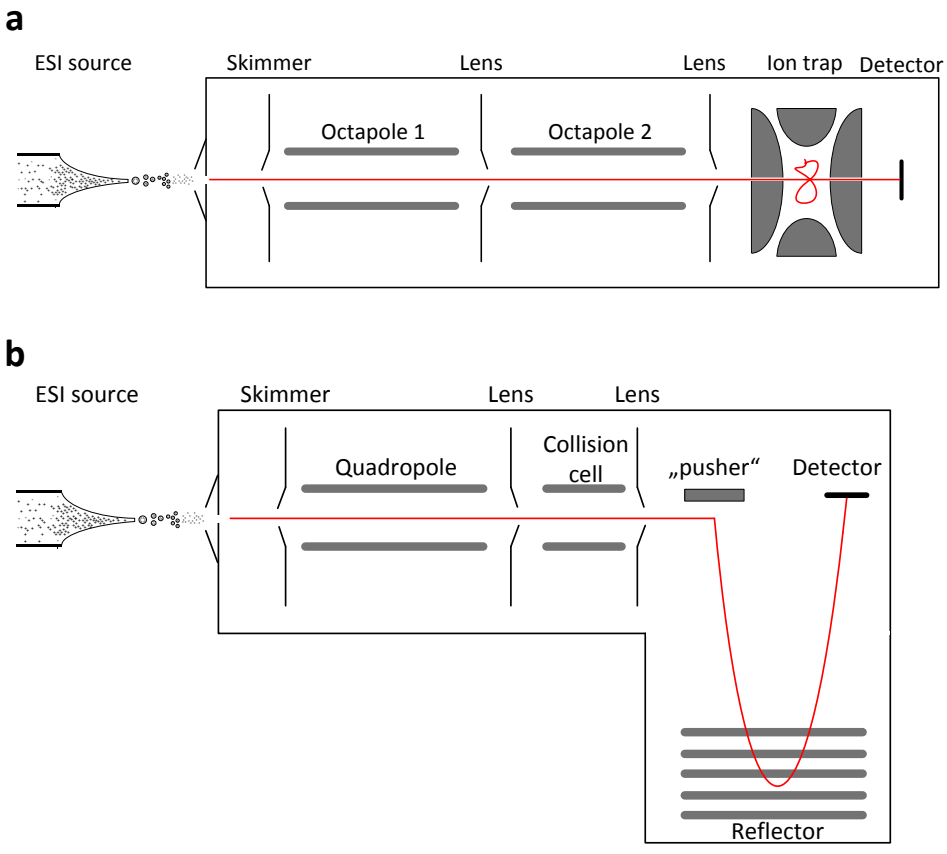

Figure 1.4. Schematic illustration of ion trap (a) and qudrupole time-of flight (QTOF) mass spectrometers. Both analyzers are equipped with an ESI source. The way of the ion beam during mass analysis is indicated by the red lines.

1.2.3 Protein identification from mass spectrometric data

The large-scale identification of proteins and peptides using MS data became possible by the availability of whole genome sequences of a variety of organisms since the 1990`s. The first method to derive protein identities from mass spectra using sequence databases was the peptide mass fingerprint (PMF) proposed in 1993 simultaneously by different groups [Mann *et al.*, 1993; Pappin *et al.*, 1993; Yates *et al.*, 1993]. In this method, peptide masses obtained from MS measurements after enzymatic digestion of proteins are compared to theoretical masses of an *in silico* digest of protein sequences (or translated gene sequences) available in a database. The masses are then matched to a specific protein according to a mathematical scoring scheme like the MOWSE score (MOlecular Weight Search) [Pappin *et al.*, 1993]. However, this method requires high purity of the protein to be identified because already when two proteins are digested together, the resulting mass spectrum can hardly be matched unambiguously to a protein fingerprint from the *in silico* digest. Hence, PMF is restricted to the identification of proteins separated by 2-DE, for example. One year after the introduction of the PMF method, another method was introduced that matched the masses of MS/MS spectra to the sequence databases and which was called peptide fragment fingerprint (PFF) [Eng *et al.*, 1994; Blueggel *et al.*, 2004]. The advantage of PFF is the additional information on underlying amino acid sequences which is deduced from the fragment ion pattern. During CID, a peptide is fragmented preferably at its peptide bonds resulting in N-terminal (b-ions) and C-terminal fragments (y-ions). Also other fragmentations can occur as it is shown in Figure 1.5 a, but b- and y-ions are the fragments most likely observed after fragmentation *via* CID.

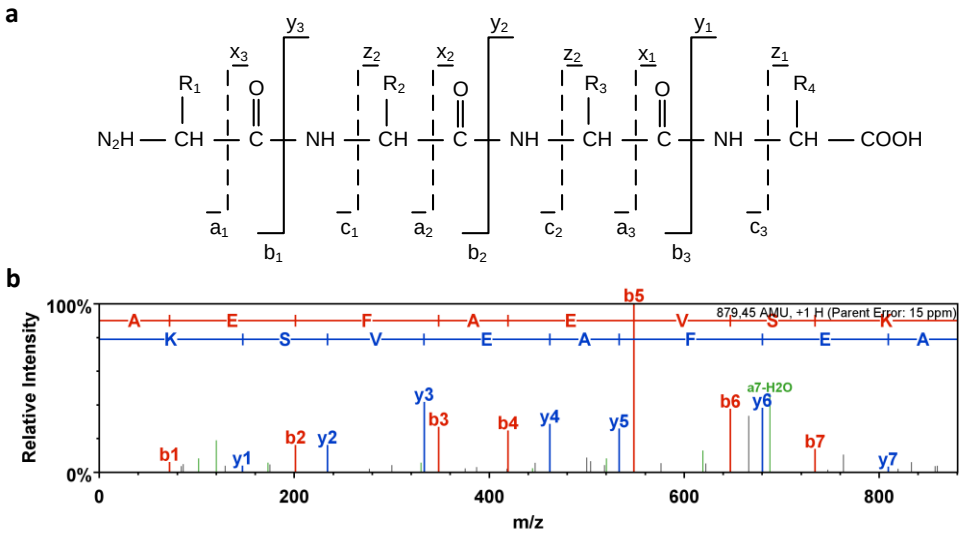

Figure 1.5. Nomenclature of peptide fragments as proposed by Roepstorff and Biemann [Roepstorff and Fohlman, 1984; Biemann, 1988] (a). MS/MS spectrum of the peptide AEFAEVSK after fragmentation *via* CID in a MALDI-TOF/TOF-MS (b).

A peptide can be fragmented at every peptide bond which results in a spectrum where each peak represents a different peptide fragment. The mass differences between the peaks can now be used to determine the amino acid sequence, because the masses of amino acids are known (see Fig.1.5b). Many algorithms have been developed to interpret MS/MS spectra of fragmented peptides, because the manual interpretation requires high expertise and becomes impractical for the application to large-scale proteomics analyses, in which several thousand peptides are analyzed at once. SEQUEST was the first being commercialized using the algorithm developed by Eng *et al.* in 1994 and which cross correlates the empirical with the theoretical data. Another widely used algorithm is Mascot, which was introduced in 1999 [Perkins *et al.*, 1999] and which uses a probability based scoring scheme. It calculates the probability that the observed match is a random event and calculates an "ion score" from this probability. The ion score is calculated as $-10*\log_{10}(P)$, where "P" is the probability of a random match. For example, a score of 200 is equivalent to a probability of 10^{-20} that the match happened by chance. The higher the ion score, the lower the probability of a random match. In order to identify significant matches, Mascot provides a second score which incorporates the number of applicants into score calculation. This "identity score" is calculated as $-10*\log_{10}(p/\text{no. of matches})$, where "p" is the probability threshold defined by the user (normally 5%) and "no. of matches" is the number of different precursor masses that matched to the spectrum. Thus, only peptides with an ion score above the identity score, i.e. when ion score minus identity score is above 0, can be considered as being confidently identified. However, for all of the algorithms used for MS/MS spectra interpretation, there is a level of uncertainty regarding the correct assignments of experimental spectra to the theoretical data. The estimation and control of this false discovery rate (FDR) in such approaches can be achieved by the use of "target-decoy" database searches [Elias and Gygi, 2007]. The principle of this technique consists in the implementation of decoy-sequences into the sequence database to be searched ("target" database). The decoy sequences are generated by reversing or randomizing the correct sequences. If a spectrum can be matched to a sequence of the decoy entries, it can be considered as a false positive identification. The score threshold for accepting identifications can now be adjusted until the number of decoy matches is at a tolerable level, usually around 1 %. Furthermore, algorithms have been introduced which calculate the possibility that the peptide and protein assignments are true, namely PeptideProphet™ and ProteinProphet™ [Keller *et al.*, 2002; Nesvizhskii *et al.*, 2003]. They use Bayesian statistics to calculate the probability of true positives from the score distributions in the underlying data set and subsequently assign the confidently identified peptides to the most probable protein (see Fig. 1.6.). Software solutions are available implementing all of the aforementioned techniques and/or algorithms providing a simple

and user friendly interface for validation of database search results such as Scaffold, for example [Searle, 2010].

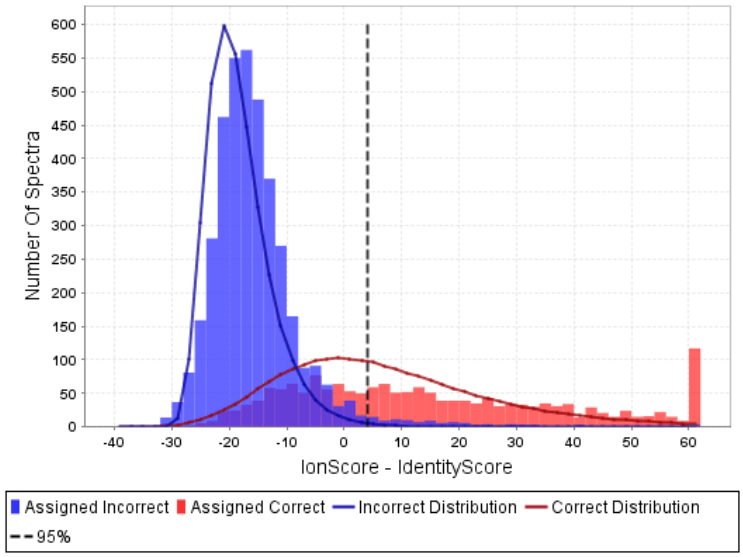

Figure 1.6. Typical score distribution obtained after a target-decoy database search using Mascot. Red bars indicate the number of correct assignments of spectra to a peptide sequence, blue bars indicate incorrect assignments, both as a function of the "ion minus identity score". The red and blue lines indicate score distributions as calculated by PeptideProphet™. The dashed line indicates the minimum ion-identity score above which PeptideProphet™ has calculated a 95% probability of a correct peptide spectrum match.

1.2.4 Quantification in Proteomics

As mentioned previously, one of the most important goals of proteomics is the determination of quantitative changes in protein expression in response to a specific perturbation [Ong and Mann, 2005]. The development of methods enabling accurate quantification of proteins in complex samples using mass spectrometry is one of the most challenging and rapidly growing areas in proteomics [Elliott *et al.*, 2009]. Most quantitative proteomics methods developed so far provide relative quantification, i.e. the up- or down-regulation of a protein compared to a control sample. In contrast, absolute quantification aims at providing absolute concentration values of a distinct protein in a sample. Actually, this absolute quantification is also achieved by relative quantification, but to an internal standard for which the absolute concentration is known.

In gel-based workflows, relative quantification is performed at the level of intact proteins by comparing spot intensities between gels. However, this approach requires high reproducibility of the gels to be compared and the quantification is limited by the low linearity range of staining techniques like Coomassie Blue in regard to the protein amount in the spot. The development of 2D fluorescence differential gel electrophoresis (2D-DIGE) significantly enhanced the performance of gel-based quantification because the compared samples are run together on the same gel,

eliminating potential gel-to-gel variation [Alban *et al.*, 2003]. However, it suffers from already mentioned restrictions imposed by the 2-DE approach like limited dynamic range and difficulties in handling proteins with extreme properties [Zhu *et al.*, 2010]. Furthermore, biases can be introduced because a spot can contain more than one protein.

Most techniques for quantification in shotgun proteomics techniques rely on the incorporation of stable heavy isotopes into the analyzed peptides. Because labeled peptides have identical chemical and physical properties as their natural counterparts except in mass, there is no difference in their behavior during applied separation techniques but they can be separated in the subsequent analysis by MS. Compared samples from which one (or more) have been labeled are mixed prior to analysis and by comparing the ion intensities or peak areas of the labeled and the unlabeled species after MS, the differences in abundance can be determined. A variety of labeling approaches have been developed like TMT [Thompson *et al.*, 2003], iTRAQ [Ross *et al.*, 2004], ICAT [Gygi *et al.*, 1999] or SILAC [Ong *et al.*, 2002]. A special quantification technique using isotope labeled peptides is the selected reaction monitoring (SRM) also called multiple reaction monitoring (MRM) if several proteins are quantified at once. This targeted quantification approach uses the ability of triple-quadrupole mass analyzers to isolate a precursor ion as well as a specific fragment ion after CID by using three quadrupoles in series. In the first quadrupole, the precursor is selected and is then fragmented in the second quadrupole which serves as collision cell. After fragmentation, the third quadrupole isolates a fragment ion, which is specific for a peptide of interest if combined with the precursor mass. The specific combination of precursor and fragment ion masses is called a “transition”. If this transition is derived from a peptide which is found only in one protein (proteotypic peptide), this technique is highly specific. Quantification is achieved by spiking the sample with this proteotypic peptide as an isotope labeled variant and comparing the intensities of the fragment ions. Because the concentration of the spiked peptide is known, the absolute concentration of a protein can be determined [Lange *et al.*, 2008]. The limitations of labeling-based approaches include the increased time and complexity of sample preparation, the high costs of the reagents as well as the possibility of incomplete labeling of analyzed samples [Zhu *et al.*, 2010]. Therefore, label-free methods are gaining more and more attention by the proteomic community [Elliott *et al.*, 2009; Neilson *et al.*, 2011].

Label-free quantification is generally based on two categories of measurements. The first is the intensity of chromatographic peak heights or peak areas, which has been shown to correlate with the abundance of the corresponding protein [Chelius and Bondarenko, 2002]. The second way of label-free quantification is based on the number of sequenced peptides of a distinct protein during MS/MS

acquisition. The more abundant a protein within a sample, the more likely is the identification of peptides derived from this protein during MS-analysis. This manifests itself in the achieved sequence coverage of a protein, i.e. the part of the amino acid sequence being covered by the identified peptides. Furthermore, protein abundance can be deduced from the total number of identified peptides (peptide hits) or from the total number of identified spectra (spectrum counts) with the latter also including redundant spectra of the same peptide. By using standard proteins spiked in a complex sample at different ratios, Liu *et al.* compared the correlation of protein abundance to sequence coverage, peptide hits as well as spectrum counts [Liu *et al.*, 2004]. They found a perfectly linear relationship between spectrum counts and protein abundance. The sequence coverage exhibited no or weak correlation to the spiked-in protein amount whereas the peptide hits showed good but not linear correlation. The latter was successfully applied to the determination of changes in protein expression in yeast after cultivation on different carbon sources as well as for the detection of protein biomarkers for inflammation in human urine [Pang *et al.*, 2002; Gao *et al.*, 2003]. Moreover, the peptide hit approach was able to identify biomarkers for idiosyncratic toxicity using primary hepatocytes which was confirmed by western blotting [Gao *et al.*, 2004].

1.3 The Secretome as a valuable source of biomarkers

According to the National Institute of Health (NIH), a biomarker is "a characteristic that is objectively measured and evaluated as an indicator of normal biologic processes, pathogenic processes, or pharmacologic responses to a therapeutic intervention" [2001]. A biomarker should be easily accessible during clinical surveillance and in this regard, the easiest way would be a simple blood sampling from the patient. Since the liver secretes many proteins directly into the blood-stream of the human organism, proteins found to be differentially secreted upon drug-application in an *in vitro* culture of primary human hepatocytes are likely to be present in plasma of patients. The main advantage of analyzing secreted proteins in the conditioned medium of cell cultures rather than in the human plasma itself for biomarker discovery is the decreased complexity of the conditioned medium regarding protein number and dynamic range. Moreover, the cells can be cultivated in a well controlled system minimizing biases due to different origins and histories of clinical samples. Thus, the biomarker discovery process is significantly facilitated [Dowling and Clynes, 2011]. In this thesis, the secretome is defined as the totality of proteins found in the conditioned medium of cultivated human hepatocytes as a result of active secretion but not leakage from cells due to damaged plasma membranes. The active secretion of proteins by a cell can be achieved by a variety of pathways. To enter the classical secretory pathway, proteins must contain a signal sequence to enter the endoplasmic reticulum and are secreted after travelling through the Golgi apparatus [Klee

and Sosa, 2007]. For secretion by unconventional or non-classical pathways, proteins do not require a signal sequence and are released by a variety of mechanisms, including efflux through plasma membrane transporters, shedding from the plasma membrane or exocytosis of secretory lysosomes and exosomes [Nickel, 2010].

1.4 The aim of the BMBF-project “HEPATOX”

The presented work was done within the german research project “3D-*in vitro* model for hepatic drug-toxicity” or “HEPATOX” funded by the Federal Ministry of Education and Research (BMBF).

The project aimed at the prediction of drug-induced toxicity using a novel 3D-cultivation technique and in-depth characterization of this culture to establish read-out parameters specific for hepatic drug toxicity. The project is based on the hypothesis that long-term maintenance of liver specific functions of human hepatocytes can be achieved by cultivation of primary human hepatocytes in a complex 3D perfusion culture device that closely reflects the microenvironment of hepatocytes in real liver tissue.

The consortium consisted of three academic and two industrial partners, each representing a subproject:

1. Pharmacelsus GmbH, Saarbrücken (Coordinator)
2. Charité Bioreactor Group, Charité University Medicine, Berlin
3. Traumatology, Technical University Munich, München
4. Technical Biochemistry, Saarland University, Saarbrücken
5. Elexopharm GmbH, Saarbrücken

The specific aim of the subproject No. 4 at the Department of Biochemical Engineering was the “Systems biotechnological characterization of the physiology of hepatic cell cultivation in 3D bioreactors” using state of the art systems biology approaches, namely metabolomics and proteomics.

The subproject aimed at providing metabolomics and proteomics data for the detailed analysis of long-term bioreactor performance and for detecting potential toxic effects after application of reference drugs. This detailed analysis should reveal biomarker candidates for the prediction of early drug toxicity.

1.5 Goal and outline of this thesis

The goal of this thesis was the identification of protein biomarker candidates for drug-induced liver toxicity in the secretome of primary human hepatocytes cultivated in a 3D-bioreactor by proteomics techniques.

To achieve this goal, the following steps had to be elaborated:

1) Long-term functional cultivation of primary liver cells for efficient secretome analysis
2) Optimization of sample preparation for in-depth characterization of the secretome
3) Setup of a nano-scale high-pressure liquid-chromatography system coupled to an automatic spotting device allowing analysis of the hepatocytes secretome *via* LC-MALDI
4) Comparison of the secretome in monolayer and bioreactor culture
5) Detect differences in the secretome upon drug-exposure

First, the serum-free cultivation had to be established for standard monolayer cultures to allow set-up and optimization of secretome analysis by LC-MALDI while establishing the serum-free cultivation of primary human hepatocytes in the 3D-bioreactor. The established workflow should be applied to bioreactor samples containing proteins secreted by primary hepatocytes and the differences upon exposure to a reference drug (diclofenac) should be detected to identify proteins related to diclofenac induced toxicity events.

2. Chemicals

All used chemicals were purchased at the highest purity/reagent grade available.

Ammonium peroxodisulfate, bromophenol blue sodium salt, formaldehyde, iodoacetamide, CHCA (α-cyano-4-hydroxycinnamic acid; MALDI matrix), [Glu1]-fibrinopeptide B human (for internal calibration), EZblue gel staining reagent was obtained from Sigma-Aldrich (Steinheim, Germany).

Tris-(hydroxymethyl)-aminomethane, sodium dodecyl sulfate (SDS), acrylamide solution Rotiphorese® Gel 30 were purchased from Carl Roth GmbH (Karlsruhe, Germany).

Glycerol, ethanol, acetic acid, methanol (for synthesis), silver nitrate (for analysis) and sodium thiosulfate pentahydrate were obtained from Chemical Storage Facility of the University of Saarland.

Dithiotreitol (DTT) was purchased from MBI Fermentas (St. Leon-Rot, Germany).

ß-Mercaptoethanol, Trifluoroacetic acid (TFA) and Temed (N,N,N´,N´-tetramethylethylendiamine) was purchased from Fluka (Steinheim, Germany).

Sequencing grade modified trypsin was obtained from Promega (Madison, WI, USA).

Deionized water (18 MΩ) for preparation of buffers was prepared using a Purelab Ultra Genetic system (ELGA, Griesheim; Germany), while HPLC grade water and acetonitrile (Chromasolv plus) for preparing solvents for chromatography were purchased from Sigma-Aldrich.

All other materials and instruments used in this work are reported in the respective methods section.

3. Material and Methods

3.1 Isolation of primary human hepatocytes

The isolation of primary human hepatocytes (PHH) was performed by Dr. Daniel Knobeloch at Charité Virchow clinic, Berlin.

Resected liver tissues from patients with primary and secondary tumors were used. Tissue was collected according to the institutional guidelines and with the patient's written consent. Hepatocytes were isolated using a two-step collagenase P (from *Clostridium histolyticum*) perfusion technique, followed by a Percoll density gradient centrifugation [Nussler *et al.*, 2009]. The purity and viability was determined under light microscopy using trypan blue exclusion.

PHH for bioreactor inocculation were shipped as suspension in Cold Storage Solution (Hepacult, Regensburg) directly after isolation according to the protocol provided by the company. For monolayer cultures, PHH were seeded after isolation on rat tail collagen coated dishes (BD Falcon) in Williams medium E, supplemented with penicillin/streptomycin (100 U/ml, 100 µg/ml), HEPES (15 mM), fetal calf serum (10%), insulin (1 mM), sodium pyruvate (1mM) and fortecortin (0.8 µg/ml). The cells were incubated in a humidified incubator with 95 % air and 5 % CO_2 at 37 °C. 24 hours after seeding, cells were shipped under standardized operating procedures. Rat tail collagen was prepared according to the protocol of Rajan et al. [Rajan *et al.*, 2006].

3.2 Monolayer cell culture

Human primary hepatocytes (department of surgery, Charité-Universitätsmedizin, Virchow-Klinikum, Berlin, Germany) were obtained in 6-well plates at a density of $1x10^6$ cells per well and the medium was changed at the day of arrival to Heparmed medium containing 1% ITG supplement (0.8 mg/l **i**nsulin, 5mg/l **t**ransferrin and 3 µg/l **g**lucagon; both Biochrome AG, Berlin, Germany), with 10 % FCS (PAA, Cölbe, Germany) and penicillin/streptomycin. After 24h, the medium was removed and the cells were washed four times with Heparmed medium (2ml) without FCS and cultured for 4 days with daily medium exchange. The medium of three wells was removed, pooled and a protease inhibitor cocktail (Complete; Roche Diagnostics, Mannheim, Germany) was added as a 25 x stock solution to avoid unspecific proteolysis. The collected medium containing the secreted proteins and metabolites from primary human hepatocytes is in the henceforth referred to "conditioned medium", while "unconditioned medium" means fresh medium.

3.3 Bioreactor cultivation

The 3D bioreactor (Stem Cell Systems GmbH, Berlin, Germany) used in this work consisted of three interwoven hollow-fiber capillary bundles integrated into a polyurethane housing resulting in four different compartments. Two bundles of hydrophilic polyethersulphone membranes with a pore size of 0.5 mm (Membrana, Wuppertal, Germany) were used for medium supply. The third bundle is made of hydrophobic multilaminate hollow-fiber membranes (MHF; Mitsubishi, Tokyo, Japan) for gas supply. However, for the bioreactor cultivations performed in our lab, the oxygen-supply was achieved by a different strategy (see Fig. 3.1 a). The medium was oxygenated using a self-developed gassing-unit consisting of a thin air-permeable silicone tubing (i.d. 1.47 mm, wall thickness 0.5 mm; Helix Medical, Carpinteria, USA) placed before the bioreactor. Thus, the medium was saturated with oxygen by diffusion of air through this tubing. The hollow-fibers originally thought for gas-supply were filled with sterile water. Additionally, 5% CO_2 was adjusted using this gassing system. The bundles for medium supply were connected to a tubing system which was equipped with two oxygen sensors (PreSens, Regensburg, Germany), one in front of the bioreactor and one behind to calculate oxygen-uptake rates for *on-line* monitoring of cell-viability [Mueller *et al.*, 2011b]. The bioreactor polyurethane housing was equipped with separate access ports for each individual capillary bundle and one additional port to inoculate the cells into the extracapillary compartment. The bioreactor and the connected tubing system were placed into a specifically developed, heatable perfusion system (Stem Cell Systems, Berlin; see Fig. 3.1 d) providing two peristaltic pumps, one for medium-recirculation (7 ml per minute) and the other for the supply of fresh medium (1.5 ml per hour). Furthermore, the perfusion system allowed proportional regulation of air and CO_2 in the gas mixture for gassing *via* built-in rotameters. The cell compartment of the “jelly-fish”-bioreactor used for cultivation in our lab (see Fig. 3.1 b) had a volume of 2 ml and was inoculated with $1x10^8$ cells while the “two-layer”-bioreactor used for the serum-free cultivation at Charité, Berlin (see Fig. 3.1 d) had a cell-compartment size of 0.5 ml and was inoculated with $2x10^7$ cells.

The continuous supply with fresh-medium resulted in an overpressure in the system, thus provoking an efflux of conditioned medium. This efflux was collected in a refrigerator in a flask containing protease inhibitors for the analysis of the extracellular proteome.

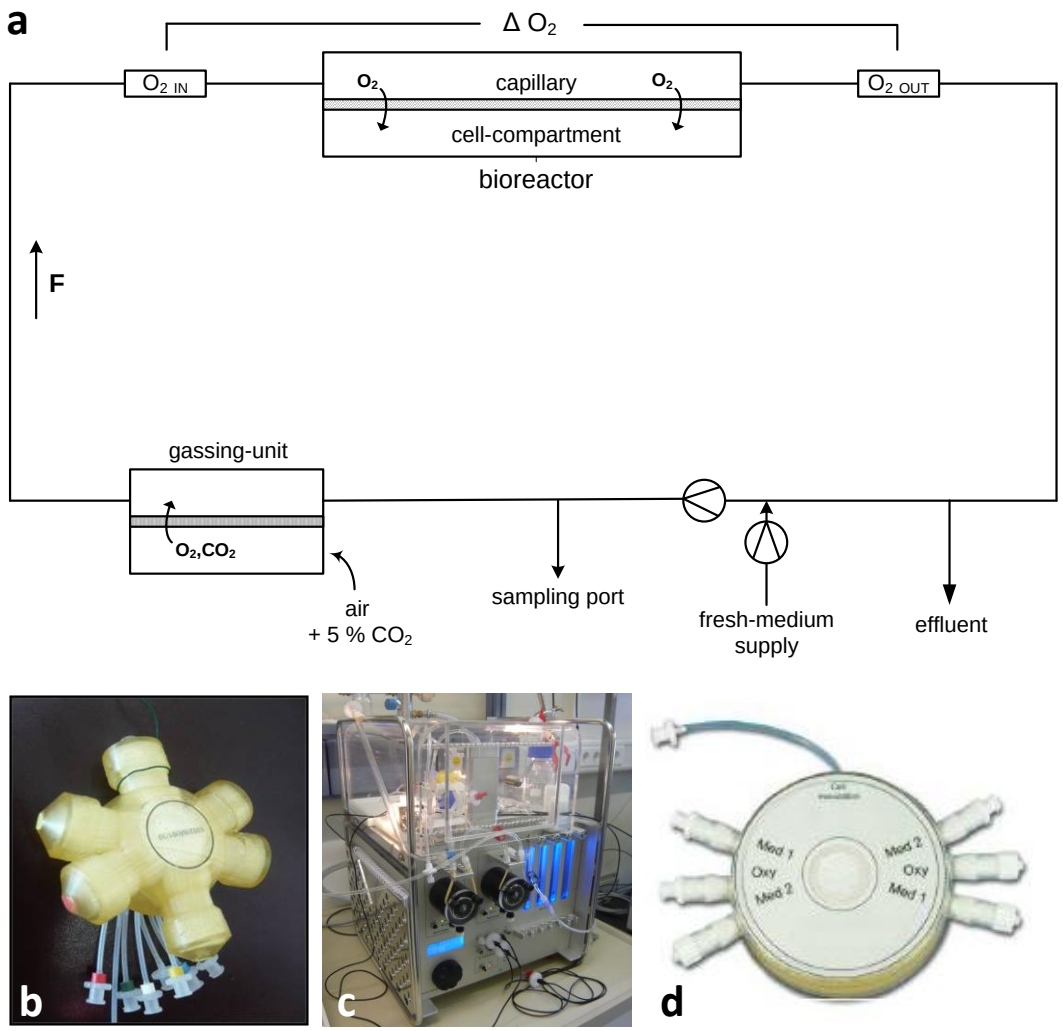

Figure 3.1. The bioreactor system used in this work. Scheme of the bioreactor with tubing system, pumps, oxygen sensors ($O_{2\,IN}$, $O_{2\,OUT}$) and the gassing-unit (a). Picture of the "jelly fish" bioreactor used for cultivations at the Saarland University (b), of the perfusion system for bioreactor operation (c) and of the "two-layer" bioreactor used for serum-free cultivation at Charité, Berlin (d, courtesy of Charité, Berlin).

3.4 Physiological characterisation of the hepatocyte cultures

To characterize the monolayer cultivation of primary human hepatocytes, supernatants of the cultures were analyzed for several parameters i.e. metabolism (*via* sugar uptake/release and lactate production), viability (*via* enzyme release) and protein production of the cells. The methods used to achieve this goal are explained in this section and the results are reported in section 4.2.

3.4.1 Determination of albumin concentrations

Albumin concentration in the culture supernatant was determined *via* an enzyme-linked immunosorbent assay (ELISA) kit, containing all required buffers and reagents (Albuwell II; Exocell, Philadelphia, PA), according to the manufacturer´s instructions in 96-well plates. In brief, samples (100 µl) were incubated for about 30 minutes at room temperature (RT) with 100 µl of CONJUGATE in the precoated 96-well plate supplied with the kit. For color development, 100 µl of COLOR DEVELOPER was added and incubated for about 10 minutes at RT. Afterwards, color development was stopped with 100 µl COLOR STOPPER and absorbance at 450 nm was determined using a microplate reader (iEMS Reader MF; Labsystems, Helsinki, Finnland). Albumin concentration was calculated using a standard of human serumalbumin derived with the kit and measured simultaneously as a 1:2 dilution series. Both standard and samples were determined as duplicates. For calculation of production rates, the value obtained for the blank (medium) was subtracted and rates were calculated by normalizing the values to the total volume of the supernatant and dividing the resulting values by the number of seeded cells (one million per well of a 6-well plate).

For calculation of daily production rates from bioreactor effluent samples, the following formula provided by the charitè was used:

$$(C_E\,(tx) - C_E\,(tx\text{-}1)) * V_E\,(tx) + ((C_E\,(tx) + C_E\,(tx\text{-}1))/2 - C_M) * V_R$$

with C_E being the analytes concentration in the effluent samples at the day of sampling (tx) and the day before (tx-1); V_E being the total volume of effluent; C_M being the medium (blank) value and V_R being the total recirculation volume of the bioreactor.

3.4.2 Determination of LDH activity

The specific activity of Lactate-Dehydrogenase (LDH) in the culture supernatant was determined using a colorimetric enzymatic assay kit (Cytotoxicity Detection Kit; Roche). LDH released in the supernatant oxidizes lactate to pyruvate with the formation of $NADH+H^+$. A catalyst (diaphorase) then uses this $NADH+H^+$ to reduce a tetrazolium salt (INT) to the corresponding formazan whose

amount can be determined photometrically. In brief, 100 µl of sample was mixed with 100 µl reaction mix (containing lactate, NAD^+ and diaphorase) in a 96-well plate and incubated for 30 minutes at RT under light-protection. Absorbance was determined at 492 nm using a microplate reader (iEMS Reader MF). For normalization, a dilution series of a standard serum (NobiCal-MULTI; HITADO, Möhnesee-Delecke) was measured simultaneously. Release rates were calculated by normalizing the values to the total volume of the supernatant and dividing this value by the number of seeded cells (one million per well of a 6-well plate). Release was calculated after subtracting the activity determined in the unconditioned cultivation medium.

3.4.3 Determination of AST activity

The activity of liver-specific aspartate aminotransferase (AST) in the culture supernatant was determined using a kinetic UV assay kit (Hitado, Möhnesee-Delecke, Germany). L-Aspartate and 2-Oxoglutarate are converted to L-Glutamate and Oxalocetate by Transamination through AST. In a second reaction, the produced Oxalocetate is oxidized to L-Malat by the enzyme Malat-Dehydrogenase under formation of NAD^+ from $NADH+H^+$. The decrease in NAD^+ can be determined photometrically at a wavelength of 340 nm and is proportional to the amount of AST in the sample. 20 µl of sample were mixed with the reaction mixture (5 parts R1 and 1 part R2), that was warmed to 37° C and the extinction was determined at 340 nm in a microplate reader (iEMS reader MF) after 1 minute and after 10 minutes. To calculate the activity of AST, a dilution series of a standard serum (NobiCal-MULTI; Hitado, Möhnesee-Delecke) was measured simultaneously. Release rates were calculated by normalizing the values to the total volume of the supernatant and dividing this value by the number of seeded cells (one million per well of a 6-well plate) after subtracting the activity of AST determined in the unconditioned medium.

3.4.4 Determination of glucose, galactose, sorbitol and lactate concentrations

D-glucose, D-galactose, D-sorbitol and L-lactate concentrations in the samples were determined using enzymatic assay kits (all from R-Biopharm, Darmstadt, Germany) after manufacturer`s instructions as described below. Release/production rates were calculated by normalizing the values to the total volume of the supernatant and dividing this value by the number of seeded cells (one million per well of a 6-well plate) after subtracting the concentration of the respective metabolite determined in the unconditioned medium.

3.4.4.1 D-Glucose

The assay is based on the conversion of D-glucose to gluconate-6-phosphate by hexokinase and glucose-6-phosphatedehydrogenase with the formation of equimolar NADPH. Absorbance of NADPH is measured at 340 nm using an Ultrospec 2000 UV/Vis spectrophotometer (Amersham Pharmacia Biotech, Buckinghamshire, UK) photometer. Samples were diluted 1:10 with distilled water. 500 µl of solution 1 of the kit was pipetted into cuvettes. 50 µl of diluted sample and 950 µl of distilled water were added and mixed. Absorbance at 340 nm (A1) was measured after 3 minutes. Reaction was started by adding 10 µl of suspension containing enzymes. After 15 min incubation at room temperature absorbance was again measured at 340 nm (A2). Blank values with all reagents except culture samples were taken at every measurement. Differences between A2 and A1 were determined. Absorbance difference of blank sample was substracted from absorbance differences of samples. D-glucose concentrations were calculated using a formula given by the manufacturer.

3.4.4.2 D-Galactose

The assay is based on the conversion of galactose to galactonic acid by galactose dehydrogenase with the formation of equimolar NADH. Absorbance of NADH is measured at 340 nm using an Ultrospec 2000 UV/Vis spectrophotometer (Amersham Pharmacia Biotech, Buckinghamshire, UK) photometer. The kit consists of solution 1 and solution 2. Samples were diluted 1:10 with distilled water. 100 µl of solution 1 was pipetted into plastic cuvettes. 50 µl of diluted sample was added, mixed and incubated for 20 min at room temperature. 500 µl of solution 2 and 975 µl distilled water were added. After 3 min, absorbance at 340 nm (A1) was measured. Reaction was started by adding 25 µl of enzyme suspension. After 20 min incubation at room temperature absorbance was again measured at 340 nm (A2). Blank values with all reagents except culture samples were taken at every measurement. Differences between A2 and A1 were determined. Absorbance difference of blank was substracted from absorbance differences of samples. D-galactose concentrations were calculated using a formula given in the manual.

3.4.4.3 D-Sorbitol

This colorimetric assay is based on the conversion of D-sorbitol to fructose by sorbitol dehydrogenase with the formation of equimolar NADH. Because equilibrium lies on the side of sorbitol, NADH is removed in a subsequent reaction, whereas formazan is formed. The absorption of formazan is measured at its maximum at 492 nm using an Ultrospec 2000 UV/Vis spectrophotometer (Amersham Pharmacia Biotech, Buckinghamshire, UK) photometer. Samples were diluted in 1:10 ratio with distilled water. 300 µl of solution 1, 100 µl of solution 2 and 3 respectively and 50 µl of

diluted samples were pipetted into plastic cuvettes. 950 µl distilled water was added and after 2 min absorbance (A1) at 492 nm was measured. Reaction was started by adding 25 µl of enzyme suspension. After 30 min incubation absorbance was again measured at 492 nm (A2). Blank values with all reagents except culture samples were taken at every measurement. Differences between A2 and A1 were determined. Absorbance difference of blank was substracted from absorbance differences of samples. D-sorbitol concentrations were calculated using formula provided with the kit.

3.4.4.4 L-Lactate

The assay is based on the conversion of L-lactate to L-alanine *via* pyruvate with formation of equimolar NADH. Absorbance of NADH is measured at 340 nm. Samples were diluted in 1:10 ratio with distilled water. 500 µl of solution 1, 100 µl solution 2 and 10 µl suspension 3 were pipetted into plastic cuvettes. 50 µl of diluted sample and 450 µl distilled water were added and mixed. After 5 min, absorbance at 340 nm (A1) was measured using an Ultrospec 2000 UV/Vis spectrophotometer (Amersham Pharmacia Biotech, Buckinghamshire, UK) photometer. Reaction was started by adding 10 µl of enzyme suspension. After 30 min incubation absorbance was again measured at 340 nm (A2). Blank values with all reagents except culture samples were taken. Differences between A2 and A1 were determined. Absorbance difference of blank was substracted from absorbance differences of samples. Again, L-lactate concentrations were calculated using the formula supplied with the kit.

3.4.5 Determination of urea concentration (HPLC)

The concentration of urea in the conditioned medium of primary human hepatocytes was determined using an HPLC-method [Clark *et al.*, 2007]. In this method, the urea present in the culture supernatant is converted to N-9H-xanthen-9-ylurea by derivatisation with xanthydrol (9H-xanthen-9-ol). After chromatographic separation on a Agilent 1100 equipped with a C18-column (Eclipse XBD RP-18 column (150 mm × 4.6 mm ID, 5 µm); Agilent Technologies, Weinheim), the derivative was detected using a fluorescence detector (λ_{ex} = 213 nm; λ_{em} = 308 nm) and quantified using a urea standard curve measured in the same way. Production rates were calculated by normalizing the values to the total volume of the supernatant and dividing this value by the number of seeded cells (one million per well of a 6-well plate).

3.5 Protein extraction from collected culture supernatants

The collected medium from the cultivations was centrifuged once (3000 x g at 4° C) to pellet dead cells and cell-debris. At this timepoint, protease inhibitors (complete, Roche, Mannheim, Germany) were added and an aliquot of 1 ml was removed for determination of physiological parameters as

depicted in section 3.4. The remainder was filtered through a 0.44 µm regenerated cellulose filter (VWR) to remove small debris. 4 ml of conditioned medium (corresponding to 2 million seeded cells in monolayer culture) was concentrated 20-fold using an ultrafiltration device with a molecular-weight cut-off of 10 kDa (Vivaspin4, Sartorius) for 30 minutes at 10000 x g at 4°C. Retenuates (50 - 100 µl) were rebuffered to an appropriate binding buffer for immunodepletion (see 3.6) by filling up the ultrafiltration device with the respective buffer and centrifugation as described before. This step was performed twice resulting in 99.9 % buffer-exchange. For the bioreactor samples, the volume of samples was between 6 and 8 ml, depending on the available material. For these samples, the first centrifugation step was performed twice after filling-up the device with the rest of the sample. After concentration, the protein content was estimated using a Bradford-based protein assay (Bio-Rad Protein Assay, Bio-Rad, München, Germany) [Bradford, 1976] and production rates were calculated by normalizing the values to the total volume of collected supernatant and dividing this value by the number of seeded cells (one million cells per well of a 6-well plate containing 2 ml of medium). For calculation of protein production rates from bioreactor samples, the same formula as for calculation of albumin production rates was used (see section 3.4.1).

3.6 Immunodepletion for the removal of high-abundant proteins

For specific depletion of high abundant proteins (albumin, transferrin, haptoglobin, antitrypsin), an antibody-based spin cartridge (Hu-6 Multiple Affinity Removal Spin Cartridge; Agilent, Böblingen) was used. Samples were rebuffered into binding buffer ("buffer A") by ultrafiltration as described in 3.5. The sample was loaded onto the column and spun at 100 x g for 1.5 minutes. 400 µl of buffer A were added and spun for 2.5 minutes. This step was conducted twice resulting in 1 ml of depleted sample. The bound fraction was eluted by pushing 2 ml of elution buffer ("buffer B") through the cartridge and re-equilibrated for the next sample with 4 ml of buffer A using a Luer-Lock syringe. Flow-through as well as bound fraction were rebuffered by ultrafiltration into 25 mM NH_4HCO_3 buffer and analyzed directly by SDS-PAGE or, alternatively, by LC-MALDI following in-solution digest of proteins using trypsin as endoprotease.

3.7 Gel electrophoresis (SDS-PAGE)

Before in-gel tryptic digestion, proteins were separated using one-dimensional discontinuous Tris-Glycine SDS-PAGE (sodium-dodecyl polyacrylamide gel-electrophoresis) under denaturing conditions [Laemmli, 1970]. Samples were denatured and reduced for 5 min at 95°C in 1x sample buffer (4 % SDS, 10 % Glycerol, 5 % ß-Mercaptoethanol, 0.02 % bromphenol blue in 125 mM Tris) and electrophoretic separation was performed at constant current (25mA per gel) on a 12.5 % separation

gel after focusing at 15 mA per gel on a 4 % stacking gel for 15 min (see table 3.1). For molecular weight estimation, 6 µl of prestained protein standard (Precision Plus Protein Standard Dual Color; Bio-Rad) was run simultaneously. Electrophoresis was stopped as the bromphenol blue front just run out of the gel. After electrophoresis, gels were stained either by colloidal Coomassie Blue (G-250) staining or by silver-ammonium staining (see section 3.8).

Table 3.1. Solutions for casting of SDS-PAGE gels

Separation gel (12.5%)		**Stacking gel (4%)**	
dH_2O	3.2 ml	dH_2O	3.05 ml
1.5 M Tris pH 8.8	2.5 ml	0.5 M Tris pH 6.8	1.5 ml
10 % SDS	100 µl	10 % SDS	50 µl
30 % acrylamide/bisacrylamide	4.1ml	30 % acrylamide/bisacrylamide	0.65 ml
TEMED	5 µl	TEMED	5 µl
10 % APS	50 µl	10 % APS	50 µl

3.8 Gel-staining

3.8.1 Colloidal Coomassie Blue staining

For colloidal Coomassie Blue staining of SDS-gels, a colloidal Coomassie-based (Coomassie Brilliant Blue G-250) staining solution (EZblue Gel Staining Reagent, Sigma-Aldrich, Steinheim) was used. After electrophoresis, gels were washed three times with water (10 minutes each) and incubated for 45 minutes to 1 hour in 20 ml EZblue reagent. Afterwards, gels were washed three to four times (or overnight) with water before scanning to minimize backround staining.

3.8.2 Silver-ammonium staining (MS-compatible)

For silver staining of SDS-gels, an silver-ammonium staining compatible with mass-spectrometry was used [Chevallet *et al.*, 2006]. Gels (containing 0.5% sodium thiosulfate as sensitivity enhancer) were impregnated 45 minutes in silver-ammonia solution (7 ml 1 M NaOH, 7.5 ml 5 M NH_4OH and 12 ml 1 M $AgNO_3$ add 500 ml with water) and developed in acidic developer (350 µM citric acid and 0.1% formalin in water) for about 10 minutes for visualization of protein bands while keeping backround staining as low as possible. Staining was stopped with 0.5% ethanolamine, 2% acetic acid in water for 1h at room temperature. For in-gel digest, excised gel-slices were washed twice with water and

destained with 15 mM potassium ferricyanide and 50 mM sodium thiosulfate in water for 5-10 min at room temperature (RT) prior to reduction and alkylation as described in the following.

3.9 In-gel digest

After staining of SDS-gels, bands were excised using a clean scalpel and transferred into a 0.5 ml Eppendorf tube. Slices were washed with 100 µl water and with 100 µl 50% acetonitrile (ACN; 2 x 5 min each; 37°C). Disulfide-bonds were reduced using 50 µl of 10 mM dithiothreitol (DTT; 1h, 60°C) and after washing with 100 µl of water, Carbamidomethylation of free cysteins was conducted with 50 µl of 55 mM iodoacetamid (IAA) for 1h at RT under light protection. Gel-slices were destained completely by washing with 100 µl 50 % ACN in water several times until the gel-slices were completely destained (for Coomassie staining; for silver-stained gels, the gel-slices were destained prior to the described protocol here; see section 3.8.2). The destained gel-bands were dehydrated with 100µl of pure ACN, 10µl of sequencing-grade modified trypsin (Promega; 12.5 ng/µl in 25 mM ABC) was added and incubated at room temperature until trypsin solution was soaked completely into the gel-slices. Remaining trypsin solution around the gel-slices was removed and the slices were covered with 25 mM ABC buffer followed by incubation overnight at 37°C for digestion. Trypsin-proteolysis was stopped by adding 10 % TFA to a final concentration of 0.2 %, mixed 1:1 with matrix (CHCA, 5 mg/ml in 70 % ACN + 0.1 % TFA) and immediately spotted onto a MALDI-target (384well Opti-TOF, Applied Biosystems).

For the analysis of whole gel lanes for the evaluation of prefractionation on different LC-MS platforms, 40 µg of sample was separated on a 12 % polyacrylamid gel and lanes were cut in 24 2x2 mm slices using a special device for gel-excision (gel-company, Tübingen). Slices were reduced and alkylated on an automated liquid handling device (MassPREP Station; Waters, Milford, MA) as described in [Weiss *et al.*, 2009]. In brief, gel pieces were washed three-times with 50 % ACN in 25 mM ABC. Cysteine residues were reduced with 10 mM DTT at 57 °C for 30 minutes and alkylated in 55 mM IAA at room temperature for 20 minutes. After dehydration with ACN, proteins were digested in gel with 10 µL of 12.5 ng/µL sequencing-grade modified trypsin (Promega, Madison, WI) in 25 mM ABC overnight at 37 °C. Tryptic peptides were extracted firstly with 60 % ACN in 0.1 % formic acid (for ESI-MS) or with 60 % ACN in 1 % TFA (for MALDI-MS). Then, a second extraction step with 100 % ACN was performed. For extractions, samples were vigorously shaken for 1 hour on an orbital shaker at 1200 rpm at room temperature. After extraction, supernatants were pooled, the volume was reduced to 5 µl in a speed-vac and the resulting sample was analysed by nanoLC-MS/MS (nanoliquid chromatography coupled to tandem mass spectrometry). The procedure was performed identically in triplicate to allow comparison of the three different LC-MS platforms.

3.10 In-solution digest

Proteins were thermally denatured for 15 minutes at 90 °C and disulfide bonds were reduced using 5 mM DTT for 30 minutes at 60 °C. Carbamidomethylation of free cysteins was performed in 15 mM IAA for 45 minutes at RT under light protection. Digestion was performed overnight with sequencing grade-modified trypsin (Promega, Madison, WI, USA) applying a trypsin to protein ratio of 1:50. After proteolysis the trypsin was inactivated by addition of TFA (final concentration 0.1%) and another ultrafiltration step (Amicon 0.5, 10 kDa MWCO, Millipore) was performed to remove the trypsin and remaining undigested proteins. The filtrate was evaporated to dryness in a speed-vac (Jouan RC 10.22, Saint-Nazaire, France) and resuspended in 2 % ACN + 0.05 % TFA for LC-MALDI analysis.

For the analyses performed together with the LSMBO (University of Strasbourg), the denaturation was performed at 95°C for 10 minutes in 25 mM ABC containing 1 % sodium desoxycholic acid (DOC) as a detergent maximizing denaturation as well as digestion of the polypeptide chains. Reduction, alkylation and proteolysis were performed as described above. Afterwards, the DOC was removed by adding TFA (or FA for the ESI-sample) to a final concentration of 0.2 %. Under these (acidic) conditions, the DOC precipitated and was removed by centrifugation for 5 minutes at 14.000 x g. The supernatant was then used for LC-MS analysis after ultrafiltration as described above.

3.11 Liquid-chromatography and fraction collection

The HPLC system used in this study was a biocompatible version of an Ultimate 3000 nano LC system consisting of a solvent degassing unit (SRD-3600), a dual low-pressure gradient pump (DGP-3600MB), a column oven with integrated 1:1000 splitting cassette (FLM-3100), a variable wavelength detector with a 3 nl z-shaped flow-cell (VWD-3400) and a thermostated autosampler (WPS-3000T/TB; all from Dionex, Sunnyvale, CA). Peptides were separated on a C18 column (PepMap, 75 µm i.d., 15 cm, 3 µm, 100 Å) at a flow rate of 300 nl/min (after splitting) in combination with a C18 precolumn (PepMap100, 300 µm i.d., 5 mm, 5 µm, 100 Å) at a flow rate of 30 µl/min. Eluent A consisted of 0.05 % TFA in water and eluent B was 90 % acetonitrile in water containing 0.04 % TFA. The UV-chromatogram was recorded at a wavelength of 214 nm. After loading the samples onto the precolumn and desalting for 5 minutes with 0.1 % TFA in water at 30 µl per minute, the precolumn was switched into the gradient flow and peptides were eluted employing a gradient from 10 % (fast rise from 5 % to 10 % in one minute) to 45 % Eluent B in 90 minutes (liquid digests). For the separation of peptides originating from in-gel digests, the employed gradient was 15 % to 55 % in 30 minutes. The column was then washed for 5 minutes with 95 % Eluent B and re-equilibrated for 15 minutes to 5 % Eluent B for the next analysis.

Fraction collection during chromatography was performed with a Probot microfraction collector (Dionex). The MALDI matrix used was α-Cyano-4-hydroxycinnamic acid (CHCA; Fluka Chemistry AG, Buchs, Switzerland) and was continuously added to the effluent at a flow rate of 1.2 µl per minute at a concentration of 3 mg/ml in 70% ACN containing 0.1 % TFA. A signal was sent to the Probot at minute 13 of the LC run to start fractionation. Fractions were collected every 12 sec for 90 minutes generating 450 spots per run. Fractions were spotted directly on a blank Opti-TOF LC/MALDI plate (Applied Biosystems, Darmstadt, Germany) using a 50 x 32 geometry (1600 spots per plate).

3.12 MALDI mass-spectrometry

MS and MS/MS analysis was performed on an Applied Biosystems 4800 MALDI TOF/TOF analyzer (Applied Biosystems, Darmstadt, Germany). Before each MALDI measurement and also before each MS run, the analyzer was externally calibrated using the 4700 Proteomics Analyzer Calibration Mixture (4700 proteomics analyzer mass standards kit, Applied Biosystems) resulting in a mass accuracy of 50 ppm. Furthermore, Glu^1-Fibrinopeptide B (1570.677 *m/z*) was added to the matrix used for LC-MALDI at a concentration of 25 nM for internal calibration of each MS spectrum to improve the average mass accuracy to 15 ppm. If internal calibration failed due to presence of high intensities of sample peptides leading to peak suppression of Glu^1-Fibrinopeptide B, the default calibration was used (i.e. 50 ppm).

MS-data was generated in positive reflector-mode in a mass range of 700-4000 m/z with 50 shots per subspectrum accumulating 1000 shots in total. An exclusion list was written to avoid fragmentation of the internal calibrant as well as common Matrix-ions. Laser frequency used was 200 Hz (at 355nm; Nd/YAG-laser) and laser intensity was adjusted individually (normally between 3100 and 3500). However, for the comparative analyses of bioreactor samples, the laser intensity was fixed at 3400 for all measurements. A maximum of 15 precursor ions per fraction were automatically selected by the software (4000 series explorer software, version 3.5.1, Applied Biosystems) for MS/MS-analysis. For the comparison of MALDI- and ESI-MS, the 6 most intense precursors were analysed by MS/MS both for the liquid and the in-gel digests. Criteria for a peak to be selected as a precursor were: minimum signal-to-noise ratio 35; precursor mass tolerance between spots 100 ppm; minimum chromatogram peak width of two fractions (i.e. spots). For acquisition of MS/MS spectra, 100 shots were fired per subspectrum with 3000 shots in total or after reaching a signal-to-noise ratio of 35 for at least 10 peaks in the MS/MS spectrum. Peptides were fragmented by 1kV collisions via CID (air as collision gas). External calibration was performed using fragments of Glu^1-Fibrinopeptide from the 4700 proteomics analyzer mass standards kit (Applied Biosystems) prior to each MS/MS run.

3.13 Analyses performed at LSMBO, CNRS; University of Strasbourg

3.13.1 Analyses using an ion trap instrument

NanoLC-MS/MS analyses were performed using an Agilent 1100 series nanoLC-Chip/MS system (Agilent Technologies, Palo Alto, USA) coupled to an amaZon ion trap (BrukerDaltonics, Bremen, Germany). The system was fully controlled by HyStar 3.2 (BrukerDaltonics). The chip contained a Zorbax 300SB-C18 column (43 mm×75 µm, 5 µm particle size) and a Zorbax 300SB-C18 enrichment column (40 nl, 5 µm particle size). The solvent system consisted of 2 % acetonitrile, 0.1 % formic acid in water (Eluent A) and 2 % water, 0.1 % formic acid in acetonitrile (Eluent B).

3 µl of each sample were loaded onto the enrichment column at a flow rate set to 3.75 µl per minute with eluent A. Elution was performed at a flow rate of 300 nl per minute with a 8–40 % linear gradient (eluent B) in 30 minutes (in gel) or 45 minutes (liquid digest), followed by a 4 minute washing step at 70 % of eluent B before reconditioning the column at 8 % of eluent B.

MS spectra were acquired with the following settings: source temperature was set to 135°C while cone gas flow was at 3 liter per minute. The nanoelectrospray voltage was optimized to −1850 V. The MS spectra were acquired in the positive ion mode on the mass range 250 to 1500 m/z using the standard enhanced resolution at a scan rate of 8.1 m/z per second. The ion charge control was fixed at 200,000 with a maximum accumulation time of 200 milliseconds. For tandem MS experiments, the system was operated with automatic switching between MS and MS/MS modes. The 6 most abundant peptides were selected on each MS spectrum for further isolation and fragmentation with a preference for doubly charged ions (absolute threshold of 5000, relative threshold 5 %). The MS/MS spectra were acquired in the mass range from 100 to 2000 m/z. The ion charge control was fixed at 300000 and 2 scans were averaged to obtain a MS/MS spectrum. Ions were excluded after acquisition of one MS/MS spectrum and the exclusion was released after 0.3 minutes. The smart parameters setting option was used for the selected precursor ions.

3.13.2 Analyses using a quadropole-time of flight (Q-TOF) instrument

NanoLC-MS/MS were performed using a nanoACQUITY Ultra-Performance-LC system (Waters, Milford, MA, USA) coupled to a MaXis 4G Q-TOF mass spectrometer (BrukerDaltonics, Bremen, Germany). The system was fully controlled by HyStar 3.2 (BrukerDaltonics). The UPLC system was equipped with a Symmetry C18 precolumn (20 x 0.18 mm, 5 µm particle size, Waters, Milford, USA) and an ACQUITY UPLC® BEH130 C18 column (75 µm × 200 mm, 1.7 µm particle size, Waters). The

solvent system consisted of 0.1 % formic acid in water (eluent A) and 0.1 % formic acid in ACN (eluent B).

3 µL of each sample were trapped during 1 min at 15 µl per minute with 99 % of A and 1 % of B. Elution was performed at 60 °C at a flow rate of 450 nl per minute, using a 6-35 % gradient of B for 21 minutes (in gel) or a 6-43.5 % gradient of B for 35 minutes (liquid sample) followed by a fast rise to 90 % of B and back to 1 % B.

The MaXis was operating in positive mode, with following settings: source temperature was set to 150°C while dry gas flow was at 4 liter per minute. The nanoelectrospray voltage was optimized to −5000 V. Mass calibration of the TOF was achieved using Tuning Mix (Agilent) in the mass range of 322-2722 m/z. Online correction of this calibration was performed with methylstearate ($[M+H]^+$ 299.2945 m/z) and hexakis(2,2,3,3,-tetrafluoropropoxy)phosphazine ($[M+H]^+$ 922.0098 m/z) as the lock-mass.

For tandem MS experiments, the system was operated with automatic switching between MS and MS/MS modes in the range of 50-2200 m/z (MS acquisition time of 0.68 s, MS/MS acquisition time between 0.68 (intensity > 26000) and 4.76 s (intensity <1000). The 4 (in gel) or 5 (liquid digest) most abundant peptides (absolute intensity threshold of 1000), preferably doubly, triply and quadruply charged ions, were selected from each MS spectrum for further isolation and CID fragmentation using argon as collision gas. Ions were excluded after acquisition of one MS/MS spectrum and the exclusion was released after 0.6 (in gel) or 0.8 minutes (liquid digest), respectively.

3.14 Database search for protein identification

The peak-lists were searched against a SwissProt-derived (January 2011) combined target-decoy database (containing 20254 target sequences plus the same number of reversed decoy sequences) of human proteins including common contaminants (human keratins and porcine trypsin). It was generated using the database generation toolbox from the laboratory of bio-organic mass-spectrometry of the University of Strasbourg (https://msda.u-strasbg.fr/index.php). Peak lists were sent to a local Mascot server (version 2.1, Matrix science, London, England) using the GPS explorer software (version 3.6, Applied Biosystems, Darmstadt, Germany) for the measurements on the MALDI instrument. Mascot generic files (.mgf) generated during analyses performed on the ESI instruments in Strasbourg were sent to the same server using Mascot deamon (version 2.0). No differences in identifications were observed when using these two different approaches for submission of peak-lists using a test dataset. Search parameters applied were: one missed cleavage

by trypsin. Variable modifications allowed were oxidation of Methionine (+16 Da) and carbamidomethylation of Cysteine (+57 Da).

Mass accuracy settings for the different instruments were as follows:

MALDI: 50 ppm for precursor ions, 0.3 Da for the fragment ions

Ion-trap: 0.25 Da for precursor as well as for fragment ions

QTOF: 5 ppm for precursor ions, 0.02 Da for fragment ions

3.15 Reprocessing of Mascot search results

After database search, the Mascot result files (.dat) were imported into Scaffold 3 software (Proteome Software Inc.) and the identified proteins were filtered both at the 1- and 2-peptide level by adjusting the Mascot "delta score" (ion minus identity score). For proteins identified by 2 peptides and more, the delta score had to be > 0, which means that the ion score had to be above the minimum identity threshold at 95% probability. For identifications with one peptide only, the filtering was more stringent (normally delta score > 5) thus minimizing false positives by only accepting high quality MS/MS spectra. All identifications above the (lower) threshold for the 2-peptide level (i.e. delta score > 0) were exported from Scaffold. Subsequently, all identifications with only one peptide and with scores below the more stringent threshold were removed in Excel. Using this approach together with a combined target-decoy database search [Elias and Gygi, 2007], the false discovery rate (FDR) could be controlled and was kept below 2 % (about 1 decoy hit in 100 identifications) for all measurements. However, for the comparison of different donors and for the immunodepletion experiment, the FDR was reduced to 0 % which means that no decoy-hit was tolerated in the final protein list.

3.16 Annotation of identified proteins

For functional annotation enrichment analysis of identified proteins, the **D**atabase for **A**nnotation, **V**isualization and **I**ntegrated **D**iscovery (DAVID, version 6.7; http://david.abcc.ncifcrf.gov/) was used [Huang da *et al.*, 2009a; Huang da *et al.*, 2009b]. Proteins were examined for the enrichment of annotations in the Panther database [Thomas *et al.*, 2003; Mi and Thomas, 2009] compared to the whole list of proteins known for *Homo sapiens* as the backround list. The information about the presence of a signal peptide required for secretion *via* classical secretion pathways was also extracted from Uniprot using DAVID. The subcellular location of identified proteins was retrieved from Uniprot (http://www.uniprot.org/) [2009].

3.17 Prediction of non-classically secreted proteins

To predict if identified proteins were secreted *via* non-classical secretion pathways, proteins not annotated to have a signal peptide in DAVID were processed using the web-based software SecretomeP (version 2.0). The algorithm underlying the prediction has been explained in detail in [Bendtsen *et al.*, 2004] but generally relies on the common properties secreted proteins are thought to share based on their amino acid sequence. All proteins with a NN-score above 0.5 were accepted as possibly secreted as proposed in the online manual.

SecretomeP is available under: http://www.cbs.dtu.dk/services/SecretomeP/

3.18 Quantification by peptide hit counting

Differentially expressed proteins were identified by the number of peptides leading to identification of a specific protein. This was done by the help of Scaffold, which applies a statistical test (one-way ANOVA in this case) to detect significant differences in the number of peptides assigned to a protein between groups (i.e. 2 treated and 1 untreated group) compared to the differences observed within a group (i.e. three replicates). The ANOVA test delivers a *p*-value and in this study, only proteins with a *p*-value < 0.05 were accepted as differentially expressed. Prior to the ANOVA test, peptide hits in each sample were normalized to the total amount of peptide hits in each sample by averaging the peptide counts across all groups, and then multiplying the peptide counts in each sample or group by the average divided by the individual sample or group sum. For example:

Two samples: A and B

Each biosample has three proteins: One, Two and Three

Protein One has 12 peptides in sample A and 8 peptides in sample B

Protein Two has 6 peptides in sample A and 3 peptides in sample B

Protein Three has 4 peptides in sample A and 3 peptides in sample B

Scaffold would normalize as follows:

Sample A has 22 peptides, sample B has 14 peptides, the average of both is 18

Scaffold would multiply all of the protein peptide counts in sample A by (18/22), and all of the peptide counts in sample B by (18/14).

3.19 Principal component analysis (PCA)

Principal component analysis to detect and visualize significant changes in protein expression by peptide counts was performed using Matlab software (version R2006a, The MathWorks). Normalized peptide counts were auto-scaled for PCA by dividing the peptide counts of one protein by the standard deviation of all peptide counts for that protein in all replicates of all groups. PCA is a type of multivariate statistics reducing the dimensions within a dataset to a set of independent and orthogonal variables, the “principal components”. The number of principal components is less or equal to the original number of variables in the underlying dataset, with the first component explaining most of the variance explaining the differences in the dataset.

4. Results

4.1 Establishment of an analytical strategy for hepatocyte secretome analysis

4.1.1 Optimizing the cultivation for efficient secretome analysis

Before sample collection for secretome analysis, the FCS-supplemented medium had to be removed and replaced by serum-free medium. This was done because the supplemented proteins mask the proteins secreted by cultured hepatocytes. The removal of FCS in standard monolayer cultures could be achieved fairly simple by washing the cells with serum-free medium. However, the removal of serum proteins from the bioreactor used in this project turned out to be not that easy, which is reported below.

4.1.1.1 FCS-free monolayer cultivation

The number of wash-cycles required to minimize the amount of FCS in the cell culture flasks was determined. Since PHH were delivered in FCS-supplemented medium and maintained in medium containing 10 % FCS for about 24h before any experiment in order to recover from “transport stress”, they had to be washed several times with serum-free medium. Thus, proteins originating from FCS were withdrawn.

After 24h of equilibration, primary human hepatocytes (PHH) were washed four times with serum-free medium. The cells were cultivated for 96h (4 days) in serum-free medium without medium exchange. The medium of washing steps and supernatants from the cultivation was concentrated by ultrafiltration and subjected to SDS-PAGE (see Figure 4.1). As shown in Figure 4.1 a and c, the protein concentration decreased rapidly within 2 washing steps and was further diminished by a third wash to a protein concentration already present in fresh medium (HM_0). Obviously, four wash-cycles were sufficient to minimize the amount of proteins from FCS leaving human transferrin (supplemented in the medium) as the only proteinaceous material detected by coomassie blue staining in the supernatant and thus allowing secretome analysis of primary human hepatocytes in monolayer culture.

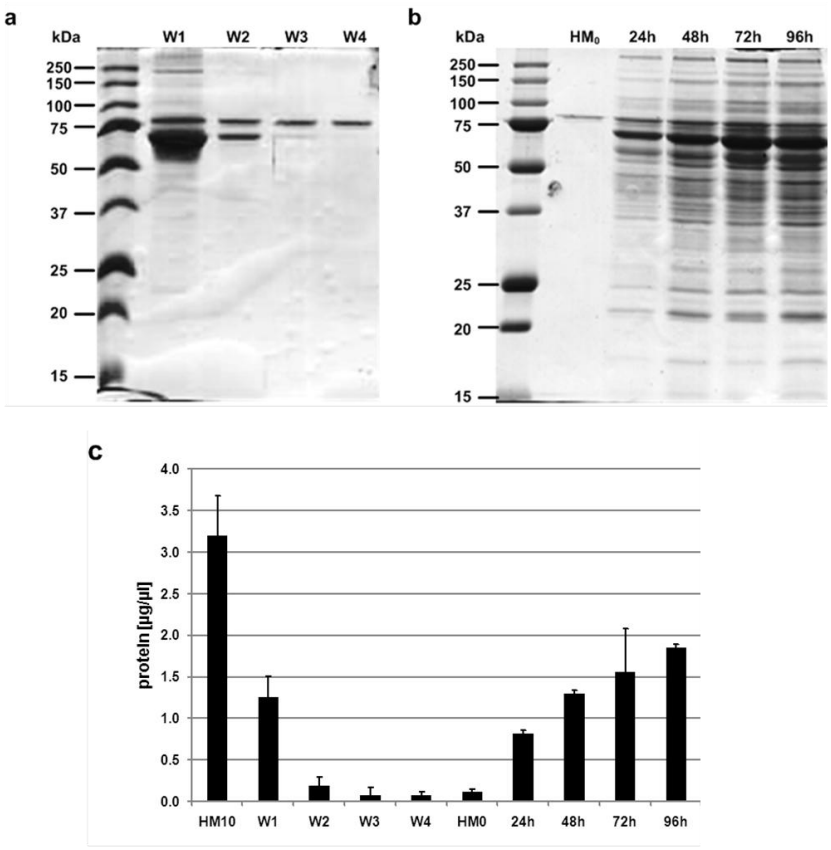

Figure 4.1. SDS-PAGE of wash-cycles (a) and supernatants (b) of PHH in conventional 2D-culture for removal of proteins originating from fetal calf serum (FCS). Cells cultivated in Heparmed +10% FCS (HM_{10}) were washed four times (W1-W4) with serum-free medium (HM_0) and cultivated for 96h in HM_0. Supernatants were concentrated by ultrafiltration (10.000 MWCO) and 7.5µl (a) or 10µl (b) were subjected to SDS-PAGE. Total protein content in the concentrated samples (c) as determined *via* Bradford-assay. Error bars indicate standard deviation of triplicate measurements (n=3).

4.1.1.2 FCS-free bioreactor cultivation

Several runs of "jelly-fish"-bioreactors were performed using FCS-supplemented medium for inoculation of cell-suspension and initial cultivation to ensure best survival of the primary hepatocytes. At day 9, the cultivation medium was replaced by serum-free medium to allow analysis of secreted proteins. The cultivation medium was concentrated by ultrafiltration and after determining the protein concentration, the concentrated samples were subjected to SDS-PAGE.

In Figure 4.2 a, the total protein concentration of bioreactor samples during a cultivation employing FCS is depicted. It is obvious that the protein concentration at the first days was entirely dominated by the supplemented FCS (2.2 µg/µl). It has to be mentioned, that the amount of FCS in the medium was already lowered from 10 % to 2.5 % at this time. After switching to serum-free conditions on day 9, the protein concentration decreased rapidly to 1.8 µg/µl at day 10 and to 0.27 µg/µl at day 11. Afterwards, the protein concentration further decreased and was estimated to 0.18 µg/µl at day 12,

0.14 µg/µl at day 13 and 0.11 µg/µl at day 14. During the final phase of cultivation (day 15 to 19), the protein concentration remained at 0.06 µg/µl. The elevated value at day 16 is most probably attributable to the fact that only little effluent was produced at day 16 and a high concentration of Protease Inhibitors was present in the sample. The Protease Inhibitors were filled into the collection bottles prior to collection as 25-fold stock solution to prevent unspecific proteolysis and may have affected the Bradford assay.

The absence of proteins in the sample of day 16 was confirmed by SDS-PAGE carried out with the concentrated samples (see Fig. 4.2 b). The electrophoresis of samples from day 3 to 11 proves the domination of proteins by bovine albumin accounting for more than 60 % of total protein in serum. Albumin has a molecular weight of about 67 kDa and there was a very intense band visible in the region of the gel where proteins of this size should migrate. This band predominated until the FCS was withdrawn from the culture at day 9. At day 10, the concentration of FCS was still quite high, even though there was already a decrease in the intensity for mostly all of the bands. After day 11, only three bands could be detected by coomassie staining. These proteins were, as confirmed by MALDI-TOF/TOF analysis of in-gel digests at day 13 and 17 from the top to the bottom: human transferrin (supplemented in the medium), bovine albumin and human liver carboxylesterase. By applying a more sensitive method for detection, namely silver-ammonium staining (see Fig. 4.2 b, small picture), many more bands could be detected in the samples from day 13 to 19, but the intensity of the bands is decreasing constantly. This decrease is most probably due to a long-lasting wash-out of proteins from FCS still residing in the bioreactor circuit.

LC-MALDI analysis of samples before (day 2) and after (day 14) withdrawing of FCS strengthened this assumption and showed that it is hardly possible to identify human proteins upon FCS addition because the bovine proteins remain in the bioreactor for many days (see Table 4.1).

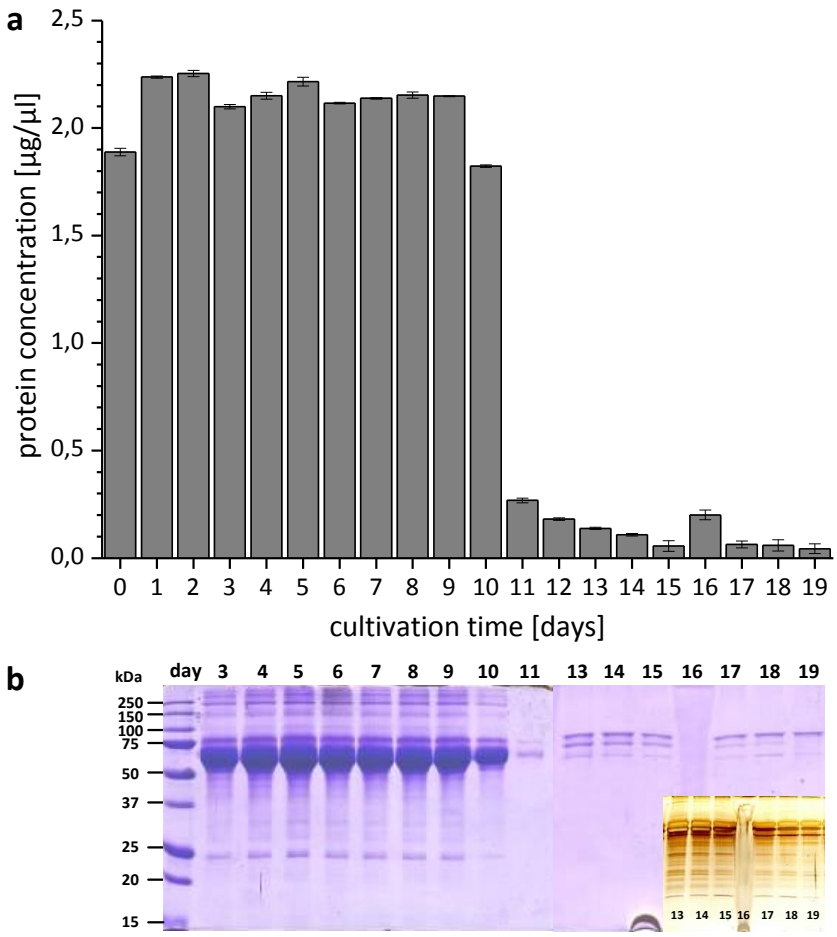

Figure 4.2. Wash-out of FCS from a 3D bioreactor containing primary human hepatocytes. Inoculation and cultivation until day 9 was performed in medium containing 2.5 % FCS. At day 9, the medium was changed for serum-free cultivation. Daily samples (effluent) were concentrated by ultrafiltration and protein concentration was determined *via* Bradford-assay (a). SDS-PAGE of the same samples starting at day 3 (b). Shown are gels stained with Coomassie Blue and silver-ammonium (small picture). 1 µl of concentrated sample was loaded from day 3 to 11, while 10 µl were loaded from day 13 to 19.

On day 2, 16 human proteins could be identified and the supplemented human transferrin was identified by only 2 peptides, while bovine transferrin was identified by 16 peptides as one of 13 bovine proteins identified in the sample. Only 3 peptides of human albumin where identified in contrast to 20 peptides that were found for the bovine albumin. Since human transferrin is present as a supplement in the cultivation medium and was identified consistently with more than 35 peptides in monolayer cultures, this strongly underlines masking of human proteins by their bovine equivalents. On day 14, the situation was slightly better but still unsatisfactory. Human transferrin was identified with 41 unique peptides and also human albumin was identified by 9 peptides, but bovine transferrin and albumin were still identified with 23 and 22 peptides, respectively. This implies, again, that the FCS leaves the bioreactor very slowly, especially the bovine albumin as the

predominant protein in fetal calf serum because many more peptides were assigned to the bovine proteins.

Table 4.1. LC-MALDI analysis of bioreactor samples before (day 2) and after (day 14) withdrawal of FCS. Number of unique peptides leading to the identification of human or bovine transferrin and albumin in the culture medium of 3D cultures of PHH as well as the total number of identified proteins.

	day 2		day 14	
	human	**bovine**	**human**	**bovine**
transferrin	2	16	41	22
albumin	3	20	9	23
identified proteins	16	13	6	11

Therefore, completely serum-free bioreactor cultivation was needed and it has been shown by the scientists who developed the 3D-bioreactor used in this study, that it is possible to inoculate primary hepatocytes and run the bioreactor under serum-free conditions without influencing the performance of the hepatocytes (Kathrin Zeilinger, personal communication). Indeed, it has been shown that cells cultivated in a serum-free environment were not inferior to hepatocytes cultivated in medium supplemented with bovine serum regarding viability and maintenance of liver-specific functions like expression of cytochrome P450 enzymes.

Finally, samples from serum-free bioreactor cultivations were available for the analysis of extracellular proteins from 3D-bioreactor cultures of primary human hepatocytes. The results are reported in section 4.4.

4.1.2 Removal of high-abundant proteins by immunodepletion

The SDS-PAGE of proteins collected in the supernatant of FCS-free cultivated hepatocytes (see Figure 4.1 b), especially in the lanes where supernatants after 24h and 48h are shown, indicates that there are few bands showing very high intensities compared to the intensities of the many other bands detected by staining with Coomassie blue. These few proteins emerge in high concentrations, while most other proteins are present at much lower concentrations in the sample. The difference in concentrations of studied analytes in biological samples often spans several orders of magnitude. In order to reduce the dynamic range within the samples, albumin, transferrin, haptoglobin and antitrypsin, four proteins that are present at high concentrations in the culture supernatant were

removed by immunodepletion. For this purpose, a commercially available antibody-based spin-cartridge was used, originally designed for the proteomic analysis of human serum. Because hepatocytes produce many of the proteins present in human serum, this technique could also be applied to the analysis of the hepatocyte secretome. The procedure is quite fast with approximately 20 minutes needed for the depletion of one sample including re-equilibration of the spin cartridge. The efficiency of the method is demonstrated by the fact that none of the four depleted proteins mentioned above was identified by LC-MALDI after depletion. Additionally, while in the undepleted sample 58 proteins were identified with 2 or more peptides (116 in total), the number of identified proteins in the depleted sample increased to 201, with 118 of them identified by 2 peptides or more (see figure 4.3 b). By applying a filtering approach to control the false discovery rate (FDR; see 3.14 for detailed description), the number of identifications increased from 74 to 134 proteins after immunodepletion. 17 proteins were identified in the bound fraction including the proteins targeted for depletion. On the other hand, eight of the proteins identified before depletion could not be found after depletion, additionally to the four highly-abundant proteins mentioned above. These eight proteins were: GSH-S-transferase, Cofilin-1, kinesin-like protein KIF15, isocitrate dehydrogenase, heat shock protein 60, galectin-1, complement factor H, and nucleotide diphosphate kinase B.

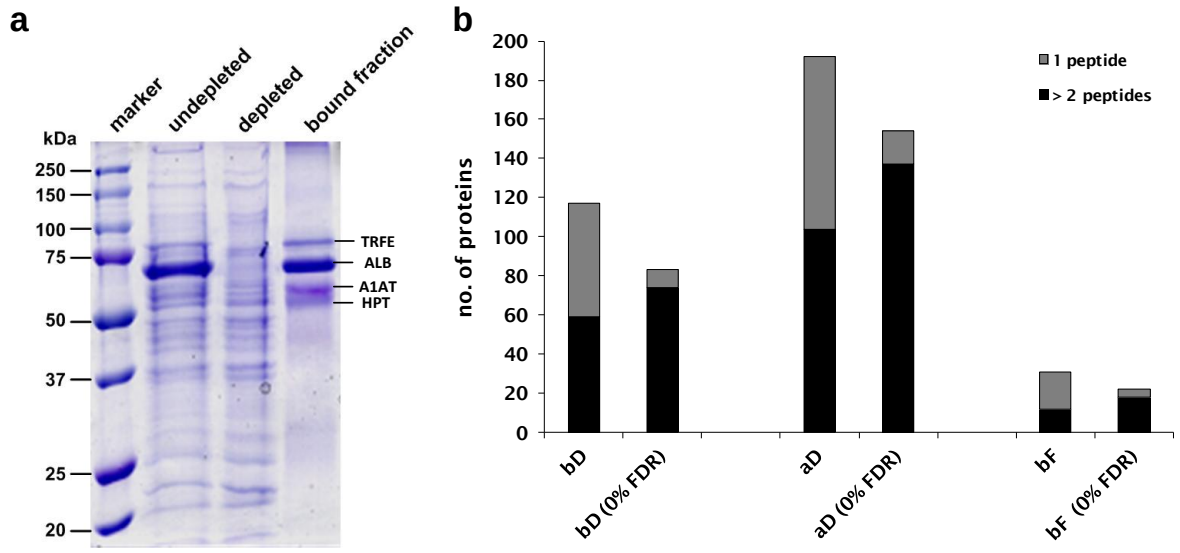

Figure 4.3. Immunodepletion of culture supernatants of primary human hepatocytes for the removal of high-abundant proteins. a, SDS-PAGE (coomassie staining) of undepleted and depleted samples of primary human hepatocytes in conventional 2D-culture as well as proteins depleted by the immunoaffinity column (bound fraction; TRFE=transferrin, ALB=albumin, A1AT=alpha-1-antitrypsin, HPT=haptoglobin). Cells were cultivated in serum-free medium for 96h; b, number of proteins identified with one or at least two peptides before (bD) and after depletion (aD) as well as in the bound fraction (bF), shown are results before and after applying a target-decoy search strategy and subsequent stringent filtering resulting in a false discovery rate (FDR) of 0%.

4.1.3 Gradient optimization for liquid-chromatographic separation of peptides

For the separation of tryptic peptides, the employed solvent gradient had to be determined. For this purpose, a commercially available mixture of peptides from tryptic digest of six standard proteins (bovine serum albumin, transferrin and cytochrome C; beta-galactosidase from *E. coli;* chicken lysozyme and alcohol dehydrogenase from Yeast) was separated applying different solvent compositions at the beginning and the end of the gradient. Solvent A was water containing 0.05 % TFA and solvent B consisted of 90 % ACN in water containing 0.04 % TFA. For the separation of the protein mixture standard, the gradient had a length of 60 minutes, starting at minute 5, the timepoint when the precolumn was switched into the flow of the separation column. After the gradient, the column was washed with 95 % of solvent B for 5 minutes and reconditioned to 5 % solvent B for 15 minutes. First, the endpoint of the gradient was determined at which all of the peptides had eluted from the column. Then, this endpoint was fixed and the starting values for solvent B were varied to spread the separation window as far as possible regarding retention time. A summary of the optimization is shown as the recorded UV-chromatograms in Figure 4.4.

The separation in reversed-phase HPLC is based on hydrophobicity of the analytes, i.e peptides in this special case. The more hydrophobic a peptide is, the later it elutes from the column if a gradient with increasing amount of organic solvent is used over time. At a certain percentage of organic solvent, all of the peptides should have eluted from the column. The determination of this percentage was the aim of the first step of optimization as shown in Figure 4.4 a. While the starting point was kept fixed at 5 % solvent B, the endpoint of the gradient was changed from 30 % B to 65 % B. In between, it was gradually increased by 5 %, but only the most informative elution profiles are given in Figure 4.4a.

When the gradient reached 35 % B (Fig. 4.4a, black chromatogram), there were many peptides not yet eluted from the column resulting in a big peak after 72 minutes. This is the time when analytes eluted during the wash of the column (starting at minute 65.1) reach the detector and is called the “dwell-time” (In this case the system has a dwell-time of 6.5 minutes). If the percentage of solvent B is increased to 40 % B (Fig. 4.4a, red chromatogram), there is still a quite large peak eluting at minute 72, indicating that there are still peptides not eluting from the column by going up to 40 % of solvent B. Finally, when the gradient is further increased to 45 % B (Fig. 4.4a, blue chromatogram), there is only a small peak appearing at minute 72, showing that nearly all of the peptides are eluted from the column using this endpoint (45 % solvent B, corresponding to about 40.5 % ACN).

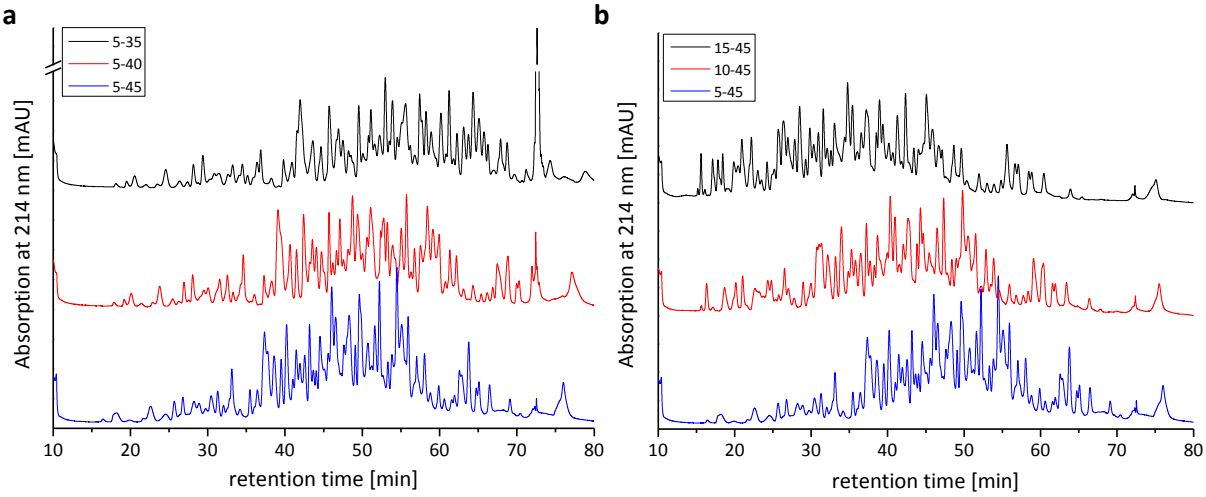

Figure 4.4. Optimization of solvent gradients for liquid-chromatographic separation of tryptic peptides. For optimization, a standard containing a mixture of peptides from a digest of six standard proteins (bovine serum albumin, transferrin and cytochrome C; beta-galactosidase from *E. coli;* chicken lysozyme and alcohol dehydrogenase from Yeast) was used. Shown are UV-chromatograms recorded at a wavelength of 214 nm for determination of the optimal solvent composition during separation, i.e. endpoint (a) and starting point (b) of the gradient. The gradient started after 5 minutes and the length was 60 minutes. Legends indicate the percentage of solvent B (90% ACN, 0.04 % TFA) employed during the gradient.

Increasing the percentage of solvent B at the end of the gradient resulted in a decrease of the wash peak and a shift of the whole chromatogram to earlier retention times. Further increase of the endpoint (55 %, 60% and 65%, data not shown) did not led to a decrease of this peak but to a shift of the whole elution profile towards earlier retention times what was not desirable. The peptides should elute over the whole time of the gradient to maximize separation.

After determining the minimum amount of solvent B needed for the elution of peptides, the starting composition of the gradient was optimized. Therefore, the endpoint was kept fixed at 45 % solvent B and the starting value was gradually increased from 5 % to 15 % solvent B (see Fig. 4.4b). As it becomes obvious from the blue chromatogram in Figure 4.4b, only few peptides eluted before minute 25 if the gradient started at 5 % solvent B and the latest peaks are observed until minute 70 of the chromatogram. By increasing the starting point of the gradient to 10 % B, the elution of the first peaks could be relocated to minute 16 to 17 of the chromatogram, but peaks detected at the end of the chromatogram eluted earlier, namely until minute 65. When the starting point was further increased to 15 % solvent B, there was no more shifting of the elution profile to earlier retention times but the early peaks eluted more condensed as with 10 % B as starting composition. Furthermore, the biggest part of the more hydrophobic peptides eluted until minute 60, which was not desired as mentioned above.

Finally, the optimal gradient for the separation of tryptic peptides was determined as 10 to 45 % solvent B, which corresponds to a percentage of ACN of 9 to 40.5 %. This gradient was used to separate secretome samples, but the time of separation was extended to 90 minutes taking into account the increased complexity of real samples after liquid digestion of proteins present in the conditioned medium from primary human hepatocytes.

4.2 Physiological characterization

The conditioned media of primary human hepatocytes were analyzed in order to investigate the performance of the primary cells regarding survival, liver specific functions and protein production during cultivation. The standard monolayer culture should serve as a control for the secretome analysis of samples from the bioreactor. Because intracellular contaminants could be released by cell death disturbing the analysis of truly secreted proteins, it was tested how much intracellular enzymes were released into the culture medium as an indicator for viability or cell-death, respectively. Additionally, the common anti-inflammatory drug Diclofenac was applied at two different concentrations as a model drug to study drug-induced hepatotoxicity.

4.2.1 Characterisation of monolayer cultures

Primary human hepatocytes were maintained for four days in monolayer culture and exposed to two concentrations of the anti-inflammatory drug diclofenac (6.4 µM and 100 µM). Physiological parameters like carbohydrate consumption and glucose or lactate production were determined to monitor the general energy metabolism of the cells. Furthermore, the release of LDH and AST was analyzed as a parameter reflecting cell viability or cell death, respectively. Albumin as well as urea production rates were determined as hepatocyte-specific parameters. Finally, protein production was calculated from the estimated protein concentrations in concentrated culture supernatants. At first, all rates were calculated as rates per day per million seeded cells. All values except the rates illustrating the carbohydrate metabolism were additionally normalized to enzyme release and total protein production with both having been normalized to production and release per day per million seeded cells. Thus, cell-death occurring during cultivation was taken into account for indirect, *a priori* estimation of contamination of the secretome by intracellular proteins. In the special case of urea production, normalization was achieved by division by the sorbitol uptake rate which has been shown to be a reliable parameter of hepatocyte viability [Gerlach *et al.*, 2010].

Figure 4.5 illustrates the carbohydrate consumption and lactate production during standard monolayer cultivation of primary human hepatocytes.

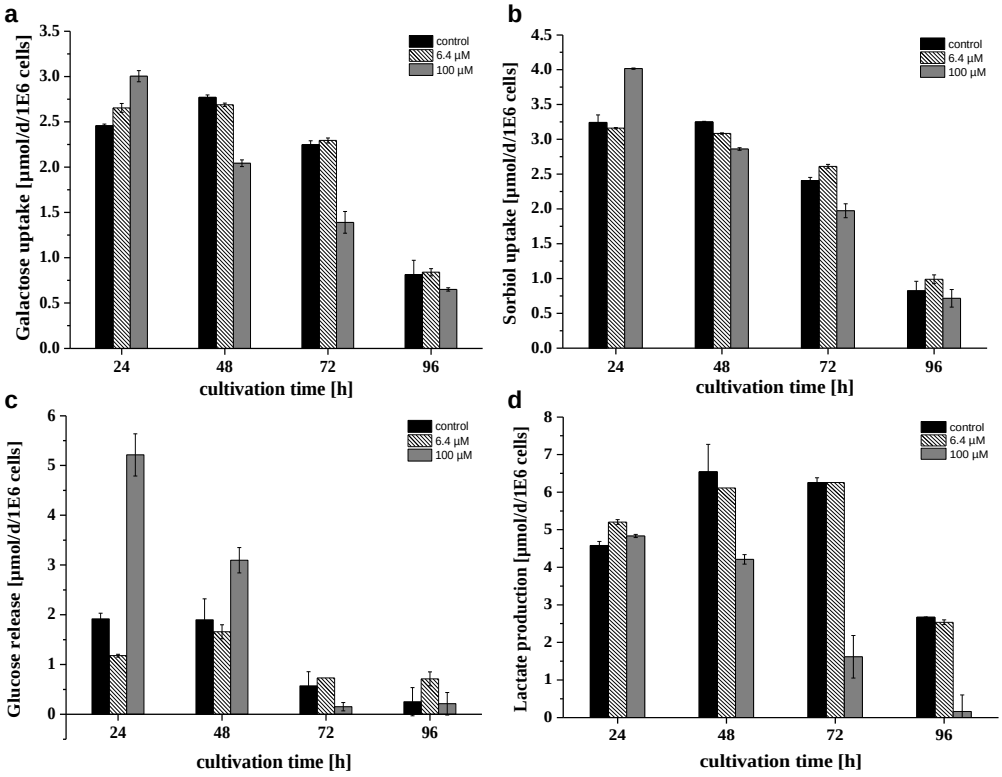

Figure 4.5. Carbohydrate metabolism in primary human hepatocytes during monolayer cultivation under diclofenac exposure. Galactose (a) and sorbitol (b) uptake, glucose release (c) and lactate production (d) are normalized to daily production (or uptake) per million seeded cells. Error bars indicating standard deviation of duplicate measurements (*n*=2).

For the untreated control, both galactose and sorbitol uptake (see Fig. 4.5 a, b; black bars) as well as glucose release (see Fig. 4.5 c; black bars) remained stable for the first 48h of cultivation with an uptake of about 2.5 µmol and 2.75 µmol sorbitol after 24h and 48h, respectively, and an uptake of about 3.25 µmol galactose as well as a release of glucose of about 2 µmol. After 72h, the consumption rates decreased (2.25 µmol galactose, 2.5 µmol sorbitol) as it was the case for the glucose release (0.5 µmol). About 0.75 µmol sorbitol and galactose were taken up and 0.5 µmol glucose was released after 96h. Lactate production increased from 4.5 µmol after 24h to about 6.5 µmol after 48h. After 72h, the untreated cells produced 6.25 µmol and after 96h the lactate production decreased to 2.5 µmol. The group exposed to the lower diclofenac concentration (6.4 µM, see Fig. 4.5, dashed bars) took up 2.7 µmol galactose and 3.2 µmol sorbitol, both after 24h as well as after 48h. After 72h the consumption of galactose decreased to 2.3 µmol and that of sorbitol to 2.7 µmol and further to 0.75 µmol for galactose and 1.0 µmol per million seeded cells for sorbitol after 96h. Glucose release was determined as 1.2 µmol after one day in culture, then increased to 1.6 µmol after 48h and afterwards decreased to 0.75 µmol of released glucose after 72h and 96h. Under these conditions (6.4 µM diclofenac), lactate production (see Fig. 4.5 d; dashed bars) increased from

5.25 µmol after 24h to about 6.1 µmol after 48h as well as 72h and decreased to 2.5 µmol lactate per million seeded cells after 96h. The cells exposed to higher concentrations of diclofenac (100 µM, see Fig. 4.5 a, b; grey bars) consumed 3 µmol galactose as well as 4 µmol sorbitol after 24h after which the daily carbohydrate uptake decreased to 2.1 µmol galactose and 2.9 µmol sorbitol after 48h. After 72h the galactose and sorbitol uptake decreased to 1.3 and 2.0 µmol galactose and sorbitol, respectively, and further decreased to 0.65 µmol galactose and 0.7 µmol sorbitol after 96h. The cells released 5 µmol glucose after 24h and 3 µmol after 48h when exposed to high concentrations of diclofenac (see Fig. 4.5 c, grey bars) while after 72h and 96h, 0.1 µmol glucose was released per day per million seeded cells. Daily lactate production decreased steadily from 4.8 µmol after 24h to 4.3 µmol, 1.5 µmol and 0.2 µmol lactate after 48h, 72h or 96h, respectively, when 100 µM diclofenac were applied (see Fig. 4.5 d; grey bars).

In order to assess cell death occurring during cultivation, the activity of intracellular enzymes was determined in the supernatant, namely the activity of Lactate dehydrogenase (LDH) and Aspartate-aminotransferase (AST). LDH is an enzyme involved in central carbon metabolism while AST is specific for hepatocytes as an enzyme involved in amino-acid metabolism. Both enzymes are indicators of cell lysis or cell death because they are localized intracellularly and are released if the cell membrane is disrupted, thus indicating dying cells. Figure 4.6 shows the determined activities of LDH and AST in the culture supernatants of standard monolayer cultures. The release of AST per day per million cells is shown in Figure 4.6 a. The control group (see Fig. 4.6 a, black bars) showed increasing AST release from 24h to 72h (45, 62 and 130 mU, respectively) which was then decreasing after 96h to 80 mU. The group exposed to 6.4 µM diclofenac (see Fig. 4.6 a, dashed bars) showed almost the same distribution with slightly less release after 24h and 72h (30 and 105 mU) and comparable releases after 48h and 96h (70 and 80 mU). The group exposed to the highest concentration of 100 µM diclofenac (Fig. 4.6 a, grey bars) released much more AST during the first two days of cultivation (100 and 112 mU) but released less AST after 72h and 96h (90 and 60 mU, respectively). Most likely, this was due to the already reduced number of cells at this time of exposure.

When the release of AST per day per million seeded cells was normalized to the total protein content in the supernatant, the profile was changing in time as shown in Figure 4.6 b. For all of the three groups, the release is increasing for the time points examined with the maximum release appearing after 96h. The control group releases more AST per protein as the group exposed to 6.4 µM diclofenac after 24h (1.25 mU versus 0.5 mU) but afterwards, the release of the two groups is comparably increasing from 1.25 mU AST per µg protein after 24h to 2.25 mU per µg protein after 96h. The cells that underwent treatment with 100 µM diclofenac, showed an increased AST release

for all 4 timepoints compared to the other two groups reaching from 1.75 mU per µg protein after 24h to almost 4.5 mU after 96h following a plateau of AST that was released after 48h and 72h (2.0 mU).

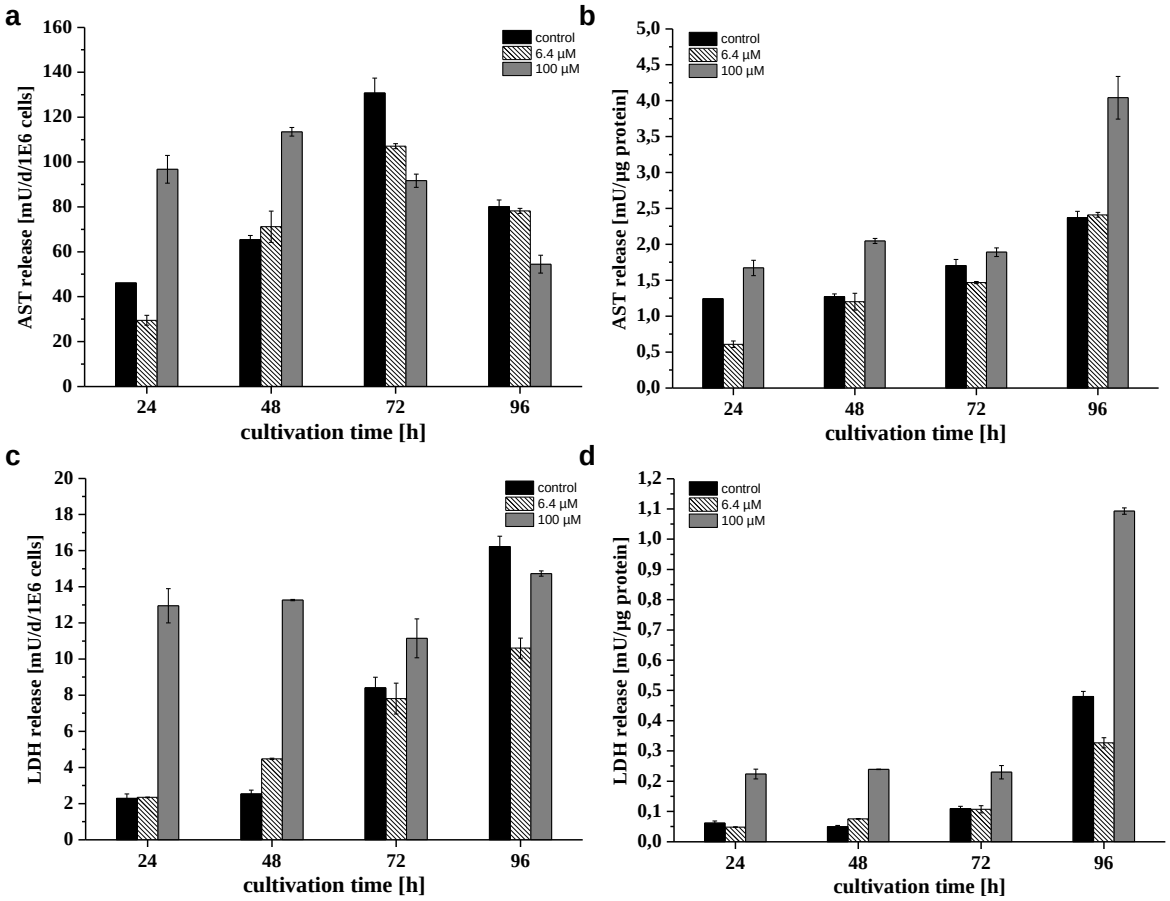

Figure 4.6. Release of intracellular enzymes (LDH, AST) by primary human hepatocytes during monolayer cultivation upon diclofenac exposure. The release is given as milliunits (mU) per million seeded cells (a, c) as well as milliunits per µg of total protein in the supernatant (b, d). Error bars indicate standard deviations of triplicate measurements (*n*=3).

The release of LDH per day by one million cells seeded in standard monolayer culture is shown in Figure 4.6 c. The untreated cells released 2 mU LDH after 24h as well as after 48h. The release is then increasing to 8 mU after 72h and to 16 mU after 96h. The group treated with 6.4 µM diclofenac is releasing as much LDH after 24h as after 72h but releases more LDH after 48h (4.5 mU) and less LDH after 96h (10 mU) compared to the control. For the cells treated with 100 µM diclofenac, the amount of enzyme released into the culture supernatant is equivalent to 13 mU for the first two days (24h and 48h, respectively) after which the release is slightly decreasing to 11 mU LDH per day per million seeded cells after 72h and is then increasing to 15 mU after 96h.

After normalizing the release of LDH to the total amount of protein released by one million cells per day, the cells that were either untreated or treated with 6.4 µM diclofenac showed almost identical profiles of LDH release (see Fig. 4.6 d; black and dashed bars). They released about 0.06 mU LDH per µg protein after 24h and 48h and 0.1 mU after 72h. After 96h the control group released 0.5 mU LDH while the group treated with 6.4 µM diclofenac released 0.35 mU only. For all of the time points, the cells treated with 100 µM diclofenac released more LDH as the other two groups when the release was normalized to the total protein amount in the supernatant (see Fig. 4.6 d; grey bars). From 24h to 72h, they released about 2.25 mU LDH per day and after 96h, the release increased to 1.1 mU.

Two of the main functions of hepatocytes exhibited *in vivo* are the production of serum proteins and the detoxification of ammonia. Ammonia is produced during protein turnover in the human body and is converted into urea by hepatocytes. This urea is then excreted through the renal system. The formation of albumin and urea should still be carried out in an *in vitro* system that should mimic the *in vivo* situation. To evaluate for how long this is applicable using monolayer culture conditions like the ones in this thesis, albumin and urea production was determined. Albumin concentration was measured using an ELISA and urea concentration was determined by HPLC as described in the methods section (see 3.4).

The production of albumin and urea is summarized in Figure 4.7. The albumin production per million seeded cells after 24h was about 4 to 4.5 µg for all of the three groups (see Fig. 4.7 a). For the untreated cells (black bars), the production remained at 4 µg after 48h, increased to 5.5 µg after 72h and decreased again to 2.5 µg after 96h. The cells treated with 6.4 µM diclofenac (dashed bars) produced 6.5, 7 and 2.5 µg after 48h, 72h and 96h, respectively. The albumin production per million cells for the group treated with 100 µM diclofenac (grey bars) was decreasing constantly with 3, 2 and 0.5 µg per day after 48h, 72h and 96h, respectively.

The albumin production was normalized to the total amount of protein in the supernatant and is reprted as the percentage of total protein as shown in Figure 4.7. The fraction of albumin in the supernatant of the control group (see Fig. 4.7 b, black bars) decreased from 11 % to 8 % from 24h to 48h and remained at 7 % after 72h and 8 % after 96h. The cells under 6.4 µM diclofenac-exposure (dashed bars) produced slightly more albumin after 48h (11 %) than after 24h (9 %). Thereafter, the fraction of albumin was 10 % after 72h and decreased to 8 % after 96h. The group under treatment with 100 µM diclofenac (grey bars) showed decreasing albumin production over time with 8 % after 24h, 5 % after 48h, 4 % after 72h and only 3 % albumin after 96h of cultivation in serum-free medium.

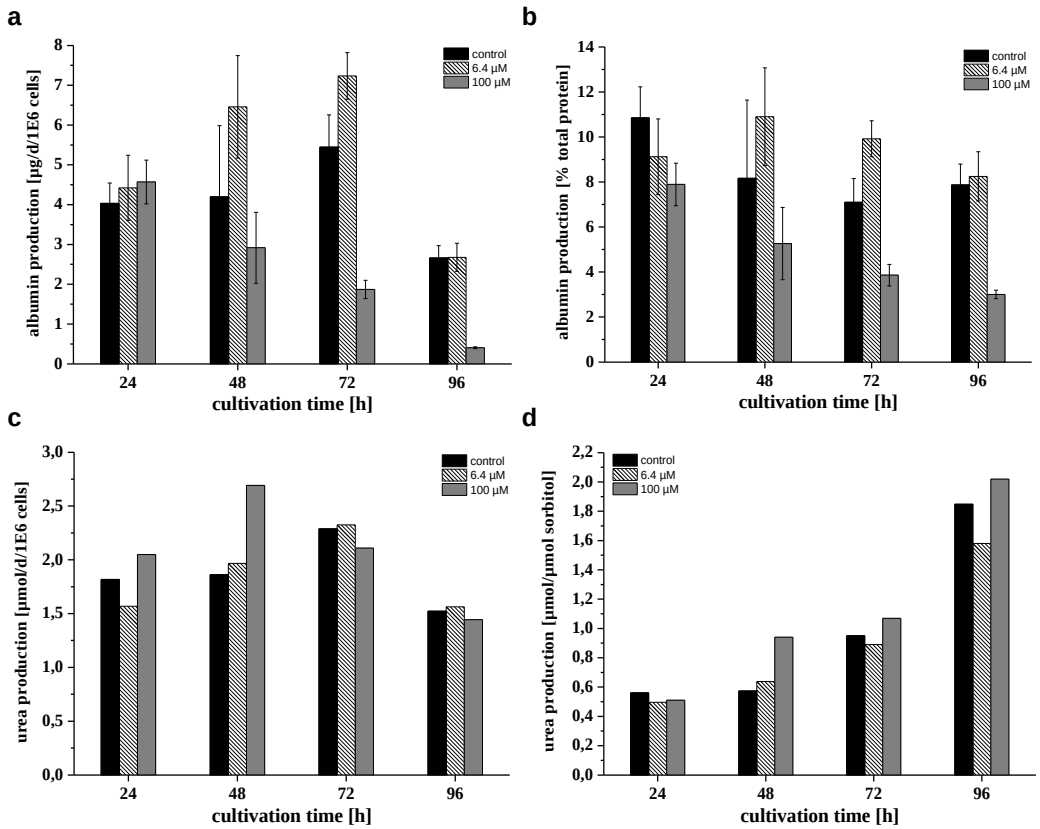

Figure 4.7. Albumin and urea production by primary human hepatocytes in standard monolayer culture under diclofenac exposure. The production is given as production per million seeded cells (a,c) as well as production per µg of total protein for albumin (b) and production per consumed sorbitol for urea (d). Error bars in a and b indicate standard deviations of duplicate measurements (*n*=2). For determination of urea concentrations using HPLC, samples were injected once.

Urea production per million seeded cells (shown in Fig. 4.7 c) for the untreated group (black bars) was 1.8 µmol after 24h and 48h, increased to 2.26 µmol after 72h and decreased again to 1.5 µmol after 96h. When the cells were treated with 6.4 µM diclofenac (Fig. 4.7 c; dashed bars) the urea production increased from 1.6 µmol after 24h over 1.9 µmol after 48h to 2.3 µmol after 72h and decreased to a value of 1.5 µmol after 96h. 2.0 µmol production of urea was determined after 24h treatment with 100 µM diclofenac (Fig. 4.7 c, grey bars) whereby production increased to 2.7 µmol after 48h. The production then decreased to 2.1 µmol and 1.5 µmol after 72h and 96h. The urea production normalized to the amount of consumed sorbitol (Figure 4.7 d) increased steadily for all three groups. The control (Fig. 4.7 d, black bars) showed values of 0.56, 0.57, 0.95 and 1.85 µmol urea per µmol sorbitol during cultivation, while the cells treated with 6.4 µM diclofenac (Fig. 4.7 d, dashed bars) delivered values of 0.5, 0.64, 0.89 and 1.57 µmol after 24h, 48h, 72h and 96h, respectively. The production of urea by the cells that underwent treatment with 100 µM diclofenac (Fig. 4.7 d, grey bars) exhibited values of 0.51 µmol after 24h, 0.94 µmol after 48h as well as 1.1 µmol after 72h and 2.0 µmol urea per µmol sorbitol after 96h.

As this thesis is dedicated to the analysis of secreted proteins by primary human hepatocytes, the first step of analyzing the proteins in the supernatant was to determine how much protein is found in the culture medium. Therefore, the culture supernatants were concentrated 20-fold as described in materials and methods and protein concentration was estimated using a Bradford-based colorimetric assay. The results of these measurements after normalization to the number of initially seeded cells and furthermore to the release of intracellular enzymes are depicted in Figure 4.8. The normalization to the amount of released LDH should provide estimates of contamination of secreted proteins by leaked intracellular proteins which would distort the secretome analysis.

The protein production per million seeded cells (see Fig. 4.8 a) increased for the control group (black bars) from 37 µg after 24h to 50 µg after 48h and further increased to 78 µg after 72h. After 96h, only 35 µg were produced. The cells treated with 6.4 µM diclofenac (see Fig. 4.8 a, dashed bars) produced 49, 60 and 74 µg after 24h, 48h or 72h, respectively. The production then decreased to 33 µg of protein per million seeded cells. The protein production for the group exposed to 100 µM diclofenac (see Fig. 4.8 a, grey bars) decreased steadily from 58 µg after 24h, over 55 µg after 48h and 50 µg after 72h. Also here, the production fell rapidly to a value of only 14 µg after 96h of cultivation under serum-free conditions.

The values after normalization of the protein production to the activity of LDH in the supernatant are shown in Figure 4.8 b. When the protein production was normalized to the activity of LDH in the culture supernatant, the group exposed to 100 µM diclofenac (see Fig. 4.8 b, grey bars) produced 4.5 µg of protein after 24h, 48h as well as 72h. However, after 96h, only 1 µg protein was produced per mU LDH. The cells that remained untreated (see Fig. 4.8 b, black bars) for the whole cultivation period produced 16 µg protein after 24h, 20.5 µg after 48h, 9.1 µg after 72h and 2 µg after 96h per mU LDH in the culture supernatant of one million cells. In the supernatant of cells treated with 6.4 µM diclofenac (see Fig. 4.8 b, dashed bars), 20.7 µg protein was produced per mU LDH after 24h and 13 µg were detected after 48h. Meanwhile, 9 µg of protein was found after 72h and 3 µg after 96h of serum-free cultivation.

Obviously, cells cultivated in standard monolayer culture perform very well during the first two days of culture in regard to central metabolism and liver-specific functions like albumin and urea production as well as protein production. Afterwards, cells start to die as it is visible from the increasing release of intracellular enzymes (AST and LDH) as well as decreasing consumption of carbohydrates and decreasing production of protein. As it was mentioned above, accompanied with the release of LDH and AST, there is also an increased release of other intracellular proteins “contaminating” the actual secretome. The protein production normalized to the LDH activity in the

supernatant can be interpreted as the fraction of “non-contaminated” protein and decreased after 72h to only half of the value obtained after 24h and 48h. Among the contaminants from the intracellular compartements is the protein Arginase I, an enzyme of the urea cycle which converts arginin to ornithin and urea [Peters *et al.*, 2008]. The release of this enzyme in the supernatant is most probably the reason for the increased urea production after 72h. Moreover, the treatment with diclofenac induced visible changes in the general cultivation profiles of the primary human hepatocytes. While the application of a subtoxic concentration (6.4 µM) seemed to have no or only little effect on the cells, the application of a more toxic concentration (100 µM) near the EC_{50} value of diclofenac led to an impairment of all of the analyzed parameters, most probably due to a high number of cells dying when applying such a high concentration of the drug.

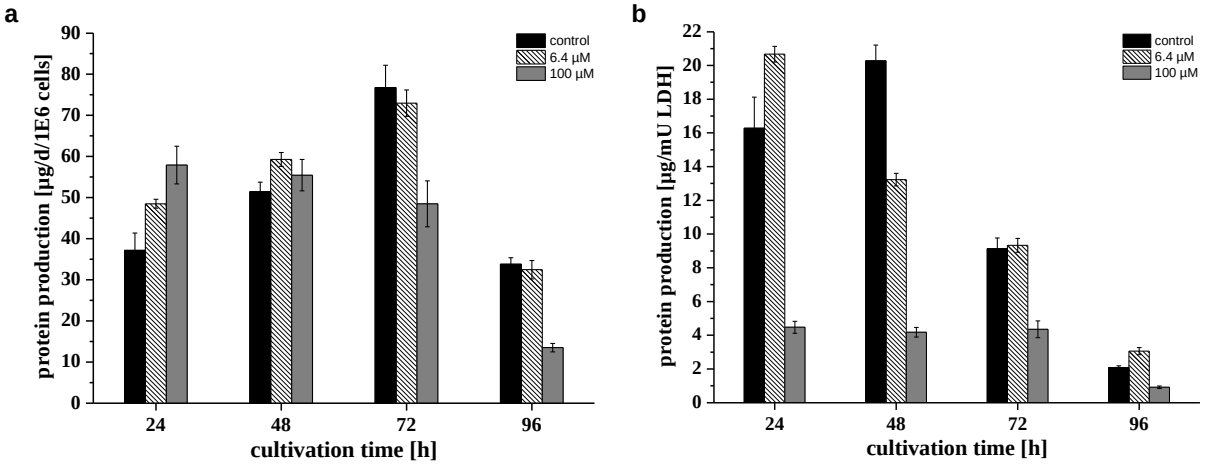

Figure 4.8. Protein production/release by primary human hepatocytes in standard monolayer culture under diclofenac exposure. Every 24h, the cultivation medium was changed and protein content was estimated in the 20-fold concentrated supernatants *via* Bradford-assay. The production is given as production per day per million seeded cells (a) as well as production per day per million seeded cells normalized to the activity of LDH (b) in the supernatant. Error bars indicate standard deviations of triplicate measurements (n=3).

According to these findings, it was decided to use samples from 24h or 48h to characterize the secretome of primary human hepatocytes cultivated in standard monolayer culture. However, later time points were used to establish the immunodepletion procedure (see section 4.1.2) and to evaluate the impact of prefractionation and instrumentation on identified proteins (see section 4.5).

4.2.2 Characterization of 3D-bioreactor cultures

The serum-free bioreactor cultivation of primary human hepatocytes described in this paragraph was performed by Stefan Hoffmann at the Brandenburg Center for Regenerative Therapies, Division of Experimental Surgery at the Charité clinic in Berlin. A publication of the detailed results is in preparation but with the emphasis on metabolism of diclofenac in this miniaturized cultivation device for use in pharmacological studies (Hoffmann *et al.*, in preparation). Bioreactors with a cell compartment volume of 0.5 ml ("two-layer") were run in Berlin under serum-free conditions for ten days. From day 3 to day 10, diclofenac was applied at two different concentrations (6.4 µM and 100 µM) plus an untreated control using three bioreactors filled with isolated liver cells from the same donor. A scheme of the experiment is shown in Figure 4.9. A suspension containing a total of 20 million cells (78 % viability) was inoculated. Daily samples from the effluent during treatment (day 4 to day 10) were supplemented with protease-inhibitors and sent to our laboratory.

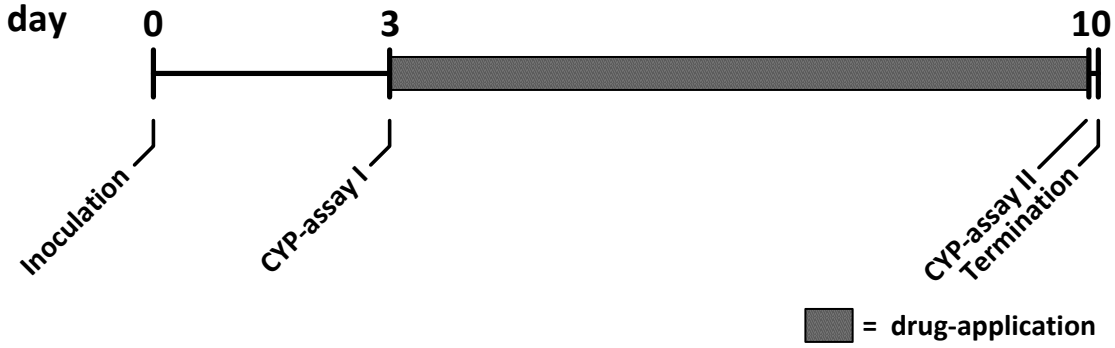

Figure 4.9. Scheme illustrating the time course of a bioreactor cultivation of primary human hepatocytes with application of the anti-inflammatory drug diclofenac performed at Charité, Berlin. The experiment lasted 10 days with the drug applied from day 3 to day 10, after which the bioreactor cultures were terminated. Cell suspension was inoculated at day 0. Both at day 3 and day 10, so-called "CYP-assays" were conducted to verify the metabolic capacity of the culture. Samples from day 4 to day 10 were sent to our laboratory and analysed as described in the text.

Protein concentrations were determined *via* Bradford assay after concentrating the samples 20-fold by ultrafiltration. These values were divided by the applied concentration factor (i.e. 20) to obtain the original concentrations in the bioreactor samples which are shown in Figure 4.10, a. The protein concentration in the bioreactor of the untreated control (Fig. 4.10 a; black bars) increased from 5.4 ng/µl at day 4 to 39.7 ng/µl at day 7, with 10.5 and 29.0 ng/µl at day 5 and 6, respectively. At day 8, the protein concentration was 37.8 ng/µl after which it increased to 95.7 ng/µl at day 9 and decreased again to 34.6 ng/µl at day 10. In the bioreactor treated with 6.4 µM diclofenac (Fig. 4.10a; dashed bars), no protein could be detected at day 4. At day 5, the concentration measured was 16.1

ng/µl, at day 6, the concentration increased to 62.3 ng/µl and at day 7 the protein content increased further to 75.3 µg/µl. Afterwards the protein concentration decreased again to 49.4 ng/µl at day 8 and to 40.6 ng/µl at day 9. In the sample of day 10 of this bioreactor, a protein concentration of 82.2 ng/µl was determined. The protein concentration in the bioreactor treated with 100 µM diclofenac (Fig. 4.10a; grey bars) increased from a non-detectable level at day 4 to 5.4 ng/µl at day 5, 19.8 ng/µl at day 6 and to 32.3 ng/µl at day 7. Thereafter, the concentration did not change much with 28.1 ng/µl at day 8 and 42.4 ng/µl determined at day 9. The protein concentration determined in the sample before termination of the experiment (day 10) was 34.6 ng/µl.

The profile for the calculated protein production normalized to one million inoculated cells is shown in Figure 4.10 b. The protein production per day per million inoculated cells for the control bioreactor (see Fig. 4.10 b, black bars) increased from 2 µg at day 4 over 8 µg at day 5 to 21 µg at day 6, and further increased to 26 µg of produced protein at day 7. After slightly decreasing to 23 µg at day 8, the protein production in the control bioreactor increased to 65 µg at day 9 after which it decreased again to 11 µg of protein per million cells. In the bioreactor treated with 6.4 µM diclofenac (see Fig. 4.10 b, dashed bars), no protein production could be detected at day 4 but at day 5, 13 µg of protein was produced and the production further increased to 53 µg at day 6. Thereafter, the production decreased to 48 µg, 25 µg and 23 µg of protein at days 7, 8 and 9, respectively. On the last day of cultivation (day 10), 59 µg of protein was produced per day per million inoculated cells. If the cells in the bioreactor were cultivated in the presence of 100 µM diclofenac (see Fig. 4.10 b, grey bars), the production increased from non-detectable levels at day 4 to 25 µg at day 7, with 4 and 17 µg of protein produced at days 5 and 6, respectively. At day 8, the production decreased to 18 µg, at day 9 the protein production was 29 µg and at day 10, 22 µg of protein was produced per day.

Albumin concentrations in the bioreactor samples were determined before concentration *via* ELISA and the determined values were calculated as production rates per day per million inoculated cells (see Figure 4.10 c). The determined albumin concentration in the cultivation medium of the control bioreactor (see Fig. 4.10 c, black bars) increased during the first four days from 0.25 µg per day per million inoculated cells at day 4 to 2.6 µg at day 7, with 0.5 and 2.2 µg of albumin produced at days 5 and 6, respectively. At day 8, the albumin production was determined as 2.1 µg, then increased to 3.6 µg at day 9 and decreased to 1.2 µg of albumin produced at the last day of the experiment (day 10). One million cells in the bioreactor treated with 6.4 µM diclofenac (see Fig. 4.10 c, dashed bars) produced 0.25 µg albumin per day at day 4, after which the production increased to 1.1 µg at day 5, 3.5 µg at day 6 and 3.8 µg at day 7. At day 8, 1.6 µg of albumin was produced per day, at day 9, 2.2 µg and at day 10, 2.3 µg of albumin was produced per day per million inoculated cells in this

bioreactor. 100 µM diclofenac were applied in the third bioreactor (see Fig. 4.10 c, grey bars) and here, the albumin production was determined as 0.22, 0.28, 1.48, 3.2 µg of albumin produced at days 4, 5, 6 and 7, respectively. 1.6, 2.5 and 1.9 µg of albumin were produced per day per million inoculated cells at days 8, 9 and 10.

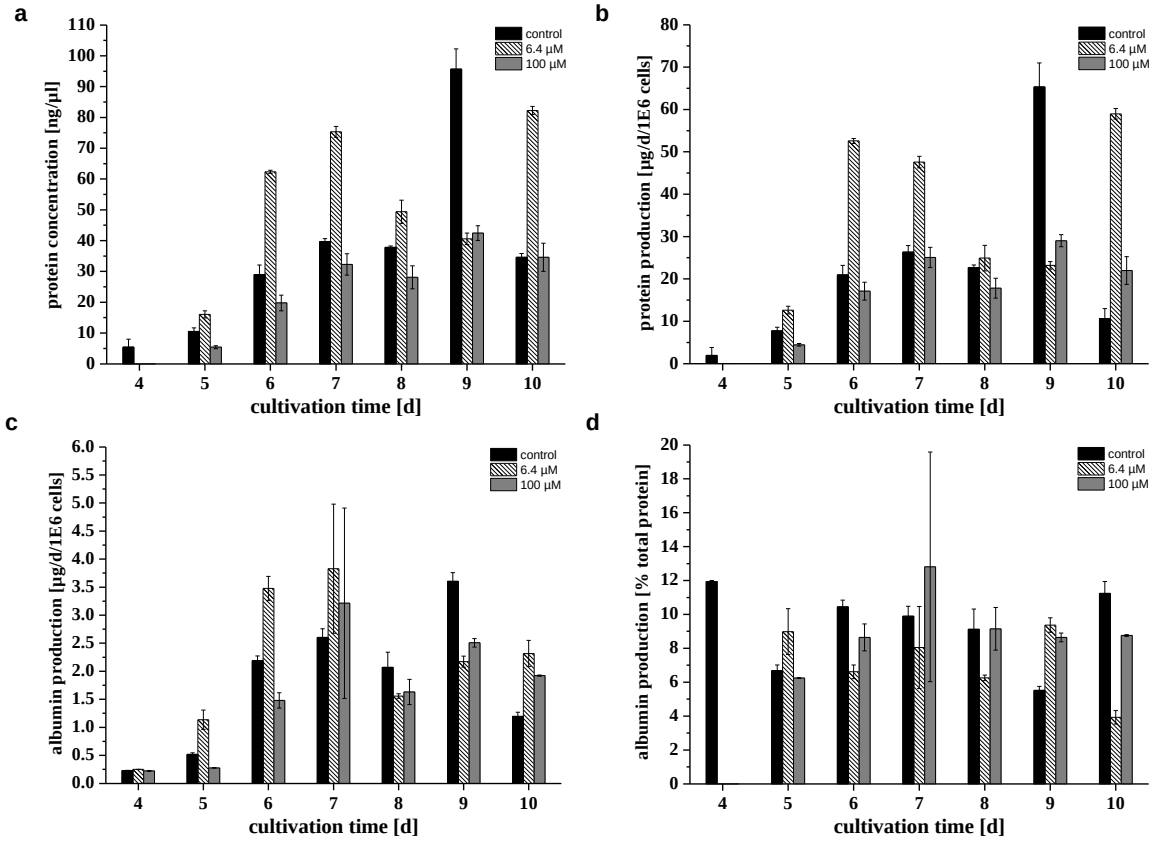

Figure 4.10. Protein and albumin production by primary human hepatocytes during 3D-bioreactor cultivation upon diclofenac exposure as determined *via* Bradford assay or ELISA, respectively. a) protein concentration in the conditioned culture medium. b) calculated protein production per million seeded cells. c) albumin production per million seeded cells. d) albumin production as percentage of total protein production as depicted in b. Error bars indicate standard deviations of multiple measurements (*n*>2).

As for the monolayer cultures, the albumin production rates were normalized to that of total protein released into the culture medium as depicted in Figure 4.10 a. The fraction of albumin in the supernatant of the untreated control (see Fig. 4.10 d, black bars) was 12 % at day 4 and decreased to 7 % at day 5. At days 6 and 7, the percentage of albumin increased again to 10 % of total protein while at days 8, 9 and 10, 9 %, 6 % and 10 % of total protein was albumin. For the cells in the bioreactor where 6.4 µM diclofenac was applied (see Fig. 4.10 d, dashed bars) the percentage increased from non-detectable levels at day 4 to 9 % at day 5. Afterwards, the calculated fraction of

albumin was 7 % (day 6), 8 % (day 7) and 6 % (day 8) of total protein in the bioreactor circuit. While 9 % of total protein was albumin was at day 9, 4 % of total protein in the culture medium from this bioreactor was determined to be albumin. The bioreactor receiving treatment with 100 µM diclofenac (see Fig. 4.10 d, grey bars) also showed non-detectable levels of albumin production if the values were normalized to the total protein amount released into the bioreactor. Thereafter, the production increased to 6 % at day 5 and further increased to 9 % at day 6. At day 7, 10 % of total protein was albumin in this bioreactor, while over the last three days of culture (days 8, 9 and 10) the fraction of proteins contained in the conditioned medium being albumin was determined as 9 %.

It has to be mentioned that for all of the three bioreactors, so-called "CYP-assays" were performed at days 3 and 10. During such a CYP-assay, specific substrates for the most important cytochrome P450 isoenzymes are injected into the bioreactor and the production of phase I metabolites of these substrates are measured by LC-MS [Zeilinger *et al.*, 2011]. After finishing this assay at day 3, the bioreactor was extensively purged with fresh medium to remove the applied substances (i.e. drugs) from the system. Hence, the protein as well as albumin concentration at day 4 was very low for all of the three bioreactors.

According to these results, the cultures were divided into two distinct phases. The first phase (phase I) from day 4 to day 6 of the bioreactor cultivation showed increasing protein concentration while the second phase (phase II) from day 7 to 10 was defined because of a more stable protein concentration in the culture-medium. Samples belonging to the same phase were pooled and analyzed by LC-MALDI after immunodepletion. The results of these experiments are reported in section 4.4.

4.3 Proteins identified in monolayer culture

The supernatant of a monolayer culture of primary human hepatocytes after 48h of serum-free cultivation (without medium change) was analyzed to get a reference set of proteins for later analysis of bioreactor samples. To eliminate inter-individual differences, the cells were obtained from the same liver resection (i.e. the same donor) as the ones used for inoculation of the bioreactor. After immunodepletion and tryptic digest, 3 µg of the resulting peptide mixture was analyzed in triplicate by LC-MALDI. In Figure 4.11 the separation and subsequent mass-spectrometric analysis is illustrated as a recorded UV-chromatogram and the resulting base-peak chromatogram for the first run. The intensity in the UV (see Fig. 4.11 a) did not necessarily correlate with the intensity in the base peak chromatogram of the MALDI analysis (see Fig. 4.11 b). During separation by nanoHPLC, the chromatogram recorded at a wavelength of 214 nm showed two high peaks having intensities of 14

mAU at minutes 22 and 47, respectively. The rest of the chromatogram showed intensities around 10 mAU with a strong increase from minute 17 and a decrease starting at minute 40, reaching the "base-line" of about 2 mAU at minute 70.

In contrast, the intensity in the mass spectrometer was quite constant over the whole base peak chromatogram with intensities between 40.000 and 50.000 counts. Noteworthy, some peaks exhibiting only very low absorptions in the UV showed much higher intensities in the mass-spectrometer. For example, for the peak at minute 67, the absorption in the UV is only 2 mAU, while the intensity in the base-peak chromatogram is 45.000, which is comparable to other peaks having much higher intensities in the UV-chromatogram. This illustrates the important problem of ion-suppression during ionization of peptides, especially during phases where many peptides co-elute from the column into one fraction (i.e. spot) as it is the case from minute 20 to 40.

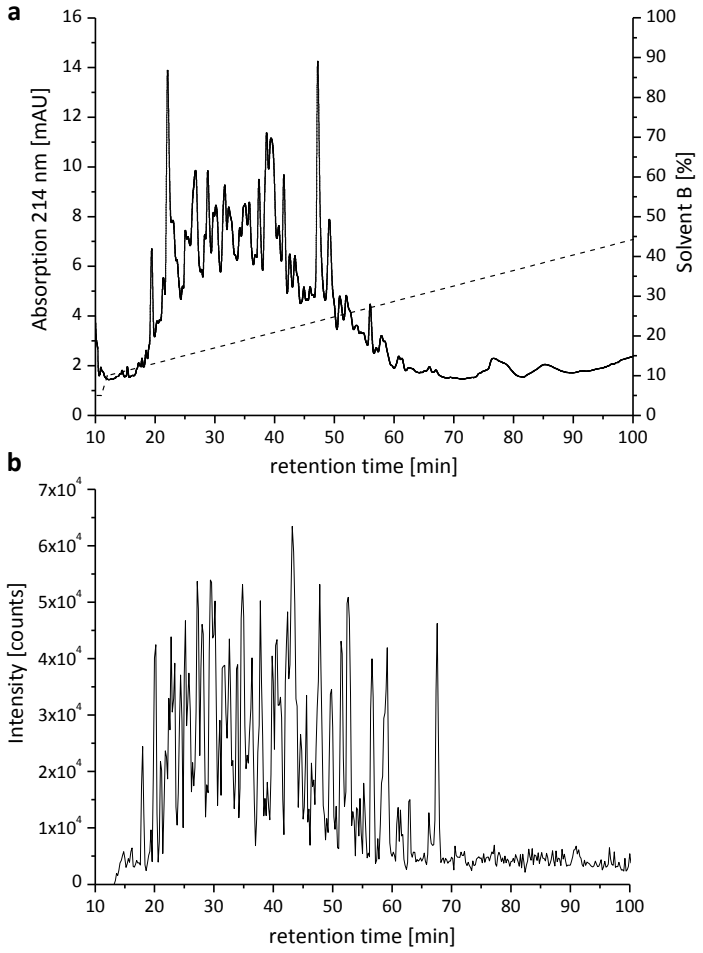

Figure 4.11. LC-MALDI analysis of a tryptic digest of the extracellular proteome of primary human hepatocytes in standard monolayer culture after 48h of serum-free cultivation. The UV-chromatogram (a) was recorded at a wavelength of 214 nm, the dashed line indicates the employed gradient (percentage of solvent B) during separation by nano-scale HPLC. Resulting base-peak chromatogram (b) of the subsequent analysis of spotted fractions by MALDI-TOF-MS.

As mentioned above, the analysis was performed in triplicates and in each run, 10 precursors were selected for fragmentation in each fraction. However, the runs should rather be called "pseudo-replicates" because during the first run, the MS/MS acquisition started with the strongest precursor, while the weakest precursors in each fraction were fragmented first during runs 2 and 3 to maximize good-quality spectra of low abundance peptides. This resulted in at most 20 fragmented peptides per fraction. The data from each run was subjected to a database search using Mascot and the results were filtered in Scaffold to control the FDR. One decoy hit was allowed for proteins identified with one peptide and more and the FDR was estimated by doubling the number of decoy hits and dividing this by the total number of hits (target + decoy hits) at a given score threshold [Elias and Gygi, 2007]. The estimated FDR in each run was kept at comparable levels (1.8 % for run 1 and 2.0 % for run 2 and 3) and afterwards, the overlap in identifications was examined (see Fig. 4.12). Almost 60 % (59.8) of the identified proteins were identified in all three runs. Another 16.7 % were identified in at least two runs, with 7.6 % identified in run 1 and run 2, 0.8 % identified in run 1 and run 3 and 8.3 % of all proteins were identified both in run 2 and run 3.

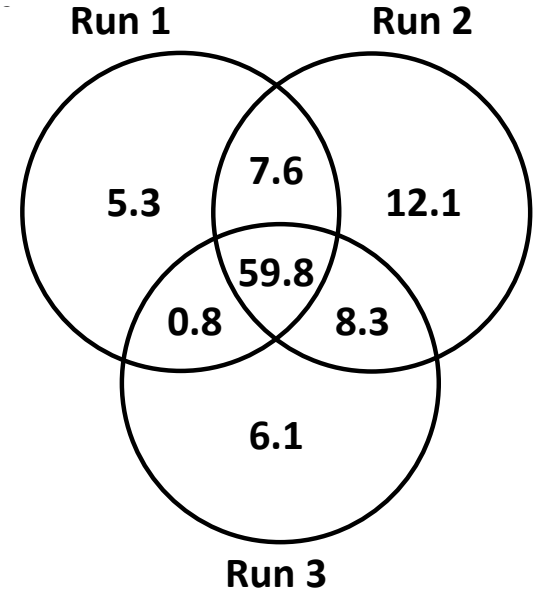

Figure 4.12. Overlap in identified proteins after LC-MALDI analysis of the same sample performed in triplicate. For all runs, 10 peptides were selected in each fraction for MS/MS analysis. In run 1, peptides having the strongest signals were fragmented first while in runs 2 and 3, the precursors showing the weakest intensites in the MS-scan of each fraction were fragmented. The numbers in the Venn diagram are given as percentage of 126 proteins identified in total.

Thus, 76.5 % of the proteins identified in total were identified in at least two runs. The remainder (23.5 %) was only found in one run of the "pseudo-triplicate" analysis. 5.3 % were identified only in run 1, 12.6 % were identified only in run 2 and 6.1 % could only be found in run 3.

For the final protein list, the results of all three runs were merged while importing the mascot result files into Scaffold software. Thus, 126 proteins were identified after database search of acquired MS/MS-spectra in a concatenated target-decoy database. The estimated false identifications in the list of identified proteins were calculated as 2 false positives in 127 total identifications which correspond to a FDR of 1.6 %. The average sequence coverage achieved was calculated as 10.5 % and the fraction of proteins identified by one peptide was 35.7 %. The complete list of identified proteins can be found in the Appendix.

For identified proteins, the subcellular location was extracted from the UniprotKB database (http://www.uniprot.org) and the results of the annotation are depicted in Figure 4.12. More than two-thirds (63.5 %) of identified proteins were annotated as secreted. 5.6 % were membrane proteins and for 3.2 % of identified proteins, no information about the localization was found in the database.

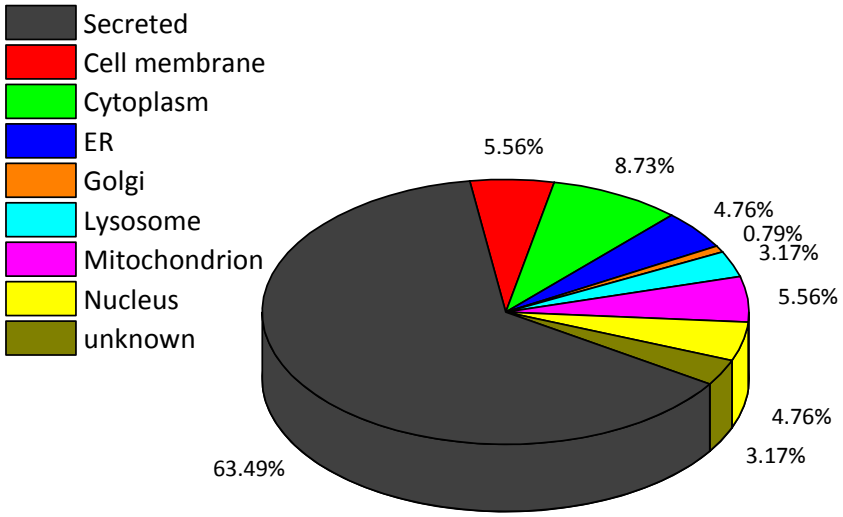

Figure 4.13. Distribution of subcellular locations of the identified proteins as described in the UniProt database. 126 proteins were identified in total by LC-MALDI-MS/MS analysis of a tryptic digest of the extracellular proteome of primary human hepatocytes in standard monolayer culture after 48h of serum-free cultivation. ER = endoplasmic reticulum

The remaining proteins were apparently released from intracellular parts, namely cytoplasm (8.7 %), endoplasmic reticulum (4.8 %), the Golgi apparatus (0.8 %), from lysosomes (3.2 %), from mitochondria (5.6 %) or from the cell nucleus (4.8 %). This indicates a significant predominance of secreted proteins in the supernatant, even though contaminant proteins from also intracellular origin were identified.

To get an overview of the biological processes the identified proteins are involved in, the list of proteins was annotated *via* DAVID [Huang da *et al.*, 2009a; Huang da *et al.*, 2009b]. This online tool calculates overrepresented ontologies in the uploaded dataset compared to a so-called "background-list". The background list used for the analysis of identified proteins discussed here was the whole list of proteins known for *homo sapiens*. The EASE-score (*p*-value) for enrichment was set to default as used by DAVID (i.e. 0.1). 14 terms were found to be significantly enriched among the 133 proteins indentified and are shown in table 4.2

Table 4.2. Over-represented biological processes of identified proteins in the supernatant of a monolayer culture of primary human hepatocytes after 48h of serum-free cultivation. Annotation was extracted from the Panther database *via* DAVID. Listed are the total number of proteins (count) annotated to a term (panther ID in brakets), the percentage (%) of involved proteins compared to total identifications as well as corresponding *p*-values as a measurement for statistical relevance of enrichment in the underlying dataset. Note that proteins can be annotated to more than one process.

Biological process	Count	%	p-value
Proteolysis (BP00071)	35	27.8	1.2E-13
Immunity and defense (BP00148)	40	31.7	8.6E-13
Blood clotting (BP00176)	12	9.5	3.5E-10
Lipid and fatty acid transport (BP00028)	11	8.7	1.2E-07
Growth factor homeostasis (BP00270)	4	3.2	2.5E-05
Blood circulation and gas exchange (BP00209)	7	5.6	9,4E-05
Extracellular matrix protein-mediated signaling (BP00275)	6	4.8	2.1E-04
Protein metabolism and modification (BP00060)	40	31.7	7.7E-04
MHCI-mediated immunity (BP00150)	3	2.4	1.0E-02
Homeostasis (BP00267)	6	4.8	2.9E-02
Lipid, fatty acid and steroid metabolism (BP00019)	13	10.3	2.8E-02
Vitamin/cofactor transport (BP00088)	3	2.4	4.7E-02
Transport (BP00141)	18	14.3	4.8E-02
Coenzyme and prosthetic group metabolism (BP00081)	5	4.0	5.4E-02
not annotated/enriched	33	24.8	

The most enriched terms were "Proteolysis" including proteases as well as protease inhibitors with 35 proteins and "Immunity and defense" (40 proteins) comprising complement factors but also proteins like coagulation factors. These classes of proteins also belonged to "blood clotting", the process being enriched at the third place if ordered by *p*-values (12 proteins). Furthermore, a significant enrichment was found for proteins related to "lipid and fatty acid metabolism and transport" with 11 and 13 proteins, respectively. The most prominent protein class to be mentioned here is the family of Apolipoproteins. 4 isoforms of the insulin-like growth factor binding protein were found ("growth factor homeostasis"), 7 proteins were annotated as part of "Bloodcirculation and gas exchange" and 6 proteins belonged to "Extracellular matrix protein-mediated signaling". 40

proteins were annotated to “Protein metabolism and modification” and 3 proteins were part of the major histocompatibility complex 1 (“MHCI-mediated immunity”) whereas 6 proteins were attributed to “Homeostasis”. 3 or 18 proteins, respectively, were annotated to “Vitamin/cofactor transport” or “transport” and 5 proteins were members of the “Coenzyme and prosthetic group metabolism”. The process of “Detoxification” was represented by 3 proteins, while the “Amino acid metabolism” was enriched with 5 proteins annotated to this term. Finally, 2 proteins were members of “Protein disulfide-isomerase reaction” and 33 proteins were not annotated or did not belong to a significantly enriched term.

4.4 Proteins identified in 3D-bioreactor cultures

As mentioned in section 4.2.2, the samples of the bioreactor experiment were divided into two phases based on protein concentration in the conditioned medium. Phase I was defined as the time from day 4 to day 6, in which protein concentration was increasing, while in phase II, the samples from day 7 to day 10 were combined because of a more stable protein concentration in the conditioned medium. The pooled samples from both phases of the bioreactor not being treated with diclofenac (control) were immunodepleted and analyzed in triplicate by LC-MALDI. The mascot results from three replicate runs were merged as mentioned in the previous section.

In the first phase of the bioreactor from day 4 to day 6, 133 proteins were identified in total with a FDR of 1.49 %. The average sequence coverage was 10.8 % and the percentage of proteins identified with one peptide was 23.3 %. For the second phase from day 7 to day 10, the number of identified proteins was 250. The calculated FDR was 0.8 % and the average sequence coverage was the same as for the first phase (10.8 %). 38.3 % of identifications were based on one assigned peptide. The complete lists of identified proteins can be found in the Appendix.

As for the monolayer cultures, information about the subcellular location of the identified proteins was obtained from Uniprot database (see Fig. 4.12). In the sample of phase I, 40.6 % of the 133 proteins identified were annotated as secreted, 3 % were proteins of the cell membrane and 6.8 % of all identifications were not annotated in the uniprot database. 24.8 % of identifications were annotated as cytoplasmic proteins, 6 % belonged to the endoplasmic reticulum (ER) and 4.5 % were lysosomal proteins. 11.3 % were of mitochondrial origin and 3 % of all proteins were from the nucleus. From the 250 proteins identified during the second phase of the bioreactor cultivation, almost one third (31.6 %) were secreted proteins and another 31.2 % were cytoplasmic proteins. 5.9 % of total identifications were proteins of the cell membrane and 5.5 % were apparently released from the ER. One protein of the golgi-apparatus was found (0.4 %) and about 4.4 % of identifications

were proteins from lysosomes. Furthermore, another 4.4 % of the identifications were annotated to be located in the mitochondrion and 5.1 % are known to be located in the cell nucleus.

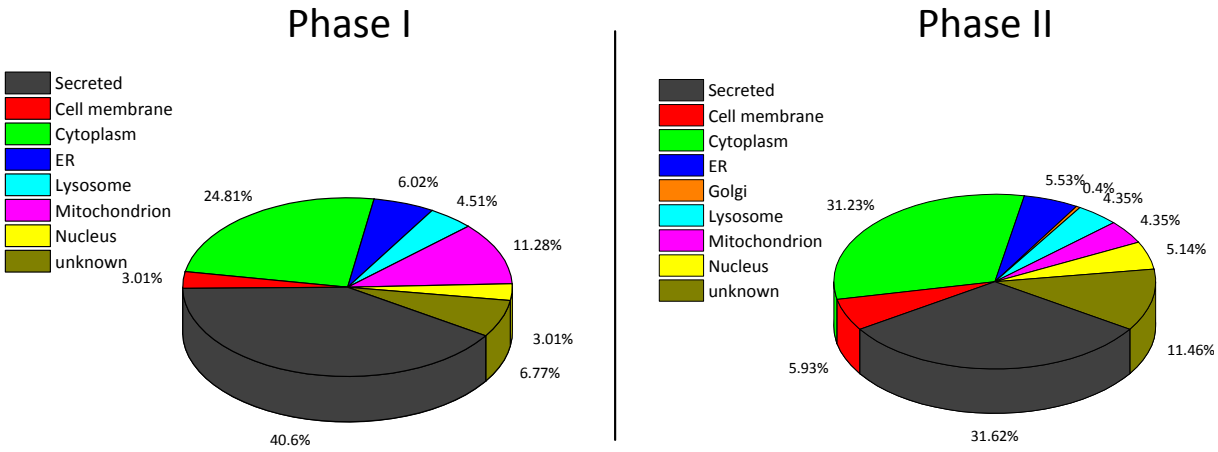

Figure 4.12. Distribution of subcellular locations of identified proteins in the culture medium of primary human hepatocytes cultured in a 3D-bioreactor under serum-free conditions. Pooled samples from days 4 to 6 (Phase I) and days 7 to 10 (Phase II) were analyzed. The total number of identified proteins was 133 (Phase I) and 250 (Phase II), respectively. Subcellular location is reported as described in the UniProt database. ER = endoplasmic reticulum

According to DAVID, the significantly enriched biological processes of the 133 identified proteins during phase I of the bioreactor culture (see Table 4.3) were “Immunity and defense” (41 proteins), “Amino acid metabolism” (15 proteins), “Carbohydrate metabolism” (21 proteins), “Proteolysis” (26 proteins) and “Coenzyme and prosthetic group metabolism” (9 proteins). Moreover, “Blood clotting” and “Lipid and fatty acid transport” (6 proteins each), “Vitamin metabolism” (4 proteins), “Fatty acid beta-oxidation” (3 proteins), “Detoxification” (4 proteins) and “Tricarboxylic acid pathway” (3 proteins) were represented by a significant number of proteins. Finally, “Protein metabolism and modification” (36 proteins), “Antioxidation and free radical removal” (3 proteins), “Vitamin/cofactor transport” (3 proteins) and “Growth factor homeostasis” (2 proteins) belonged to the terms showing significant enrichment during phase I of the bioreactor culture. 22 proteins were not annotated or did not belong to one of the 15 significantly enriched terms.

Table 4.3. Over-represented biological processes of identified proteins in the culture medium of primary human hepatocytes cultured in a 3D-bioreactor under serum-free conditions in the pooled samples from day 4, 5 and 6 (phase I). Annotation was extracted from the Panther database *via* DAVID. The total number of proteins (count) annotated to a term (panther ID in brakets), the percentage (%) of involved proteins compared to total identifications as well as corresponding *p*-values as a measurement for statistical relevance of enrichment in the underlying dataset are listed. Note that proteins can be annotated to more than one process.

Biological process	Count	%	p-value
Immunity and defense (BP00148)	41	30.6	6.2E-12
Amino acid metabolism (BP00013)	15	11.2	3.5E-08
Carbohydrate metabolism (BP00001)	21	15.7	4.1E-07
Proteolysis (BP00071)	26	19.4	1.4E-06
Coenzyme and prosthetic group metabolism (BP00081)	9	6.7	1.8E-04
Blood clotting (BP00176)	6	4.5	1.8E-03
Lipid and fatty acid transport (BP00028)	6	4.5	6.8E-03
Vitamin metabolism (BP00083)	4	3.0	7.5E-03
Fatty acid beta-oxidation (BP00022)	3	2.2	2.6E-02
Detoxification (BP00180)	4	3.0	2.9E-02
Tricarboxylic acid pathway (BP00008)	3	2.2	3.6E-02
Protein metabolism and modification (BP00060)	36	26.9	4.3E-02
Antioxidation and free radical removal (BP00268)	3	2.2	5.1E-02
Vitamin/cofactor transport (BP00088)	3	2.2	5.6E-02
Growth factor homeostasis (BP00270)	2	1.5	6.8E-02
not enriched/annotated	22	16.4	

During phase II of the bioreactor cultivation, 19 processes were found to be significantly enriched, while 65 of the 250 identified proteins were not in the list of enriched terms. The processes found to be statistically over-represented were in particular (see Tab. 4.4): “Immunity and defense” (66 proteins), “Proteolysis” (40 proteins), “Blood clotting” (11 proteins), “Carbohydrate metabolism” (27 proteins), “Other protein targeting and localization” (6 proteins), “Amino acid metabolism” (15 proteins), “Lipid and fatty acid transport” (11 proteins) and “Other carbon metabolism” as well as “Blood circulation and gas exchange” (8 proteins each). Additionally, “Coenzyme and prosthetic group metabolism” (9 proteins), “Other metabolism” (18 proteins), “Tricarboxylic acid pathway” (4 proteins), “Extracellular matrix protein-mediated signaling” (5 proteins) and “Nitrogen metabolism” (3 proteins) represented terms enriched during the second phase. Finally, “Protein disulfide-isomerase reaction” (3 proteins), “Protein folding” (7 proteins), “Other carbohydrate metabolism” (4 proteins) as well as “Lipid, fatty acid and steroid metabolism” (19 proteins) showed significant enrichment.

Table 4.4. Over-represented biological processes of identified proteins in the culture medium of primary human hepatocytes cultured in a 3D-bioreactor under serum-free conditions in the pooled samples from day 7 to day 10 (phase II). Annotation was extracted from the Panther database *via* DAVID. Total number of proteins (count) annotated to a term (panther ID in brakets), the percentage (%) of involved proteins compared to total identifications as well as corresponding *p*-values as a measurement for statistical relevance of enrichment in the underlying dataset are listed. Note that proteins can be annotated to more than one process.

Biological process	Count	%	p-value
Immunity and defense (BP00148)	66	26.5	1.5E-16
Proteolysis (BP00071)	40	16.1	6.7E-08
Blood clotting (BP00176)	11	4.4	3.3E-06
Carbohydrate metabolism (BP00001)	27	10.8	3.9E-06
Other protein targeting and localization (BP00140)	6	2.4	9.0E-06
Amino acid metabolism (BP00013)	15	6.0	3.3E-05
Lipid and fatty acid transport (BP00028)	11	4.4	4.9E-05
Other carbon metabolism (BP00292)	8	3.2	3.7E-04
Blood circulation and gas exchange (BP00209)	8	3.2	6.0E-04
Antioxidation and free radical removal (BP00268)	5	2.0	3.7E-03
Coenzyme and prosthetic group metabolism (BP00081)	9	3.6	6.9E-03
Other metabolism (BP00289)	18	7.2	1.2E-02
Tricarboxylic acid pathway (BP00008)	4	1.6	1.6E-02
Extracellular matrix protein-mediated signaling (BP00275)	5	2.0	2.2E-02
Nitrogen metabolism (BP00090)	3	1.2	3.6E-02
Protein disulfide-isomerase reaction (BP00069)	3	1.2	3.6E-02
Protein folding (BP00062)	7	2.8	6.1E-02
Other carbohydrate metabolism (BP00012)	4	1.6	6.6E-02
Lipid, fatty acid and steroid metabolism (BP00019)	19	7.6	8.4E-02
not enriched/annotated	65	26.1	

4.5 Comparison of LC-MALDI and LC-ESI with and without prior fractionation

Parts of the sample preparation (SDS-PAGE, reduction and alkylation of gel-slices) and mass-spectrometric analysis described in this section was performed in the laboratory of Dr. Alain van Dorsselaer at the Laboratory of bio-organic mass-spectrometry (LSMBO) at CNRS, University of Strasbourg.

To evaluate the established LC-MALDI workflow for secretome-analysis of primary human hepatocytes, a sample was analyzed on two commonly used LC-ESI-MS platforms, namely a hybrid quadropole-time of flight (Q-TOF; MaXis, Bruker daltonics, Bremen) and an ion-trap (Amazon, also Bruker daltonics) mass-spectrometer following reversed-phase liquid chromatography of tryptic peptides (LC-MS). Furthermore, the extent prefractionation of the sample via one-dimensional electrophoresis prior to LC-MS analysis (GeLC-MS) enhances the identification of secreted proteins was evaluated. After mass spectrometric analysis of separated peptides, the resulting peak lists were searched against the same database using the same Mascot-version to minimize artifacts resulting from different protein databases and search algorithms. Furthermore, the adjacent data reprocessing was performed equally by the same operator (i.e. myself) to exclude deviations by differently interpreted search results. The injected amount of peptides was also the same, except for the GeLC-MS analysis, where only half of the amount was injected for LC-MALDI. However, the gradient for the liquid chromatography on the different instruments used was different, especially for the liquid digest, because it was optimized empirically on each instrument (see methods section for details).

As it is shown in Figure 4.14 a, the MALDI-based workflow identified 94 proteins if the sample was analyzed *via* LC-MS after in-solution digestion. The average sequence coverage of identified proteins was 10.2 % and the average mascot ion-score was calculated as 50.3 (see Fig. 4.14, a; black bars). The Q-TOF identified 84 proteins with identified peptides covering 8.3 % of the protein sequence and having an average ion-score of 31.7 (see Fig. 4.14 a, white bars). The ion-trap could identify 49 proteins with an average sequence coverage of 8.9 % and an average ion-score of the fragmented peptides of 30.8 (see Fig. 4.14 a, dashed bars). After merging the mascot results of the three instruments within Scaffold, the number of identified proteins was increased to 118 and the sequence coverage was 12.2 %, while the average observed ion-score was 45.2 (see Fig. 4.14 a, grey bars). These identifications were all based on a FDR of 0 %, i.e. that no decoy hit was tolerated while adjusting the score threshold for accepted identifications. This was done because the number of identifications was well below 100 proteins and for such small datasets, the target-decoy approach was shown to be inappropriate. But because the number of identified proteins was above 100 after

merging the results from the different instruments, the score threshold adjustment was repeated and adjusted to 1.6 % (i.e. one decoy hit in 127 (target + decoy hits) total identifications). This led to 126 identified proteins with an average sequence coverage of 11.5 % and an average ion-score of 45 (see Fig. 4.14 a, chequered bars).

The GeLC-MS analysis was evaluated similarly (see Fig. 4.14 b). After analysis on the MALDI-MS, 540 proteins were identified in the 24 gel-bands with an average sequence coverage of 14.9 % and an average ion-score of 74.1 (see Fig. 4.14 b, black bars). The ion-trap identified 538 proteins while these proteins were identified with an average sequence coverage of 19.2 % and an average ion-score of 38.5 (see Fig. 4.14 b, dashed bars). When the sample was analyzed on the Q-TOF instrument, 512 proteins were identified with a sequence coverage of 27.9 %. The average ion-score achieved was 35.3 (see Fig. 4.14 b, white bars). For all analyses by GeLC-MS mentioned, the FDR was below 0.8 % (see Fig. 4.14 b, legend). After merging the results in Scaffold, the number of proteins being identified increased to 681 at a FDR of 0.58 % (see Fig. 4.14 b, grey bars). The identified peptides spanned in average 26.1 % of the amino acid sequences and were identified with an average ion-score of 51.1.

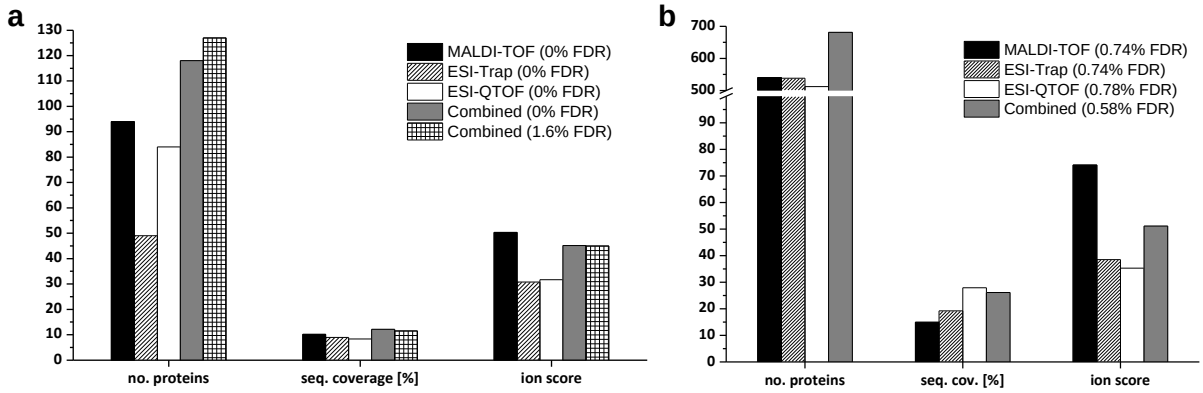

Figure 4.14. Comparison of different LC-MS platforms for the analysis of secreted proteins of primary human hepatocytes in 2D-culture. a) performance parameters for the analysis of a liquid digest (LC-MS); b) analysis of the same sample employing prefractionation by SDS-PAGE and subsequent analysis of in-gel digests of 24 adjacent bands (GeLC-MS). Values obtained for each instrument as well as after merging the database results of all three instruments are shown. In the legend, the corresponding false discovery rates (FDR) are reported.

As for previously mentioned identifications, information about the subcellular location of identified proteins was obtained from Uniprot database and is shown in Figure 4.15. Without prefractionation, 49.2 % of 126 proteins identified were annotated as secreted, 3.2 % were proteins of the cell membrane and 5.6 % were not annotated in the uniprot database. 28.6 % of identifications were annotated as cytoplasmic proteins, 3.2 % belonged to the endoplasmic reticulum (ER) and 1.6 % were lysosomal proteins. 4.8 % were mitochondrial proteins and 4 % were proteins from the cell

nucleus. Out of 681 proteins identified after prefractionation by SDS-PAGE, 23.6 % were secreted proteins and almost 39 % were cytoplasmic proteins. 8.7 % were proteins of the cell membrane and 3.7 % were annotated as being located to the ER. The amount of golgi-derived proteins was 1.8 % and about 2.9 % of identifications were proteins from lysosomes. Furthermore, 6.9 % of the identifications were annotated to the mitochondrion and 3.7 % are located in the cell nucleus. Finally, 0.7 % were annotated as peroxisomal proteins and for 11.2 %, the subcellular location was unknown.

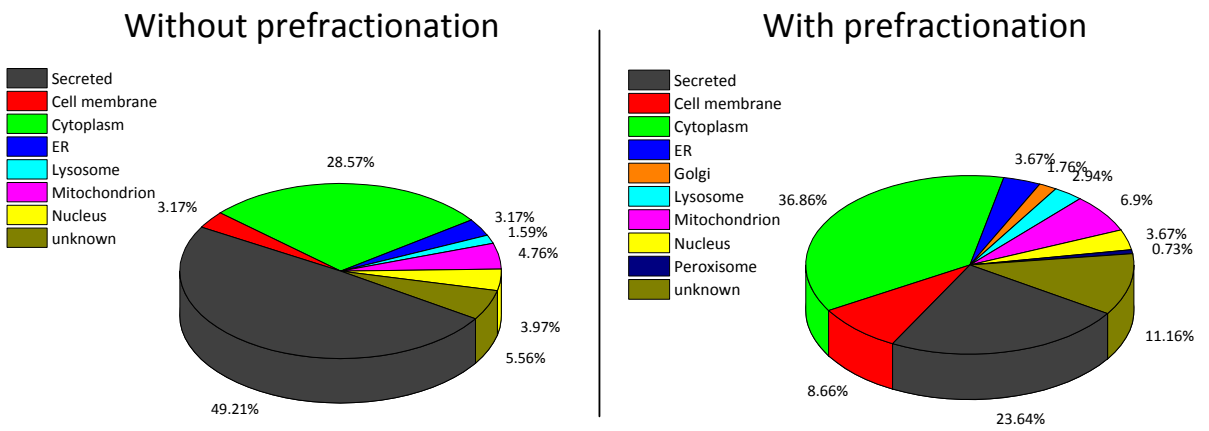

Figure 4.15. Distribution of subcellular locations of identified proteins in the culture medium of primary human hepatocytes cultured in a monolayer culture after merging of results from three different MS-platforms without and with prefractionation of proteins using SDS-PAGE. Subcellular location is reported as described in the UniProt database. ER = endoplasmic reticulum

4.6 Effects of diclofenac on the extracellular proteome of PHH in the bioreactor

Samples from phase II (day 7 to day 10) of the bioreactor cultures treated with diclofenac were analyzed by LC-MALDI and tested for differences in protein expression levels as a result of diclofenac-treatment. The estimation of abundances of identified proteins was performed using Scaffold by means of peptide hit counting, i.e. the number of peptides that led to the identification of a protein, which has been found to be a rough estimate of relative abundances of proteins identified in complex mixtures [Pang *et al.*, 2002; Gao *et al.*, 2003]. Only proteins identified at or above 99 % confidence with at least 4 peptides identified at or above 95 % confidence were included in the analysis. The probabilities were calculated by Scaffold based on algorithms used in PeptideProphet™ [Keller *et al.*, 2002] and ProteinProphet™ [Nesvizhskii *et al.*, 2003]. Although these algorithms are more stringent than the "Mascot delta-score approach" which was employed for protein identification, it was used for quantification because acquired data could be converted into normalized peptide hits directly in Scaffold. Additionally, a one-way Analysis Of Variance (ANOVA) could be applied in Scaffold to detect significant differences in peptide hits. Furthermore, only high-confident identifications were considered for quantification with differences in peptide hits improbably based on under-sampling of peptides. The latter is often observed in proteomic analyses of complex samples when proteins are identified with only few (i.e. 1-3) peptides [Old *et al.*, 2005; Mueller *et al.*, 2008].

20 proteins showed significant differences in assigned peptide hits among the 66 proteins identified with 4 peptides and more in at least one of the three bioreactor cultures as calculated by Scaffold (ANOVA p-vaue < 0.05). After discarding intracellular proteins not being predicted to be possibly secreted *via* non-classical pathways according to SecretomeP, 12 secreted proteins left exhibiting significant differences in peptide hits after application of diclofenac. The normalized peptide hits of these proteins are shown in Figure 4.16 and the estimated up- or down-regulation as well as corresponding ANOVA p-values are listed in Table 4.5.

Four proteins showed an up-regulation upon 6.4 µM diclofenac, namely alpha-1-antitrypsin, fibrinogen gamma chain, histidine-rich glycoprotein and leucine-rich alpha-2-glycoprotein. One protein was found to be down-regulated (4-hydroxyphenylpyruvate dioxygenase) under these conditions. In the group treated with 100 µM diclofenac, eight proteins were up-regulated and two proteins were down-regulated. The proteins with increased abundances in the sample were, in particular: Apolipoproteins A-I and A-IV, Fibrinogen gamma chain, inter-alpha-trypsin inhibitor heavy chain H2, retinol-binding protein 4, histidine-rich glycoprotein, ceruloplasmin as well as alpha-2-

macroglobulin. The two proteins with decreased abundances upon application of 100 µM diclofenac were: cytoplasmic isocitrate dehydrogenase and 4-hydroxyphenylpyruvate dioxygenase. The two down-regulated proteins were the only proteins predicted to be possibly secreted *via* non-classical secretion pathways by SecretomeP.

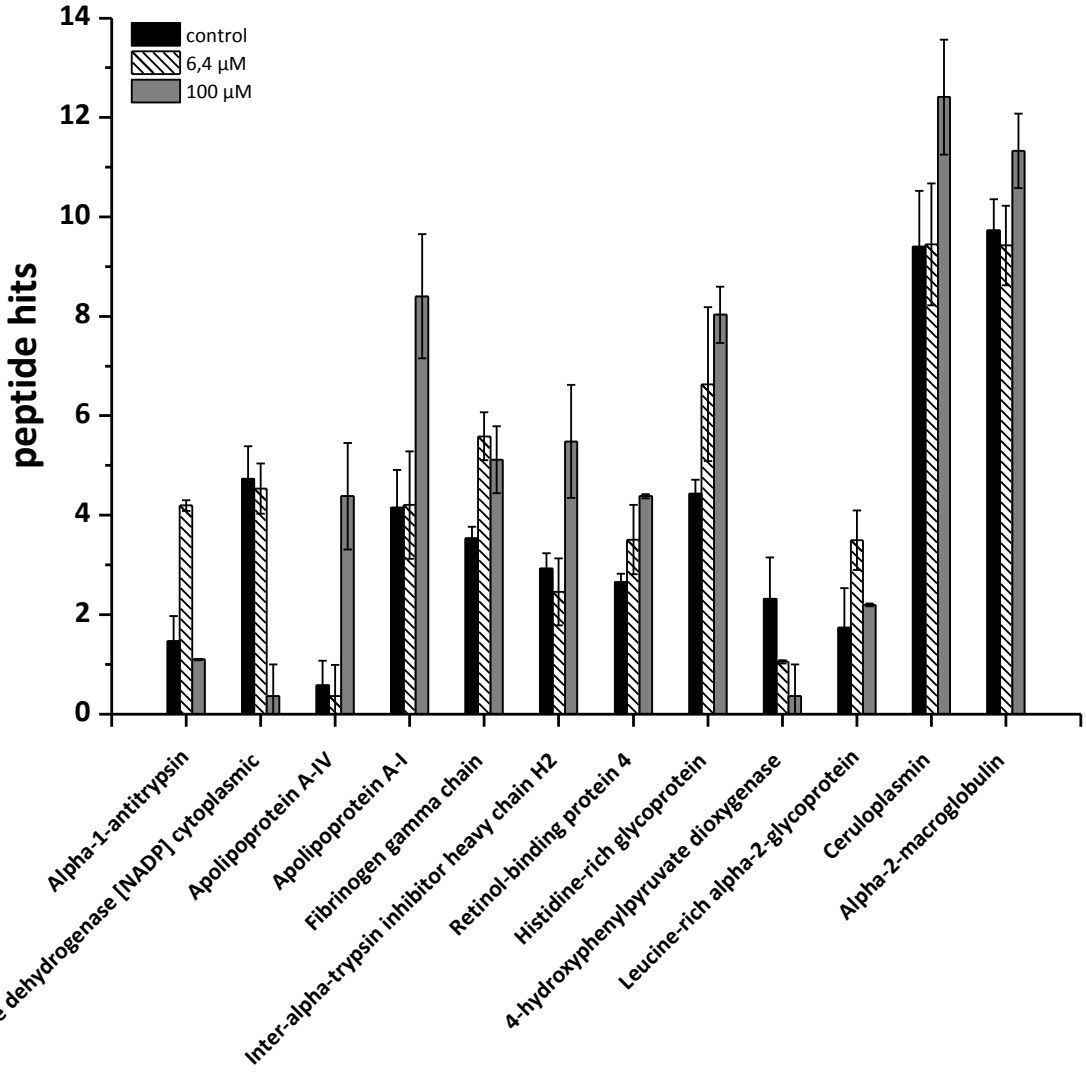

Figure 4.16. Analysis of proteins identified in the culture medium of primary human hepatocytes in a 3D-bioreactor in the pooled samples from day 7 to day 10 (phase II) during application of 6.4 µM and 100 µM diclofenac, respectively. Peptide hits of proteins showing significant deviations in assigned peptides according to a one-way ANOVA test performed in Scaffold are shown. A change in hits indicates a significant change in the abundance of a protein in the sample. Peptide hits were normalized to the total amount of peptide hits in each sample by averaging the peptide counts across all groups, and then multiplying the peptide counts in each sample or group by the average divided by the individual sample or group sum. Error bars indicate standard deviations of three replicate measurements (*n*=3).

Table 4.5. Global regulation of secreted proteins identified in the culture medium of primary human hepatocytes in a 3D-bioreactor in the pooled samples from day 7 to day 10 (phase II) during application of 6.4 µM and 100 µM diclofenac, respectively. all proteins showing significant deviations in peptide hits according to a one-way ANOVA test performed in Scaffold and contain either a signal peptide to enter the classical secretion pathway or are predicted to be secreted *via* non-classical secretion pathways according to SecretomeP are listed. Regarding the regulation, up-regulation of a protein is indicated by +, down-regulation is indicated by -, while no change is indicated by •.

Protein name	ANOVA (p-Value)	Regulation	
		6.4 µM	100 µM
Alpha-1-antitrypsin	0.000026	+	•
Isocitrate dehydrogenase [NADP] cytoplasmic	0.00018	•	-
Apolipoprotein A-IV	0.0011	•	+
Apolipoprotein A-I	0.0038	•	+
Fibrinogen gamma chain	0.0054	+	+
Inter-alpha-trypsin inhibitor heavy chain H2	0.0067	•	+
Retinol-binding protein 4	0.0067	•	+
Histidine-rich glycoprotein	0.011	+	+
4-hydroxyphenylpyruvate dioxygenase	0.020	-	-
Leucine-rich alpha-2-glycoprotein	0.023	+	•
Ceruloplasmin	0.031	•	+
Alpha-2-macroglobulin	0.038	•	+

To independently confirm the significance of changes in peptide hits during diclofenac exposure and to exclude the impact of the "pseudo-replicates", a principal component analysis (PCA) was performed for the 66 identified proteins fulfilling the criteria for identification as stated above. PCA is an approach of multivariate statistics reducing a large number of variables present in a dataset to a fewer number of independent and orthogonal variables, the "principal components", ideally explaining most of the variance within the dataset. As it is shown in Figure 4.17, the three replicates of each group formed clusters while no overlap was observed between the three groups within the 95 % confidence interval. Furthermore, the cluster of the group treated with 6.4 µM diclofenac (see Fig. 4.17, circles) is closer to the control group (see Fig. 4.17, squares) than the group treated with 100 µM (triangles) what is in concordance with the normalized peptide hits also showing larger differences in the group treated with 100 µM diclofenac (see Fig. 4.16). The first two principal components describe the biggest part of variance observed between the three groups. In this case, the percentage of variance described was 48 %.

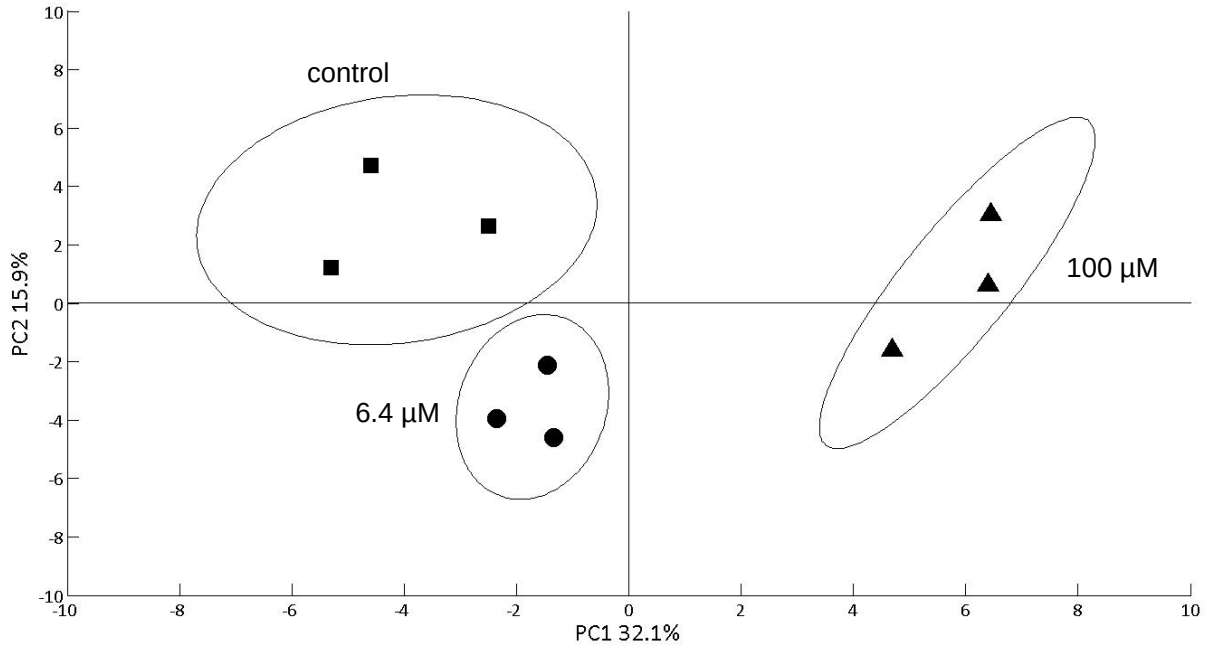

Figure 4.17. Principal component analysis (PCA) of spectral counts of identified proteins in the conditioned medium from PHH during phase II (days 7 to 10) of a 3D-bioreactor culture. Proteins identified with 4 peptides and more were included in the analysis. Diclofenac was applied at two concentrations, 6.4 µM (dots), 100 µM (triangles) plus an untreated control (squares) in three bioreactors filled with hepatocytes from the same donor. 95 % confidence intervals are indicated as ellipses around the clusters. Shown is the PCA-plot for the first two principal components (PC1, PC2) explaining 48 % of total variance within the dataset.

The contribution of the different proteins to variances in the dataset is described by the calculated loading-coefficients ("loadings") in each principal component. The loadings of the first two principal components calculated from observed peptide counts of identified proteins are shown in Figure 4.18. Most of the proteins reported by Scaffold to have significantly different peptide counts as calculated by a one-way ANOVA test (proteins marked with an asterisk in Fig. 4.18) also show the highest loadings for the first principal component. The proteins having low loadings for the first component, however, have a high loading in the second principal component.

Figure 4.18. Principal component analysis (PCA) of peptide counts of identified proteins in the conditioned medium from PHH during phase II (days 7 to 10) of a 3D-bioreactor culture. Calculated loadings for all identified proteins with minimum 4 peptides for the first and second principal component. Proteins likely to be secreted and showing significant differnces in peptide counts are marked with an asterisk.

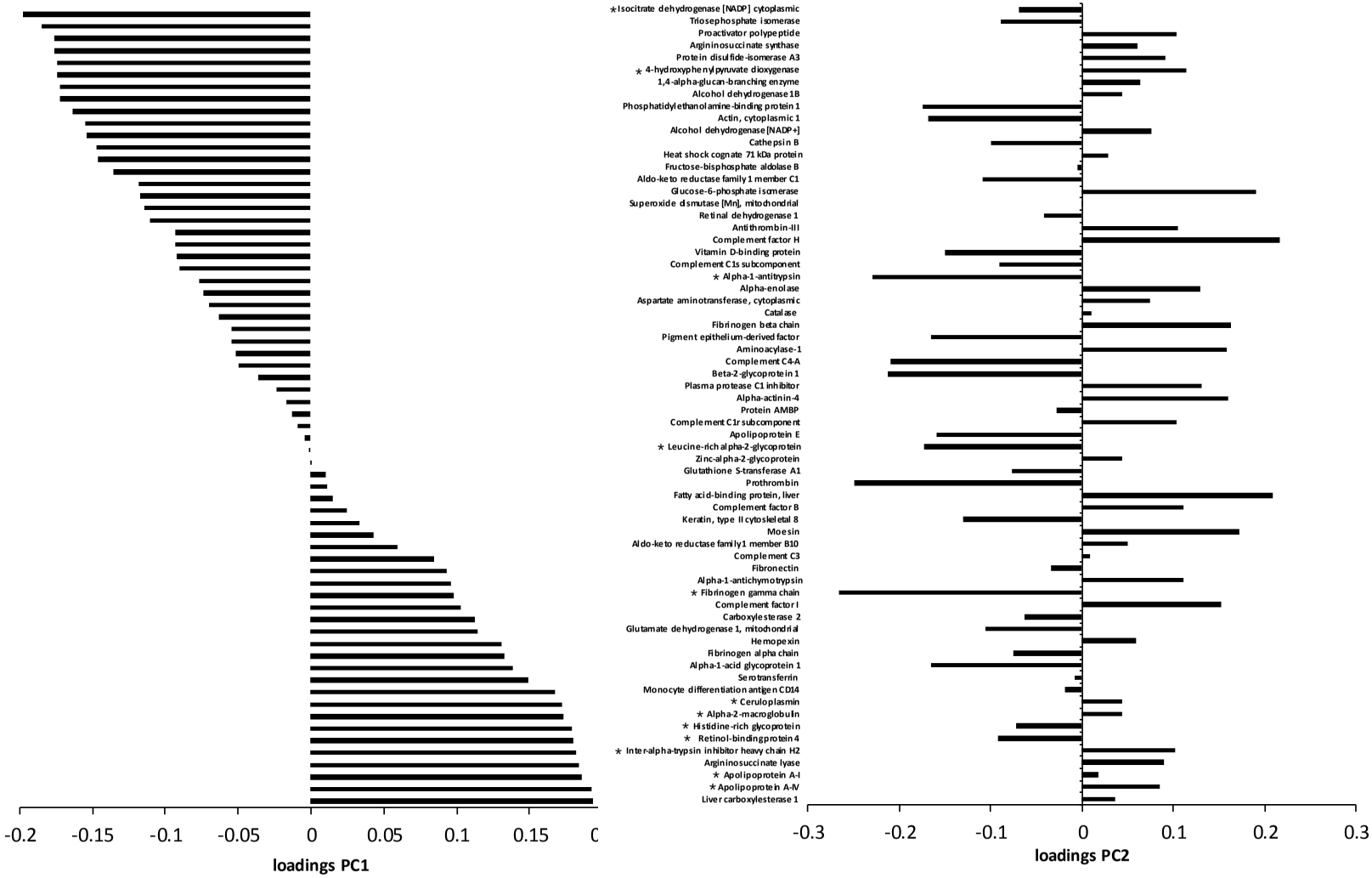

5. Discussion

In the presented thesis, the extracellular proteome ("secretome") of primary human hepatocytes was analyzed by a proteomics approach. For this purpose, an analytical strategy was elaborated which is depicted schematically in Figure 5.1. The workflow comprises sample preparation and LC-MALDI analysis of tryptic peptides after ensuring efficient secretome-analysis by serum-free cultivation of primary human hepatocytes.

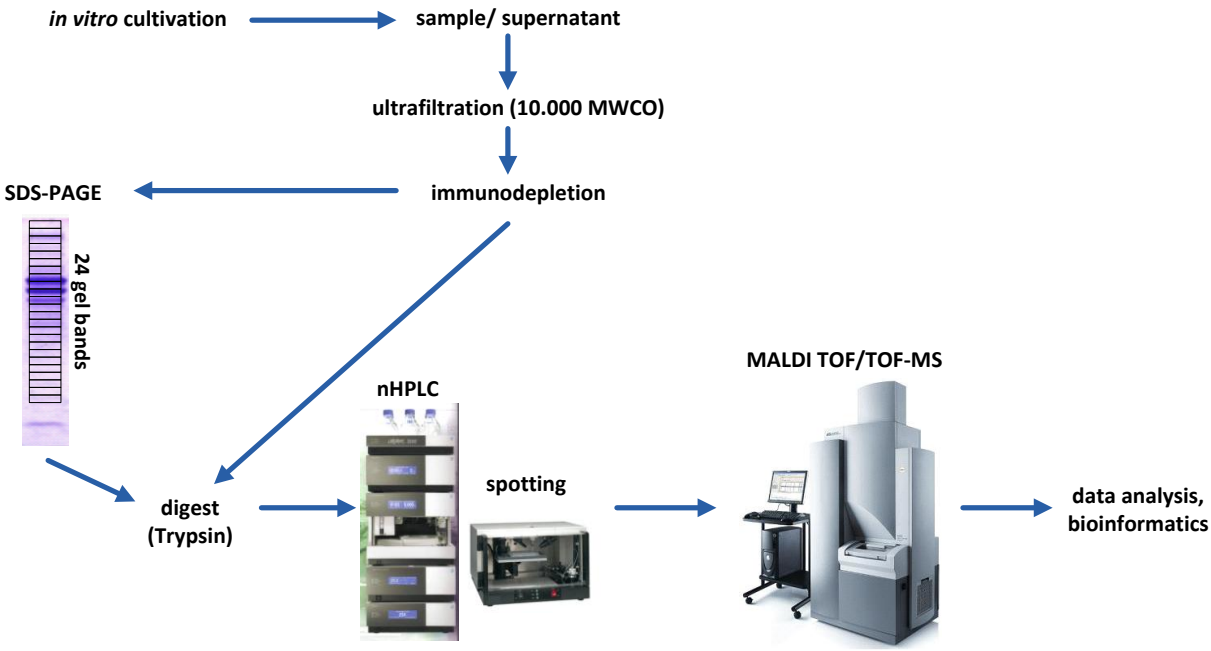

Figure 5.1. Schematic illustration of the workflow for proteomic analysis of the extracellular proteome of primary human hepatocytes elaborated in the course of this thesis. Hepatocytes are cultivated in *in vitro* systems and collected conditioned media are first concentrated and rebuffered by ultrafiltration. High abundant proteins are removed by immunodepletion and the remaining proteins are either directly digested in-solution or in-gel after prefractionation by SDS-PAGE. Resulting peptide mixtures are separated by nano-scale liquid-chromatography (nHPLC) and fractions are automatically mixed with matrix and spotted onto a MALDI-target for subsequent mass spectrometric analysis. Identified proteins after database search are verified and characterized using bioinformatic tools.

The workflow was applied to standard monolayer cultures and results were compared to an organotypic bioreactor culture. Furthermore, the impact of drug-treatment on the secretome of hepatocytes cultivated in the 3D-bioreactor was examined semi-quantitatively by label-free quantification of identified proteins *via* peptide counting. On the following pages, the workflow as well as the obtained results will be critically discussed and compared to the current literature.

5.1 Serum-free cultivation

Each proteomic analysis starts with a sample with both origin and preparation of the sample being crucial for meaningful results. Because artifacts introduced during sample generation and processing are carried through the whole analysis process, these artifacts can lead to wrong conclusions and interpretations made from generated data. Therefore, both steps have to be tightly controlled and optimized.

The first step was to optimize the cultivation of primary human hepatocytes to allow secretome analysis using conditioned media. Fetal calf serum (FCS) is commonly used in mammalian cell culture because attachment to the surface of culture dishes and survival of cells *in vitro* is strongly dependent on such a supplement. However, it is a known obstacle in secretome analysis because proteins of bovine origin hamper identification of proteins secreted by the cells of interest. Even if the amount of supplemented serum is reduced from the commonly applied 10 % to amounts as low as 0.5 %, efficient secretome analysis remains extremely difficult [Dowling and Clynes, 2011]. In the case of hepatocytes, this obstacle is even more challenging to overcome because the proteins present in bovine serum closely resemble proteins secreted by hepatocytes. *In vivo*, the liver is the organ producing the major part of serum proteins such as carrier-proteins (e.g. albumin, transferrin, haptoglobin), protease-inhibitors (e.g. antitrypsin) or complement factors [Miller and Bale, 1954]. These proteins show a high degree of homology between different species. For example, human and bovine albumins share more than 76 % of their amino-acid sequences. Because MS-based protein identification relies on determination of amino-acid sequences of peptides which are subsequently assigned to a specific protein, this approach can hardly distinguish between human or bovine proteins in the supernatant of hepatocytes. An unambiguous identification is possible only if “unique” peptides, i.e. peptides only present in the protein of one species, are identified, which is not guaranteed in complex samples. Furthermore, the sequence coverage of a protein, i.e. the fraction of the amino acid sequence that could be identified by LC-MS is - amongst others - a function of its abundance in the sample. Generally speaking, the lower the concentration of a protein in a sample, the lower is the sequence coverage. In fact, this correlation is the basis of label-free quantification of proteins by peptide hit counting [Pang *et al.*, 2002] and spectral counting [Liu *et al.*, 2004], in which the number of identified peptides/spectra for a specific protein is used as an estimate of its abundance in the sample. Adding fetal calf serum means adding complexity, both in terms of protein number and protein abundance. Especially for low abundant proteins which are most likely to serve as biomarker candidates, the presence of serum proteins can eliminate the possibility of identification and quantification. As such, FCS has to be removed from cultures prior to collection of

conditioned medium or better completely avoided during cultivation of mammalian cells for efficient analysis of secreted proteins. The masking of secreted proteins by supplemented serum proteins was proven by LC-MALDI analysis of samples from FCS-supplemented bioreactor cultures before and after switching to serum free conditions. The bovine proteins remained in the bioreactor for at least 5 days, especially the bovine albumin as the most abundant protein in bovine serum. Identifications were severely impaired with only low numbers of both human and bovine proteins being identified. The possibility of serum-free cultivation of primary hepatocytes in the bioreactor was previously not considered by the scientists at the Charité, because the bioreactor was predominantly used in morphologic and drug metabolism studies which can be performed in the presence of FCS. However, with beginning of the HEPATOX project and realizing the problems for proteome analysis, the possibility of serum-free inoculation and cultivation was tested and shown to be possible without reduction of culture quality. This fact points out the exceptional position of the hollow-fiber bioreactor among the 3D-culture systems, because no cultivation technique using standard medium without specific growth factors is able to keep primary hepatocytes alive for more than a few days. In regard to proteome analysis, conducting a FCS-free cultivation in the bioreactor was, as expected, very advantageous. The number of identified proteins was more than ten times higher but this is discussed later. Finally, ethical concerns evolving from conducting animal experiments in toxicological studies and other disciplines of life-science also imply the necessity for banishment of animal serum from *in vitro* cultivation. Additionally, because of large batch-to-batch variances, any new batch of purchased FCS has to be tested for applicability for primary hepatocytes. This is another reason for the need of standardized media ensuring survival of cells and replacing animal serum.

The general physiological and biochemical parameters during serum-free monolayer cultivation were determined to identify the optimal timepoint for secretome collection. Both carbohydrate metabolism and enzyme release indicated that the cultivation of primary hepatocytes for a longer period than 48h resulted in a decreased carbohydrate uptake and increased release of intracellular enzymes. Additionally, the amount of produced protein per day was decreasing rapidly after 48h when it was normalized to the amount of released LDH as a measure of occurring cell death. This finding is in accordance with other secretome studies in hepatic, but also other cell lines in which the period of serum-free cultivation was not exceeding 48h to avoid contamination by intracellular proteins leaking from dead cells [Chevallet *et al.*, 2007; Planque *et al.*, 2009; Lewis *et al.*, 2010; Van Summeren *et al.*, 2011]. However, the monolayer cultures examined here exhibited liver specific functions over the whole cultivation time of 96 h as it was shown by a constant release of albumin and urea, but the values started to decrease after 72h. Other groups already showed that primary hepatocytes cannot be cultivated in standard monolayer cultures for a longer period (i.e. more than

72h) because cells start to dedifferentiate and lose their liver specific functions regardless of presence or absence of FCS [Tuschl and Mueller, 2006; Godoy *et al.*, 2009; Zeilinger *et al.*, 2011]. If the aim is to perform short-term toxicoproteomics studies, the limited lifespan of monolayer cultures is not a constraint, but when it comes to long-term studies aiming to detect biomarkers for late-onset or chronic toxicity of a drug, other cultivation techniques must be applied. The introduction of the bioreactor was a big step towards the possibility of examining longer-term and chronic toxicity especially after recent down-scaling [Zeilinger *et al.*, 2011]. In earlier studies, porcine hepatocytes were shown to maintain liver functionality for up to one month using this bioreactor technique [Zeilinger *et al.*, 2004]. Also our group confirmed that bioreactor cultures of primary human hepatocytes maintain liver like properties for up to 2 weeks and constant oxygen consumption rates indicated viability even 3 weeks after inoculation with a constantly low release of intracellular enzymes [Mueller *et al.*, 2011b]. During FCS-free bioreactor cultivation, constant protein and albumin production rates were observed.

5.2 Sample preparation

The proteins secreted by hepatocytes are extremely diluted in the large volume of cultivation medium with concentrations in the low µg/ml range requiring concentration of conditioned media before analysis. Furthermore, culture media contain large amount of salts interfering with most proteomic techniques. Different strategies have been employed for desalting and concentrating conditioned media from cell cultures but the most often applied techniques are ultrafiltration and precipitation by trichloroacetic acid (TCA), the latter being carried out with and without the help of carriers like sodium lauroyl sarcosinate [Chevallet *et al.*, 2007; Skalnikova *et al.*, 2011]. Dowell and co-workers found ultrafiltration to be superior to TCA-precipitation regarding sample recovery [Dowell *et al.*, 2009]. More recently, it was shown that each of the concentration methods has its advantages, either in sample recovery (ultrafiltration) or number of identifiable proteins (precipitation). But they also give different information about the secretome and should therefore be considered as complementary approaches [Cao *et al.*, 2011]. In this thesis, the choice was made towards ultrafiltration because it allowed fast concentration and rebuffering. Proteins could be recovered in high yields and in their native forms which was required for the immunodepletion procedure following the concentration/desalting step.

Immunodepletion became a standard technique in preprocessing of human plasma and serum samples because it allows analysis of low abundant proteins not detectable without depletion of the high abundant proteins present in serum [Echan *et al.*, 2005]. In this thesis, the application of immunodepletion to the analysis of the hepatocyte secretome was shown to be a valuable tool

reducing the range of protein concentrations in the samples. The number of identified proteins in the supernatant of monolayer cultures was almost doubled by depletion of four high abundant proteins, namely transferrin, albumin, alpha-1-antitrypsin and haptoglobin illustrating the beneficial contribution of this technique to secretome analysis of hepatocytes. However, as for (almost) all steps in proteomic sample preparation, there is a risk of losing sample material in the course of the depletion procedure. The observed sample loss was estimated to almost 25 % as determined *via* Bradford assay performed before and after depletion. Additionally, 50 % of total protein was removed as high abundant proteins reducing the amount of depleted material to be analyzed and thus increasing the required quantity of starting material. What should be mentioned is the fact, that albumin binds many molecules including small proteins and peptides. It binds so diversely, that a distinct term called Albuminome [Gundry *et al.*, 2007] has emerged. The risk of removing possible identification candidates by the depletion of albumin is well known but for the immunodepletion column used during this work it has been shown that it removes the lowest number of non-targeted proteins compared to other depletion devices [Gundry *et al.*, 2009; Bellei *et al.*, 2011]. Analysis of the bound fraction led to identification of 13 proteins. Undesired removal of albumin-bound proteins could partially be overcome by using an organic solvent during ultrafiltration (e.g. 10 % Acetonitrile), thus reducing the non-covalent interactions. But this could also diminish the binding-efficiency to the depletion column and also lead to a faster degradation of the affinity resin. Therefore, and because the advantages outweighed the disadvantages, the depletion column was used as proposed by the manufacturer without any modifications. One drawback of the spin-cartridge format used in this work is the low throughput but a column-format is available which can be implemented in standard HPLC-instruments increasing the number of processed samples per time in an automated work-flow. Furthermore, there are columns available capable of removing up to 14 high abundant proteins from human plasma samples with 10 of them also being identified during this thesis in the upper third of identifications if ordered by identified peptides and thus by their abundance in the sample. These columns could be applied for immunodepletion of samples from hepatocyte cultures, further increasing the depth of the analysis. Only one other study was found in PubMed using immunodepletion for *in vitro* secretome analysis, in this case using HepG2 cells [Lewis *et al.*, 2010].

5.3 LC-MALDI analysis

The solvent composition used for chromatographic separation of tryptic peptides was optimized using a commercial peptide standard and was determined to be 9 to 40.5 % acetonitrile. When this gradient was applied to real samples, it became obvious that there is still room for further optimization. The fraction of more hydrophilic peptides was much larger in the real sample than in

the protein standard used for gradient optimization. When separating the standard mixture, the first minutes showed only few well-separated peptides (see Fig. 4.4 b, red chromatogram). In contrast, the chromatogram of the real sample showed many peptides from minute 20 to 40. Furthermore, the elution window of the real sample is not that broad towards the end of the gradient as determined for the digest of six standard proteins. No peptides elute after 70 minutes which corresponds to a percentage of acetonitrile of about 31.5 %, in contrast to the determined amount of 40.5 % for elution of the biggest part of peptides from the six-protein standard mixture. This could be due to a loss of hydrophobic peptides during sample preparation, i.e. adsorption of these peptides to the wall of the reaction tube and/or the HPLC vial, even though special tubes were used during sample preparation for which protein binding is reduced to a minimum. Another reason could be aggregation of hydrophobic parts of the proteins during digestion protecting them from being thoroughly digested and consequently from being detected after the second ultrafiltration step designated for the removal of trypsin and uncompletely digested polypeptide chains from the digestion mixture. For further optimization studies, more appropriate standards should be applied that contain many proteins in different - but known - concentrations to simulate a complex sample more realistically. One such standard was recently introduced as the SC-200 proteomics standard mixture [Bauman *et al.*, 2011]. It was developed at the **S**eattle **C**hildren`s Hospital and consists of **200** proteins with known identities and molar concentrations derived from 6 microbial genomes, thus ideally suited to develop and optimize proteomic workflows for analysis of complex samples. Containing 200 proteins, this standard is in the same range as the number of identified proteins in the secretome of primary human hepatocytes described in this work. Additionally, as this standard consists of proteins, the optimization would start already at the sample preparation, i.e. digestion step which was not the case for the commercial standard that consisted of peptides after digestion. In this thesis, the success of digestion of real samples was confirmed by SDS-PAGE as the absence of distinct protein bands after over-night digestion (data not shown).

A nano-scale HPLC was purchased and coupled to an automated fraction collection robot capable of automatic matrix addition and deposition of eluting fractions as spots on a blank target for LC-MALDI analysis. The ratio of added matrix was the same as described for the analysis of proteins from *C. glutamicum* [Lasaosa *et al.*, 2009a; Lasaosa *et al.*, 2009b], i.e. 4 parts of matrix (3 mg/ml CHCA) were mixed at a flow-rate of 1.2 µl/min with one part of sample eluting from the column at a flow rate of 0.3 µl/min. This provided an appropriate matrix concentration on the target (i.e. 2.4 mg/ml) comparable to the determined optimal concentration used for manual spotting of in-gel digests. Additionally, when the fraction collection interval at these flow-rates was set to 12 seconds, the applied flow-rate and mixing-ratio provided spot volumes of about 0.3 µl per fraction, ensuring

homogenous co-crystallization within the spots as well as appropriate spot diameters (about 1.2 mm) after evaporation of solvents. Larger spot volumes obtained by increasing the fractionation intervals would increase the measurement time because more laser shots had to be accumulated and would cause a loss of separation. Smaller spot volumes would result in a loss of sensitivity by limited sample amounts within each fraction and a reduced number of acquirable MS/MS spectra per spot. The latter was also the reason for fragmenting the weakest precursors per fraction first in the second and third run because the amount of peptides in each fraction decreases during acquisition of several MS/MS spectra. The laser desorbs not only the precursor that is meant for fragmentation but rather all peptides contained in the spot or at least the peptides that ionize well. The selection of a specific mass (i.e. peptide) for fragmentation is achieved after the ion source by the timed-ion-selector (TIS) of the MALDI-TOF/TOF instrument. Hence, the probability of acquiring a high-quality fragment spectrum of a peptide present at low amounts in the spot is increased if this low-abundant peptide is analyzed as early as possible during MS/MS acquisitions. The choice of this strategy is supported by the fact that more than a quarter (26.5 %) of identified proteins in the monolayer culture could have been identified only in the two runs (runs 2 and 3) in which the acquisition started with the weakest precursor. If the acquisition started with the strongest precursor, the percentage of identifications unique to this run was only 5.3 %. An additional strategy to increase the number of identifications could be the generation of an exclusion list of all identified peptides during the first and second run to minimize redundant acquisition in the third run as described in [Chen *et al.*, 2005]. Future studies should also optimize the matrix to analyte ratio, which is a critical parameter when performing MALDI as it influences the ionization efficiency of the analytes. This could be done by varying the injected amount and/or applied matrix concentration.

5.4 Influence of the type of ionisation and sample prefractionation

A sample after 96h of serum-free monolayer cultivation with and without prior prefractionation by SDS-PAGE was analyzed on three different MS-platforms commonly used in proteomic analyses. On one hand the LC-MALDI platform used in our laboratory coupling chromatographic separation off-line to a MALDI-TOF/TOF instrument and on the other hand, two MS-platforms in which chromatographic separation is coupled on-line to either a linear ion-trap or a hybrid quadropole time-of-flight instrument (QTOF) employing electrospray-ionization (ESI). It was shown that the number of identified proteins was increased for both unfractionated and fractionated samples using the MALDI-instrument. One reason for the differences may lie in the mass accuracy of the three mass analyzers. The MALDI-instrument is able to achieve an average mass accuracy of about 15 ppm using internal calibraton of the mass spectra, the Q-TOF has an accuracy of less than 2 ppm using the lock-

mass option and the ion-trap is only capable of an average mass-accuracy around 80 ppm. The number of “applicants” for determination of the identity score in mascot algorithm is accuracy-dependent, i.e. the lower the mass accuracy, the higher the number of peptides that could match to a precursor mass. This results in a higher identity threshold and reduces the number of assigned peptides for a given ion score. One reason why the MALDI-TOF/TOF could outplay the high-mass accuracy of the Q-TOF probably lies in the different ways of spectra acquisition. During ESI-MS, the MS/MS spectra are acquired “on the fly” during elution with a specific exclusion of peptides (i.e. mass values) for a specific time (usually in the range of 5-15 seconds). The offline LC-MALDI approach, however, uses the advantage of deposition of fractions on a MALDI-target and thus “freezes” the separation in time. This provides the opportunity to acquire MS/MS spectra at the apex of the elution-peak of a precursor after a MS scan of all spotted fractions, significantly increasing the sensitivity. Furthermore, more time can be spent on one single MS/MS spectrum gaining intensity of fragment peaks and thus increasing the average score and overall identifications. The most probable reason, however, is the applied solvent gradient used for peptide separation. For LC-MALDI analysis, the slope of the solvent gradient was 0.38 % ACN per minute while during LC-ESI, the slope was 0.71 and 0.82 % ACN per minute for the ion trap and for the Q-TOF, respectively.

For the analysis of in-gel digests, the slopes were only slightly different (1.1-1.4 % per minute) and consequently, the difference in number of identified proteins between the three instruments was marginally. The separation by SDS-PAGE is a common approach for reduction of complexity prior to LC-MS [Brewis and Brennan, 2010]. In this thesis, it increased the number of identified proteins tremendously. More than five times the number of identifications could be achieved using the GeLC-MS approach in contrast to the 1D-LCMS analysis of the liquid digest for all of the three platforms, for the ion-trap the increase is even 10-fold. Furthermore, the sequence-coverage was more than doubled for the two ESI-instruments, for the MALDI the increase was 1.5-fold. The average ion-score also increased by the reduction of sample complexity, especially for the MALDI-workflow (increase from 50 to 74). However, the differences in identified proteins are not as large as in the unfractionated sample. This could imply that MALDI is better in identifying proteins from very complex samples but if the complexity is reduced, the instruments are not as different regarding identification efficiency. Notably, the amount of injected material from in-gel digests in the MALDI-based analyses was only half of the amount used in the ESI-based analyses because of detector saturation when injecting the whole extract from in-gel digests as it was done in ESI-analyses. Of course, this could also be the reason for the lower increase in the number of identified proteins.

The combination of mascot search results from three instruments for each of the analytical strategies resulted in an increased number of identifications as well as sequence coverage for both approaches. 110 proteins were identified by both approaches and, as expected, many of the proteins were identified only in the sample that underwent prefractionation by SDS-PAGE (571 proteins). One could assume that all of the proteins identified in the liquid digest should also be identified by the GeLC-MS approach because of decreased sample complexity due to prior prefractionation. However, there were 16 proteins present in the liquid digest that were not captured by the gel-based strategy (see Table 5.1).

Table 5.1. Identified proteins in the supernatant of primary human hepatocytes by one dimensional LC-MS only. Given are the Swiss-Prot accession number (no.), the protein name, the molecular weight (MW) and the number of peptides assigned to each protein (pep.)

accession no.	protein name	MW [kDa]	pep.
Q96M02	Uncharacterized protein C10orf90	77.9	1
Q13505	Metaxin-1	51.5	1
Q99969	Retinoic acid receptor responder protein 2	18.6	2
P07737	Profilin-1	15.0	2
P09382	Galectin-1	14.7	2
P52758	Ribonuclease UK114	14.5	3
P07148	fatty acid binding protein liver	14.0	5
O60814	Histone H2-B	14.0	3
P14174	Macrophage migration inhibitory factor	12.5	2
P10599	Thioredoxin	11.7	1
P20962	Parathymosin	11.5	2
P62805	Histone H4	11.4	2
P02655	Apolipoprotein C-II	11.3	2
P04080	Cystatin-B	11.1	1
P61604	10 heat shock protein, mitochondrial	10.9	1
P02656	Apolipoprotein C-III	10.8	1

Most of these proteins were in the low-molecular weight range between 10 and 19 kDa, while the tool to cut the gel-lanes reached from the top of the gel to about 20 kDa. Hence, these proteins could not be identified, just because they were not cut. The liquid digest did not suffer from this kind of restrictions, thus allowing the identification of small proteins down to the applied cut-off during ultrafiltration, in this case 10 kDa. The two proteins identified having a molecular weight above 20 kDa, namely Metaxin-1 and an uncharacterized protein which gene lies on chromosome 10, orf 90, were identified by one peptide. A big advantage of the GeLC-MS approach is the increased sequence coverage, facilitating unambiguous identification of proteins. As an example, Complement 4-A was

reported for the liquid digest together with Complement 4-B, two genes for the same protein that have a distinct polymorphism and lie on different alleles in the human genome. However, in the gel-based analysis, only Complement 4-B was reported, because the specific peptide distinguishing the two isoforms was identified leading to the exclusion of 4-A isoform as a possible candidate.

Summarizing, the three different instruments or better the two different ionization methods are highly complementary in regard to protein identification as it was already shown previously [Bodnar *et al.*, 2003]. Furthermore, the prefractionation step was very advantageous for the in-depth analysis of proteins in the conditioned medium of primary human hepatocytes. The almost 6-fold increase in identified proteins favours this prefractionation step for secretome analysis, although the fraction of secreted proteins is reduced. However, because the total number of identifications is that much higher, the total number of secreted proteins is also elevated. An important drawback of the prefractionation is the tremendous increase in analysis time. One sample is divided in at least 24 samples, increasing the measurement time by a factor of about 12. For the MALDI analysis, this corresponds to an increase from 11 hours to almost 130 hours just regarding the measurement time, excluding increased time needed for sample preparation and post-processing of the acquired data. This could be reduced in future experiments by shortening the run-time of the SDS-PAGE just until the proteins are separated in the first third of the separation gel. This would prefractionate the sample but with a reduced number of fractions being a compromise between complexity- and analysis time reduction. In this strategy, the whole sample could be analyzed without losing low molecular-weight proteins as mentioned above.

5.5 Donor-to-donor variance of identified proteins

During preliminary experiments, the supernatants from monolayer cultures of primary human hepatocytes from three different donors were analyzed without prior immunodepletion. Supernatants were collected after 24h of cultivation and analyzed by LC-MALDI. 144 proteins were identified in the sample of donor 1. In the sample of donor 2, 72 proteins were identified and for donor 3, 74 proteins were identified. For all Identifications, the FDR was adjusted to 0% by not allowing any decoy hit during score threshold adjustment. The total number of proteins identified from these three samples was 163, and the distribution of the proteins among the samples is shown in Figure 5.2.

Only 25 % (40) of proteins were identified in all three samples, which is much below the run-to-run reproducibility of the analytical workflow (60 %), thus indicating differences in sample composition due to the different donors. Interestingly, 37 % of identifications were only found in the sample of

donor 1 and it was assumed that this could be due to a higher amount of intracellular proteins leaked into the culture medium during cultivation. However, the percentage of intracellular proteins was found to be 55 %, which is exactly the same as for donor 2.

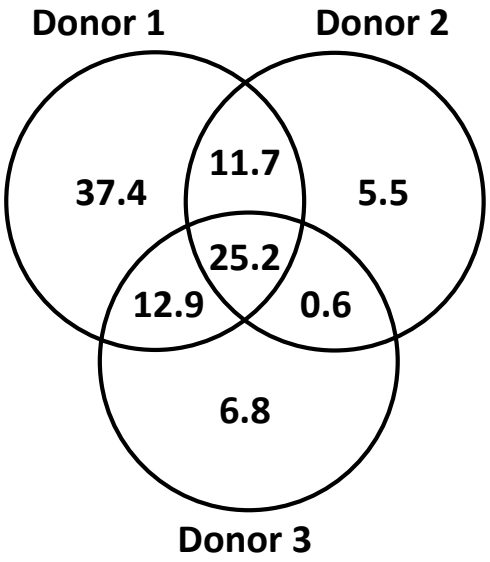

Figure 5.2. Overlap in identified proteins in the secretome of PHH of three different donors after 24h in monolayer culture. Samples were concentrated by ultrafiltration, digested using trypsin and analyzed by LC-MALDI. Overlaps are given as percentage of total identified proteins.

For donor 3, the intracellular proteins accounted for only 28 % of total identifications. 69 % of the commonly identified proteins in all three donors were annotated as secreted and 50 % of the proteins overlapped in at least two donors indicating that there exists donor to donor variability in secreted proteins already at the qualitative level. This is in consistence with other studies where several donors were compared regarding general physiological and metabolic parameters [Mueller *et al.*, 2011b].

5.6 Prediction of secreted proteins

In this thesis, the secretome is defined as the whole range of proteins released by the hepatocytes into the culture medium by active secretion, either by classical or non-classical secretion pathways. To enter the well-described classical secretion pathway, proteins need a signal peptide that directs the translating ribosomes to the endoplasmic reticulum (ER). The nascent polypeptide chain is co-translationally translocated into the lumen of the ER and proteins are secreted by exocytosis after traveling through the Golgi apparatus [van Vliet *et al.*, 2003]. Alternatively, proteins can be secreted via non-classical secretion pathways circumventing the route through the ER and Golgi but these pathways are not yet fully understood [Nickel and Rabouille, 2009]. However, it exists an online tool

(SecretomeP) that was shown to predict secretion via non-classical pathways of candidate proteins quite accurately based on their amino acid sequence [Bendtsen *et al.*, 2004]. The subcellular localization of identified proteins reported in the results section was based on the annotations in Uniprot. These annotations come mostly from the published literature and are manually reviewed, but proteins could also have different localizations that were not yet discovered. Hence, all identified proteins were examined for the presence of a signal peptide as reported in the Uniprot database using DAVID and if this feature was lacking, proteins were checked for possible secretion using SecretomeP to predict all possibly secreted proteins and also find proteins having a signal peptide not annotated in Uniprot. Meanwhile, this strategy is commonly applied when secretomes are analyzed [Skalnikova *et al.*, 2011].

In the supernatant of the monolayer culture, a total of 126 proteins were identified. 75 % of these proteins possessed a signal peptide and another 11 % were predicted to be secreted by SecretomeP. In the sample of phase I of the bioreactor culture, 133 proteins were identified in total. 53 % featured a signal peptide while another 20 % were predicted to be non-classically secreted. Among the 250 proteins identified in the sample of the second phase of the bioreactor culture, 46 % contained a signal peptide and further 20 % were possibly non-classically secreted. In summary, 86 % (109 proteins) of proteins identified in monolayer culture, 73 % (98 proteins) of proteins during phase I and 66 % (165 proteins) of proteins identified in the sample of phase II of the bioreactor were found in the conditioned medium as a result of active secretion.

Several studies analyzed the liver secretome using hepatocellular carcinoma cell lines [Zwickl *et al.*, 2005; Yamashita *et al.*, 2007; Lewis *et al.*, 2010], primary rat hepatocytes in sandwich culture [Farkas *et al.*, 2005] or perfused rat liver [Zhang *et al.*, 2010]. But so far, only one study analyzed the secretome of primary human hepatocytes (PHH) in monolayer culture [Slany *et al.*, 2010]. In this study, the cytoplasmic and extracellular proteomes of PHH and two hepatocellular carcinoma cell lines (HepG2 and Hep3B) were analyzed by two-dimensional gel-electrophoresis and LC-MS. Secreted proteins were accepted based on the same criteria as in this thesis, namely the presence of a signal peptide or positive prediction by SecretomeP. The authors found 72 secreted proteins in the conditioned medium of a standard monolayer culture of human hepatocytes collected after 24h of serum-free cultivation. 46 of them were reported to be plasma proteins. As mentioned above, the number of possibly secreted proteins identified in monolayer culture in this work was almost 50 % higher (109), with 56 of them being known plasma proteins. Furthermore, among the proteins we identified in the secretome of PHH, there were 11 proteins that were claimed by Slany *et al.* to be expressed only in HepG2 cells. On the other hand, Slany and co-workers identified 19 proteins in the

secretome of PHH that were not found in this thesis. One of the proteins identified by Slany but not in this work was albumin, which could not been identified due to the preceeding immunodepletion. Another one was alpha-fetoprotein, a known marker for hepatic tumors that should only be expressed by fetal liver and liver tumors but not adult hepatocytes [Wu, 1990; Marrero and Lok, 2004] and should not be present in cultures of primary hepatocytes derived of an adult liver. 13 of the 19 proteins were identified with only one peptide, thus indicating that these proteins were present in low abundance and may have been lost during immunodepletion which was not performed during sample preparation by Slany *et al.* However, most of the 11 proteins identified in this thesis and not found by Slany (i.e. 8) were identified with more than three peptides. Another reason for the differences could be the different instruments used for identification. Since Slany et al. used an LC-ESI-MS for identification of proteins the differences could be a result of the different ionization methods, especially for proteins detected with only few peptides. Nevertheless, the list of proteins found to be secreted by PHH in monolayer culture during this thesis is the most extended reported up to now, but further studies will surely lead to identification of additional secretory proteins of PHH especially because of the plethora of complementary proteomics techniques that can and will be used for secretome analysis in the future.

5.7 Impact of cultivation technique on the secretome

An interesting question is if the secretome of PHH in monolayer culture differs to the secretome when the cells are cultivated in a three-dimensional environment like the bioreactor used in this work. A first investigation was performed on the level of detectability. In the bioreactor, the secreted proteins have to pass the membranes surrounding the cell compartment of the bioreactor to be identified in the conditioned medium, while the monolayer culture does not suffer of such limitations since proteins are released directly into the conditioned medium covering the cells. Although the membranes in the bioreactor have a molecular weight cut-off of about 500 kDa [Zeilinger *et al.*, 2004], it was questionable if proteins could diffuse through the membranes and subsequently be identified in the conditioned medium. Therefore, the identified proteins in each culture condition were ordered by size and the distribution between the different culture conditions and/or culture phases in the bioreactor was examined (see Fig. 5.2).

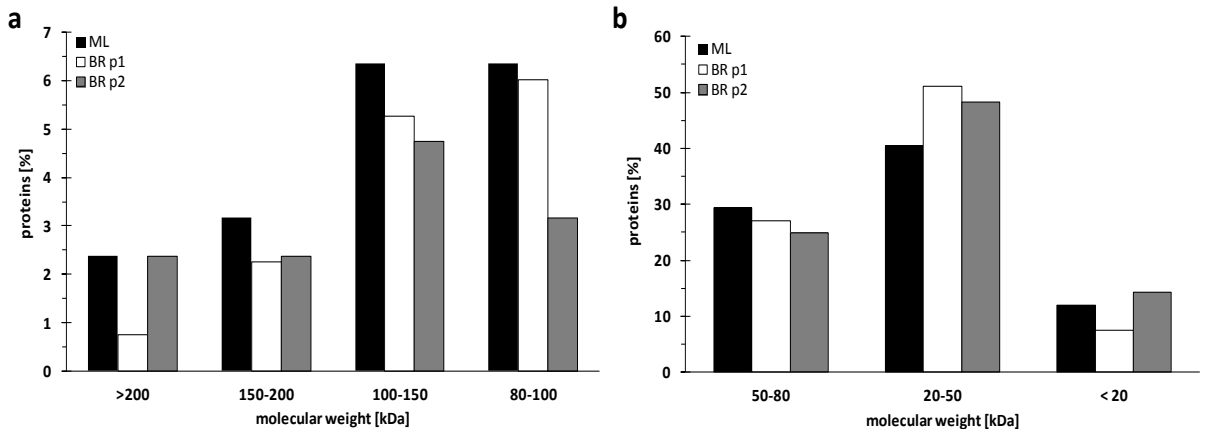

Figure 5.2. Size distribution (in kDa) of identified proteins in the secretome of PHH in monolayer culture (ML) and during phase I (days 4-6; BR p1) and phase II (days 7-10; BR p2) of a three-dimensional bioreactor culture. The percentage of identified proteins with a molecular weight above (a) and below (b) 80 kDa is shown.

Indeed, more proteins with a molecular weight above 200 kDa were identified in the monolayer culture and the later phase of the bioreactor but not in the early phase of the three-dimensional culture (see Fig.5.2 a). This indicates that larger proteins need longer to diffuse out of the cell compartment but can, in principle, be detected. Smaller proteins were comparably distributed in the two culture conditions and the two phases of the bioreactor, except for the proteins between 80 kDa and 100 kDa, for which the percentage was lower in the second phase of the bioreactor. In conclusion, the presence of the membrane-barrier showed only minimal effects on the detectable proteins in regard to their protein size, but a delayed appearance of larger proteins in the conditioned medium of bioreactor cultures was observed.

A further concern was the contamination of the secretome by intracellular proteins released into the bioreactor. Compared to the proteins identified in monolayer culture, the proportion of proteins known to be secreted in the samples from the bioreactor cultivation was reduced. During phase I of the bioreactor, the percentage of secreted proteins is about two-third the number of secreted proteins in monolayer culture, while in the second phase, the number of proteins known to be secreted is only one half of the proteins in standard monolayer culture. Most probably, this is due to the fact that the bioreactor is perfused in recirculation mode with fresh medium being added in low rates of about 0.5 ml per hour. This results, at first sight, in a complete replacement of medium in the bioreactor circuit (total volume is 12 ml) during one day of cultivation, comparable to the daily medium change in monolayer cultures. But, in fact, the medium in the bioreactor is rather continuously diluted with fresh medium. Thus, the intracellular proteins released from dying cells can accumulate in the system resulting in a reduced fraction of secreted proteins. Consequently, the percentage of intracellular proteins is increasing or, vice versa, the percentage of secreted proteins is

decreasing. The accumulation of intracellular proteins is confirmed by the biological processes found to be enriched in the bioreactor culture, both in phase I and phase II. Many processes taking place in intracellular compartments of the cell like “Amino acid metabolism” and “Carbohydrate metabolism”, “Vitamin metabolism”, “Fatty acid beta-oxidation” and “Tricarboxylic acid pathway” or “Protein folding” were enriched in the samples of the bioreactor culture but not in the monolayer culture. In summary, due to the increased fraction of intracellular proteins in the conditioned medium of PHH cultivated in the 3D-bioreactor, there is an increase in enriched intracellular processes like metabolic pathways from the cytosol (Glycolysis) or pathways that take place in intacellular organelles like the endoplasmic reticulum (protein folding) or mitochondria (TCA-cycle, beta oxidation).

After discarding proteins not likely to be secreted based on a lacking signal peptide and non-prediction by SecretomeP, the resulting protein lists were compared to identify differences in the secretome as a result of different cultivation conditions. It has already been shown by histological observations that hepatocytes cultivated in the bioreactor exhibit liver-morphology including structures resembling bile canaliculi [Gerlach *et al.*, 2003a; Schmelzer *et al.*, 2009]. To build up these tissue-like structures, the inoculated hepatocytes have to undergo well-regulated reorganization and regeneration processes which *in vivo* are accompanied by extensive cell communication [Zimmermann, 2004]. Several proteins involved in such processes were found in the bioreactor samples but not in the corresponding monolayer culture and are reported as follows. **Thrombospondin-1**, an adhesive glycoprotein involved in cell-to-cell and cell-to-matrix interactions was identified and it was shown to be upregulated in congenital fibrosis [El-Youssef *et al.*, 1999]. Another protein, **laminin γ**, mediates attachment and migration but also organization of cells into tissues [Ishibashi *et al.*, 2005], stimulates proliferation of epithelial cells [Virtanen *et al.*, 2003] and was recently shown to be expressed in the basement membrane influencing cell polarity [Li *et al.*, 2011]. The **junctional adhesion molecule A (F11 receptor)** has claimed to play a role in early tight-junction assembly according to gene ontology database based on protein homology. Furthermore, two proteins involved in angiogenesis were identified: **Aminopeptidase N** was found to be upregulated in tissues undergoing extensive angiogenesis like tumors and the corpus luteum and antagonists of this protein specifically inhibited angiogenesis [Pasqualini *et al.*, 2000]. **Complement C5** is a protein indirectly involved in angiogenisis by positive regulation of vascular endothelial growth factor (VEGF) production [Ambati *et al.*, 2003; Nozaki *et al.*, 2006]. VEGF not only stimulates blood-vessel formation but also proliferation and migration of endothelial cells [Patan, 2004; Evans *et al.*, 2010; Skalnikova *et al.*, 2011]. A role of VEGF during late phases of liver regeneration (resinusoidation) was also reported [LeCouter *et al.*, 2003; Zimmermann, 2004]. Moreover, **vanin-1**

was identified in the bioreactor culture. Martin and co-workers showed that the mouse homologue of this protein is secreted and involved in tissue repair in the context of oxidative stress [Martin *et al.*, 2001]. Very recently, a study showed the significant upregulation of interferon-gamma (INFγ) in rats following partial hepatectomy and thus indicating a function of this cytokine in liver regeneration [Batusic *et al.*, 2011]. One protein involved in the INFγ-mediated signaling pathway that was found in the bioreactor was **INFγ inducible protein 30**. The expression of this protein is positively influenced by INFγ and a secreted isoform was postulated to play a role in intra- and interchain disulfide bonding [Luster *et al.*, 1988] which could possibly play a role in reorganization of extracellular matrix during tissue reconstruction. Another protein found in the bioreactor that is induced by INFγ is **metallothionein-2** [Kusari *et al.*, 1987]. This protein was shown to interact with protein kinase D1 [Rao *et al.*, 2003] which, in turn, stimulates angiogenisis and cell proliferation [Johannes *et al.*, 1994; Storz and Toker, 2003; Ha *et al.*, 2008]. Metallothioneins are also thought to be involved in the cells response to oxidative stress [Baird *et al.*, 2006].

The aforementioned proteins take part in many processes required for liver remodeling like cell proliferation, cell differentiation, cell migration, angiogenesis, tight junction assembly and cell-to-cell or cell-to-matrix interactions. These findings serve as complementary confirmation of former histological studies indicating that the primary hepatocytes undergo tissue reconstruction in this hollow-fiber system. The proteins were not found in monolayer culture after 48h. However, almost all of these proteins were found in the sample that underwent prefractionation by SDS-PAGE. This sample was collected after 96h of cultivation in monolayer culture thus indicating that the cells start to produce these proteins in the later phase of cultivation. Indeed, these proteins were not found in phase I of the bioreactor but in phase II. Notably, the first day of phase II is corresponding to 96h of serum-free monolayer cultivation in respect of timepoint of cell isolation and seeding or inoculation into the bioreactor, respectively. The hepatocytes obviously try to reorganize in both cultures by expressing the required proteins but in standard monolayer culture, there is no possibility to build-up tissue-like structures and subsequently cells cannot survive for a longer period. In contrast, the cells in the bioreactor are able to reorganize and survive because the high-density three-dimensional culture in the bioreactor provides an optimal environment. Additionally to the proteins involved in cell proliferation, some proteins were found that are indicative of oxidative stress in the bioreactor culture. However, proteins that are involved in protection against oxidative stress have also a connection to liver regeneration [Beyer *et al.*, 2008]. Furthermore, the presence of proteins being part of the oxidative stress response could be a result of the way of oxygenation in the bioreactor. Oxygen is directly introduced into the cell compartment through the gassing capillaries which is not really physiological but overcame the problem of limited oxygen supply in this bioreactor. Using a

modified gassing system as developed during this thesis [Mueller *et al.*, 2011b] in which the medium is saturated with oxygen before the entrance into the bioreactor could lead to an oxygen supply closer to the situation found *in vivo*. From the difference in oxygen concentration in the medium before and after the bioreactor, the oxygen uptake rate of the cells can be determined which could furthermore serve as an online parameter for cell viability during cultivation. A strategy ideally mimicking the *in vivo* situation would be an oxygen transport system in the medium based on hemoglobin. Recently, such a technique was published using hemoglobin-based oxygen carriers in an hepatic hollow-fiber bioreactor [Chen and Palmer, 2010].

5.8 Effects of diclofenac on the secretome

Diclofenac is a widely used non-steroidal anti-inflammatory drug (NSAID) and is a typical example for idiosyncratic drug toxicity causing liver injury, cholestasis as well as lipid accumulation disorders (i.e. steatosis) by inhibition of fatty acid oxidation [Banks *et al.*, 1995; Baldwin *et al.*, 1998]. There is evidence that both oxidative stress and mitochondrial dysfunction, alone or in combination play a role in liver injury during treatment with this NSAID [Galati *et al.*, 2002; Masubuchi *et al.*, 2002]. Also immune-mediated liver injury was reported as a result of allergic responses to protein adducts of drug-glucuronides formed during diclofenac detoxification in mice [Yang, 1996]. Furthermore, diclofenac induced apoptosis both in leukemia cells and in hepatoma cells [Franceschelli *et al.*, 2011; Singh *et al.*, 2011]. Although the incidence rate of diclofenac induced liver failure in clinics is very low, the wide use of this drug causes an impressive absolute number of cases worldwide but the toxic effect is exhibited only after chronic treatment [Walker, 1997; Boelsterli, 2003]. *In vitro*, only very high doses of diclofenac cause acute toxicity in human hepatocytes [Bort *et al.*, 1999]. In this thesis, diclofenac was applied at two different concentrations plus an untreated control to bioreactor cultures of primary human hepatocytes. One lower concentration was applied (6.4 µM) corresponding to the maximal therapeutic concentration in human patients [Hinz *et al.*, 2005] while the second concentration (100µM) was more closer to the EC_{50} value of diclofenac but still in the subtoxic range [Bort *et al.*, 1999]. The effects of diclofenac on the secretome were investigated during the later phase of the culture (days 7 to 10) and differences were detected by peptide hit counting. Although this technique is not as sensitive and robust in detecting differences in protein expression as isotopic labeling or spectrum counting, it provides approximates of protein abundance in compared samples [Pang *et al.*, 2002; Gao *et al.*, 2003; Gao *et al.*, 2004; Liu *et al.*, 2004]. Proteins exhibiting differences in peptide hits during analysis of the conditioned medium of the bioreactor cultures will in the following be referred to as being “regulated”. However, it has to be kept in mind that an altered abundance of a protein in the conditioned medium is not necessarily caused solely by

an altered gene expression. Other processes down-stream of transcription could be affected by the drug treatment and lead to altered amounts of a protein in the extracellular space. Post transcriptional regulation on the level of mRNA or altered protein degradation but also impacts on the secretion mechanism itself could result in observed differences upon treatment with diclofenac.

Twelve proteins were found to have significant differences in peptide counts upon application of diclofenac compared to the control. Overall, only two proteins were down-regulated while ten proteins showed up-regulation. Furthermore, five proteins exhibited regulation already upon application of the lower, therapeutic concentration and except for one protein all of them were up-regulated. One of the up-regulated proteins was **α-1-antitrypsin** but this protein should have been removed by the immunodepletion column. Since the difference in peptide counts could be a result of insufficient depletion, this protein will not be discussed in detail but it cannot be excluded that this protein was up-regulated and exceeded the binding capacity of the antibody resin. **Leucine-rich α-2-glycoprotein** was up-regulated in the group treated with the lower concentration of diclofenac only but not in the group treated with the higher dose. It was recently identified as an inflammatory biomarker for autoimmune diseases [Serada *et al.*, 2010]. **Fibrinogen γ chain** and **histidine-rich glycoprotein** were up-regulated in both groups treated with diclofenac. The latter acts as a protective protein in autoimmune processes [Gorgani and Theofilopoulos, 2007] and the former protein, fibrinogen, has been found to be up-regulated in blood plasma during xenobiotic-induced cholestatic liver injury in mice [Luyendyk *et al.*, 2011]. The higher abundance of these proteins upon diclofenac treatment indicates that already at a therapeutic concentration, diclofenac induces inflammatory immune responses and cholestatic processes. One protein was down-regulated in both treated groups, **4-hydroxyphenylpyruvate dioxygenase (Hpd)**, but for this protein, no direct link to diclofenac toxicity could be made. It is part of the tyrosine catabolic pathway and mice hepatocytes carrying a mutation in the gene encoding Hpd and the gene for the last enzyme in the tyrosine catabolic pathway (fumarylacetoacetate hydrolase) rapidly underwent apoptosis, but only when homogentisate (intermediate metabolite of tyrosine degradation) was administered [Nakamura *et al.*, 2007]. This probably indicates an anti-apoptotic function of this protein counteracting the pro-apoptotic effect exhibited by diclofenac [Gomez-Lechon *et al.*, 2003b]. Additionally, a recent study of our lab showed significant decrease in tyrosine uptake of PHH upon diclofenac treatment indicating that this metabolic pathway is somehow affected by this drug [Mueller *et al.*, 2012].

The abundance of seven proteins was altered in the condidioned medium of the bioreactor treated with 100 µM diclofenac. One up-regulated protein was **retinol-binding-protein 4**. Actually being an important protein in vitamin A metabolism and transport, it was significantly up-regulated in plasma

of children with non-alcoholic fatty liver disease and therefore claimed to be a biomarker for intrahepatic lipid content [Romanowska *et al.*, 2011]. This is indicative of accumulation of lipids in the cells due to diclofenac treatment which has been reported for colorectal carcinoma cells [Baldwin *et al.*, 1998]. Additionally, two apolipoproteins were highly up-regulated, **apolipoprotein A-I** and **apolipoprotein A-IV**. Both proteins are involved in lipid transport and have been shown to promote efflux of excess cellular lipids [Remaley *et al.*, 2001]. They could possibly provide elimination of accumulated lipids out of the cells. In addition, **apolipoprotein A-IV** possesses antioxidant activity by removal of free radicals [Wong *et al.*, 2007]. **Ceruloplasmin** was also up-regulated upon 100 µM diclofenac. Besides its function in copper- and iron transport, it is an effective antioxidant [Gutteridge, 1992; Patel *et al.*, 2002]. **NADPH dependent isocitrate dehydrogenase** was down-regulated and a decrease in transcripts of this protein was demonstrated to accompany development of apoptosis in rat liver [Tsvetikova *et al.*, 2010]. The differential expression of these proteins supports the apoptotic effect of diclofenac that was linked to the formation of reactive oxygen species [Gomez-Lechon *et al.*, 2003a]. Another up-regulated protein, **α-2-macroglobulin**, has strong anti-inflammatory effects by binding of proinflammatory cytokines like tumor necrosis factor alpha and Interleukin-6 [Webb and Gonias, 1998] with the former being a known inductor of liver injury [Schwabe and Brenner, 2006]. The last protein up-regulated in the bioreactor treated with 100µM diclofenac was **inter-α-trypsin inhibitor heavy chain H2**, which was demonstrated to also play a significant role in inflammation [Zhuo *et al.*, 2004].

Taken together, all proteins that exhibited significant differences in peptide counts upon application of diclofenac could, directly or indirectly, be connected to mechanisms of toxicity known for this NSAID. Observed differences in secreted proteins were larger in the group treated with a higher concentration of diclofenac than in the group treated with a therapeutic concentration. More proteins showed significantly altered peptide counts according to a one way ANOVA test and the observed change in identified peptides was larger upon application of the higher concentration. This was confirmed statistically by PCA of the acquired data. The cluster of the group undergoing high-dose treatment showed a higher separation from the control group than the cluster of cells exposed to the therapeutic concentration. Moreover, the respective groups were well separated and did not overlap within the 95 % confidence intervals. In both treated groups, regulated proteins were identified being indicative of or protective against rather sensitive pathways like immune-mediated inflammatory reactions. Immunological processes are thought to play an essential role in idiosyncratic toxicity of diclofenac [Yang, 1996; Bessone, 2010]. However, the occurrence of such events could be questioned because of the absence of cells of the immune system in the bioreactor. Even though the applied method for cell isolation results in a high purity of hepatocytes up to almost

100 %, it cannot be excluded that liver macrophages (stellate cells) found their way into the bioreactor. On the other hand, the altering in secretion of proteins related to immune-mediated inflammatory responses could be interpreted as an initial step for recruiting of immune cells which results in onset of inflammation *in vivo*. Moreover, proteins providing hints for ongoing cholestasis and apoptosis were identified already at a therapeutic concentration of diclofenac pinpointing the high sensitivity of the proteomic approach. When a higher concentration was applied, the differences in the secretome could be correlated to the occurrence of severe drug adverse reactions like lipid accumulation and apoptosis but also oxidative stress, all of them being known effects of diclofenac treatment. This work proved, for the first time, the proposed mechanisms of diclofenac induced hepatotoxicity based on proteomic analysis of secreted proteins. Several studies investigated the effect of diclofenac on the intracellular proteome of primary rat cardiomyocytes, on rat bile as well as human plasma, but none of the proteins found to be altered in this thesis were reported in these studies [Jones *et al.*, 2003; Baek *et al.*, 2010; van Erk *et al.*, 2010]. Thus, the secreted proteins found to be affected by diclofenac display new findings worth further investigation to confirm and evaluate these new biomarker candidates for diclofenac induced hepatotoxicity.

6. Conclusion and outlook

In the presented thesis, the secreted proteins of primary human hepatocytes in a 3D-bioreactor have been analyzed by proteomics. It was evident from the results that the use of FCS for cultivation has to be avoided if a proteomic analysis is aspired, particularly if the extracellular proteome is to be analyzed. The tissue-like behavior of cells cultivated in the bioreactor was confirmed which makes this device a suitable tool for the investigation of human specific hepatotoxicity during early drug testing. However, the high number of required cells for inoculation (2.5×10^7) and the high costs as well as the needed expertise to run this system restrict its use to few laboratories and make it unsuitable for high-throughput screenings. To overcome this problem, the bioreactor should be further down-scaled which is currently under development. Other three-dimensional cultivation techniques for *in vitro* drug testing should be considered ensuring tissue reconstruction and allowing the use in large-scale drug testing. A quite novel cultivation format applied to hepatocytes is the spheroid culture. These are spherical tissue-like structures which can be easily obtained by cultivation of cells in a hanging drop in a 96-well format. First experiments already proved the applicability of spheroids for *in vitro* drug testing using HepG2 cells [Mueller *et al.*, 2011a] and also HepaRG cells using quite low cell numbers (2,000-10,000). The HepaRG cell line is derived from a human hepatocellular carcinoma and has recently gained much attention from the toxicological community because it shows metabolic activities comparable to primary hepatocytes and maintains these features for many weeks. This cell line could overcome the problem of donor-to-donor variability as well as limited availability of primary human hepatocytes and will be investigated and characterized for the use in toxicoproteomic research in the future.

To the best of my knowledge, no other proteomic study investigated the effects of diclofenac on the secretome of primary human hepatocytes so far. Several proteins were found to exhibit altered abundances in the secretome upon diclofenac exposure and almost all proteins could be connected to the proposed mechanisms of toxicity. Of course, these findings have to be confirmed by additional experiments to select possible biomarker candidates for diclofenac-induced hepatotoxicity. The samples from 2D monolayer cultures treated with diclofenac generated during this thesis could unfortunately not be analyzed because of paucity of time but this should be made up to validate the findings obtained with the bioreactor. In order to discover predictive biomarkers that can be used as universal indicators of drug induced hepatotoxicity, other drugs will have to be administered and possible overlaps in changes of protein abundances have to be unveiled. However, it is not likely, but also not excluded, that one common biomarker for all drugs will be discovered. It is rather likely that

the different mechanisms of toxicity are represented by different (sets of) proteins that have to be monitored together to predict toxicity of a new drug. Furthermore, these proteins are likely to be present in very low amounts in plasma of patients during clinical surveillance which could be below the sensitivity of commonly used proteomic workflows. Therefore, a more sensitive quantification method like MRM should be applied. MRM is furthermore capable of absolute quantification as well as multiplexing thus allowing targeted quantification of several proteins at once which would increase the throughput. In any case, the preliminary examination of a new drug by discovery proteomics techniques like 2D-DIGE can be used for preclinical toxicity studies but also for classification of the drug´s mode of action.

The application of proteomics techniques on toxicological research will for sure provide deeper insights into the mechanisms of drug toxicity in the future, especially if applied together with other fields of systems biology like genomics, transcriptomics and metabolomics. The cross-linking of such techniques in toxicology by means of computational methods is very promising to understand the general processes affected by treatment with a drug and to find new biomarkers that are indicative of adverse drug reactions. This will lead to improvements not only in early drug development but also clinical surveillance in the future.

7. References

(2009). "The Universal Protein Resource (UniProt) 2009." *Nucleic Acids Res* 37(Database issue): D169-174.

Aebersold, R. and Mann, M. (2003). "Mass spectrometry-based proteomics." *Nature* 422(6928): 198-207.

Aithal, G. P. (2004). "Diclofenac-induced liver injury: a paradigm of idiosyncratic drug toxicity." *Expert Opin Drug Saf* 3(6): 519-523.

Alban, A., David, S. O., Bjorkesten, L., Andersson, C., Sloge, E., Lewis, S. and Currie, I. (2003). "A novel experimental design for comparative two-dimensional gel analysis: two-dimensional difference gel electrophoresis incorporating a pooled internal standard." *Proteomics* 3(1): 36-44.

Amacher, D. E. (2012). "The primary role of hepatic metabolism in idiosyncratic drug-induced liver injury." *Expert Opin Drug Metab Toxicol*.

Ambati, J., Anand, A., Fernandez, S., Sakurai, E., Lynn, B. C., Kuziel, W. A., Rollins, B. J. and Ambati, B. K. (2003). "An animal model of age-related macular degeneration in senescent Ccl-2- or Ccr-2-deficient mice." *Nat Med* 9(11): 1390-1397.

Anderson, N. L. and Anderson, N. G. (2002). "The human plasma proteome: history, character, and diagnostic prospects." *Mol Cell Proteomics* 1(11): 845-867.

Baek, S. M., Ahn, J. S., Noh, H. S., Park, J., Kang, S. S. and Kim, D. R. (2010). "Proteomic analysis in NSAIDs-treated primary cardiomyocytes." *J Proteomics* 73(4): 721-732.

Baird, S. K., Kurz, T. and Brunk, U. T. (2006). "Metallothionein protects against oxidative stress-induced lysosomal destabilization." *Biochem J* 394(Pt 1): 275-283.

Baldwin, G. S., Murphy, V. J., Yang, Z. and Hashimoto, T. (1998). "Binding of nonsteroidal antiinflammatory drugs to the alpha-subunit of the trifunctional protein of long chain fatty acid oxidation." *J Pharmacol Exp Ther* 286(2): 1110-1114.

Bandara, L. R. and Kennedy, S. (2002). "Toxicoproteomics -- a new preclinical tool." *Drug Discov Today* 7(7): 411-418.

Banks, A. T., Zimmerman, H. J., Ishak, K. G. and Harter, J. G. (1995). "Diclofenac-associated hepatotoxicity: analysis of 180 cases reported to the Food and Drug Administration as adverse reactions." *Hepatology* 22(3): 820-827.

Batusic, D. S., von Bargen, A., Blaschke, S., Dudas, J. and Ramadori, G. (2011). "Different physiology of interferon-alpha/-gamma in models of liver regeneration in the rat." *Histochem Cell Biol* 136(2): 131-144.

Bauman, A., Higdon, R., Rapson, S., Loiue, B., Hogan, J., Stacy, R., Napuli, A., Guo, W., van Voorhis, W., Roach, J., Lu, V., Landorf, E., Stewart, E., Kolker, N., Collart, F., Myler, P., van Belle, G. and Kolker, E. (2011). "Design and initial characterization of the SC-200 proteomics standard mixture." *OMICS* 15(1-2): 73-82.

Bellei, E., Bergamini, S., Monari, E., Fantoni, L. I., Cuoghi, A., Ozben, T. and Tomasi, A. (2011). "High-abundance proteins depletion for serum proteomic analysis: concomitant removal of non-targeted proteins." *Amino Acids* 40(1): 145-156.

Bendtsen, J. D., Jensen, L. J., Blom, N., Von Heijne, G. and Brunak, S. (2004). "Feature-based prediction of non-classical and leaderless protein secretion." *Protein Eng Des Sel* 17(4): 349-356.

Bessone, F. (2010). "Non-steroidal anti-inflammatory drugs: What is the actual risk of liver damage?" *World J Gastroenterol* 16(45): 5651-5661.

Beyer, T. A., Xu, W., Teupser, D., auf dem Keller, U., Bugnon, P., Hildt, E., Thiery, J., Kan, Y. W. and Werner, S. (2008). "Impaired liver regeneration in Nrf2 knockout mice: role of ROS-mediated insulin/IGF-1 resistance." *EMBO J* 27(1): 212-223.

Biemann, K. (1988). "Contributions of mass spectrometry to peptide and protein structure." *Biomed Environ Mass Spectrom* 16(1-12): 99-111.

Blueggel, M., Chamrad, D. and Meyer, H. E. (2004). "Bioinformatics in proteomics." *Curr Pharm Biotechnol* 5(1): 79-88.

Bodnar, W. M., Blackburn, R. K., Krise, J. M. and Moseley, M. A. (2003). "Exploiting the complementary nature of LC/MALDI/MS/MS and LC/ESI/MS/MS for increased proteome coverage." *J Am Soc Mass Spectrom* 14(9): 971-979.

Boelsterli, U. A. (2003). "Diclofenac-induced liver injury: a paradigm of idiosyncratic drug toxicity." *Toxicol Appl Pharmacol* 192(3): 307-322.

Bort, R., Ponsoda, X., Jover, R., Gomez-Lechon, M. J. and Castell, J. V. (1999). "Diclofenac toxicity to hepatocytes: a role for drug metabolism in cell toxicity." *J Pharmacol Exp Ther* 288(1): 65-72.

Bradford, M. M. (1976). "A rapid and sensitive method for the quantitation of microgram quantities of protein utilizing the principle of protein-dye binding." *Anal Biochem* 72: 248-254.

Brewis, I. A. and Brennan, P. (2010). "Proteomics technologies for the global identification and quantification of proteins." *Adv Protein Chem Struct Biol* 80: 1-44.

Cao, J., Shen, C., Zhang, J., Yao, J., Shen, H., Liu, Y., Lu, H. and Yang, P. (2011). "Comparison of alternative extraction methods for secretome profiling in human hepatocellular carcinoma cells." *Sci China Life Sci* 54(1): 34-38.

Chelius, D. and Bondarenko, P. V. (2002). "Quantitative profiling of proteins in complex mixtures using liquid chromatography and mass spectrometry." *J Proteome Res* 1(4): 317-323.

Chen, G. and Palmer, A. F. (2010). "Mixtures of hemoglobin-based oxygen carriers and perfluorocarbons exhibit a synergistic effect in oxygenating hepatic hollow fiber bioreactors." *Biotechnol Bioeng* 105(3): 534-542.

Chen, H. S., Rejtar, T., Andreev, V., Moskovets, E. and Karger, B. L. (2005). "Enhanced characterization of complex proteomic samples using LC-MALDI MS/MS: exclusion of redundant peptides from MS/MS analysis in replicate runs." *Anal Chem* 77(23): 7816-7825.

Chevallet, M., Diemer, H., Van Dorssealer, A., Villiers, C. and Rabilloud, T. (2007). "Toward a better analysis of secreted proteins: the example of the myeloid cells secretome." *Proteomics* 7(11): 1757-1770.

Chevallet, M., Luche, S. and Rabilloud, T. (2006). "Silver staining of proteins in polyacrylamide gels." *Nat Protoc* 1(4): 1852-1858.

Clark, S., Francis, P. S., Conlan, X. A. and Barnett, N. W. (2007). "Determination of urea using high-performance liquid chromatography with fluorescence detection after automated derivatisation with xanthydrol." *J Chromatogr A* 1161(1-2): 207-213.

Collins, B. C., Clarke, A., Kitteringham, N. R., Gallagher, W. M. and Pennington, S. R. (2007). "Use of proteomics for the discovery of early markers of drug toxicity." *Expert Opin Drug Metab Toxicol* 3(5): 689-704.

Cukierman, E., Pankov, R., Stevens, D. R. and Yamada, K. M. (2001). "Taking cell-matrix adhesions to the third dimension." *Science* 294(5547): 1708-1712.

De Hoffmann, E. and Stroobant, V. (2008). "Mass Spectrometry: Principles and Applications", John Wiley & Sons.

Delmotte, N., Lasaosa, M., Tholey, A., Heinzle, E. and Huber, C. G. (2007). "Two-dimensional reversed-phase x ion-pair reversed-phase HPLC: an alternative approach to high-resolution peptide separation for shotgun proteome analysis." *J Proteome Res* 6(11): 4363-4373.

DiMasi, J. A., Hansen, R. W. and Grabowski, H. G. (2003). "The price of innovation: new estimates of drug development costs." *J Health Econ* 22(2): 151-185.

Dowell, J. A., Johnson, J. A. and Li, L. (2009). "Identification of astrocyte secreted proteins with a combination of shotgun proteomics and bioinformatics." *J Proteome Res* 8(8): 4135-4143.

Dowling, P. and Clynes, M. (2011). "Conditioned media from cell lines: a complementary model to clinical specimens for the discovery of disease-specific biomarkers." *Proteomics* 11(4): 794-804.

Echan, L. A., Tang, H. Y., Ali-Khan, N., Lee, K. and Speicher, D. W. (2005). "Depletion of multiple high-abundance proteins improves protein profiling capacities of human serum and plasma." *Proteomics* 5(13): 3292-3303.

El-Youssef, M., Mu, Y., Huang, L., Stellmach, V. and Crawford, S. E. (1999). "Increased expression of transforming growth factor-beta1 and thrombospondin-1 in congenital hepatic fibrosis: possible role of the hepatic stellate cell." *J Pediatr Gastroenterol Nutr* 28(4): 386-392.

Elias, J. E. and Gygi, S. P. (2007). "Target-decoy search strategy for increased confidence in large-scale protein identifications by mass spectrometry." *Nat Methods* 4(3): 207-214.

Elliott, M. H., Smith, D. S., Parker, C. E. and Borchers, C. (2009). "Current trends in quantitative proteomics." *J Mass Spectrom* 44(12): 1637-1660.

Eng, J., McCormack, A. and Yates, J. (1994). "An approach to correlate tandem mass spectral data of peptides with amino acid sequences in a protein database." *J Am Soc Mass Spectrom* 5(11): 976-989.

Evans, I. M., Bagherzadeh, A., Charles, M., Raynham, T., Ireson, C., Boakes, A., Kelland, L. and Zachary, I. C. (2010). "Characterization of the biological effects of a novel protein kinase D inhibitor in endothelial cells." *Biochem J* 429(3): 565-572.

Farkas, D., Bhat, V. B., Mandapati, S., Wishnok, J. S. and Tannenbaum, S. R. (2005). "Characterization of the secreted proteome of rat hepatocytes cultured in collagen sandwiches." *Chem Res Toxicol* 18(7): 1132-1139.

Fenn, J. B., Mann, M., Meng, C. K., Wong, S. F. and Whitehouse, C. M. (1989). "Electrospray ionization for mass spectrometry of large biomolecules." *Science* 246(4926): 64-71.

Franceschelli, S., Moltedo, O., Amodio, G., Tajana, G. and Remondelli, P. (2011). "In the Huh7 Hepatoma Cells Diclofenac and Indomethacin Activate Differently the Unfolded Protein Response and Induce ER Stress Apoptosis." *Open Biochem J* 5: 45-51.

Galati, G., Tafazoli, S., Sabzevari, O., Chan, T. S. and O'Brien, P. J. (2002). "Idiosyncratic NSAID drug induced oxidative stress." *Chem Biol Interact* 142(1-2): 25-41.

Gao, J., Ann Garulacan, L., Storm, S. M., Hefta, S. A., Opiteck, G. J., Lin, J. H., Moulin, F. and Dambach, D. M. (2004). "Identification of in vitro protein biomarkers of idiosyncratic liver toxicity." *Toxicol In Vitro* 18(4): 533-541.

Gao, J., Opiteck, G. J., Friedrichs, M. S., Dongre, A. R. and Hefta, S. A. (2003). "Changes in the protein expression of yeast as a function of carbon source." *J Proteome Res* 2(6): 643-649.

Gao, Y., Holland, R. D. and Yu, L. R. (2009). "Quantitative proteomics for drug toxicity." *Brief Funct Genomic Proteomic* 8(2): 158-166.

Geng, X. and Regnier, F. E. (1984). "Retention model for proteins in reversed-phase liquid chromatography." *J Chromatogr* 296: 15-30.

Gerlach, J. C., Brayfield, C., Puhl, G., Borneman, R., Muller, C., Schmelzer, E. and Zeilinger, K. (2010). "Lidocaine/monoethylglycinexylidide test, galactose elimination test, and sorbitol elimination test for metabolic assessment of liver cell bioreactors." *Artif Organs* 34(6): 462-472.

Gerlach, J. C., Mutig, K., Sauer, I. M., Schrade, P., Efimova, E., Mieder, T., Naumann, G., Grunwald, A., Pless, G., Mas, A., Bachmann, S., Neuhaus, P. and Zeilinger, K. (2003a). "Use of primary human liver cells originating from discarded grafts in a bioreactor for liver support therapy and the prospects of culturing adult liver stem cells in bioreactors: a morphologic study." *Transplantation* 76(5): 781-786.

Gerlach, J. C., Zeilinger, K., Grebe, A., Puhl, G., Pless, G., Sauer, I., Grunwald, A., Schnoy, N., Muller, C. and Neuhaus, P. (2003b). "Recovery of preservation-injured primary human hepatocytes and nonparenchymal cells to tissuelike structures in large-scale bioreactors for liver support: an initial transmission electron microscopy study." *J Invest Surg* 16(2): 83-92.

Godoy, P., Hengstler, J. G., Ilkavets, I., Meyer, C., Bachmann, A., Muller, A., Tuschl, G., Mueller, S. O. and Dooley, S. (2009). "Extracellular matrix modulates sensitivity of hepatocytes to fibroblastoid dedifferentiation and transforming growth factor beta-induced apoptosis." *Hepatology* 49(6): 2031-2043.

Gomez-Lechon, M. J., Ponsoda, X., O'Connor, E., Donato, T., Castell, J. V. and Jover, R. (2003a). "Diclofenac induces apoptosis in hepatocytes by alteration of mitochondrial function and generation of ROS." *Biochem Pharmacol* 66(11): 2155-2167.

Gomez-Lechon, M. J., Ponsoda, X., O'Connor, E., Donato, T., Jover, R. and Castell, J. V. (2003b). "Diclofenac induces apoptosis in hepatocytes." *Toxicol In Vitro* 17(5-6): 675-680.

Gorg, A., Weiss, W. and Dunn, M. J. (2004). "Current two-dimensional electrophoresis technology for proteomics." *Proteomics* 4(12): 3665-3685.

Gorgani, N. N. and Theofilopoulos, A. N. (2007). "Contribution of histidine-rich glycoprotein in clearance of immune complexes and apoptotic cells: implications for ameliorating autoimmune diseases." *Autoimmunity* 40(4): 260-266.

Gundry, R. L., Fu, Q., Jelinek, C. A., Van Eyk, J. E. and Cotter, R. J. (2007). "Investigation of an albumin-enriched fraction of human serum and its albuminome." *Proteomics Clin Appl* 1(1): 73-88.

Gundry, R. L., White, M. Y., Nogee, J., Tchernyshyov, I. and Van Eyk, J. E. (2009). "Assessment of albumin removal from an immunoaffinity spin column: critical implications for proteomic examination of the albuminome and albumin-depleted samples." *Proteomics* 9(7): 2021-2028.

Guo, D. C., Mant, C. T. and Hodges, R. S. (1987). "Effects of ion-pairing reagents on the prediction of peptide retention in reversed-phase high-performance liquid chromatography." *J Chromatogr* 386: 205-222.

Gutteridge, J. M. (1992). "Iron and oxygen radicals in brain." *Ann Neurol* 32 Suppl: S16-21.

Gygi, S. P., Rist, B., Gerber, S. A., Turecek, F., Gelb, M. H. and Aebersold, R. (1999). "Quantitative analysis of complex protein mixtures using isotope-coded affinity tags." *Nat Biotechnol* 17(10): 994-999.

Ha, C. H., Wang, W., Jhun, B. S., Wong, C., Hausser, A., Pfizenmaier, K., McKinsey, T. A., Olson, E. N. and Jin, Z. G. (2008). "Protein kinase D-dependent phosphorylation and nuclear export of histone deacetylase 5 mediates vascular endothelial growth factor-induced gene expression and angiogenesis." *J Biol Chem* 283(21): 14590-14599.

Hartung, T. (2009). "Toxicology for the twenty-first century." *Nature* 460(7252): 208-212.

Hinz, B., Chevts, J., Renner, B., Wuttke, H., Rau, T., Schmidt, A., Szelenyi, I., Brune, K. and Werner, U. (2005). "Bioavailability of diclofenac potassium at low doses." *Br J Clin Pharmacol* 59(1): 80-84.

Huang da, W., Sherman, B. T. and Lempicki, R. A. (2009a). "Bioinformatics enrichment tools: paths toward the comprehensive functional analysis of large gene lists." *Nucleic Acids Res* 37(1): 1-13.

Huang da, W., Sherman, B. T. and Lempicki, R. A. (2009b). "Systematic and integrative analysis of large gene lists using DAVID bioinformatics resources." *Nat Protoc* 4(1): 44-57.

Ishibashi, M., Bottone, F. G., Jr., Taniura, S., Kamitani, H., Watanabe, T. and Eling, T. E. (2005). "The cyclooxygenase inhibitor indomethacin modulates gene expression and represses the extracellular matrix protein laminin gamma1 in human glioblastoma cells." *Exp Cell Res* 302(2): 244-252.

Jaeschke, H., McGill, M. R. and Ramachandran, A. (2011). "Pathophysiological relevance of proteomics investigations of drug-induced hepatotoxicity in HepG2 cells." *Toxicol Sci* 121(2): 428-430; author reply 431-423.

Jaskolla, T. W. and Karas, M. (2011). "Compelling evidence for Lucky Survivor and gas phase protonation: the unified MALDI analyte protonation mechanism." *J Am Soc Mass Spectrom* 22(6): 976-988.

Johannes, F. J., Prestle, J., Eis, S., Oberhagemann, P. and Pfizenmaier, K. (1994). "PKCu is a novel, atypical member of the protein kinase C family." *J Biol Chem* 269(8): 6140-6148.

Jones, J. A., Kaphalia, L., Treinen-Moslen, M. and Liebler, D. C. (2003). "Proteomic characterization of metabolites, protein adducts, and biliary proteins in rats exposed to 1,1-dichloroethylene or diclofenac." *Chem Res Toxicol* 16(10): 1306-1317.

Karas, M., Gluckmann, M. and Schafer, J. (2000). "Ionization in matrix-assisted laser desorption/ionization: singly charged molecular ions are the lucky survivors." *J Mass Spectrom* 35(1): 1-12.

Karas, M. and Hillenkamp, F. (1988). "Laser desorption ionization of proteins with molecular masses exceeding 10,000 daltons." *Anal Chem* 60(20): 2299-2301.

Keller, A., Nesvizhskii, A. I., Kolker, E. and Aebersold, R. (2002). "Empirical statistical model to estimate the accuracy of peptide identifications made by MS/MS and database search." *Anal Chem* 74(20): 5383-5392.

Kenrick, K. G. and Margolis, J. (1970). "Isoelectric focusing and gradient gel electrophoresis: a two-dimensional technique." *Anal Biochem* 33(1): 204-207.

Klee, E. W. and Sosa, C. P. (2007). "Computational classification of classically secreted proteins." *Drug Discov Today* 12(5-6): 234-240.

Klose, J. (1975). "Protein mapping by combined isoelectric focusing and electrophoresis of mouse tissues. A novel approach to testing for induced point mutations in mammals." *Humangenetik* 26(3): 231-243.

Knochenmuss, R. and Zenobi, R. (2003). "MALDI ionization: the role of in-plume processes." *Chem Rev* 103(2): 441-452.

Kusari, J., Tiwari, R. K., Kumar, R. and Sen, G. C. (1987). "Expression of interferon-inducible genes in RD-114 cells." *J Virol* 61(5): 1524-1531.

Laemmli, U. K. (1970). "Cleavage of structural proteins during the assembly of the head of bacteriophage T4." *Nature* 227(5259): 680-685.

Lange, V., Picotti, P., Domon, B. and Aebersold, R. (2008). "Selected reaction monitoring for quantitative proteomics: a tutorial." *Mol Syst Biol* 4: 222.

Lasaosa, M., Delmotte, N., Huber, C. G., Melchior, K., Heinzle, E. and Tholey, A. (2009a). "A 2D reversed-phase x ion-pair reversed-phase HPLC-MALDI TOF/TOF-MS approach for shotgun proteome analysis." *Anal Bioanal Chem* 393(4): 1245-1256.

Lasaosa, M., Jakoby, T., Delmotte, N., Huber, C. G., Heinzle, E. and Tholey, A. (2009b). "Rapid selection of peptide containing fractions in off-line 2-D HPLC in shotgun proteome analysis by screening with MALDI TOF MS." *Proteomics* 9(19): 4577-4581.

LeCouter, J., Moritz, D. R., Li, B., Phillips, G. L., Liang, X. H., Gerber, H. P., Hillan, K. J. and Ferrara, N. (2003). "Angiogenesis-independent endothelial protection of liver: role of VEGFR-1." *Science* 299(5608): 890-893.

Lewis, J. A., Dennis, W. E., Hadix, J. and Jackson, D. A. (2010). "Analysis of secreted proteins as an in vitro model for discovery of liver toxicity markers." *J Proteome Res* 9(11): 5794-5802.

Li, Y. N., Radner, S., French, M. M., Pinzon-Duarte, G., Daly, G. H., Burgeson, R. E., Koch, M. and Brunken, W. J. (2011). "The gamma3 chain of laminin is widely but differentially expressed in murine basement membranes: Expression and functional studies." *Matrix Biol*.

Liu, H., Sadygov, R. G. and Yates, J. R., 3rd (2004). "A model for random sampling and estimation of relative protein abundance in shotgun proteomics." *Anal Chem* 76(14): 4193-4201.

Lottspeich, F. (1999). "Proteome Analysis: A Pathway to the Functional Analysis of Proteins." *Angew Chem Int Ed Engl* 38(17): 2476-2492.

Luster, A. D., Weinshank, R. L., Feinman, R. and Ravetch, J. V. (1988). "Molecular and biochemical characterization of a novel gamma-interferon-inducible protein." *J Biol Chem* 263(24): 12036-12043.

Luyendyk, J. P., Mackman, N. and Sullivan, B. P. (2011). "Role of fibrinogen and protease-activated receptors in acute xenobiotic-induced cholestatic liver injury." *Toxicol Sci* 119(1): 233-243.

Mann, M., Hojrup, P. and Roepstorff, P. (1993). "Use of mass spectrometric molecular weight information to identify proteins in sequence databases." *Biol Mass Spectrom* 22(6): 338-345.

Marrero, J. A. and Lok, A. S. (2004). "Newer markers for hepatocellular carcinoma." *Gastroenterology* 127(5 Suppl 1): S113-119.

Martin, F., Malergue, F., Pitari, G., Philippe, J. M., Philips, S., Chabret, C., Granjeaud, S., Mattei, M. G., Mungall, A. J., Naquet, P. and Galland, F. (2001). "Vanin genes are clustered (human 6q22-24 and mouse 10A2B1) and encode isoforms of pantetheinase ectoenzymes." *Immunogenetics* 53(4): 296-306.

Masubuchi, Y., Nakayama, S. and Horie, T. (2002). "Role of mitochondrial permeability transition in diclofenac-induced hepatocyte injury in rats." *Hepatology* 35(3): 544-551.

Mazzoleni, G., Di Lorenzo, D. and Steimberg, N. (2009). "Modelling tissues in 3D: the next future of pharmaco-toxicology and food research?" *Genes Nutr* 4(1): 13-22.

Medzihradszky, K. F., Campbell, J. M., Baldwin, M. A., Falick, A. M., Juhasz, P., Vestal, M. L. and Burlingame, A. L. (2000). "The characteristics of peptide collision-induced dissociation using a high-performance MALDI-TOF/TOF tandem mass spectrometer." *Anal Chem* 72(3): 552-558.

Mi, H. and Thomas, P. (2009). "PANTHER pathway: an ontology-based pathway database coupled with data analysis tools." *Methods Mol Biol* 563: 123-140.

Miller, L. L. and Bale, W. F. (1954). "Synthesis of all plasma protein fractions except gamma globulins by the liver; the use of zone electrophoresis and lysine-epsilon-C14 to define the plasma proteins synthesized by the isolated perfused liver." *J Exp Med* 99(2): 125-132.

Mitulovic, G. and Mechtler, K. (2006). "HPLC techniques for proteomics analysis--a short overview of latest developments." *Brief Funct Genomic Proteomic* 5(4): 249-260.

Mueller, D., Koetemann, A. and Noor, F. (2011a). "Organotypic cultures of HepG2 cells for in vitro toxicity studies." *J Bioengineer & Biomedical Sci*.

Mueller, D., Muller-Vieira, U., Biemel, K. M., Tascher, G., Nussler, A. K. and Noor, F. (2012). "Biotransformation of diclofenac and effects on the metabolome of primary human hepatocytes upon repeated dose exposure." *Eur J Pharm Sci*.

Mueller, D., Tascher, G., Muller-Vieira, U., Knobeloch, D., Nuessler, A. K., Zeilinger, K., Heinzle, E. and Noor, F. (2011b). "In-depth physiological characterization of primary human hepatocytes in a 3D hollow-fiber bioreactor." *J Tissue Eng Regen Med*.

Mueller, L. N., Brusniak, M. Y., Mani, D. R. and Aebersold, R. (2008). "An assessment of software solutions for the analysis of mass spectrometry based quantitative proteomics data." *J Proteome Res* 7(1): 51-61.

Nakamura, K., Tanaka, Y., Mitsubuchi, H. and Endo, F. (2007). "Animal models of tyrosinemia." *J Nutr* 137(6 Suppl 1): 1556S-1560S; discussion 1573S-1575S.

Neilson, K. A., Ali, N. A., Muralidharan, S., Mirzaei, M., Mariani, M., Assadourian, G., Lee, A., van Sluyter, S. C. and Haynes, P. A. (2011). "Less label, more free: approaches in label-free quantitative mass spectrometry." *Proteomics* 11(4): 535-553.

Nesvizhskii, A. I., Keller, A., Kolker, E. and Aebersold, R. (2003). "A statistical model for identifying proteins by tandem mass spectrometry." *Anal Chem* 75(17): 4646-4658.

Nickel, W. (2010). "Pathways of unconventional protein secretion." *Curr Opin Biotechnol* 21(5): 621-626.

Nickel, W. and Rabouille, C. (2009). "Mechanisms of regulated unconventional protein secretion." *Nat Rev Mol Cell Biol* 10(2): 148-155.

NIH (2001). "Biomarkers and surrogate endpoints: preferred definitions and conceptual framework." *Clin Pharmacol Ther* 69(3): 89-95.

Nozaki, M., Raisler, B. J., Sakurai, E., Sarma, J. V., Barnum, S. R., Lambris, J. D., Chen, Y., Zhang, K., Ambati, B. K., Baffi, J. Z. and Ambati, J. (2006). "Drusen complement components C3a and C5a promote choroidal neovascularization." *Proc Natl Acad Sci U S A* 103(7): 2328-2333.

Nussler, A. K., Nussler, N. C., Merk, V., Brulport, M., Schormann, W. and Hengstler, J. G. (2009). The Holy Grail of Hepatocyte Culturing and Therapeutic Use. *Strategies in Regenerative Medicine*. M. Santin. New York, NY, USA, Springer**:** 1-38.

O'Farrell, P. H. (1975). "High resolution two-dimensional electrophoresis of proteins." *J Biol Chem* 250(10): 4007-4021.

Old, W. M., Meyer-Arendt, K., Aveline-Wolf, L., Pierce, K. G., Mendoza, A., Sevinsky, J. R., Resing, K. A. and Ahn, N. G. (2005). "Comparison of label-free methods for quantifying human proteins by shotgun proteomics." *Mol Cell Proteomics* 4(10): 1487-1502.

Olson, H., Betton, G., Stritar, J. and Robinson, D. (1998). "The predictivity of the toxicity of pharmaceuticals in humans from animal data--an interim assessment." *Toxicol Lett* 102-103: 535-538.

Ong, S. E., Blagoev, B., Kratchmarova, I., Kristensen, D. B., Steen, H., Pandey, A. and Mann, M. (2002). "Stable isotope labeling by amino acids in cell culture, SILAC, as a simple and accurate approach to expression proteomics." *Mol Cell Proteomics* 1(5): 376-386.

Ong, S. E. and Mann, M. (2005). "Mass spectrometry-based proteomics turns quantitative." *Nat Chem Biol* 1(5): 252-262.

Pampaloni, F., Reynaud, E. G. and Stelzer, E. H. (2007). "The third dimension bridges the gap between cell culture and live tissue." *Nat Rev Mol Cell Biol* 8(10): 839-845.

Pang, J. X., Ginanni, N., Dongre, A. R., Hefta, S. A. and Opitek, G. J. (2002). "Biomarker discovery in urine by proteomics." *J Proteome Res* 1(2): 161-169.

Pappin, D. J., Hojrup, P. and Bleasby, A. J. (1993). "Rapid identification of proteins by peptide-mass fingerprinting." *Curr Biol* 3(6): 327-332.

Pasqualini, R., Koivunen, E., Kain, R., Lahdenranta, J., Sakamoto, M., Stryhn, A., Ashmun, R. A., Shapiro, L. H., Arap, W. and Ruoslahti, E. (2000). "Aminopeptidase N is a receptor for tumor-homing peptides and a target for inhibiting angiogenesis." *Cancer Res* 60(3): 722-727.

Patan, S. (2004). "Vasculogenesis and angiogenesis." *Cancer Treat Res* 117: 3-32.

Patel, B. N., Dunn, R. J., Jeong, S. Y., Zhu, Q., Julien, J. P. and David, S. (2002). "Ceruloplasmin regulates iron levels in the CNS and prevents free radical injury." *J Neurosci* 22(15): 6578-6586.

Perkins, D. N., Pappin, D. J., Creasy, D. M. and Cottrell, J. S. (1999). "Probability-based protein identification by searching sequence databases using mass spectrometry data." *Electrophoresis* 20(18): 3551-3567.

Peters, S. J., Haagsman, H. P. and van Norren, K. (2008). "Arginase release by primary hepatocytes and liver slices results in rapid conversion of arginine to urea in cell culture media." *Toxicol In Vitro* 22(4): 1094-1098.

Planque, C., Kulasingam, V., Smith, C. R., Reckamp, K., Goodglick, L. and Diamandis, E. P. (2009). "Identification of five candidate lung cancer biomarkers by proteomics analysis of conditioned media of four lung cancer cell lines." *Mol Cell Proteomics* 8(12): 2746-2758.

Rabilloud, T. (2002). "Two-dimensional gel electrophoresis in proteomics: old, old fashioned, but it still climbs up the mountains." *Proteomics* 2(1): 3-10.

Rajan, N., Habermehl, J., Cote, M. F., Doillon, C. J. and Mantovani, D. (2006). "Preparation of ready-to-use, storable and reconstituted type I collagen from rat tail tendon for tissue engineering applications." *Nat Protoc* 1(6): 2753-2758.

Rao, P. S., Jaggi, M., Smith, D. J., Hemstreet, G. P. and Balaji, K. C. (2003). "Metallothionein 2A interacts with the kinase domain of PKCmu in prostate cancer." *Biochem Biophys Res Commun* 310(3): 1032-1038.

Remaley, A. T., Stonik, J. A., Demosky, S. J., Neufeld, E. B., Bocharov, A. V., Vishnyakova, T. G., Eggerman, T. L., Patterson, A. P., Duverger, N. J., Santamarina-Fojo, S. and Brewer, H. B., Jr.

(2001). "Apolipoprotein specificity for lipid efflux by the human ABCAI transporter." *Biochem Biophys Res Commun* 280(3): 818-823.

Roepstorff, P. and Fohlman, J. (1984). "Proposal for a common nomenclature for sequence ions in mass spectra of peptides." *Biomed Mass Spectrom* 11(11): 601.

Romanowska, A., Lebensztejn, D. M., Skiba, E., Tarasow, E. and Kaczmarski, M. (2011). "Retinol binding protein-4 as a serum biomarker of intrahepatic lipid content in obese children--preliminary report." *Acta Biochim Pol* 58(1): 35-38.

Rosenfeld, J., Capdevielle, J., Guillemot, J. C. and Ferrara, P. (1992). "In-gel digestion of proteins for internal sequence analysis after one- or two-dimensional gel electrophoresis." *Anal Biochem* 203(1): 173-179.

Ross, P. L., Huang, Y. N., Marchese, J. N., Williamson, B., Parker, K., Hattan, S., Khainovski, N., Pillai, S., Dey, S., Daniels, S., Purkayastha, S., Juhasz, P., Martin, S., Bartlet-Jones, M., He, F., Jacobson, A. and Pappin, D. J. (2004). "Multiplexed protein quantitation in Saccharomyces cerevisiae using amine-reactive isobaric tagging reagents." *Mol Cell Proteomics* 3(12): 1154-1169.

Sauer, I. M., Neuhaus, P. and Gerlach, J. C. (2002). "Concept for modular extracorporeal liver support for the treatment of acute hepatic failure." *Metab Brain Dis* 17(4): 477-484.

Schmelzer, E., Mutig, K., Schrade, P., Bachmann, S., Gerlach, J. C. and Zeilinger, K. (2009). "Effect of human patient plasma ex vivo treatment on gene expression and progenitor cell activation of primary human liver cells in multi-compartment 3D perfusion bioreactors for extra-corporeal liver support." *Biotechnol Bioeng* 103(4): 817-827.

Schwabe, R. F. and Brenner, D. A. (2006). "Mechanisms of Liver Injury. I. TNF-alpha-induced liver injury: role of IKK, JNK, and ROS pathways." *Am J Physiol Gastrointest Liver Physiol* 290(4): G583-589.

Searle, B. C. (2010). "Scaffold: a bioinformatic tool for validating MS/MS-based proteomic studies." *Proteomics* 10(6): 1265-1269.

Serada, S., Fujimoto, M., Ogata, A., Terabe, F., Hirano, T., Iijima, H., Shinzaki, S., Nishikawa, T., Ohkawara, T., Iwahori, K., Ohguro, N., Kishimoto, T. and Naka, T. (2010). "iTRAQ-based proteomic identification of leucine-rich alpha-2 glycoprotein as a novel inflammatory biomarker in autoimmune diseases." *Ann Rheum Dis* 69(4): 770-774.

Shevchenko, A., Wilm, M., Vorm, O. and Mann, M. (1996). "Mass spectrometric sequencing of proteins silver-stained polyacrylamide gels." *Anal Chem* 68(5): 850-858.

Singh, R., Cadeddu, R. P., Frobel, J., Wilk, C. M., Bruns, I., Zerbini, L. F., Prenzel, T., Hartwig, S., Brunnert, D., Schroeder, T., Lehr, S., Haas, R. and Czibere, A. (2011). "The non-steroidal anti-inflammatory drugs Sulindac sulfide and Diclofenac induce apoptosis and differentiation in human acute myeloid leukemia cells through an AP-1 dependent pathway." *Apoptosis* 16(9): 889-901.

Skalnikova, H., Motlik, J., Gadher, S. J. and Kovarova, H. (2011). "Mapping of the secretome of primary isolates of mammalian cells, stem cells and derived cell lines." *Proteomics* 11(4): 691-708.

Slany, A., Haudek, V. J., Zwickl, H., Gundacker, N. C., Grusch, M., Weiss, T. S., Seir, K., Rodgarkia-Dara, C., Hellerbrand, C. and Gerner, C. (2010). "Cell characterization by proteome profiling applied to primary hepatocytes and hepatocyte cell lines Hep-G2 and Hep-3B." *J Proteome Res* 9(1): 6-21.

Storz, P. and Toker, A. (2003). "Protein kinase D mediates a stress-induced NF-kappaB activation and survival pathway." *EMBO J* 22(1): 109-120.

Syka, J. E., Coon, J. J., Schroeder, M. J., Shabanowitz, J. and Hunt, D. F. (2004). "Peptide and protein sequence analysis by electron transfer dissociation mass spectrometry." *Proc Natl Acad Sci U S A* 101(26): 9528-9533.

Tanaka, K., Waki, H., Ido, Y., Akita, S., Yoshida, Y., Yoshida, T. and Matsuo, T. (1988). "Protein and polymer analyses up to m/z 100 000 by laser ionization time-of-flight mass spectrometry." *Rapid Communications in Mass Spectrometry* 2(8): 151-153.

Thomas, P. D., Kejariwal, A., Campbell, M. J., Mi, H., Diemer, K., Guo, N., Ladunga, I., Ulitsky-Lazareva, B., Muruganujan, A., Rabkin, S., Vandergriff, J. A. and Doremieux, O. (2003). "PANTHER: a browsable database of gene products organized by biological function, using curated protein family and subfamily classification." *Nucleic Acids Res* 31(1): 334-341.

Thome-Kromer, B., Bonk, I., Klatt, M., Nebrich, G., Taufmann, M., Bryant, S., Wacker, U. and Kopke, A. (2003). "Toward the identification of liver toxicity markers: a proteome study in human cell culture and rats." *Proteomics* 3(10): 1835-1862.

Thompson, A., Schafer, J., Kuhn, K., Kienle, S., Schwarz, J., Schmidt, G., Neumann, T., Johnstone, R., Mohammed, A. K. and Hamon, C. (2003). "Tandem mass tags: a novel quantification strategy for comparative analysis of complex protein mixtures by MS/MS." *Anal Chem* 75(8): 1895-1904.

Tsvetikova, L. N., Popova, T. N., Rakhmanova, T. I. and Iskusnykh, I. (2010). "[Expression and catalytic properties NADP-isocitrate dehydrogenase from the rat liver under normal conditions and following administration of tumor necrosis factor-alpha or thioctic acid]." *Biomed Khim* 56(2): 220-229.

Tuschl, G., Hrach, J., Walter, Y., Hewitt, P. G. and Mueller, S. O. (2009). "Serum-free collagen sandwich cultures of adult rat hepatocytes maintain liver-like properties long term: a valuable model for in vitro toxicity and drug-drug interaction studies." *Chem Biol Interact* 181(1): 124-137.

Tuschl, G. and Mueller, S. O. (2006). "Effects of cell culture conditions on primary rat hepatocytes-cell morphology and differential gene expression." *Toxicology* 218(2-3): 205-215.

van Erk, M. J., Wopereis, S., Rubingh, C., van Vliet, T., Verheij, E., Cnubben, N. H., Pedersen, T. L., Newman, J. W., Smilde, A. K., van der Greef, J., Hendriks, H. F. and van Ommen, B. (2010). "Insight in modulation of inflammation in response to diclofenac intervention: a human intervention study." *BMC Med Genomics* 3: 5.

Van Summeren, A., Renes, J., Bouwman, F. G., Noben, J. P., van Delft, J. H., Kleinjans, J. C. and Mariman, E. C. (2011). "Proteomics investigations of drug-induced hepatotoxicity in HepG2 cells." *Toxicol Sci* 120(1): 109-122.

van Summeren, A., Renes, J., van Delft, J. H., Kleinjans, J. C. and Mariman, E. C. (2012). "Proteomics in the search for mechanisms and biomarkers of drug-induced hepatotoxicity." *Toxicol In Vitro*.

van Vliet, C., Thomas, E. C., Merino-Trigo, A., Teasdale, R. D. and Gleeson, P. A. (2003). "Intracellular sorting and transport of proteins." *Prog Biophys Mol Biol* 83(1): 1-45.

Virtanen, I., Korhonen, M., Petajaniemi, N., Karhunen, T., Thornell, L. E., Sorokin, L. M. and Konttinen, Y. T. (2003). "Laminin isoforms in fetal and adult human adrenal cortex." *J Clin Endocrinol Metab* 88(10): 4960-4966.

Walker, A. M. (1997). "Quantitative studies of the risk of serious hepatic injury in persons using nonsteroidal antiinflammatory drugs." *Arthritis Rheum* 40(2): 201-208.

Washburn, M. P., Wolters, D. and Yates, J. R., 3rd (2001). "Large-scale analysis of the yeast proteome by multidimensional protein identification technology." *Nat Biotechnol* 19(3): 242-247.

Wasinger, V. C., Cordwell, S. J., Cerpa-Poljak, A., Yan, J. X., Gooley, A. A., Wilkins, M. R., Duncan, M. W., Harris, R., Williams, K. L. and Humphery-Smith, I. (1995). "Progress with gene-product mapping of the Mollicutes: Mycoplasma genitalium." *Electrophoresis* 16(7): 1090-1094.

Webb, D. J. and Gonias, S. L. (1998). "A modified human alpha 2-macroglobulin derivative that binds tumor necrosis factor-alpha and interleukin-1 beta with high affinity in vitro and reverses lipopolysaccharide toxicity in vivo in mice." *Lab Invest* 78(8): 939-948.

Weiss, S., Carapito, C., Cleiss, J., Koechler, S., Turlin, E., Coppee, J. Y., Heymann, M., Kugler, V., Stauffert, M., Cruveiller, S., Medigue, C., Van Dorsselaer, A., Bertin, P. N. and Arsene-Ploetze, F. (2009). "Enhanced structural and functional genome elucidation of the arsenite-oxidizing strain Herminiimonas arsenicoxydans by proteomics data." *Biochimie* 91(2): 192-203.

Wilkins, M. R., Pasquali, C., Appel, R. D., Ou, K., Golaz, O., Sanchez, J. C., Yan, J. X., Gooley, A. A., Hughes, G., Humphery-Smith, I., Williams, K. L. and Hochstrasser, D. F. (1996). "From proteins to proteomes: large scale protein identification by two-dimensional electrophoresis and amino acid analysis." *Biotechnology (N Y)* 14(1): 61-65.

Wolters, D. A., Washburn, M. P. and Yates, J. R., 3rd (2001). "An automated multidimensional protein identification technology for shotgun proteomics." *Anal Chem* 73(23): 5683-5690.

Wong, W. M., Gerry, A. B., Putt, W., Roberts, J. L., Weinberg, R. B., Humphries, S. E., Leake, D. S. and Talmud, P. J. (2007). "Common variants of apolipoprotein A-IV differ in their ability to inhibit low density lipoprotein oxidation." *Atherosclerosis* 192(2): 266-274.

Wu, J. T. (1990). "Serum alpha-fetoprotein and its lectin reactivity in liver diseases: a review." *Ann Clin Lab Sci* 20(2): 98-105.

Yamashita, R., Fujiwara, Y., Ikari, K., Hamada, K., Otomo, A., Yasuda, K., Noda, M. and Kaburagi, Y. (2007). "Extracellular proteome of human hepatoma cell, HepG2 analyzed using two-dimensional liquid chromatography coupled with tandem mass spectrometry." *Mol Cell Biochem* 298(1-2): 83-92.

Yang, D. Y., Benet L.Z. (1996). "Immunogenicity of diclofenac protein conjugates formed via drug-glucuronide intermediate." *ISSX proceedings, 7th North American ISSX Meeting, San Diego, CA 85*.

Yates, J. R., 3rd, Speicher, S., Griffin, P. R. and Hunkapiller, T. (1993). "Peptide mass maps: a highly informative approach to protein identification." *Anal Biochem* 214(2): 397-408.

Zeilinger, K., Holland, G., Sauer, I. M., Efimova, E., Kardassis, D., Obermayer, N., Liu, M., Neuhaus, P. and Gerlach, J. C. (2004). "Time course of primary liver cell reorganization in three-dimensional high-density bioreactors for extracorporeal liver support: an immunohistochemical and ultrastructural study." *Tissue Eng* 10(7-8): 1113-1124.

Zeilinger, K., Schreiter, T., Darnell, M., Soderdahl, T., Lubberstedt, M., Dillner, B., Knobeloch, D., Nussler, A. K., Gerlach, J. C. and Andersson, T. B. (2011). "Scaling down of a clinical three-dimensional perfusion multicompartment hollow fiber liver bioreactor developed for extracorporeal liver support to an analytical scale device useful for hepatic pharmacological in vitro studies." *Tissue Eng Part C Methods* 17(5): 549-556.

Zhang, Y., Wang, Y., Sun, W., Jia, L., Ma, S. and Gao, Y. (2010). "Strategy for studying the liver secretome on the organ level." *J Proteome Res* 9(4): 1894-1901.

Zhu, W., Smith, J. W. and Huang, C. M. (2010). "Mass spectrometry-based label-free quantitative proteomics." *J Biomed Biotechnol* 2010: 840518.

Zhuo, L., Hascall, V. C. and Kimata, K. (2004). "Inter-alpha-trypsin inhibitor, a covalent protein-glycosaminoglycan-protein complex." *J Biol Chem* 279(37): 38079-38082.

Zimmermann, A. (2004). "Regulation of liver regeneration." *Nephrol Dial Transplant* 19 Suppl 4: iv6-10.

Zwickl, H., Traxler, E., Staettner, S., Parzefall, W., Grasl-Kraupp, B., Karner, J., Schulte-Hermann, R. and Gerner, C. (2005). "A novel technique to specifically analyze the secretome of cells and tissues." *Electrophoresis* 26(14): 2779-2785.

Appendix

Appendix I: Curriculum vitae

Appendix II: Lists of identified proteins

Curriculum vitae

Name:	Georg Claudius Tascher
Adress:	Saarlouiser Straße 21
	66346 Püttlingen, Saarland
Date of birth:	04.12.1981
Place of birth:	Ottweiler, Germany

Education

8/1988 - 6/1992	primary school (Grundschule Köllerbach)
9/1992 - 6/2001	secondary school (Marie-Luise-Kaschnitz Gymnasium, Völklingen Abitur, grade: 2.6)
10/2002 - 12/2007	studies of human- and molecularbiology at the Saarland University
03/2007 - 12/2007	Diploma thesis at the institute for medical biochemistry and molecularbiology at the Saarland University in the group of PD Dr. Susanne Bailer, title: „Strukturelle und funktionelle Analyse des Membranankers des Herpes simplex Virus 1 Proteins UL34“ (degree: Diplom Biologe; grade: 1.3)
05/2008 - 02/2012	PhD studies at the institute for biochemical engineering at the Saarland University, Saarbrücken in the group of Prof. Elmar Heinzle; Title of the thesis: “The secretome of primary human hepatocytes in an organotypic bioreactor culture for the identification of biomarkers of drug-induced hepatotoxicity”

Publications

"In-depth physiological characterization of primary human hepatocytes in a 3D-hollow fiber bioreactor"

Mueller D, Tascher G, Müller-Vieira U, Knobeloch D, Nuessler AK, Zeilinger K, Heinzle E and Noor F (2011)

Journal of Tissue Engineering and Regenerative Medicine, 5: e207-e218, DOI: 10.1002/term.418

"Biotransformation of diclofenac and effects on the metabolome of primary human hepatocytes upon repeated dose exposure"

Mueller D, Müller-Vieira U, Biemel KM, Tascher G, Nüssler AK and Noor F (2012)

European Journal of Pharmaceutical Sciences, DOI: 10.1016/j.ejps.2012.01.014

"Real-time *in situ* viability assessment in 3D bioreactor with liver cells using resazurin assay during drug exposure"

Mueller D, Tascher G, Damm G, Nüssler AK, Heinzle E and Noor F (2011)

submitted

"GC-TOFMS based metabolomics for the assessment of therapeutic drug concentration effects on human liver cells"

Mueller D, Tascher G, Müller-Vieira U, Knobeloch D, Nüssler AK, Heinzle E and Noor F (2011)

submitted

"*In vivo* veritas: Secretome analysis of primary human hepatocytes in an organotypic 3D-bioreactor"

Tascher G, Hoffmann S, Mueller D, Zeillinger K, Heinzle E and Noor F

in preparation

"Label-free quantification to detect diclofenac-induced changes in the secretome of primary human hepatocytes using LC-MALDI"

Tascher G, Hoffmann S, Mueller D, Zeillinger K, Heinzle E and Noor F

in preparation

Contributions to scientific meetings

Presentations

"Secretome analysis of primary human hepatocytes in 2D- and 3D-culture for *in-vitro* toxicology"

Selected presenter in the students session of the European Society of Toxicology In Vitro (ESTIV)

Congress on Alternatives to Animal Testing, 02. - 04.09.2010, Linz, Austria

Posters

Tascher G, Noor F, Mueller D, Knobeloch D, Nüssler AK, Zeilinger K and Heinzle E

"Toxicoproteomic analysis on primary human hepatocytes in a 3D-jellyfish bioreactor"

ADMET Europe 2010 08. - 09.04.10, München, Germany

Tascher G, Mueller D, Knobeloch D, Nüssler AK, Zeilinger K, Heinzle E and Noor F

"Secretome analysis of primary human hepatocytes in 2D- and 3D-culture for *in-vitro* toxicology"

Congress on Alternatives to Animal Testing, 02.-04.09.2010, Linz, Austria (selected for presentation in the students session; see above)

Tascher G, Mueller D, Knobeloch D, Nüssler AK, Zeilinger K, Heinzle E and Noor F

"Secretome analysis of human hepatocytes in 2D- and 3D-culture for *in-vitro* toxicology"

4th EuPA Meeting, 23. - 27.10.2010, Estoril, Portugal

Mueller D, Tascher G, Zeilinger K, Lübberstedt M, Noor F and Heinzle E

"3D *in vitro* bioreactor system for the assessment of drug toxicity using human hepatic cells"

ADMET EUROPE 24. - 25.02.2009, Berlin, Germany (eposters.net Best Poster Award)

Mueller D, Müller S, Tascher G, Noor F, Knobeloch D, Nüssler AK and Heinzle E

"A metabonomic approach for the investigation of drug induced hepatic toxicity using GC-ToFMS"

Metabolomics and More, 10. – 12.03.2010, Freising, Germany

Mueller D, Mueller S, Tascher G, Knobeloch D, Nüssler AK, Heinzle E and Noor F

"Sensitive assessment of drug-induced changes in primary human hepatocyte metabolome using a combination of GC-MS and multivariate statistics" (Altex Best Poster Award)

Congress on Alternatives to Animal Testing, 02. - 04.09.2010, Linz, Austria

Mueller D, Tascher G, Müller-Vieira U, Knobeloch D, Nüssler AK, Lübberstedt M, Zeilinger K, Heinzle E and Noor F

"Cultivation of primary human hepatocytes in a 3D membrane bioreactor as an alternative to 2D culture systems for improved hepatotoxicity testing"

Congress on Alternatives to Animal Testing, 02. - 04.09.2010, Linz, Austria

Table I. Identified proteins in the conditioned medium of PHH in monolayer culture after 24h using LC-MALDI. Gene name (GN), Swiss-Prot Accesion number (Acc. no.), identified peptides (pep), sequence coverage (seq. cov.), signal peptide (SP),SecretomeP prediction status (SecP)

No.	Protein name	Acc. no.	MW [Da]	pep	seq. cov.	SP	SecP
1	Complement C3 GN=C3	P01024	187,131.10	38	22.5%	yes	
2	Apolipoprotein A-IV GN=APOA4	P06727	45,381.30	19	43.2%	yes	
3	Complement C4-A GN=C4A	P0C0L4	192,754.80	19	10.7%	yes	
4	Fibronectin GN=FN1	P02751	262,598.90	18	9.01%	yes	
5	Apolipoprotein E GN=APOE	P02649	36,135.50	14	41.6%	yes	
6	Complement factor B GN=CFB	P00751	85,515.20	13	15.6%	yes	
7	Alpha-1-antichymotrypsin GN=SERPINA3	P01011	47,634.90	13	28.1%	yes	
8	Complement C1s subcomponent GN=C1S	P09871	76,666.20	12	17.9%	yes	
9	Apolipoprotein A-I GN=APOA1	P02647	30,760.50	12	35.6%	yes	
10	Complement C1r subcomponent GN=C1R	P00736	80,101.60	10	16.9%	yes	
11	Prothrombin GN=F2	P00734	70,018.80	10	19.6%	yes	
12	Protein AMBP GN=AMBP	P02760	38,981.50	10	35.2%	yes	
13	Alpha-1-antitrypsin GN=SERPINA1	P01009	46,719.90	9	24.6%	yes	
14	Ceruloplasmin GN=CP	P00450	122,189.90	9	8.92%	yes	
15	Apolipoprotein B-100 GN=APOB	P04114	515,596.80	8	1.86%	yes	
16	Hemopexin GN=HPX	P02790	51,658.50	8	16.5%	yes	
17	Alpha-2-macroglobulin GN=A2M	P01023	163,271.90	8	6.51%	yes	
18	Beta-2-glycoprotein 1 GN=APOH	P02749	38,280.50	8	28.1%	yes	
19	Serum amyloid A protein GN=SAA1	P02735	13,514.50	7	54.9%	yes	
20	Complement factor H GN=CFH	P08603	139,078.20	7	8.45%	yes	
21	Vitronectin GN=VTN	P04004	54,288.10	7	16.1%	yes	
22	Vitamin D-binding protein GN=GC	P02774	52,946.60	7	24.1%	yes	
23	Zinc-alpha-2-glycoprotein GN=AZGP1	P25311	34,240.60	7	22.8%	yes	
24	Alcohol dehydrogenase 1B GN=ADH1B	P00325	39,836.30	6	16.8%		no
25	Haptoglobin GN=HP	P00738	45,186.90	6	16.00%	yes	
26	Hyaluronan-binding protein 2 GN=HABP2	Q14520	62,653.40	6	12.00%	yes	
27	Fibrinogen gamma chain GN=FGG	P02679	51,495.30	6	14.8%	yes	
28	Fibrinogen alpha chain GN=FGA	P02671	94,955.40	6	9.93%	yes	
29	Plasminogen GN=PLG	P00747	90,549.40	5	9.38%	yes	
30	Kininogen-1 GN=KNG1	P01042	71,939.60	5	7.61%	yes	
31	Plasma protease C1 inhibitor GN=SERPING1	P05155	55,137.50	5	9.8%	yes	
32	Fibrinogen beta chain GN=FGB	P02675	55,910.60	5	11.4%	yes	
33	Alpha-1-acid glycoprotein 1 GN=ORM1	P02763	23,494.10	5	19.9%	yes	
34	Alpha-2-HS-glycoprotein GN=AHSG	P02765	39,305.40	5	15.8%	yes	
35	Inter-alpha-trypsin inhibitor heavy chain H2 GN=ITIH2	P19823	106,447.50	5	5.81%	yes	
36	Glutamate dehydrogenase 1, mitochondrial GN=GLUD1	P00367	61,381.70	4	6.81%		no
37	Neutrophil gelatinase-associated lipocalin GN=LCN2	P80188	22,570.90	4	25.3%	yes	
38	Complement C2 GN=C2	P06681	83,250.80	4	6.91%	yes	
39	Clusterin GN=CLU	P10909	52,476.90	4	10.0%	yes	
40	Insulin-like growth factor-binding protein 2 GN=IGFBP2	P18065	34,795.60	4	14.2%	yes	
41	Pigment epithelium-derived factor GN=SERPINF1	P36955	46,296.30	4	8.13%	yes	
42	Beta-2-microglobulin GN=B2M	P61769	13,696.90	4	24.4%	yes	
43	Serotransferrin GN=TF	P02787	77,046.30	4	7.74%	yes	
44	Actin, cytoplasmic 1 GN=ACTB	P60709	41,719.80	4	15.2%		no
45	Calreticulin GN=CALR	P27797	48,124.90	4	11.00%	yes	
46	Inter-alpha-trypsin inhibitor heavy chain H4 GN=ITIH4	Q14624	103,340.40	3	3.66%	yes	
47	Glutathione S-transferase A1 GN=GSTA1	P08263	25,615.00	3	11.7%		no
48	Alpha-2-antiplasmin GN=SERPINF2	P08697	54,548.60	3	6.72%	yes	
49	Complement component C8 gamma chain GN=C8G	P07360	22,259.30	3	16.8%	yes	
50	Nucleobindin-1 GN=NUCB1	Q02818	53,861.60	3	9.11%	yes	
51	Angiotensinogen GN=AGT	P01019	53,136.80	3	7.63%	yes	

52	Fructose-1,6-bisphosphatase 1 GN=FBP1	P09467	36,825.20	3	12.1%		0.515
53	Retinol-binding protein 4 GN=RBP4	P02753	22,992.30	3	15.9%	yes	
54	Apolipoprotein C-III GN=APOC3	P02656	10,834.30	3	34.3%	yes	
55	Plasminogen activator inhibitor 1 GN=SERPINE1	P05121	45,042.20	3	6.72%	yes	
56	Histidine-rich glycoprotein GN=HRG	P04196	59,558.60	3	6.1%	yes	
57	Insulin-like growth factor-binding protein complex acid labile subunit GN=IGFALS	P35858	66,020.60	3	6.12%	yes	
58	Fibrinogen-like protein 1 GN=FGL1	Q08830	36,361.90	3	10.9%	yes	
59	Histone H4 GN=HIST1H4A	P62805	11,349.70	3	29.1%		no
60	Transforming growth factor-beta-induced protein ig-h3 GN=TGFBI	Q15582	74,664.90	3	5.71%	yes	
61	Insulin-like growth factor-binding protein 4 GN=IGFBP4	P22692	27,915.70	2	9.3%	yes	
62	Apolipoprotein C-II GN=APOC2	P02655	11,266.10	2	19.8%	yes	
63	Coagulation factor XII GN=F12	P00748	67,772.60	2	3.9%	yes	
64	Coagulation factor X GN=F10	P00742	54,714.10	2	6.76%	yes	
65	Metalloproteinase inhibitor 1 GN=TIMP1	P01033	23,153.10	2	11.1%	yes	
66	Insulin-like growth factor-binding protein 1 GN=IGFBP1	P08833	27,884.90	2	11.6%	yes	
67	Cytochrome b5 GN=CYB5A	P00167	15,312.30	2	20.1%		0.567
68	3-ketoacyl-CoA thiolase, mitochondrial GN=ACAA2	P42765	41,906.20	2	6.55%		no
69	Leucine-rich alpha-2-glycoprotein GN=LRG1	P02750	38,161.70	2	5.76%	yes	
70	Retinoic acid receptor responder protein 2 GN=RARRES2	Q99969	18,599.30	2	14.7%	yes	
71	Inter-alpha-trypsin inhibitor heavy chain H3 GN=ITIH3	Q06033	99,832.90	2	2.81%	yes	
72	Betaine--homocysteine S-methyltransferase 1 GN=BHMT	Q93088	44,980.60	2	7.88%		no
73	Protein disulfide-isomerase GN=P4HB	P07237	57,100.10	2	5.51%	yes	
74	Polymeric immunoglobulin receptor GN=PIGR	P01833	83,265.40	2	2.36%	yes	
75	Fructose-bisphosphate aldolase B GN=ALDOB	P05062	39,455.30	2	6.04%		no
76	Galectin-3-binding protein GN=LGALS3BP	Q08380	65,314.10	2	3.93%	yes	
77	HLA class I histocompatibility antigen, A-25 alpha chain GN=HLA-A	P18462	41,199.70	2	6.58%	yes	
78	Liver carboxylesterase 1 GN=CES1	P23141	62,504.40	2	4.06%	yes	
79	Chitinase-3-like protein 1 GN=CHI3L1	P36222	42,609.00	2	5.22%	yes	
80	Agrin GN=AGRN	O00468	214,820.00	2	1.32%	yes	
81	Cathepsin Z GN=CTSZ	Q9UBR2	33,850.20	2	7.26%	yes	
82	Syndecan-1 GN=SDC1	P18827	32,443.40	1	5.48%	yes	
83	Antithrombin-III GN=SERPINC1	P01008	52,586.00	1	3.66%	yes	
84	Cathepsin B GN=CTSB	P07858	37,803.20	1	5.01%	yes	
85	Triosephosphate isomerase GN=TPI1	P60174	26,651.10	1	5.22%		0.51
86	Fatty acid-binding protein, liver GN=FABP1	P07148	14,190.70	1	8.66%		no
87	Inter-alpha-trypsin inhibitor heavy chain H1 GN=ITIH1	P19827	101,371.80	1	1.32%	yes	
88	Cathepsin L1 GN=CTSL1	P07711	37,546.10	1	3.6%	yes	
89	Ornithine carbamoyltransferase, mitochondrial GN=OTC	P00480	39,919.00	1	3.95%		no
90	Alpha-1-acid glycoprotein 2 GN=ORM2	P19652	23,585.20	1	12.4%	yes	
91	Proprotein convertase subtilisin/kexin type 9 GN=PCSK9	Q8NBP7	74,266.40	1	1.88%	yes	
92	Serum amyloid A-4 protein GN=SAA4	P35542	14,729.20	1	8.46%	yes	
93	Cell adhesion molecule 1 GN=CADM1	Q9BY67	48,491.30	1	2.94%	yes	
94	Malate dehydrogenase, cytoplasmic GN=MDH1	P40925	36,408.90	1	3.59%		no
95	Amyloid beta A4 protein GN=APP	P05067	86,923.30	1	1.69%	yes	
96	Ezrin GN=EZR	P15311	69,396.60	1	1.71%		0.563
97	Zinc finger imprinted 2 GN=ZIM2	Q9NZV7	61,145.50	1	2.28%		0.666
98	Cystatin-C GN=CST3	P01034	15,781.20	1	7.53%	yes	
99	Alcohol dehydrogenase 1C GN=ADH1C	P00326	39,849.60	1	10.1%		no
100	Carboxylesterase 2 GN=CES2	O00748	61,789.30	1	2.15%	yes	
101	Angiopoietin-related protein 3 GN=ANGPTL3	Q9Y5C1	53,621.30	1	3.04%	yes	
102	SPARC GN=SPARC	P09486	34,613.90	1	4.29%	yes	
103	Histone H3.1 GN=HIST1H3A	P68431	15,386.70	1	6.62%		0.681
104	Histone H2A type 1-B/E GN=HIST1H2AB	P04908	14,118.00	1	6.92%		0.536
105	Plasma serine protease inhibitor GN=SERPINA5	P05154	45,684.80	1	2.46%	yes	
106	Proactivator polypeptide GN=PSAP	P07602	58,094.00	1	2.1%	yes	
107	Complement factor I GN=CFI	P05156	65,731.80	1	1.2%	yes	
108	Rab GDP dissociation inhibitor alpha GN=GDI1	P31150	50,566.10	1	4.25%		no

109	Malate dehydrogenase, mitochondrial GN=MDH2	P40926	35,485.70	1	3.85%		0.644
110	Protein disulfide-isomerase A4 GN=PDIA4	P13667	72,916.00	1	1.71%	yes	
111	Nck-associated protein 1-like GN=NCKAP1L	P55160	128,140.30	1	0.71%		0.552
112	Protein FAM83H GN=FAM83H	Q6ZRV2	127,105.90	1	0.594%		no
113	Plasma kallikrein GN=KLKB1	P03952	71,351.70	1	1.57%	yes	
114	Apolipoprotein A-II GN=APOA2	P02652	11,157.20	1	9.00%	yes	
115	Alpha-actinin-4 GN=ACTN4	O43707	104,839.20	1	0.988%		no
116	Osteopontin GN=SPP1	P10451	35,404.60	1	5.41%	yes	
117	Apolipoprotein C-I GN=APOC1	P02654	9,314.30	1	10.8%	yes	
118	S-adenosylmethionine synthase isoform type-1 GN=MAT1A	Q00266	43,629.50	1	2.28%		no
119	Leucine-rich repeat-containing protein 16B GN=LRRC16B	Q8ND23	150,214.80	1	0.583%		no
120	4-aminobutyrate aminotransferase, mitochondrial GN=ABAT	P80404	56,422.80	1	2.8%		0.575
121	Superoxide dismutase [Cu-Zn] GN=SOD1	P00441	15,917.30	1	9.09%		0.648
122	Mannan-binding lectin serine protease 2 GN=MASP2	O00187	75,685.40	1	1.17%	yes	
123	Phosphatidylethanolamine-binding protein 1 GN=PEBP1	P30086	21,038.90	1	8.02%		0.672
124	Angiopoietin-related protein 4 GN=ANGPTL4	Q9BY76	45,196.00	1	2.71%	yes	
125	Delta(3,5)-Delta(2,4)-dienoyl-CoA isomerase, mitochondrial GN=ECH1	Q13011	35,798.20	1	3.05%		0.696
126	39S ribosomal protein L21, mitochondrial GN=MRPL21	Q7Z2W9	22,797.10	1	3.9%		0.695

Table II. Identified proteins in the conditioned medium of PHH in bioreactor culture during phase I (day 4-6) using LC-MALDI. Gene name (GN), Swiss-Prot Accesion number (Acc. no.), identified peptides (Pep), sequence coverage (Seq. cov.), signal peptide (SP), SecretomeP prediction status (SecP)

No.	Protein name	Acc. no.	MW [Da]	Pep	Seq. cov.	SP	SecP
1	Complement C3 GN=C3	P01024	187,131.10	22	15.9%	yes	
2	Complement C4-A GN=C4A	P0C0L4	192,754.80	17	9.98%	yes	
3	Ceruloplasmin GN=CP	P00450	122,189.90	14	16.1%	yes	
4	Complement factor B GN=CFB	P00751	85,515.20	13	19.6%	yes	
5	Liver carboxylesterase 1 GN=CES1	P23141	62,504.40	13	25.7%	yes	
6	Glutamate dehydrogenase 1, mitochondrial GN=GLUD1	P00367	61,381.70	12	28.7%		no
7	Alpha-1-antichymotrypsin GN=SERPINA3	P01011	47,634.90	12	29.8%	yes	
8	Complement factor H GN=CFH	P08603	139,078.20	11	10.7%	yes	
9	Alpha-2-macroglobulin GN=A2M	P01023	163,271.90	10	8.34%	yes	
10	Protein AMBP GN=AMBP	P02760	38,981.50	9	30.4%	yes	
11	Vitamin D-binding protein GN=GC	P02774	52,946.60	9	24.1%	yes	
12	Protein disulfide-isomerase A3 GN=PDIA3	P30101	56,766.60	9	19.6%	yes	
13	Antithrombin-III GN=SERPINC1	P01008	52,586.00	8	20.3%	yes	
14	Hemopexin GN=HPX	P02790	51,658.50	8	22.9%	yes	
15	Catalase GN=CAT	P04040	59,738.50	8	17.3%		no
16	Alpha-1-acid glycoprotein 1 GN=ORM1	P02763	23,494.10	7	35.3%	yes	
17	Alpha-1B-glycoprotein GN=A1BG	P04217	54,235.30	7	17.2%	yes	
18	Complement C1r subcomponent GN=C1R	P00736	80,101.60	6	10.4%	yes	
19	Apolipoprotein A-I GN=APOA1	P02647	30,760.50	6	23.6%	yes	
20	Beta-2-glycoprotein 1 GN=APOH	P02749	38,280.50	6	22.0%	yes	
21	Fibronectin GN=FN1	P02751	262,598.90	6	2.93%	yes	
22	Glutathione S-transferase A2 GN=GSTA2	P09210	25,647.90	6	18.0%		no
23	Complement C1s subcomponent GN=C1S	P09871	76,666.20	6	9.45%	yes	
24	Alcohol dehydrogenase [NADP+] GN=AKR1A1	P14550	36,555.60	6	23.4%		no
25	Insulin-like growth factor-binding protein complex acid labile subunit GN=IGFALS	P35858	66,020.60	6	11.4%	yes	
26	Malate dehydrogenase, mitochondrial GN=MDH2	P40926	35,485.70	6	20.7%		0.644
27	Triosephosphate isomerase GN=TPI1	P60174	26,651.10	6	32.5%		0.51
28	POTE ankyrin domain family member F GN=POTEF	A5A3E0	121,429.10	5	5.67%		no
29	Aspartate aminotransferase, mitochondrial GN=GOT2	P00505	47,500.60	5	12.1%		0.505
30	Superoxide dismutase [Mn], mitochondrial GN=SOD2	P04179	24,704.60	5	20.3%	yes	
31	Alpha-enolase GN=ENO1	P06733	47,152.20	5	15.9%		0.536
32	Fructose-1,6-bisphosphatase 1 GN=FBP1	P09467	36,825.20	5	19.2%		0.515
33	Aspartate aminotransferase, cytoplasmic GN=GOT1	P17174	46,230.10	5	11.9%		no
34	Phosphatidylethanolamine-binding protein 1 GN=PEBP1	P30086	21,038.90	5	39.0%		0.672
35	Pigment epithelium-derived factor GN=SERPINF1	P36955	46,296.30	5	11.0%	yes	
36	Aminoacylase-1 GN=ACY1	Q03154	45,866.30	5	11.3%		no
37	Carboxylesterase 2 GN=CES2	O00748	61,789.30	4	8.59%	yes	
38	Angiotensinogen GN=AGT	P01019	53,136.80	4	10.7%	yes	
39	Serotransferrin GN=TF	P02787	77,046.30	4	7.16%	yes	
40	Histidine-rich glycoprotein GN=HRG	P04196	59,558.60	4	7.81%	yes	
41	Fructose-bisphosphate aldolase B GN=ALDOB	P05062	39,455.30	4	15.1%		no
42	Plasminogen activator inhibitor 1 GN=SERPINE1	P05121	45,042.20	4	9.45%	yes	
43	Plasma protease C1 inhibitor GN=SERPING1	P05155	55,137.50	4	9.2%	yes	
44	Complement factor I GN=CFI	P05156	65,731.80	4	6.52%	yes	
45	Fatty acid-binding protein, liver GN=FABP1	P07148	14,190.70	4	33.9%		no
46	Cathepsin B GN=CTSB	P07858	37,803.20	4	15.6%	yes	
47	Heat shock cognate 71 kDa protein GN=HSPA8	P11142	70,881.80	4	8.51%		no
48	Inter-alpha-trypsin inhibitor heavy chain H2 GN=ITIH2	P19823	106,447.50	4	4.76%	yes	
49	Serine--pyruvate aminotransferase GN=AGXT	P21549	42,993.40	4	12.2%		0.747
50	Peptidyl-prolyl cis-trans isomerase B GN=PPIB	P23284	23,725.20	4	19.0%	yes	
51	Endoplasmic reticulum resident protein 29 GN=ERP29	P30040	28,976.90	4	18.0%	yes	
52	Chitinase-3-like protein 1 GN=CHI3L1	P36222	42,609.00	4	16.2%	yes	
53	L-lactate dehydrogenase A chain GN=LDHA	P00338	36,671.20	3	8.13%		0.549
54	Phosphoglycerate kinase 1 GN=PGK1	P00558	44,597.30	3	11.8%		no
55	Apolipoprotein E GN=APOE	P02649	36,135.50	3	11.0%	yes	
56	Serum amyloid P-component GN=APCS	P02743	25,369.70	3	12.6%	yes	
57	Leucine-rich alpha-2-glycoprotein GN=LRG1	P02750	38,161.70	3	8.07%	yes	

58	Retinol-binding protein 4 GN=RBP4	P02753	22,992.30	3	15.4%	yes	
59	Glucose-6-phosphate isomerase GN=GPI	P06744	63,130.40	3	6.63%		no
60	Monocyte differentiation antigen CD14 GN=CD14	P08571	40,058.60	3	12.5%	yes	
61	Thioredoxin GN=TXN	P10599	11,719.30	3	32.4%		no
62	Fumarylacetoacetase GN=FAH	P16930	46,357.60	3	8.59%		0.582
63	Glycine amidinotransferase, mitochondrial GN=GATM	P50440	48,438.60	3	6.38%		0.699
64	10 kDa heat shock protein, mitochondrial GN=HSPE1	P61604	10,913.70	3	19.6%		0.57
65	Beta-2-microglobulin GN=B2M	P61769	13,696.90	3	21.8%	yes	
66	Neutrophil gelatinase-associated lipocalin GN=LCN2	P80188	22,570.90	3	21.7%	yes	
67	4-aminobutyrate aminotransferase, mitochondrial GN=ABAT	P80404	56,422.80	3	6.4%		0.575
68	Inter-alpha-trypsin inhibitor heavy chain H3 GN=ITIH3	Q06033	99,832.90	3	3.71%	yes	
69	Delta(3,5)-Delta(2,4)-dienoyl-CoA isomerase, mitochondrial GN=ECH1	Q13011	35,798.20	3	12.2%		0.696
70	Selenium-binding protein 1 GN=SELENBP1	Q13228	52,374.00	3	6.36%		no
71	Thioredoxin domain-containing protein 5 GN=TXNDC5	Q8NBS9	47,611.10	3	9.49%	yes	
72	Isocitrate dehydrogenase [NADP] cytoplasmic GN=IDH1	O75874	46,642.50	2	5.31%		0.547
73	Cytochrome b5 GN=CYB5A	P00167	15,312.30	2	20.1%		0.567
74	Alcohol dehydrogenase 1C GN=ADH1C	P00326	39,849.60	2	4.27%		no
75	Retinal dehydrogenase 1 GN=ALDH1A1	P00352	54,844.80	2	4.59%		0.501
76	Ornithine carbamoyltransferase, mitochondrial GN=OTC	P00480	39,919.00	2	6.78%		no
77	Prothrombin GN=F2	P00734	70,018.80	2	3.54%	yes	
78	Plasminogen GN=PLG	P00747	90,549.40	2	3.58%	yes	
79	Coagulation factor XII GN=F12	P00748	67,772.60	2	4.39%	yes	
80	Metalloproteinase inhibitor 1 GN=TIMP1	P01033	23,153.10	2	11.1%	yes	
81	Kininogen-1 GN=KNG1	P01042	71,939.60	2	3.11%	yes	
82	Polymeric immunoglobulin receptor GN=PIGR	P01833	83,265.40	2	3.93%	yes	
83	Argininosuccinate lyase GN=ASL	P04424	51,641.00	2	6.68%		no
84	Complement C2 GN=C2	P06681	83,250.80	2	2.66%	yes	
85	Apolipoprotein A-IV GN=APOA4	P06727	45,381.30	2	5.3%	yes	
86	Beta-glucuronidase GN=GUSB	P08236	74,714.70	2	2.61%	yes	
87	Mannose-binding protein C GN=MBL2	P11226	26,126.10	2	6.85%	yes	
88	Delta-aminolevulinic acid dehydratase GN=ALAD	P13716	36,277.30	2	6.06%		0.637
89	Inter-alpha-trypsin inhibitor heavy chain H1 GN=ITIH1	P19827	101,371.80	2	3.29%	yes	
90	Insulin-like growth factor-binding protein 4 GN=IGFBP4	P22692	27,915.70	2	11.2%	yes	
91	Zinc-alpha-2-glycoprotein GN=AZGP1	P25311	34,240.60	2	8.05%	yes	
92	Moesin GN=MSN	P26038	67,803.80	2	3.29%		0.53
93	D-dopachrome decarboxylase GN=DDT	P30046	12,694.20	2	19.5%		no
94	4-hydroxyphenylpyruvate dioxygenase GN=HPD	P32754	44,916.90	2	8.4%		0.517
95	Phosphoglucomutase-1 GN=PGM1	P36871	61,433.00	2	4.27%		no
96	Aldo-keto reductase family 1 member C2 GN=AKR1C2	P52895	36,717.90	2	8.36%		no
97	Glutathione S-transferase omega-1 GN=GSTO1	P78417	27,549.20	2	9.96%		no
98	Complement factor H-related protein 1 GN=CFHR1	Q03591	37,632.40	2	12.4%	yes	
99	3-hydroxyisobutyryl-CoA hydrolase, mitochondrial GN=HIBCH	Q6NVY1	43,466.00	2	4.15%		0.549
100	Gamma-glutamyl hydrolase GN=GGH	Q92820	35,947.90	2	8.49%	yes	
101	Ester hydrolase C11orf54 GN=C11orf54	Q9H0W9	35,099.70	2	6.67%		no
102	Dimethylglycine dehydrogenase, mitochondrial GN=DMGDH	Q9UI17	96,794.90	2	3.46%	yes	
103	Alpha-actinin-4 GN=ACTN4	O43707	104,839.20	1	0.988%		no
104	GDH/6PGL endoplasmic bifunctional protein GN=H6PD	O95479	88,875.60	1	1.52%	yes	
105	Glutathione reductase, mitochondrial GN=GSR	P00390	56,239.40	1	2.3%		0.54
106	Superoxide dismutase [Cu-Zn] GN=SOD1	P00441	15,917.30	1	9.09%		0.648
107	Purine nucleoside phosphorylase GN=PNP	P00491	32,100.00	1	5.19%		0.509
108	Complement component C9 GN=C9	P02748	63,156.80	1	2.15%	yes	
109	Tissue alpha-L-fucosidase GN=FUCA1	P04066	53,671.90	1	2.36%	yes	
110	Proactivator polypeptide GN=PSAP	P07602	58,094.00	1	2.1%	yes	
111	Cathepsin L1 GN=CTSL1	P07711	37,546.10	1	3.6%	yes	
112	Corticosteroid-binding globulin GN=SERPINA6	P08185	45,124.10	1	3.21%	yes	
113	Alpha-2-antiplasmin GN=SERPINF2	P08697	54,548.60	1	1.83%	yes	
114	60 kDa heat shock protein, mitochondrial GN=HSPD1	P10809	61,037.70	1	3.14%		no
115	Lysosome-associated membrane glycoprotein 2 GN=LAMP2	P13473	44,942.90	1	1.95%	yes	
116	Phosphoglycerate mutase 1 GN=PGAM1	P18669	28,786.80	1	4.33%		no
117	Alpha-1-acid glycoprotein 2 GN=ORM2	P19652	23,585.20	1	13.4%	yes	
118	14-3-3 protein theta GN=YWHAQ	P27348	27,747.40	1	3.67%		no
119	Cystathionine gamma-lyase GN=CTH	P32929	44,490.50	1	3.46%		0.526
120	Serine hydroxymethyltransferase, cytosolic GN=SHMT1	P34896	53,065.80	1	2.28%		no

121	Transaldolase GN=TALDO1	P37837	37,523.70	1	3.56%		no
122	Malate dehydrogenase, cytoplasmic GN=MDH1	P40925	36,408.90	1	3.59%		no
123	3-hydroxyanthranilate 3,4-dioxygenase GN=HAAO	P46952	32,538.20	1	3.5%		no
124	Ribonuclease UK114 GN=HRSP12	P52758	14,476.10	1	11.7%		0.714
125	Calmodulin GN=CALM1	P62158	16,820.00	1	11.4%		0.676
126	Peptidyl-prolyl cis-trans isomerase A GN=PPIA	P62937	17,994.90	1	8.48%		no
127	Aldehyde oxidase GN=AOX1	Q06278	147,902.70	1	0.822%		no
128	Enoyl-CoA hydratase domain-containing protein 2, mitochondrial GN=ECHDC2	Q86YB7	31,108.70	1	5.14%	yes	
129	Betaine--homocysteine S-methyltransferase 1 GN=BHMT	Q93088	44,980.60	1	4.19%		no
130	N-acetylmuramoyl-L-alanine amidase GN=PGLYRP2	Q96PD5	62,199.90	1	2.6%	yes	
131	Phospholysine phosphohistidine inorganic pyrophosphate phosphatase GN=LHPP	Q9H008	29,147.40	1	4.44%		no
132	Cathepsin Z GN=CTSZ	Q9UBR2	33,850.20	1	3.3%		0.861
133	Phosphoserine aminotransferase GN=PSAT1	Q9Y617	40,405.30	1	2.43%		no

Table III. Identified proteins in the conditioned medium of PHH in bioreactor culture during phase II (day 7-10) using LC-MALDI. Gene name (GN), Swiss-Prot Accesion number (Acc. no.), identified peptides (Pep), sequence coverage (Seq. cov.), signal peptide (SP), SecretomeP prediction status (SecP)

No.	Protein name	Acc. no.	MW [Da]	Pep	Seq. cov.	SP	SecP
1	Complement C3 GN=C3	P01024	187,131.10	33	24.4%	yes	
2	Complement factor H GN=CFH	P08603	139,078.20	19	19.3%	yes	
3	Ceruloplasmin GN=CP	P00450	122,189.90	15	17.5%	yes	
4	Alpha-2-macroglobulin GN=A2M	P01023	163,271.90	13	10.8%	yes	
5	Alpha-1-antichymotrypsin GN=SERPINA3	P01011	47,634.90	12	27.4%	yes	
6	Protein AMBP GN=AMBP	P02760	38,981.50	12	38.1%	yes	
7	Complement C4-A GN=C4A	P0C0L4	192,754.80	12	7.68%	yes	
8	Alpha-actinin-4 GN=ACTN4	O43707	104,839.20	11	14.5%		no
9	Complement factor B GN=CFB	P00751	85,515.20	11	16.1%	yes	
10	Vitamin D-binding protein GN=GC	P02774	52,946.60	11	32.7%	yes	
11	Moesin GN=MSN	P26038	67,803.80	11	13.7%		0.53
12	Apolipoprotein E GN=APOE	P02649	36,135.50	10	27.8%	yes	
13	Fibronectin GN=FN1	P02751	262,598.90	9	4.15%	yes	
14	Alpha-enolase GN=ENO1	P06733	47,152.20	9	26.3%		0.536
15	Aspartate aminotransferase, cytoplasmic GN=GOT1	P17174	46,230.10	9	23.2%		no
16	Liver carboxylesterase 1 GN=CES1	P23141	62,504.40	9	19.2%	yes	
17	Triosephosphate isomerase GN=TPI1	P60174	26,651.10	9	48.2%		0.51
18	Aldo-keto reductase family 1 member C1 GN=AKR1C1	Q04828	36,771.10	9	28.2%		no
19	Isocitrate dehydrogenase [NADP] cytoplasmic GN=IDH1	O75874	46,642.50	8	18.1%		0.547
20	Retinal dehydrogenase 1 GN=ALDH1A1	P00352	54,844.80	8	23.4%		0.501
21	Hemopexin GN=HPX	P02790	51,658.50	8	21.9%	yes	
22	Heat shock cognate 71 kDa protein GN=HSPA8	P11142	70,881.80	8	17.2%		no
23	Actin, cytoplasmic 1 GN=ACTB	P60709	41,719.80	8	25.9%		no
24	Aldo-keto reductase family 1 member B10 GN=AKR1B10	O60218	36,003.40	7	26.9%		no
25	Alcohol dehydrogenase 1C GN=ADH1C	P00326	39,849.60	7	18.4%		no
26	Glutamate dehydrogenase 1, mitochondrial GN=GLUD1	P00367	61,381.70	7	16.3%		no
27	Alpha-1-acid glycoprotein 1 GN=ORM1	P02763	23,494.10	7	38.8%	yes	
28	Complement C1s subcomponent GN=C1S	P09871	76,666.20	7	12.6%	yes	
29	Phosphatidylethanolamine-binding protein 1 GN=PEBP1	P30086	21,038.90	7	48.1%		0.672
30	Protein disulfide-isomerase A3 GN=PDIA3	P30101	56,766.60	7	16.6%	yes	
31	Aminoacylase-1 GN=ACY1	Q03154	45,866.30	7	18.9%		no
32	Complement C1r subcomponent GN=C1R	P00736	80,101.60	6	10.2%	yes	
33	Fibrinogen gamma chain GN=FGG	P02679	51,495.30	6	15.2%	yes	
34	Beta-2-glycoprotein 1 GN=APOH	P02749	38,280.50	6	24.6%	yes	
35	Catalase GN=CAT	P04040	59,738.50	6	13.3%		no
36	Superoxide dismutase [Mn], mitochondrial GN=SOD2	P04179	24,704.60	6	30.2%	yes	
37	Histidine-rich glycoprotein GN=HRG	P04196	59,558.60	6	11.8%	yes	
38	Glucose-6-phosphate isomerase GN=GPI	P06744	63,130.40	6	12.2%		no
39	Glutathione S-transferase A2 GN=GSTA2	P09210	25,647.90	6	18.0%		no
40	Inter-alpha-trypsin inhibitor heavy chain H2 GN=ITIH2	P19823	106,447.50	6	5.6%	yes	
41	1,4-alpha-glucan-branching enzyme GN=GBE1	Q04446	80,444.90	6	9.26%		no
42	Argininosuccinate synthase GN=ASS1	P00966	46,513.30	5	9.95%		no
43	Antithrombin-III GN=SERPINC1	P01008	52,586.00	5	13.6%	yes	
44	Kininogen-1 GN=KNG1	P01042	71,939.60	5	6.83%	yes	
45	Apolipoprotein A-I GN=APOA1	P02647	30,760.50	5	20.6%	yes	
46	Fibrinogen alpha chain GN=FGA	P02671	94,955.40	5	9.01%	yes	
47	Fibrinogen beta chain GN=FGB	P02675	55,910.60	5	10.8%	yes	
48	Serotransferrin GN=TF	P02787	77,046.30	5	9.03%	yes	
49	Apolipoprotein B-100 GN=APOB	P04114	515,596.80	5	1.49%	yes	
50	Fructose-bisphosphate aldolase B GN=ALDOB	P05062	39,455.30	5	20.1%		no
51	Fatty acid-binding protein, liver GN=FABP1	P07148	14,190.70	5	41.7%		no
52	Pigment epithelium-derived factor GN=SERPINF1	P36955	46,296.30	5	13.4%	yes	
53	L-lactate dehydrogenase A chain GN=LDHA	P00338	36,671.20	4	11.7%		0.549
54	Retinol-binding protein 4 GN=RBP4	P02753	22,992.30	4	20.9%	yes	
55	Keratin, type II cytoskeletal 1 GN=KRT1	P04264	66,022.30	4	10.4%		no
56	Plasma protease C1 inhibitor GN=SERPING1	P05155	55,137.50	4	9.2%	yes	
57	Complement factor I GN=CFI	P05156	65,731.80	4	9.78%	yes	

58	Proactivator polypeptide GN=PSAP	P07602	58,094.00	4	7.63%	yes	
59	Cathepsin B GN=CTSB	P07858	37,803.20	4	18.3%	yes	
60	Heat shock 70 kDa protein 1A/1B GN=HSPA1A	P08107	70,036.00	4	8.89%		no
61	Monocyte differentiation antigen CD14 GN=CD14	P08571	40,058.60	4	14.9%	yes	
62	Thioredoxin GN=TXN	P10599	11,719.30	4	41.0%		no
63	Alcohol dehydrogenase [NADP+] GN=AKR1A1	P14550	36,555.60	4	16.3%		no
64	Zinc-alpha-2-glycoprotein GN=AZGP1	P25311	34,240.60	4	15.4%	yes	
65	4-hydroxyphenylpyruvate dioxygenase GN=HPD	P32754	44,916.90	4	10.4%		0.517
66	Peptidyl-prolyl cis-trans isomerase A GN=PPIA	P62937	17,994.90	4	24.2%		no
67	14-3-3 protein zeta/delta GN=YWHAZ	P63104	27,727.90	4	13.9%		no
68	Peroxiredoxin-1 GN=PRDX1	Q06830	22,092.90	4	26.1%		0.528
69	Phosphoglycerate kinase 1 GN=PGK1	P00558	44,597.30	3	12.0%		no
70	Prothrombin GN=F2	P00734	70,018.80	3	5.14%	yes	
71	Plasminogen GN=PLG	P00747	90,549.40	3	4.81%	yes	
72	Metalloproteinase inhibitor 1 GN=TIMP1	P01033	23,153.10	3	20.3%	yes	
73	Prelamin-A/C GN=LMNA	P02545	74,122.60	3	4.82%		no
74	Leucine-rich alpha-2-glycoprotein GN=LRG1	P02750	38,161.70	3	8.93%	yes	
75	Metallothionein-2 GN=MT2A	P02795	6,023.60	3	34.4%		0.856
76	Alpha-1B-glycoprotein GN=A1BG	P04217	54,235.30	3	5.45%	yes	
77	Argininosuccinate lyase GN=ASL	P04424	51,641.00	3	9.7%		no
78	Keratin, type I cytoskeletal 18 GN=KRT18	P05783	48,041.00	3	7.44%		0.725
79	Protein disulfide-isomerase GN=P4HB	P07237	57,100.10	3	7.09%	yes	
80	Cathepsin D GN=CTSD	P07339	44,535.00	3	6.31%	yes	
81	Fructose-1,6-bisphosphatase 1 GN=FBP1	P09467	36,825.20	3	10.7%		0.515
82	Delta-aminolevulinic acid dehydratase GN=ALAD	P13716	36,277.30	3	11.8%		0.637
83	Nucleoside diphosphate kinase A GN=NME1	P15531	17,130.70	3	25.7%		no
84	Fumarylacetoacetase GN=FAH	P16930	46,357.60	3	9.07%		0.582
85	Serine--pyruvate aminotransferase GN=AGXT	P21549	42,993.40	3	9.69%		0.747
86	Insulin-like growth factor-binding protein 4 GN=IGFBP4	P22692	27,915.70	3	11.2%	yes	
87	Calreticulin GN=CALR	P27797	48,124.90	3	9.59%	yes	
88	Transketolase GN=TKT	P29401	67,861.40	3	8.51%		no
89	Endoplasmic reticulum resident protein 29 GN=ERP29	P30040	28,976.90	3	11.1%	yes	
90	Peroxiredoxin-6 GN=PRDX6	P30041	25,018.10	3	15.2%		no
91	Serine hydroxymethyltransferase, cytosolic GN=SHMT1	P34896	53,065.80	3	7.87%		no
92	Chitinase-3-like protein 1 GN=CHI3L1	P36222	42,609.00	3	12.5%	yes	
93	Rho GDP-dissociation inhibitor 1 GN=ARHGDIA	P52565	23,189.50	3	18.6%		no
94	10 kDa heat shock protein, mitochondrial GN=HSPE1	P61604	10,913.70	3	19.6%		0.57
95	Beta-2-microglobulin GN=B2M	P61769	13,696.90	3	21.8%	yes	
96	Glutathione S-transferase omega-1 GN=GSTO1	P78417	27,549.20	3	13.3%		no
97	Nucleobindin-1 GN=NUCB1	Q02818	53,861.60	3	9.54%	yes	
98	Complement factor H-related protein 1 GN=CFHR1	Q03591	37,632.40	3	13.9%	yes	
99	Inter-alpha-trypsin inhibitor heavy chain H3 GN=ITIH3	Q06033	99,832.90	3	4.38%	yes	
100	Selenium-binding protein 1 GN=SELENBP1	Q13228	52,374.00	3	6.36%		no
101	Spectrin alpha chain, brain GN=SPTAN1	Q13813	284,524.70	3	1.74%		no
102	Betaine--homocysteine S-methyltransferase 1 GN=BHMT	Q93088	44,980.60	3	10.1%		no
103	Cathepsin Z GN=CTSZ	Q9UBR2	33,850.20	3	12.2%	yes	
104	Carboxylesterase 2 GN=CES2	O00748	61,789.30	2	3.4%	yes	
105	Cytochrome b5 GN=CYB5A	P00167	15,312.30	2	25.4%		0.567
106	Alcohol dehydrogenase 1B GN=ADH1B	P00325	39,836.30	2	18.4%		no
107	Superoxide dismutase [Cu-Zn] GN=SOD1	P00441	15,917.30	2	13.6%		0.648
108	Ornithine carbamoyltransferase, mitochondrial GN=OTC	P00480	39,919.00	2	7.91%		no
109	Aspartate aminotransferase, mitochondrial GN=GOT2	P00505	47,500.60	2	5.12%		0.505
110	Coagulation factor XII GN=F12	P00748	67,772.60	2	4.39%	yes	
111	Alpha-1-antitrypsin GN=SERPINA1	P01009	46,719.90	2	5.26%	yes	
112	Angiotensinogen GN=AGT	P01019	53,136.80	2	4.54%	yes	
113	Polymeric immunoglobulin receptor GN=PIGR	P01833	83,265.40	2	2.75%	yes	
114	Hemoglobin subunit delta GN=HBD	P02042	16,037.10	2	12.9%		no
115	Apolipoprotein C-III GN=APOC3	P02656	10,834.30	2	27.3%	yes	
116	Serum amyloid A protein GN=SAA1	P02735	13,514.50	2	27.9%	yes	
117	Heat shock protein beta-1 GN=HSPB1	P04792	22,764.60	2	12.7%		0.74
118	Plasminogen activator inhibitor 1 GN=SERPINE1	P05121	45,042.20	2	4.23%	yes	
119	Intercellular adhesion molecule 1 GN=ICAM1	P05362	57,806.50	2	4.32%	yes	
120	Complement C2 GN=C2	P06681	83,250.80	2	3.19%	yes	

121	Apolipoprotein A-IV GN=APOA4	P06727	45,381.30	2	5.3%	yes	
122	Beta-hexosaminidase subunit alpha GN=HEXA	P06865	60,686.00	2	4.16%	yes	
123	Acyl-CoA-binding protein GN=DBI	P07108	10,026.80	2	32.2%		0.553
124	Profilin-1 GN=PFN1	P07737	15,036.30	2	16.4%		no
125	Beta-glucuronidase GN=GUSB	P08236	74,714.70	2	2.61%	yes	
126	Alcohol dehydrogenase 4 GN=ADH4	P08319	40,204.80	2	5.53%		0.532
127	Alpha-2-antiplasmin GN=SERPINF2	P08697	54,548.60	2	4.07%	yes	
128	Galectin-1 GN=LGALS1	P09382	14,697.80	2	16.3%		no
129	Clusterin GN=CLU	P10909	52,476.90	2	4.45%	yes	
130	Alpha-actinin-1 GN=ACTN1	P12814	103,043.00	2	10.2%		no
131	Xaa-Pro dipeptidase GN=PEPD	P12955	54,529.70	2	5.27%		no
132	Farnesyl pyrophosphate synthase GN=FDPS	P14324	48,258.70	2	5.49%	yes	
133	Aminopeptidase N GN=ANPEP	P15144	109,524.40	2	1.76%	yes	
134	Aldo-keto reductase family 1 member C4 GN=AKR1C4	P17516	37,049.40	2	13.0%		no
135	Phosphoglycerate mutase 1 GN=PGAM1	P18669	28,786.80	2	11.4%		no
136	Inter-alpha-trypsin inhibitor heavy chain H1 GN=ITIH1	P19827	101,371.80	2	2.74%	yes	
137	Peptidyl-prolyl cis-trans isomerase B GN=PPIB	P23284	23,725.20	2	8.8%	yes	
138	D-dopachrome decarboxylase GN=DDT	P30046	12,694.20	2	19.5%		no
139	UMP-CMP kinase GN=CMPK1	P30085	22,205.00	2	10.7%		0.604
140	Transaldolase GN=TALDO1	P37837	37,523.70	2	7.42%		no
141	Malate dehydrogenase, cytoplasmic GN=MDH1	P40925	36,408.90	2	5.99%		no
142	Aldo-keto reductase family 1 member C3 GN=AKR1C3	P42330	36,836.10	2	25.7%		0.709
143	3-hydroxyanthranilate 3,4-dioxygenase GN=HAAO	P46952	32,538.20	2	5.94%		no
144	NADP-dependent malic enzyme GN=ME1	P48163	64,133.40	2	3.5%		no
145	14-3-3 protein gamma GN=YWHAG	P61981	28,285.10	2	13.8%		no
146	Calmodulin GN=CALM1	P62158	16,820.00	2	16.8%		0.676
147	Histone H4 GN=HIST1H4A	P62805	11,349.70	2	17.5%		no
148	Quinone oxidoreductase GN=CRYZ	Q08257	35,189.30	2	7.6%		0.511
149	Insulin-like growth factor-binding protein 7 GN=IGFBP7	Q16270	29,111.80	2	12.4%	yes	
150	Thioredoxin domain-containing protein 5 GN=TXNDC5	Q8NBS9	47,611.10	2	7.41%	yes	
151	Ester hydrolase C11orf54 GN=C11orf54	Q9H0W9	35,099.70	2	6.67%		no
152	Omega-amidase NIT2 GN=NIT2	Q9NQR4	30,590.80	2	11.6%		0.663
153	Ribosome-binding protein 1 GN=RRBP1	Q9P2E9	152,452.50	2	2.48%		no
154	Phosphoserine aminotransferase GN=PSAT1	Q9Y617	40,405.30	2	5.14%		no
155	Membrane-associated progesterone receptor component 1 GN=PGRMC1	O00264	21,654.20	1	10.3%		no
156	Agrin GN=AGRN	O00468	214,820.00	1	0.7%	yes	
157	Pirin GN=PIR	O00625	32,095.70	1	4.48%		
158	Pantetheinase GN=VNN1	O95497	56,994.30	1	2.92%	yes	
159	Glutathione reductase, mitochondrial GN=GSR	P00390	56,239.40	1	2.3%		0.54
160	Carbonic anhydrase 2 GN=CA2	P00918	29,228.60	1	3.46%		no
161	Complement C5 GN=C5	P01031	188,291.20	1	1.01%	yes	
162	Insulin-like growth factor II GN=IGF2	P01344	20,122.80	1	5.0%	yes	
163	Apolipoprotein A-II GN=APOA2	P02652	11,157.20	1	9.0%	yes	
164	Serum amyloid P-component GN=APCS	P02743	25,369.70	1	5.83%	yes	
165	Complement component C9 GN=C9	P02748	63,156.80	1	2.15%	yes	
166	Alpha-2-HS-glycoprotein GN=AHSG	P02765	39,305.40	1	5.72%	yes	
167	Transthyretin GN=TTR	P02766	15,868.90	1	9.52%	yes	
168	Ferritin light chain GN=FTL	P02792	20,002.60	1	8.57%		no
169	Vitronectin GN=VTN	P04004	54,288.10	1	3.14%	yes	
170	Tissue alpha-L-fucosidase GN=FUCA1	P04066	53,671.90	1	2.36%	yes	
171	Cystatin-B GN=CSTB	P04080	11,121.30	1	12.2%		no
172	Histone H2A type 1-B/E GN=HIST1H2AB	P04908	14,118.00	1	6.92%		0.536
173	Heparin cofactor 2 GN=SERPIND1	P05546	57,054.90	1	1.4%	yes	
174	Complement component C8 gamma chain GN=C8G	P07360	22,259.30	1	7.43%	yes	
175	Beta-hexosaminidase subunit beta GN=HEXB	P07686	63,095.30	1	1.98%	yes	
176	Cathepsin L1 GN=CTSL1	P07711	37,546.10	1	3.6%	yes	
177	Thrombospondin-1 GN=THBS1	P07996	129,363.70	1	1.03%	yes	
178	Ribonuclease pancreatic GN=RNASE1	P07998	17,625.80	1	4.49%	yes	
179	Heme oxygenase 1 GN=HMOX1	P09601	32,801.10	1	5.56%		0.526
180	Tissue factor pathway inhibitor GN=TFPI	P10646	34,998.10	1	5.26%	yes	
181	Laminin subunit gamma-1 GN=LAMC1	P11047	177,583.30	1	1.37%	yes	
182	Gamma-interferon-inducible lysosomal thiol reductase GN=IFI30	P13284	29,131.20	1	4.21%	yes	
183	Lysosome-associated membrane glycoprotein 2 GN=LAMP2	P13473	44,942.90	1	1.95%	yes	

184	Translationally-controlled tumor protein GN=TPT1	P13693	19,578.20	1	5.81%		0.581
185	Plastin-2 GN=LCP1	P13796	70,273.20	1	1.44%		0.502
186	CD59 glycoprotein GN=CD59	P13987	14,159.20	1	9.38%	yes	
187	Macrophage migration inhibitory factor GN=MIF	P14174	12,458.50	1	7.83%		0.776
188	Arylsulfatase A GN=ARSA	P15289	53,571.20	1	2.76%	yes	
189	Ezrin GN=EZR	P15311	69,396.60	1	6.31%		0.563
190	Ribosyldihydronicotinamide dehydrogenase [quinone] GN=NQO2	P16083	25,900.80	1	7.79%		no
191	Insulin-like growth factor-binding protein 2 GN=IGFBP2	P18065	34,795.60	1	7.08%	yes	
192	Vinculin GN=VCL	P18206	123,783.20	1	0.882%		no
193	Syndecan-1 GN=SDC1	P18827	32,443.40	1	5.48%	yes	
194	Alpha-1-acid glycoprotein 2 GN=ORM2	P19652	23,585.20	1	17.4%	yes	
195	Nucleoside diphosphate kinase B GN=NME2	P22392	17,280.20	1	25.7%		no
196	Heterogeneous nuclear ribonucleoproteins A2/B1 GN=HNRNPA2B1	P22626	37,412.30	1	3.4%		no
197	Cofilin-1 GN=CFL1	P23528	18,485.10	1	8.43%		0.628
198	Cathepsin S GN=CTSS	P25774	37,477.60	1	2.42%	yes	
199	Peptidyl-prolyl cis-trans isomerase FKBP2 GN=FKBP2	P26885	15,631.60	1	8.45%	yes	
200	14-3-3 protein theta GN=YWHAQ	P27348	27,747.40	1	13.9%		no
201	Flavin reductase GN=BLVRB	P30043	22,100.70	1	7.28%		0.834
202	Leukocyte elastase inhibitor GN=SERPINB1	P30740	42,725.80	1	2.37%		0.516
203	14-3-3 protein beta/alpha GN=YWHAB	P31946	28,065.10	1	13.8%		no
204	Cystathionine gamma-lyase GN=CTH	P32929	44,490.50	1	3.46%		0.526
205	Ribonuclease 4 GN=RNASE4	P34096	16,822.40	1	8.84%	yes	
206	Serpin B6 GN=SERPINB6	P35237	42,604.80	1	3.99%		no
207	Radixin GN=RDX	P35241	68,547.50	1	8.06%		no
208	Phosphoglucomutase-1 GN=PGM1	P36871	61,433.00	1	2.67%		no
209	Dihydrolipoyllysine-residue succinyltransferase component of 2-oxoglutarate dehydrogenase complex, mitochondrial GN=DLST	P36957	48,737.20	1	2.43%		0.634
210	Malate dehydrogenase, mitochondrial GN=MDH2	P40926	35,485.70	1	3.55%		0.644
211	Nicotinamide phosphoribosyltransferase GN=NAMPT	P43490	55,504.50	1	1.43%		no
212	Proteasome subunit beta type-2 GN=PSMB2	P49721	22,819.50	1	7.46%		no
213	Rab GDP dissociation inhibitor beta GN=GDI2	P50395	50,647.50	1	4.27%		no
214	Aldo-keto reductase family 1 member C2 GN=AKR1C2	P52895	36,717.90	1	22.6%		no
215	Nck-associated protein 1-like GN=NCKAP1L	P55160	128,140.30	1	0.71%		0.552
216	Galectin-4 GN=LGALS4	P56470	35,923.30	1	4.33%		no
217	Actin-related protein 2/3 complex subunit 4 GN=ARPC4	P59998	19,649.40	1	4.76%		0.646
218	Proteasome subunit alpha type-6 GN=PSMA6	P60900	27,381.50	1	4.07%		no
219	Epididymal secretory protein E1 GN=NPC2	P61916	16,552.00	1	10.6%	yes	
220	14-3-3 protein epsilon GN=YWHAE	P62258	29,157.00	1	8.24%		no
221	Nuclease-sensitive element-binding protein 1 GN=YBX1	P67809	35,905.70	1	3.7%		0.733
222	Hemoglobin subunit alpha GN=HBA1	P69905	15,239.60	1	10.6%		no
223	Neutrophil gelatinase-associated lipocalin GN=LCN2	P80188	22,570.90	1	7.58%	yes	
224	Spectrin beta chain, brain 1 GN=SPTBN1	Q01082	274,595.40	1	0.338%		no
225	14-3-3 protein eta GN=YWHAH	Q04917	28,201.60	1	8.13%		no
226	Aldehyde oxidase GN=AOX1	Q06278	147,902.70	1	0.822%		no
227	Bile salt sulfotransferase GN=SULT2A1	Q06520	33,763.30	1	3.51%		0.538
228	Galectin-3-binding protein GN=LGALS3BP	Q08380	65,314.10	1	2.74%	yes	
229	Fibrinogen-like protein 1 GN=FGL1	Q08830	36,361.90	1	3.53%	yes	
230	Nicotinate-nucleotide pyrophosphorylase [carboxylating] GN=QPRT	Q15274	30,827.30	1	4.04%	yes	
231	Hydroxyacyl-coenzyme A dehydrogenase, mitochondrial GN=HADH	Q16836	34,276.10	1	2.87%		no
232	Coiled-coil domain-containing protein 96 GN=CCDC96	Q2M329	62,693.30	1	2.88%		0.622
233	Beta-lactamase-like protein 2 GN=LACTB2	Q53H82	32,788.70	1	3.12%		no
234	RUN domain-containing protein 3A GN=RUNDC3A	Q59EK9	49,730.60	1	1.57%		no
235	Protein Smaug homolog 2 GN=SAMD4B	Q5PRF9	75,466.60	1	2.16%		no
236	Enoyl-CoA hydratase domain-containing protein 2, mitochondrial GN=ECHDC2	Q86YB7	31,108.70	1	5.14%	yes	
237	Uncharacterized protein KIAA0528 GN=KIAA0528	Q86YS7	110,430.70	1	0.7%		no
238	Hornerin GN=HRNR	Q86YZ3	282,354.70	1	0.667%		no
239	Serine protease HTRA1 GN=HTRA1	Q92743	51,269.30	1	2.5%	yes	
240	Protein DJ-1 GN=PARK7	Q99497	19,873.10	1	6.88%		no
241	Retinoic acid receptor responder protein 2 GN=RARRES2	Q99969	18,599.30	1	7.36%	yes	
242	Phospholysine phosphohistidine inorganic pyrophosphate phosphatase GN=LHPP	Q9H008	29,147.40	1	4.44%		no
243	SH3 domain-binding glutamic acid-rich-like protein 3 GN=SH3BGRL3	Q9H299	10,419.80	1	16.1%		0.768
244	Interferon kappa GN=IFNK	Q9P0W0	25,201.40	1	4.83%	yes	
245	Peroxisomal sarcosine oxidase GN=PIPOX	Q9P0Z9	44,049.10	1	3.59%		0.534

246	Beta-ureidopropionase GN=UPB1	Q9UBR1	43,148.10	1	4.69%		0.539
247	Protein canopy homolog 2 GN=CNPY2	Q9Y2B0	20,634.50	1	5.49%	yes	
248	Heme-binding protein 2 GN=HEBP2	Q9Y5Z4	22,857.70	1	7.32%		0.793
249	Junctional adhesion molecule A GN=F11R	Q9Y624	32,565.10	1	3.68%	yes	

Table IV. Identified proteins in the conditioned medium of PHH in monolayer culture after 96h. Shown are proteins identified after merging the mascot search results of analyses on three different LC-MS systems (LC-MALDI, LC-ESI ion trap and LC-ESI QTOF). Gene name (GN), Swiss-Prot Accesion number (Acc. no.), identified peptides (Pep), sequence coverage (Seq. cov.)

No.	Protein name	Acc. no.	MW [Da]	pep	seq. cov.
1	Complement C3 OS=Homo sapiens GN=C3 PE=1 SV=2	P01024	187,131.10	43	28.30%
2	Complement C4-B OS=Homo sapiens GN=C4B PE=1 SV=1	P0C0L4	192,776.80	17	11.00%
3	Actin, cytoplasmic 1 OS=Homo sapiens GN=ACTB PE=1 SV=1	P60709	41,719.80	14	34.10%
4	Apolipoprotein E OS=Homo sapiens GN=APOE PE=1 SV=1	P02649	36,135.50	14	45.40%
5	Complement factor B OS=Homo sapiens GN=CFB PE=1 SV=2	P00751	85,515.20	12	16.40%
6	Vitamin D-binding protein OS=Homo sapiens GN=GC PE=1 SV=1	P02774	52,946.60	12	28.10%
7	Protein AMBP OS=Homo sapiens GN=AMBP PE=1 SV=1	P02760	38,981.50	12	39.20%
8	Fibronectin OS=Homo sapiens GN=FN1 PE=1 SV=4	P02751	262,598.90	12	7.00%
9	Complement C1s subcomponent OS=Homo sapiens GN=C1S PE=1 SV=1	P09871	76,666.20	12	17.60%
10	Apolipoprotein A-IV OS=Homo sapiens GN=APOA4 PE=1 SV=3	P06727	45,381.30	10	27.00%
11	Clusterin OS=Homo sapiens GN=CLU PE=1 SV=1	P10909	52,476.90	10	25.60%
12	Ceruloplasmin OS=Homo sapiens GN=CP PE=1 SV=1	P00450	122,189.90	10	10.50%
13	Apolipoprotein A-I OS=Homo sapiens GN=APOA1 PE=1 SV=1	P02647	30,760.50	10	36.30%
14	Alpha-1-antichymotrypsin OS=Homo sapiens GN=SERPINA3 PE=1 SV=2	P01011	47,634.90	9	22.90%
15	Alpha-1-antitrypsin OS=Homo sapiens GN=SERPINA1 PE=1 SV=3	P01009	46,719.90	9	21.80%
16	Plasminogen activator inhibitor 1 OS=Homo sapiens GN=SERPINE1 PE=1 SV=1	P05121	45,042.20	7	15.20%
17	Alcohol dehydrogenase 1B OS=Homo sapiens GN=ADH1B PE=1 SV=2	P00325	39,836.30	7	21.30%
18	Alpha-2-macroglobulin OS=Homo sapiens GN=A2M PE=1 SV=3	P01023	163,271.90	7	6.92%
19	Beta-2-glycoprotein 1 OS=Homo sapiens GN=APOH PE=1 SV=3	P02749	38,280.50	7	20.00%
20	Complement factor H OS=Homo sapiens GN=CFH PE=1 SV=4	P08603	139,078.20	7	6.66%
21	Alpha-enolase OS=Homo sapiens GN=ENO1 PE=1 SV=2	P06733	47,152.20	6	16.40%
22	Vitronectin OS=Homo sapiens GN=VTN PE=1 SV=1	P04004	54,288.10	6	13.20%
23	Glutamate dehydrogenase 1, mitochondrial OS=Homo sapiens GN=GLUD1 PE=1 SV=2	P00367	61,381.70	5	10.60%
24	Apolipoprotein B-100 OS=Homo sapiens GN=APOB PE=1 SV=2	P04114	515,596.80	5	1.34%
25	Insulin-like growth factor-binding protein 2 OS=Homo sapiens GN=IGFBP2 PE=1 SV=2	P18065	34,795.60	5	22.20%
26	Haptoglobin OS=Homo sapiens GN=HP PE=1 SV=1	P00738	45,186.90	5	14.50%
27	Complement C1r subcomponent OS=Homo sapiens GN=C1R PE=1 SV=2	P00736	80,101.60	5	8.65%
28	Prothrombin OS=Homo sapiens GN=F2 PE=1 SV=2	P00734	70,018.80	5	12.70%
29	Kininogen-1 OS=Homo sapiens GN=KNG1 PE=1 SV=2	P01042	71,939.60	5	7.30%
30	Alpha-2-HS-glycoprotein OS=Homo sapiens GN=AHSG PE=1 SV=1	P02765	39,305.40	5	16.90%
31	Fructose-bisphosphate aldolase B OS=Homo sapiens GN=ALDOB PE=1 SV=2	P05062	39,455.30	5	20.30%
32	Fatty acid synthase OS=Homo sapiens GN=FASN PE=1 SV=3	P49327	273,409.10	5	2.35%
33	Fatty acid-binding protein, liver OS=Homo sapiens GN=FABP1 PE=1 SV=1	P07148	14,190.70	5	37.80%
34	Triosephosphate isomerase OS=Homo sapiens GN=TPI1 PE=1 SV=2	P60174	26,651.10	5	24.90%
35	Inter-alpha-trypsin inhibitor heavy chain H2 OS=Homo sapiens GN=ITIH2 PE=1 SV=2	P19823	106,447.50	5	5.50%
36	Aspartate aminotransferase, cytoplasmic OS=Homo sapiens GN=GOT1 PE=1 SV=3	P17174	46,230.10	5	14.00%
37	Pigment epithelium-derived factor OS=Homo sapiens GN=SERPINF1 PE=1 SV=4	P36955	46,296.30	4	9.81%
38	Phosphatidylethanolamine-binding protein 1 OS=Homo sapiens GN=PEBP1 PE=1 SV=3	P30086	21,038.90	4	26.70%
39	Hyaluronan-binding protein 2 OS=Homo sapiens GN=HABP2 PE=1 SV=1	Q14520	62,653.40	4	8.39%
40	Heat shock cognate 71 kDa protein OS=Homo sapiens GN=HSPA8 PE=1 SV=1	P11142	70,881.80	4	8.36%
41	Retinol-binding protein 4 OS=Homo sapiens GN=RBP4 PE=1 SV=3	P02753	22,992.30	4	15.90%
42	Glyceraldehyde-3-phosphate dehydrogenase OS=Homo sapiens GN=GAPDH PE=1 SV=3	P04406	36,035.30	4	17.00%
43	Peroxiredoxin-1 OS=Homo sapiens GN=PRDX1 PE=1 SV=1	Q06830	22,092.90	4	19.10%
44	Liver carboxylesterase 1 OS=Homo sapiens GN=CES1 PE=1 SV=2	P23141	62,504.40	4	8.47%
45	Fructose-bisphosphate aldolase A OS=Homo sapiens GN=ALDOA PE=1 SV=2	P04075	39,402.60	3	9.34%
46	L-lactate dehydrogenase A chain OS=Homo sapiens GN=LDHA PE=1 SV=2	P00338	36,671.20	3	9.64%
47	Inter-alpha-trypsin inhibitor heavy chain H4 OS=Homo sapiens GN=ITIH4 PE=1 SV=4	Q14624	103,340.40	3	4.19%
48	Alcohol dehydrogenase 4 OS=Homo sapiens GN=ADH4 PE=1 SV=5	P08319	40,204.80	3	8.16%
49	Keratin, type II cytoskeletal 8 OS=Homo sapiens GN=KRT8 PE=1 SV=7	P05787	53,688.20	3	6.21%
50	Keratin, type I cytoskeletal 18 OS=Homo sapiens GN=KRT18 PE=1 SV=2	P05783	48,041.00	3	6.74%
51	Alpha-2-antiplasmin OS=Homo sapiens GN=SERPINF2 PE=1 SV=3	P08697	54,548.60	3	6.72%
52	Cathepsin D OS=Homo sapiens GN=CTSD PE=1 SV=1	P07339	44,535.00	3	9.95%
53	Heat shock protein HSP 90-alpha OS=Homo sapiens GN=HSP90AA1 PE=1 SV=5	P07900	84,645.20	3	4.78%
54	Cathepsin B OS=Homo sapiens GN=CTSB PE=1 SV=3	P07858	37,803.20	3	12.10%
55	Alpha-1-acid glycoprotein 1 OS=Homo sapiens GN=ORM1 PE=1 SV=1	P02763	23,494.10	3	8.96%

56	Angiotensinogen OS=Homo sapiens GN=AGT PE=1 SV=1	P01019	53,136.80	3	6.39%
57	UTP--glucose-1-phosphate uridylyltransferase OS=Homo sapiens GN=UGP2 PE=1 SV=5	Q16851	56,924.00	3	6.30%
58	Monocyte differentiation antigen CD14 OS=Homo sapiens GN=CD14 PE=1 SV=2	P08571	40,058.60	3	9.60%
59	Plasma protease C1 inhibitor OS=Homo sapiens GN=SERPING1 PE=1 SV=2	P05155	55,137.50	3	7.40%
60	Fibrinogen alpha chain OS=Homo sapiens GN=FGA PE=1 SV=2	P02671	94,955.40	3	4.85%
61	Phosphoglycerate kinase 1 OS=Homo sapiens GN=PGK1 PE=1 SV=3	P00558	44,597.30	3	10.10%
62	Histone H2B type 1-K OS=Homo sapiens GN=HIST1H2BK PE=1 SV=3	O60814	13,872.60	3	21.40%
63	Protein disulfide-isomerase OS=Homo sapiens GN=P4HB PE=1 SV=3	P07237	57,100.10	3	7.28%
64	Ribonuclease UK114 OS=Homo sapiens GN=HRSP12 PE=1 SV=1	P52758	14,476.10	3	27.00%
65	Galectin-3-binding protein OS=Homo sapiens GN=LGALS3BP PE=1 SV=1	Q08380	65,314.10	3	5.81%
66	Superoxide dismutase [Cu-Zn] OS=Homo sapiens GN=SOD1 PE=1 SV=2	P00441	15,917.30	3	24.70%
67	Glutathione S-transferase A1 OS=Homo sapiens GN=GSTA1 PE=1 SV=3	P08263	25,615.00	2	8.56%
68	Fibrinogen beta chain OS=Homo sapiens GN=FGB PE=1 SV=2	P02675	55,910.60	2	4.89%
69	Insulin-like growth factor-binding protein 4 OS=Homo sapiens GN=IGFBP4 PE=1 SV=2	P22692	27,915.70	2	10.50%
70	Neutrophil gelatinase-associated lipocalin OS=Homo sapiens GN=LCN2 PE=1 SV=2	P80188	22,570.90	2	16.20%
71	Insulin-like growth factor-binding protein 1 OS=Homo sapiens GN=IGFBP1 PE=1 SV=1	P08833	27,884.90	2	11.60%
72	Macrophage migration inhibitory factor OS=Homo sapiens GN=MIF PE=1 SV=4	P14174	12,458.50	2	17.40%
73	Transketolase OS=Homo sapiens GN=TKT PE=1 SV=3	P29401	67,861.40	2	4.33%
74	Aminoacylase-1 OS=Homo sapiens GN=ACY1 PE=1 SV=1	Q03154	45,866.30	2	6.37%
75	Trypsin precursor - Sus scrofa	P00761	24,391.30	2	7.79%
76	1,4-alpha-glucan-branching enzyme OS=Homo sapiens GN=GBE1 PE=1 SV=2	Q04446	80,444.90	2	3.85%
77	Elongation factor 1-alpha 1 OS=Homo sapiens GN=EEF1A1 PE=1 SV=1	P68104	50,123.20	2	4.33%
78	Beta-2-microglobulin OS=Homo sapiens GN=B2M PE=1 SV=1	P61769	13,696.90	2	13.40%
79	Aldo-keto reductase family 1 member C2 OS=Homo sapiens GN=AKR1C2 PE=1 SV=3	P52895	36,717.90	2	5.57%
80	Nicotinate-nucleotide pyrophosphorylase [carboxylating] OS=Homo sapiens GN=QPRT PE=1 SV=3	Q15274	30,827.30	2	6.40%
81	Phosphoglucomutase-1 OS=Homo sapiens GN=PGM1 PE=1 SV=3	P36871	61,433.00	2	4.80%
82	Parathymosin OS=Homo sapiens GN=PTMS PE=1 SV=2	P20962	11,511.60	2	22.50%
83	Fructose-1,6-bisphosphatase 1 OS=Homo sapiens GN=FBP1 PE=1 SV=5	P09467	36,825.20	2	7.99%
84	60 kDa heat shock protein, mitochondrial OS=Homo sapiens GN=HSPD1 PE=1 SV=2	P10809	61,037.70	2	3.66%
85	Leucine-rich alpha-2-glycoprotein OS=Homo sapiens GN=LRG1 PE=1 SV=2	P02750	38,161.70	2	5.76%
86	Retinoic acid receptor responder protein 2 OS=Homo sapiens GN=RARRES2 PE=1 SV=1	Q99969	18,599.30	2	14.70%
87	Galectin-1 OS=Homo sapiens GN=LGALS1 PE=1 SV=2	P09382	14,697.80	2	16.30%
88	Betaine--homocysteine S-methyltransferase 1 OS=Homo sapiens GN=BHMT PE=1 SV=2	Q93088	44,980.60	2	6.16%
89	HLA class I histocompatibility antigen, A-32 alpha chain OS=Homo sapiens GN=HLA-A PE=2 SV=2	P10314	41,029.90	2	10.10%
90	Heat shock protein beta-1 OS=Homo sapiens GN=HSPB1 PE=1 SV=2	P04792	22,764.60	2	13.20%
91	Plasma serine protease inhibitor OS=Homo sapiens GN=SERPINA5 PE=1 SV=2	P05154	45,684.80	2	5.67%
92	Fibrinogen gamma chain OS=Homo sapiens GN=FGG PE=1 SV=3	P02679	51,495.30	2	4.64%
93	Histone H4 OS=Homo sapiens GN=HIST1H4A PE=1 SV=2	P62805	11,349.70	2	19.40%
94	Profilin-1 OS=Homo sapiens GN=PFN1 PE=1 SV=2	P07737	15,036.30	2	20.00%
95	Apolipoprotein C-II OS=Homo sapiens GN=APOC2 PE=1 SV=1	P02655	11,266.10	2	17.80%
96	14-3-3 protein zeta/delta OS=Homo sapiens GN=YWHAZ PE=1 SV=1	P63104	27,727.90	2	8.98%
97	Glutathione S-transferase omega-1 OS=Homo sapiens GN=GSTO1 PE=1 SV=2	P78417	27,549.20	2	9.96%
98	Carboxypeptidase N subunit 2 OS=Homo sapiens GN=CPN2 PE=1 SV=2	P22792	60,598.80	2	3.30%
99	Insulin-like growth factor-binding protein complex acid labile subunit OS=Homo sapiens GN=IGFALS PE=1 SV=1	P35858	66,020.60	2	4.63%
100	Malate dehydrogenase, cytoplasmic OS=Homo sapiens GN=MDH1 PE=1 SV=4	P40925	36,408.90	2	8.68%
101	Apolipoprotein C-III OS=Homo sapiens GN=APOC3 PE=1 SV=1	P02656	10,834.30	1	16.20%
102	Calreticulin OS=Homo sapiens GN=CALR PE=1 SV=1	P27797	48,124.90	1	3.12%
103	Hemopexin OS=Homo sapiens GN=HPX PE=1 SV=2	P02790	51,658.50	1	2.38%
104	Transthyretin OS=Homo sapiens GN=TTR PE=1 SV=1	P02766	15,868.90	1	8.84%
105	Superoxide dismutase [Mn], mitochondrial OS=Homo sapiens GN=SOD2 PE=1 SV=2	P04179	24,704.60	1	6.31%
106	Nucleoside diphosphate kinase A OS=Homo sapiens GN=NME1 PE=1 SV=1	P15531	17,130.70	1	7.89%
107	10 kDa heat shock protein, mitochondrial OS=Homo sapiens GN=HSPE1 PE=1 SV=2	P61604	10,913.70	1	13.70%
108	Tubulin alpha-1B chain OS=Homo sapiens GN=TUBA1B PE=1 SV=1	P68363	50,133.70	1	3.33%
109	Cystatin-B OS=Homo sapiens GN=CSTB PE=1 SV=2	P04080	11,121.30	1	12.20%
110	14-3-3 protein beta/alpha OS=Homo sapiens GN=YWHAB PE=1 SV=3	P31946	28,065.10	1	5.69%
111	Endoplasmin OS=Homo sapiens GN=HSP90B1 PE=1 SV=1	P14625	92,453.70	1	1.37%
112	Peroxiredoxin-6 OS=Homo sapiens GN=PRDX6 PE=1 SV=3	P30041	25,018.10	1	5.36%
113	Alpha-actinin-4 OS=Homo sapiens GN=ACTN4 PE=1 SV=2	O43707	104,839.20	1	1.32%
114	THUMP domain-containing protein 1 OS=Homo sapiens GN=THUMPD1 PE=1 SV=2	Q9NXG2	39,297.50	1	2.27%
115	Polymeric immunoglobulin receptor OS=Homo sapiens GN=PIGR PE=1 SV=4	P01833	83,265.40	1	2.09%
116	Thioredoxin OS=Homo sapiens GN=TXN PE=1 SV=3	P10599	11,719.30	1	8.57%
117	Uncharacterized protein C10orf90 OS=Homo sapiens GN=C10orf90 PE=2 SV=2	Q96M02	77,893.30	1	1.00%
118	Complement factor I OS=Homo sapiens GN=CFI PE=1 SV=2	P05156	65,731.80	1	3.26%

119	Serotransferrin OS=Homo sapiens GN=TF PE=1 SV=3	P02787	77,046.30	1	2.01%
120	Zinc-alpha-2-glycoprotein OS=Homo sapiens GN=AZGP1 PE=1 SV=2	A8MT79	34,240.60	1	3.36%
121	Proprotein convertase subtilisin/kexin type 9 OS=Homo sapiens GN=PCSK9 PE=1 SV=3	Q8NBP7	74,266.40	1	1.45%
122	Acyl-coenzyme A thioesterase 2, mitochondrial OS=Homo sapiens GN=ACOT2 PE=1 SV=6	P49753	53,201.40	1	2.28%
123	Proline-rich acidic protein 1 OS=Homo sapiens GN=PRAP1 PE=2 SV=2	Q96NZ9	17,189.20	1	5.96%
124	Metaxin-1 OS=Homo sapiens GN=MTX1 PE=1 SV=2	Q13505	51,460.00	1	1.29%
125	Thioredoxin-dependent peroxide reductase, mitochondrial OS=Homo sapiens GN=PRDX3 PE=1 SV=3	P30048	27,674.70	1	4.30%
126	Histidine-rich glycoprotein OS=Homo sapiens GN=HRG PE=1 SV=1	P04196	59,558.60	1	1.71%

Table V. Identified proteins in the conditioned medium of PHH in monolayer culture after 96h after prefractionation by SDS-PAGE. Shown are proteins identified after merging the mascot search results of analyses on three different LC-MS systems (LC-MALDI, LC-ESI ion trap and LC-ESI QTOF) with 24 gel bands each. Gene name (GN), Swiss-Prot Accesion number (Acc. no.), identified peptides (Pep), sequence coverage (Seq. cov.)

No.	Protein name	Acc. no.	MW [Da]	pep	seq. cov.
1	Apolipoprotein B-100 GN=APOB	P04114	515,596.80	189	46.00%
2	Complement C3 GN=C3	P01024	187,131.10	127	81.20%
3	Fatty acid synthase GN=FASN	P49327	273,409.10	91	47.60%
4	Complement C4-B GN=C4B	P0C0L5	192,776.80	81	58.30%
5	Fibronectin GN=FN1	P02751	262,598.90	68	38.00%
6	Alpha-2-macroglobulin GN=A2M	P01023	163,271.90	63	58.40%
7	Filamin-B GN=FLNB	O75369	278,140.80	56	30.00%
8	Complement factor H GN=CFH	P08603	139,078.20	55	54.70%
9	Carbamoyl-phosphate synthase [ammonia], mitochondrial GN=CPS1	P31327	164,924.70	53	43.90%
10	Ceruloplasmin GN=CP	P00450	122,189.90	51	55.50%
11	Alpha-actinin-4 GN=ACTN4	O43707	104,839.20	42	54.90%
12	Inter-alpha-trypsin inhibitor heavy chain H2 GN=ITIH2	P19823	106,447.50	40	43.10%
13	Complement factor B GN=CFB	P00751	85,515.20	35	46.60%
14	Inter-alpha-trypsin inhibitor heavy chain H4 GN=ITIH4	Q14624	103,340.40	34	44.30%
15	Apolipoprotein A-I GN=APOA1	P02647	30,760.50	33	86.50%
16	Alpha-1-antitrypsin GN=SERPINA1	P01009	46,719.90	33	69.10%
17	Complement C1s subcomponent GN=C1S	P09871	76,666.20	33	55.10%
18	Heat shock protein HSP 90-alpha GN=HSP90AA1	P07900	84,645.20	31	42.50%
19	Vitamin D-binding protein GN=GC	P02774	52,946.60	31	63.30%
20	Moesin GN=MSN	P26038	67,803.80	30	49.20%
21	Apolipoprotein A-IV GN=APOA4	P06727	45,381.30	30	71.00%
22	Thrombospondin-1 GN=THBS1	P07996	129,363.70	30	35.10%
23	Serotransferrin GN=TF	P02787	77,046.30	30	55.00%
24	Elongation factor 2 GN=EEF2	P13639	95,322.10	29	39.20%
25	Alpha-enolase GN=ENO1	P06733	47,152.20	29	71.40%
26	Liver carboxylesterase 1 GN=CES1	P23141	62,504.40	29	57.10%
27	Fibrinogen beta chain GN=FGB	P02675	55,910.60	28	67.40%
28	Apolipoprotein E GN=APOE	P02649	36,135.50	28	80.40%
29	Inter-alpha-trypsin inhibitor heavy chain H3 GN=ITIH3	Q06033	99,832.90	28	37.30%
30	Complement C1r subcomponent GN=C1R	P00736	80,101.60	27	45.80%
31	Prothrombin GN=F2	P00734	70,018.80	27	52.70%
32	Aldehyde oxidase GN=AOX1	Q06278	147,902.70	27	21.50%
33	Kininogen-1 GN=KNG1	P01042	71,939.60	26	35.90%
34	Complement C5 GN=C5	P01031	188,291.20	26	18.60%
35	L-lactate dehydrogenase A chain GN=LDHA	P00338	36,671.20	26	83.10%
36	Aspartate aminotransferase, cytoplasmic GN=GOT1	P17174	46,230.10	26	73.10%
37	Retinal dehydrogenase 1 GN=ALDH1A1	P00352	54,844.80	25	57.70%
38	Glucose-6-phosphate isomerase GN=GPI	P06744	63,130.40	25	46.10%
39	Keratin, type II cytoskeletal 8 GN=KRT8	P05787	53,688.20	25	44.70%
40	Alpha-1-antichymotrypsin GN=SERPINA3	P01011	47,634.90	24	57.20%
41	10-formyltetrahydrofolate dehydrogenase GN=ALDH1L1	O75891	98,812.20	24	32.00%
42	Actin, cytoplasmic 1 GN=ACTB	P60709	41,719.80	23	68.30%
43	Haptoglobin GN=HP	P00738	45,186.90	23	55.90%
44	Glutamate dehydrogenase 1, mitochondrial GN=GLUD1	P00367	61,381.70	23	44.60%
45	Plasminogen activator inhibitor 1 GN=SERPINE1	P05121	45,042.20	23	63.40%
46	Alcohol dehydrogenase 1B GN=ADH1B	P00325	39,836.30	22	72.30%
47	Pigment epithelium-derived factor GN=SERPINF1	P36955	46,296.30	22	59.10%
48	Fibrinogen gamma chain GN=FGG	P02679	51,495.30	22	60.70%
49	Isocitrate dehydrogenase [NADP] cytoplasmic GN=IDH1	O75874	46,642.50	22	63.30%
50	Inter-alpha-trypsin inhibitor heavy chain H1 GN=ITIH1	P19827	101,371.80	22	32.70%
51	UTP--glucose-1-phosphate uridylyltransferase GN=UGP2	Q16851	56,924.00	22	49.00%
52	Complement C2 GN=C2	P06681	83,250.80	22	32.20%
53	Aldo-keto reductase family 1 member B10 GN=AKR1B10	O60218	36,003.40	21	78.80%
54	Clusterin GN=CLU	P10909	52,476.90	21	43.40%

55	Agrin GN=AGRN	O00468	214,820.00	21	13.20%
56	Aldo-keto reductase family 1 member C1 GN=AKR1C1	Q04828	36,771.10	21	71.20%
57	Protein disulfide-isomerase GN=P4HB	P07237	57,100.10	21	44.90%
58	Transforming growth factor-beta-induced protein ig-h3 GN=TGFBI	Q15582	74,664.90	21	41.40%
59	Rab GDP dissociation inhibitor beta GN=GDI2	P50395	50,647.50	21	60.20%
60	Phosphoglycerate kinase 1 GN=PGK1	P00558	44,597.30	20	57.60%
61	Aminoacylase-1 GN=ACY1	Q03154	45,866.30	20	63.50%
62	Fibrinogen alpha chain GN=FGA	P02671	94,955.40	20	30.30%
63	Plasminogen GN=PLG	P00747	90,549.40	20	30.00%
64	Plasma protease C1 inhibitor GN=SERPING1	P05155	55,137.50	20	38.00%
65	Keratin, type I cytoskeletal 18 GN=KRT18	P05783	48,041.00	20	50.70%
66	Plasma kallikrein GN=KLKB1	P03952	71,351.70	20	32.10%
67	Transketolase GN=TKT	P29401	67,861.40	19	39.80%
68	Fructose-bisphosphate aldolase B GN=ALDOB	P05062	39,455.30	19	76.60%
69	Prostaglandin reductase 1 GN=PTGR1	Q14914	35,852.50	19	63.50%
70	Triosephosphate isomerase GN=TPI1	P60174	26,651.10	19	86.70%
71	Fructose-bisphosphate aldolase A GN=ALDOA	P04075	39,402.60	19	71.40%
72	14-3-3 protein zeta/delta GN=YWHAZ	P63104	27,727.90	19	62.90%
73	Peroxiredoxin-6 GN=PRDX6	P30041	25,018.10	19	79.90%
74	Heat shock cognate 71 kDa protein GN=HSPA8	P11142	70,881.80	19	40.90%
75	Protein AMBP GN=AMBP	P02760	38,981.50	19	56.50%
76	4-hydroxyphenylpyruvate dioxygenase GN=HPD	P32754	44,916.90	19	62.30%
77	1,4-alpha-glucan-branching enzyme GN=GBE1	Q04446	80,444.90	19	29.60%
78	Antithrombin-III GN=SERPINC1	P01008	52,586.00	18	45.30%
79	Phosphoglucomutase-1 GN=PGM1	P36871	61,433.00	18	38.60%
80	Argininosuccinate synthase GN=ASS1	P00966	46,513.30	18	43.20%
81	Hemopexin GN=HPX	P02790	51,658.50	18	43.70%
82	Complement factor I GN=CFI	P05156	65,731.80	18	37.60%
83	Plastin-3 GN=PLS3	P13797	70,795.90	18	33.80%
84	60 kDa heat shock protein, mitochondrial GN=HSPD1	P10809	61,037.70	18	43.60%
85	Polymeric immunoglobulin receptor GN=PIGR	P01833	83,265.40	18	26.70%
86	Histidine-rich glycoprotein GN=HRG	P04196	59,558.60	18	39.40%
87	Proteasome subunit alpha type-1 GN=PSMA1	P25786	29,538.00	17	65.40%
88	Alpha-actinin-1 GN=ACTN1	P12814	103,043.00	17	47.50%
89	Tubulin beta chain GN=TUBB	P07437	49,652.60	17	54.70%
90	Alcohol dehydrogenase [NADP+] GN=AKR1A1	P14550	36,555.60	17	51.40%
91	Fructose-1,6-bisphosphatase 1 GN=FBP1	P09467	36,825.20	17	53.30%
92	Plasma serine protease inhibitor GN=SERPINA5	P05154	45,684.80	17	49.50%
93	Phosphoglycerate mutase 1 GN=PGAM1	P18669	28,786.80	17	77.60%
94	Amyloid beta A4 protein GN=APP	P05067	86,923.30	16	23.40%
95	Peroxiredoxin-1 GN=PRDX1	Q06830	22,092.90	16	78.90%
96	Argininosuccinate lyase GN=ASL	P04424	51,641.00	16	40.30%
97	Glyceraldehyde-3-phosphate dehydrogenase GN=GAPDH	P04406	36,035.30	16	56.10%
98	Heat shock protein beta-1 GN=HSPB1	P04792	22,764.60	16	68.80%
99	Vinculin GN=VCL	P18206	123,783.20	16	19.30%
100	Protein disulfide-isomerase A3 GN=PDIA3	P30101	56,766.60	16	39.20%
101	Hyaluronan-binding protein 2 GN=HABP2	Q14520	62,653.40	16	29.80%
102	Nucleobindin-1 GN=NUCB1	Q02818	53,861.60	16	39.50%
103	Betaine--homocysteine S-methyltransferase 1 GN=BHMT	Q93088	44,980.60	16	56.90%
104	3-ketoacyl-CoA thiolase, mitochondrial GN=ACAA2	P42765	41,906.20	16	58.40%
105	Heparin cofactor 2 GN=SERPIND1	P05546	57,054.90	16	38.70%
106	Malate dehydrogenase, mitochondrial GN=MDH2	P40926	35,485.70	16	59.50%
107	Proteasome activator complex subunit 1 GN=PSME1	Q06323	28,705.80	16	65.10%
108	Cytoplasmic aconitate hydratase GN=ACO1	P21399	98,383.00	16	23.80%
109	Bifunctional ATP-dependent dihydroxyacetone kinase/FAD-AMP lyase (cyclizing) GN=DAK	Q3LXA3	58,930.10	16	42.30%
110	Serine hydroxymethyltransferase, cytosolic GN=SHMT1	P34896	53,065.80	16	39.10%
111	Glycogen debranching enzyme GN=AGL	P35573	174,749.60	16	13.10%
112	Superoxide dismutase [Mn], mitochondrial GN=SOD2	P04179	24,704.60	15	68.00%
113	Transgelin-2 GN=TAGLN2	P37802	22,373.90	15	79.40%
114	Carbonyl reductase [NADPH] 1 GN=CBR1	P16152	30,356.80	15	70.40%
115	Catalase GN=CAT	P04040	59,738.50	15	35.30%
116	Insulin-like growth factor-binding protein 2 GN=IGFBP2	P18065	34,795.60	15	53.50%
117	Selenium-binding protein 1 GN=SELENBP1	Q13228	52,374.00	15	34.70%

118	Zinc-alpha-2-glycoprotein GN=AZGP1	P25311	34,240.60	15	54.00%
119	Phosphatidylethanolamine-binding protein 1 GN=PEBP1	P30086	21,038.90	15	86.60%
120	Cathepsin D GN=CTSD	P07339	44,535.00	15	43.90%
121	Neutrophil gelatinase-associated lipocalin GN=LCN2	P80188	22,570.90	15	66.70%
122	Glutathione S-transferase omega-1 GN=GSTO1	P78417	27,549.20	15	49.40%
123	Galectin-3-binding protein GN=LGALS3BP	Q08380	65,314.10	15	27.20%
124	Nicotinamide phosphoribosyltransferase GN=NAMPT	P43490	55,504.50	14	43.80%
125	Serine--pyruvate aminotransferase GN=AGXT	P21549	42,993.40	14	48.50%
126	Aspartate aminotransferase, mitochondrial GN=GOT2	P00505	47,500.60	14	35.80%
127	Peptidyl-prolyl cis-trans isomerase B GN=PPIB	P23284	23,725.20	14	57.40%
128	Tubulin alpha-1B chain GN=TUBA1B	P68363	50,133.70	14	42.40%
129	Glutathione S-transferase A2 GN=GSTA2	P09210	25,647.90	14	48.60%
130	14-3-3 protein epsilon GN=YWHAE	P62258	29,157.00	14	69.40%
131	Complement component C8 beta chain GN=C8B	P07358	67,028.90	14	27.90%
132	Annexin A2 GN=ANXA2	P07355	38,588.10	14	45.40%
133	Heat shock protein HSP 90-beta GN=HSP90AB1	P08238	83,249.30	14	39.40%
134	Monocyte differentiation antigen CD14 GN=CD14	P08571	40,058.60	14	48.50%
135	Glycine amidinotransferase, mitochondrial GN=GATM	P50440	48,438.60	14	45.40%
136	Keratin, type II cytoskeletal 1 GN=KRT1	P04264	66,022.30	14	32.80%
137	Retinol-binding protein 4 GN=RBP4	P02753	22,992.30	14	77.10%
138	Chitinase-3-like protein 1 GN=CHI3L1	P36222	42,609.00	14	43.60%
139	Arginase-1 GN=ARG1	P05089	34,718.00	14	55.30%
140	Endoplasmin GN=HSP90B1	P14625	92,453.70	13	21.20%
141	Alcohol dehydrogenase 4 GN=ADH4	P08319	40,204.80	13	48.90%
142	6-phosphogluconate dehydrogenase, decarboxylating GN=PGD	P52209	53,123.90	13	40.60%
143	Purine nucleoside phosphorylase GN=PNP	P00491	32,100.00	13	60.20%
144	Protein DJ-1 GN=PARK7	Q99497	19,873.10	13	81.00%
145	Complement component C8 gamma chain GN=C8G	P07360	22,259.30	13	82.70%
146	Malate dehydrogenase, cytoplasmic GN=MDH1	P40925	36,408.90	13	50.00%
147	Lipopolysaccharide-binding protein GN=LBP	P18428	53,368.00	13	28.50%
148	Fumarate hydratase, mitochondrial GN=FH	P07954	54,619.80	13	37.30%
149	Calreticulin GN=CALR	P27797	48,124.90	13	33.10%
150	Insulin-like growth factor-binding protein 1 GN=IGFBP1	P08833	27,884.90	13	47.50%
151	Tropomyosin alpha-4 chain GN=TPM4	P67936	28,504.40	13	41.10%
152	Cathepsin B GN=CTSB	P07858	37,803.20	12	43.10%
153	Chloride intracellular channel protein 1 GN=CLIC1	O00299	26,905.30	12	59.30%
154	Angiotensinogen GN=AGT	P01019	53,136.80	12	34.60%
155	Omega-amidase NIT2 GN=NIT2	Q9NQR4	30,590.80	12	59.80%
156	Vitronectin GN=VTN	P04004	54,288.10	12	33.30%
157	Cytosolic non-specific dipeptidase GN=CNDP2	Q96KP4	52,861.70	12	27.60%
158	Proteasome subunit beta type-8 GN=PSMB8	P28062	30,336.80	12	43.80%
159	Insulin-like growth factor-binding protein complex acid labile subunit GN=IGFALS	P35858	66,020.60	12	26.00%
160	Fibrinogen-like protein 1 GN=FGL1	Q08830	36,361.90	12	51.90%
161	14-3-3 protein gamma GN=YWHAG	P61981	28,285.10	12	63.60%
162	Aminopeptidase N GN=ANPEP	P15144	109,524.40	12	16.20%
163	Nicotinamide N-methyltransferase GN=NNMT	P40261	29,557.00	12	65.50%
164	Glycogen phosphorylase, liver form GN=PYGL	P06737	97,134.40	12	16.60%
165	3-hydroxyanthranilate 3,4-dioxygenase GN=HAAO	P46952	32,538.20	12	61.50%
166	Laminin subunit gamma-1 GN=LAMC1	P11047	177,583.30	12	10.20%
167	Proteasome activator complex subunit 2 GN=PSME2	Q9UL46	27,384.20	12	62.30%
168	Alpha-1-acid glycoprotein 1 GN=ORM1	P02763	23,494.10	12	53.20%
169	L-xylulose reductase GN=DCXR	Q7Z4W1	25,894.20	12	69.30%
170	Beta-2-glycoprotein 1 GN=APOH	P02749	38,280.50	12	46.70%
171	Carbonic anhydrase 2 GN=CA2	P00918	29,228.60	12	61.90%
172	Bile salt sulfotransferase GN=SULT2A1	Q06520	33,763.30	12	46.30%
173	Cytosol aminopeptidase GN=LAP3	P28838	56,149.70	11	22.00%
174	Lambda-crystallin homolog GN=CRYL1	Q9Y2S2	35,401.30	11	40.80%
175	Delta(3,5)-Delta(2,4)-dienoyl-CoA isomerase, mitochondrial GN=ECH1	Q13011	35,798.20	11	47.60%
176	Sorbitol dehydrogenase GN=SORD	Q00796	38,306.60	11	38.10%
177	Proteasome subunit alpha type-4 GN=PSMA4	P25789	29,466.80	11	54.80%
178	Alpha-2-antiplasmin GN=SERPINF2	P08697	54,548.60	11	30.10%
179	Ornithine carbamoyltransferase, mitochondrial GN=OTC	P00480	39,919.00	11	42.70%
180	Vimentin GN=VIM	P08670	53,634.60	11	25.50%

181	Gamma-glutamyl hydrolase GN=GGH	Q92820	35,947.90	11	43.10%
182	Leukocyte elastase inhibitor GN=SERPINB1	P30740	42,725.80	11	35.10%
183	Nidogen-1 GN=NID1	P14543	136,357.60	11	9.94%
184	Insulin-like growth factor-binding protein 7 GN=IGFBP7	Q16270	29,111.80	11	44.70%
185	Spectrin alpha chain, brain GN=SPTAN1	Q13813	284,524.70	11	6.80%
186	Fumarylacetoacetase GN=FAH	P16930	46,357.60	11	38.40%
187	Proteasome subunit alpha type-7 GN=PSMA7	O14818	27,869.10	11	55.20%
188	Proteasome subunit alpha type-6 GN=PSMA6	P60900	27,381.50	11	45.90%
189	Transaldolase GN=TALDO1	P37837	37,523.70	11	35.00%
190	78 kDa glucose-regulated protein GN=HSPA5	P11021	72,316.70	11	25.70%
191	Low-density lipoprotein receptor GN=LDLR	P01130	95,356.70	11	15.00%
192	Basement membrane-specific heparan sulfate proteoglycan core protein GN=HSPG2	P98160	468,792.60	10	3.17%
193	Farnesyl pyrophosphate synthase GN=FDPS	P14324	48,258.70	10	33.90%
194	Carboxypeptidase N subunit 2 GN=CPN2	P22792	60,598.80	10	29.50%
195	Elongation factor 1-alpha 1 GN=EEF1A1	P68104	50,123.20	10	32.50%
196	Galectin-4 GN=LGALS4	P56470	35,923.30	10	38.40%
197	Angiopoietin-related protein 3 GN=ANGPTL3	Q9Y5C1	53,621.30	10	21.30%
198	Kallistatin GN=SERPINA4	P29622	48,526.00	10	30.20%
199	6-phosphogluconolactonase GN=PGLS	O95336	27,529.50	10	57.80%
200	Protein disulfide-isomerase A4 GN=PDIA4	P13667	72,916.00	10	18.60%
201	UMP-CMP kinase GN=CMPK1	P30085	22,205.00	10	54.10%
202	Endoplasmic reticulum resident protein 29 GN=ERP29	P30040	28,976.90	10	45.60%
203	4-aminobutyrate aminotransferase, mitochondrial GN=ABAT	P80404	56,422.80	10	26.60%
204	Alpha-1B-glycoprotein GN=A1BG	P04217	54,235.30	10	36.60%
205	Hydroxyacyl-coenzyme A dehydrogenase, mitochondrial GN=HADH	Q16836	34,276.10	10	45.50%
206	Alpha-2-HS-glycoprotein GN=AHSG	P02765	39,305.40	10	29.20%
207	Leucine-rich alpha-2-glycoprotein GN=LRG1	P02750	38,161.70	10	33.40%
208	Transthyretin GN=TTR	P02766	15,868.90	10	73.50%
209	Proprotein convertase subtilisin/kexin type 9 GN=PCSK9	Q8NBP7	74,266.40	10	20.80%
210	Aflatoxin B1 aldehyde reductase member 3 GN=AKR7A3	O95154	37,188.80	10	43.20%
211	Acetyl-CoA acetyltransferase, cytosolic GN=ACAT2	Q9BWD1	41,332.40	9	40.30%
212	Intercellular adhesion molecule 1 GN=ICAM1	P05362	57,806.50	9	20.30%
213	Pyruvate kinase isozymes M1/M2 GN=PKM2	P14618	57,919.50	9	21.30%
214	Quinone oxidoreductase GN=CRYZ	Q08257	35,189.30	9	41.00%
215	Adenylate kinase 2, mitochondrial GN=AK2	P54819	26,461.00	9	46.90%
216	Thymidine phosphorylase GN=TYMP	P19971	49,937.80	9	30.10%
217	SPARC GN=SPARC	P09486	34,613.90	9	27.40%
218	Glyoxalase domain-containing protein 4 GN=GLOD4	Q9HC38	34,776.10	9	37.40%
219	Coagulation factor XII GN=F12	P00748	67,772.60	9	16.10%
220	Homogentisate 1,2-dioxygenase GN=HGD	Q93099	49,946.70	9	33.00%
221	Keratin, type I cytoskeletal 9 GN=KRT9	P35527	62,047.80	9	19.70%
222	Keratin, type I cytoskeletal 10 GN=KRT10	P13645	58,810.80	9	16.80%
223	Carboxymethylenebutenolidase homolog GN=CMBL	Q96DG6	28,030.60	9	40.40%
224	Glutathione S-transferase Mu 1 GN=GSTM1	P09488	25,695.70	9	44.00%
225	Actin-related protein 2/3 complex subunit 2 GN=ARPC2	O15144	34,315.70	9	33.30%
226	Dihydropteridine reductase GN=QDPR	P09417	25,771.50	9	52.00%
227	Receptor-type tyrosine-protein phosphatase F GN=PTPRF	P10586	212,860.00	9	5.77%
228	Filamin-A GN=FLNA	P21333	280,711.40	9	6.31%
229	Aldo-keto reductase family 1 member C3 GN=AKR1C3	P42330	36,836.10	9	68.10%
230	UDP-glucose 6-dehydrogenase GN=UGDH	O60701	55,007.30	9	25.50%
231	Ferritin heavy chain GN=FTH1	P02794	21,208.20	9	51.40%
232	Ferritin light chain GN=FTL	P02792	20,002.60	9	54.30%
233	Serum amyloid P-component GN=APCS	P02743	25,369.70	9	35.90%
234	Matrix metalloproteinase-9 GN=MMP9	P14780	78,441.70	9	16.10%
235	Glutathione S-transferase theta-1 GN=GSTT1	P30711	27,317.90	9	37.90%
236	Spectrin beta chain, brain 1 GN=SPTBN1	Q01082	274,595.40	9	6.09%
237	Lactoylglutathione lyase GN=GLO1	Q04760	20,760.80	9	47.30%
238	Proteasome subunit beta type-1 GN=PSMB1	P20618	26,472.50	8	41.90%
239	Vesicular integral-membrane protein VIP36 GN=LMAN2	Q12907	40,211.50	8	31.20%
240	Eukaryotic initiation factor 4A-I GN=EIF4A1	P60842	46,137.30	8	24.90%
241	Beta-Ala-His dipeptidase GN=CNDP1	Q96KN2	56,689.30	8	21.30%
242	Cullin-associated NEDD8-dissociated protein 1 GN=CAND1	Q86VP6	136,363.10	8	9.76%
243	Proteasome subunit alpha type-3 GN=PSMA3	P25788	28,415.70	8	28.20%

244	Proteasome subunit alpha type-2 GN=PSMA2	P25787	25,880.90	8	46.20%
245	Superoxide dismutase [Cu-Zn] GN=SOD1	P00441	15,917.30	8	68.20%
246	Insulin-like growth factor-binding protein 4 GN=IGFBP4	P22692	27,915.70	8	41.10%
247	14-3-3 protein eta GN=YWHAH	Q04917	28,201.60	8	56.50%
248	Delta-aminolevulinic acid dehydratase GN=ALAD	P13716	36,277.30	8	31.50%
249	Proteasome subunit beta type-5 GN=PSMB5	P28074	28,463.00	8	30.80%
250	Translationally-controlled tumor protein GN=TPT1	P13693	19,578.20	8	67.40%
251	Complement component C6 GN=C6	P13671	104,768.20	8	11.60%
252	Glyoxylate reductase/hydroxypyruvate reductase GN=GRHPR	Q9UBQ7	35,651.10	8	33.50%
253	Dipeptidyl peptidase 4 GN=DPP4	P27487	88,263.00	8	11.40%
254	Thioredoxin-dependent peroxide reductase, mitochondrial GN=PRDX3	P30048	27,674.70	8	43.00%
255	Flavin reductase GN=BLVRB	P30043	22,100.70	8	63.60%
256	Beta-hexosaminidase subunit beta GN=HEXB	P07686	63,095.30	8	18.90%
257	Peroxiredoxin-2 GN=PRDX2	P32119	21,874.40	8	40.40%
258	Glycerol-3-phosphate dehydrogenase [NAD+], cytoplasmic GN=GPD1	P21695	37,549.60	8	31.20%
259	Apoptosis regulator BAX GN=BAX	Q07812	21,167.20	8	54.70%
260	14-3-3 protein theta GN=YWHAQ	P27348	27,747.40	8	51.80%
261	Heterogeneous nuclear ribonucleoproteins A2/B1 GN=HNRNPA2B1	P22626	37,412.30	8	26.60%
262	F-actin-capping protein subunit beta GN=CAPZB	P47756	31,333.60	8	32.10%
263	Adenylate kinase isoenzyme 1 GN=AK1	P00568	21,617.10	7	40.20%
264	ATP-citrate synthase GN=ACLY	P53396	120,824.80	7	9.08%
265	Inorganic pyrophosphatase GN=PPA1	Q15181	32,642.60	7	35.30%
266	Transmembrane protein 132A GN=TMEM132A	Q24JP5	110,089.40	7	9.19%
267	Phosphoserine aminotransferase GN=PSAT1	Q9Y617	40,405.30	7	19.70%
268	Cathepsin S GN=CTSS	P25774	37,477.60	7	24.80%
269	3,2-trans-enoyl-CoA isomerase, mitochondrial GN=DCI	P42126	32,798.50	7	32.10%
270	HLA class I histocompatibility antigen, A-25 alpha chain GN=HLA-A	P18462	41,199.70	7	29.00%
271	Metalloproteinase inhibitor 1 GN=TIMP1	P01033	23,153.10	7	53.10%
272	Procollagen-lysine,2-oxoglutarate 5-dioxygenase 1 GN=PLOD1	Q02809	83,534.50	7	13.10%
273	Hepatocyte growth factor-like protein GN=MST1	P26927	80,299.80	7	14.50%
274	Protein disulfide-isomerase A6 GN=PDIA6	Q15084	48,104.30	7	20.00%
275	Proteasome subunit alpha type-5 GN=PSMA5	P28066	26,393.30	7	47.70%
276	Maleylacetoacetate isomerase GN=GSTZ1	O43708	24,195.00	7	32.40%
277	GTP:AMP phosphotransferase, mitochondrial GN=AK3	Q9UIJ7	25,548.30	7	36.60%
278	3-mercaptopyruvate sulfurtransferase GN=MPST	P25325	33,160.80	7	32.00%
279	Complement component C8 alpha chain GN=C8A	P07357	65,145.80	7	12.80%
280	Adenylyl cyclase-associated protein 1 GN=CAP1	Q01518	51,883.60	7	22.10%
281	Calcineurin-like phosphoesterase domain-containing protein 1 GN=CPPED1	Q9BRF8	35,530.60	7	25.80%
282	Alcohol dehydrogenase 6 GN=ADH6	P28332	39,070.80	7	23.10%
283	Tropomyosin alpha-1 chain GN=TPM1	P09493	32,692.00	7	32.40%
284	Histamine N-methyltransferase GN=HNMT	P50135	33,278.60	7	30.80%
285	Alcohol dehydrogenase 1C GN=ADH1C	P00326	39,849.60	7	57.10%
286	Abhydrolase domain-containing protein 14B GN=ABHD14B	Q96IU4	22,328.00	7	42.90%
287	Elongation factor 1-gamma GN=EEF1G	P26641	50,101.40	7	23.10%
288	Talin-1 GN=TLN1	Q9Y490	269,747.10	7	4.25%
289	Peroxiredoxin-4 GN=PRDX4	Q13162	30,523.10	7	44.60%
290	Ester hydrolase C11orf54 GN=C11orf54	Q9H0W9	35,099.70	7	34.30%
291	N-acetylmuramoyl-L-alanine amidase GN=PGLYRP2	Q96PD5	62,199.90	7	21.00%
292	Nicotinate-nucleotide pyrophosphorylase [carboxylating] GN=QPRT	Q15274	30,827.30	7	27.30%
293	Enoyl-CoA hydratase, mitochondrial GN=ECHS1	P30084	31,370.20	7	35.20%
294	14-3-3 protein beta/alpha GN=YWHAB	P31946	28,065.10	7	61.80%
295	Glucosidase 2 subunit beta GN=PRKCSH	P14314	59,407.70	7	16.30%
296	Importin subunit beta-1 GN=KPNB1	Q14974	97,153.30	6	9.59%
297	Eukaryotic translation initiation factor 5A-1 GN=EIF5A	P63241	16,814.70	6	47.40%
298	Guanine deaminase GN=GDA	Q9Y2T3	50,985.90	6	18.10%
299	Alpha-mannosidase 2 GN=MAN2A1	Q16706	131,127.70	6	6.64%
300	Chloride intracellular channel protein 4 GN=CLIC4	Q9Y696	28,755.60	6	33.20%
301	Phospholysine phosphohistidine inorganic pyrophosphate phosphatase GN=LHPP	Q9H008	29,147.40	6	37.40%
302	Nucleoside diphosphate kinase A GN=NME1	P15531	17,130.70	6	53.30%
303	BH3-interacting domain death agonist GN=BID	P55957	21,977.30	6	47.70%
304	Sulfotransferase 1A1 GN=SULT1A1	P50225	34,147.90	6	25.40%
305	C-reactive protein GN=CRP	P02741	25,021.00	6	23.20%
306	ATP synthase subunit beta, mitochondrial GN=ATP5B	P06576	56,542.50	6	16.40%

307	Proactivator polypeptide GN=PSAP	P07602	58,094.00	6	14.30%
308	Keratin, type II cytoskeletal 2 epidermal GN=KRT2	P35908	65,415.90	6	19.60%
309	Ubiquitin-like modifier-activating enzyme 1 GN=UBA1	P22314	117,832.30	6	10.40%
310	Isopentenyl-diphosphate Delta-isomerase 1 GN=IDI1	Q13907	26,302.30	6	26.40%
311	Prelamin-A/C GN=LMNA	P02545	74,122.60	6	12.50%
312	Proteasome subunit beta type-7 GN=PSMB7	Q99436	29,947.90	6	36.10%
313	Coagulation factor X GN=F10	P00742	54,714.10	6	15.60%
314	Proteasome subunit beta type-4 GN=PSMB4	P28070	29,187.00	6	31.80%
315	Proteasome subunit beta type-9 GN=PSMB9	P28065	23,246.40	6	33.80%
316	Hydroxymethylglutaryl-CoA synthase, cytoplasmic GN=HMGCS1	Q01581	57,277.00	6	16.00%
317	Adenosylhomocysteinase GN=AHCY	P23526	47,699.10	6	18.10%
318	Interleukin-18 GN=IL18	Q14116	22,309.40	6	38.30%
319	14-3-3 protein sigma GN=SFN	P31947	27,756.80	6	49.20%
320	3-hydroxyisobutyrate dehydrogenase, mitochondrial GN=HIBADH	P31937	35,312.00	6	25.90%
321	Hepatocyte growth factor receptor GN=MET	P08581	155,525.40	6	5.11%
322	60S acidic ribosomal protein P0 GN=RPLP0	P05388	34,256.30	6	32.50%
323	Spondin-2 GN=SPON2	Q9BUD6	35,828.40	6	17.80%
324	Alpha-1-acid glycoprotein 2 GN=ORM2	P19652	23,585.20	6	52.20%
325	Protein-L-isoaspartate(D-aspartate) O-methyltransferase GN=PCMT1	P22061	24,618.80	6	35.20%
326	Heme-binding protein 1 GN=HEBP1	Q9NRV9	21,079.40	6	49.20%
327	Serum paraoxonase/arylesterase 1 GN=PON1	P27169	39,714.40	6	24.50%
328	Aldehyde dehydrogenase, mitochondrial GN=ALDH2	P05091	56,363.40	6	17.80%
329	Alcohol dehydrogenase class-3 GN=ADH5	P11766	39,705.80	6	22.20%
330	Collagen alpha-1(XVIII) chain GN=COL18A1	P39060	178,169.70	6	4.45%
331	Ezrin GN=EZR	P15311	69,396.60	6	20.00%
332	Complement component C9 GN=C9	P02748	63,156.80	6	11.60%
333	Guanidinoacetate N-methyltransferase GN=GAMT	Q14353	26,300.60	6	39.80%
334	Ketohexokinase GN=KHK	P50053	32,712.10	6	22.10%
335	Actin-related protein 2 GN=ACTR2	P61160	44,743.70	6	19.00%
336	Peroxidasin homolog GN=PXDN	Q92626	165,257.70	6	6.56%
337	Alanyl-tRNA synthetase, cytoplasmic GN=AARS	P49588	106,795.20	6	7.44%
338	Mannosyl-oligosaccharide 1,2-alpha-mannosidase IA GN=MAN1A1	P33908	72,953.70	6	10.70%
339	Hepatocellular carcinoma-associated protein TD26 GN=UNQ599/PRO1185	Q6UXH0	22,087.40	6	29.80%
340	Acidic leucine-rich nuclear phosphoprotein 32 family member A GN=ANP32A	P39687	28,568.10	6	20.50%
341	Coagulation factor XIII B chain GN=F13B	P05160	75,493.70	5	12.00%
342	Dipeptidyl peptidase 3 GN=DPP3	Q9NY33	82,573.60	5	8.96%
343	Glutathione synthetase GN=GSS	P48637	52,367.90	5	12.40%
344	Beta-1,4-galactosyltransferase 1 GN=B4GALT1	P15291	43,903.00	5	19.30%
345	Glypican-1 GN=GPC1	P35052	61,663.30	5	12.70%
346	Guanine nucleotide-binding protein subunit beta-2-like 1 GN=GNB2L1	P63244	35,058.90	5	16.10%
347	Ribonuclease inhibitor GN=RNH1	P13489	49,956.40	5	13.70%
348	Proteoglycan 4 GN=PRG4	Q92954	151,062.20	5	4.27%
349	Protein Z-dependent protease inhibitor GN=SERPINA10	Q9UK55	50,690.70	5	15.10%
350	Leukotriene A-4 hydrolase GN=LTA4H	P09960	69,269.10	5	11.10%
351	Regucalcin GN=RGN	Q15493	33,234.90	5	21.70%
352	SPRY domain-containing protein 4 GN=SPRYD4	Q8WW59	23,110.10	5	24.60%
353	60S ribosomal protein L10a GN=RPL10A	P62906	24,814.00	5	24.00%
354	Adenine phosphoribosyltransferase GN=APRT	P07741	19,590.50	5	36.10%
355	C-1-tetrahydrofolate synthase, cytoplasmic GN=MTHFD1	P11586	101,543.50	5	6.84%
356	Epoxide hydrolase 1 GN=EPHX1	P07099	52,933.10	5	16.50%
357	Serpin A11 GN=SERPINA11	Q86U17	46,973.10	5	15.40%
358	Insulin-like growth factor-binding protein 3 GN=IGFBP3	P17936	31,656.10	5	22.70%
359	Mannan-binding lectin serine protease 2 GN=MASP2	O00187	75,685.40	5	6.85%
360	Proteasome subunit beta type-2 GN=PSMB2	P49721	22,819.50	5	32.30%
361	Proteasome subunit beta type-3 GN=PSMB3	P49720	22,931.60	5	34.10%
362	S-phase kinase-associated protein 1 GN=SKP1	P63208	18,640.30	5	30.70%
363	V-type proton ATPase subunit S1 GN=ATP6AP1	Q15904	52,009.20	5	16.60%
364	N(G),N(G)-dimethylarginine dimethylaminohydrolase 1 GN=DDAH1	O94760	31,103.70	5	27.40%
365	Cathepsin Z GN=CTSZ	Q9UBR2	33,850.20	5	21.80%
366	Lysosomal protective protein GN=CTSA	P10619	54,449.60	5	11.90%
367	Serum amyloid A-4 protein GN=SAA4	P35542	14,729.20	5	40.80%
368	ES1 protein homolog, mitochondrial GN=C21orf33	P30042	28,151.60	5	26.50%
369	Acetyl-CoA acetyltransferase, mitochondrial GN=ACAT1	P24752	45,181.80	5	15.90%

370	Ubiquitin-conjugating enzyme E2 K GN=UBE2K	P61086	22,389.10	5	34.50%
371	Actin-related protein 2/3 complex subunit 3 GN=ARPC3	O15145	20,529.80	5	30.90%
372	Heat shock 70 kDa protein 4 GN=HSPA4	P34932	94,313.90	5	8.21%
373	Fibroblast growth factor 21 GN=FGF21	Q9NSA1	22,282.60	5	40.70%
374	Acyl-coenzyme A thioesterase 2, mitochondrial GN=ACOT2	P49753	53,201.40	5	16.10%
375	Interferon-induced guanylate-binding protein 1 GN=GBP1	P32455	67,914.50	5	7.77%
376	Rho GDP-dissociation inhibitor 1 GN=ARHGDIA	P52565	23,189.50	5	25.50%
377	Corticosteroid-binding globulin GN=SERPINA6	P08185	45,124.10	5	13.60%
378	S-methyl-5'-thioadenosine phosphorylase GN=MTAP	Q13126	31,218.30	5	30.40%
379	Heat shock 70 kDa protein 1A/1B GN=HSPA1A	P08107	70,036.00	5	14.20%
380	Growth/differentiation factor 15 GN=GDF15	Q99988	34,122.80	5	17.20%
381	Neutral alpha-glucosidase AB GN=GANAB	Q14697	106,857.90	5	7.42%
382	Putative L-aspartate dehydrogenase GN=ASPDH	A6ND91	29,927.80	5	30.70%
383	Eukaryotic translation initiation factor 6 GN=EIF6	P56537	26,580.20	5	37.10%
384	Coagulation factor V GN=F5	P12259	251,692.50	5	2.88%
385	Annexin A5 GN=ANXA5	P08758	35,920.60	4	15.60%
386	40S ribosomal protein S3 GN=RPS3	P23396	26,670.50	4	23.00%
387	4-trimethylaminobutyraldehyde dehydrogenase GN=ALDH9A1	P49189	53,784.00	4	8.91%
388	Glutathione reductase, mitochondrial GN=GSR	P00390	56,239.40	4	14.80%
389	S-formylglutathione hydrolase GN=ESD	P10768	31,445.60	4	26.60%
390	Fructose-bisphosphate aldolase C GN=ALDOC	P09972	39,438.20	4	27.70%
391	NADP-dependent malic enzyme GN=ME1	P48163	64,133.40	4	9.97%
392	Translin GN=TSN	Q15631	26,165.40	4	20.20%
393	Heme-binding protein 2 GN=HEBP2	Q9Y5Z4	22,857.70	4	23.40%
394	Prostaglandin E synthase 3 GN=PTGES3	Q15185	18,679.90	4	21.90%
395	Acylamino-acid-releasing enzyme GN=APEH	P13798	81,206.00	4	5.74%
396	Hornerin GN=HRNR	Q86YZ3	282,354.70	4	2.49%
397	Cystathionine gamma-lyase GN=CTH	P32929	44,490.50	4	15.60%
398	Threonyl-tRNA synthetase, cytoplasmic GN=TARS	P26639	83,419.80	4	7.19%
399	Protocadherin Fat 1 GN=FAT1	Q14517	506,250.70	4	1.46%
400	Ubiquitin carboxyl-terminal hydrolase isozyme L3 GN=UCHL3	P15374	26,164.80	4	25.70%
401	Annexin A4 GN=ANXA4	P09525	35,866.30	4	16.90%
402	Transitional endoplasmic reticulum ATPase GN=VCP	P55072	89,306.80	4	7.44%
403	Actin-related protein 3 GN=ACTR3	P61158	47,353.80	4	14.60%
404	Dual specificity protein phosphatase 3 GN=DUSP3	P51452	20,460.80	4	29.20%
405	Tissue factor pathway inhibitor GN=TFPI	P10646	34,998.10	4	15.50%
406	Proteasome subunit beta type-6 GN=PSMB6	P28072	25,339.90	4	15.10%
407	Prolow-density lipoprotein receptor-related protein 1 GN=LRP1	Q07954	504,573.80	4	1.14%
408	Beta-ureidopropionase GN=UPB1	Q9UBR1	43,148.10	4	18.80%
409	Attractin GN=ATRN	O75882	158,518.30	4	3.43%
410	Syndecan-4 GN=SDC4	P31431	21,624.10	4	24.70%
411	3-hydroxyisobutyryl-CoA hydrolase, mitochondrial GN=HIBCH	Q6NVY1	43,466.00	4	9.84%
412	Ribosyldihydronicotinamide dehydrogenase [quinone] GN=NQO2	P16083	25,900.80	4	17.30%
413	GTP-binding nuclear protein Ran GN=RAN	P62826	24,405.10	4	19.90%
414	Isochorismatase domain-containing protein 1 GN=ISOC1	Q96CN7	32,218.70	4	19.80%
415	F-actin-capping protein subunit alpha-1 GN=CAPZA1	P52907	32,905.10	4	20.30%
416	Aldo-keto reductase family 1 member C4 GN=AKR1C4	P17516	37,049.40	4	36.80%
417	Actin-related protein 2/3 complex subunit 1B GN=ARPC1B	O15143	40,931.80	4	15.30%
418	SEC14-like protein 2 GN=SEC14L2	O76054	46,128.40	4	15.90%
419	Carboxypeptidase B2 GN=CPB2	Q96IY4	48,406.70	4	12.80%
420	UDP-glucose:glycoprotein glucosyltransferase 1 GN=UGGT1	Q9NYU2	177,176.90	4	3.28%
421	Biotinidase GN=BTD	P43251	61,115.40	4	10.50%
422	Mannose-binding protein C GN=MBL2	P11226	26,126.10	4	17.30%
423	Tripeptidyl-peptidase 2 GN=TPP2	P29144	138,334.90	4	4.88%
424	Monoglyceride lipase GN=MGLL	Q99685	33,243.70	4	18.50%
425	Renin receptor GN=ATP6AP2	O75787	38,991.10	4	12.30%
426	Beta-lactamase-like protein 2 GN=LACTB2	Q53H82	32,788.70	4	16.00%
427	Catechol O-methyltransferase GN=COMT	P21964	30,019.60	4	24.40%
428	Sepiapterin reductase GN=SPR	P35270	28,031.50	4	26.80%
429	WD repeat-containing protein 1 GN=WDR1	O75083	66,175.20	4	6.44%
430	Thioredoxin domain-containing protein 5 GN=TXNDC5	Q8NBS9	47,611.10	4	11.80%
431	Villin-1 GN=VIL1	P09327	92,677.20	4	6.17%
432	Platelet-activating factor acetylhydrolase IB subunit beta GN=PAFAH1B2	P68402	25,551.50	4	18.80%

433	Valacyclovir hydrolase GN=BPHL	Q86WA6	32,525.40	3	14.80%
434	Tryptophanyl-tRNA synthetase, cytoplasmic GN=WARS	P23381	53,149.60	3	11.70%
435	Gamma-glutamylcyclotransferase GN=GGCT	O75223	20,990.00	3	18.10%
436	Dihydrolipoyl dehydrogenase, mitochondrial GN=DLD	P09622	54,159.40	3	8.45%
437	Bone morphogenetic protein 1 GN=BMP1	P13497	111,231.20	3	4.26%
438	GDH/6PGL endoplasmic bifunctional protein GN=H6PD	O95479	88,875.60	3	5.44%
439	Microsomal triglyceride transfer protein large subunit GN=MTTP	P55157	99,337.10	3	4.25%
440	Apolipoprotein L1 GN=APOL1	O14791	43,957.30	3	8.54%
441	Staphylococcal nuclease domain-containing protein 1 GN=SND1	Q7KZF4	101,980.50	3	4.29%
442	Kynureninase GN=KYNU	Q16719	52,335.30	3	9.25%
443	Haloacid dehalogenase-like hydrolase domain-containing protein 1 GN=HDHD1	Q08623	25,232.00	3	21.90%
444	Adapter molecule crk GN=CRK	P46108	33,812.80	3	13.20%
445	Fumarylacetoacetate hydrolase domain-containing protein 1 GN=FAHD1	Q6P587	24,825.40	3	12.90%
446	Proline-rich acidic protein 1 GN=PRAP1	Q96NZ9	17,189.20	3	17.90%
447	Procollagen C-endopeptidase enhancer 1 GN=PCOLCE	Q15113	47,954.50	3	8.69%
448	Polyubiquitin-B GN=UBB	P0CG47	25,744.80	3	16.60%
449	Tubulin beta-2C chain GN=TUBB2C	P68371	49,812.70	3	51.20%
450	Glutathione S-transferase P GN=GSTP1	P09211	23,338.70	3	22.40%
451	Proliferation-associated protein 2G4 GN=PA2G4	Q9UQ80	43,768.70	3	9.90%
452	Glycyl-tRNA synthetase GN=GARS	P41250	83,149.60	3	6.36%
453	2,4-dienoyl-CoA reductase, mitochondrial GN=DECR1	Q16698	36,050.90	3	14.30%
454	Laminin subunit alpha-5 GN=LAMA5	O15230	399,707.10	3	1.11%
455	Protein NipSnap homolog 3A GN=NIPSNAP3A	Q9UFN0	28,448.90	3	12.10%
456	Acyl-protein thioesterase 2 GN=LYPLA2	O95372	24,719.20	3	10.40%
457	C4b-binding protein alpha chain GN=C4BPA	P04003	67,015.00	3	4.19%
458	Vitamin K-dependent protein S GN=PROS1	P07225	75,105.40	3	5.03%
459	Leucine-rich repeat transmembrane protein FLRT3 GN=FLRT3	Q9NZU0	72,988.90	3	5.55%
460	Calsyntenin-1 GN=CLSTN1	O94985	109,773.60	3	3.57%
461	26S proteasome non-ATPase regulatory subunit 1 GN=PSMD1	Q99460	105,821.20	3	3.36%
462	Metalloproteinase inhibitor 2 GN=TIMP2	P16035	24,381.90	3	22.70%
463	Enoyl-CoA hydratase domain-containing protein 2, mitochondrial GN=ECHDC2	Q86YB7	31,108.70	3	15.80%
464	Radixin GN=RDX	P35241	68,547.50	3	15.10%
465	Peptidyl-prolyl cis-trans isomerase FKBP3 GN=FKBP3	Q00688	25,159.40	3	16.50%
466	Heterogeneous nuclear ribonucleoprotein A1 GN=HNRNPA1	P09651	38,729.00	3	14.50%
467	Dystroglycan GN=DAG1	Q14118	97,424.20	3	5.81%
468	Glycogen phosphorylase, brain form GN=PYGB	P11216	96,680.30	3	8.07%
469	60S ribosomal protein L12 GN=RPL12	P30050	17,801.10	3	26.70%
470	Phenazine biosynthesis-like domain-containing protein GN=PBLD	P30039	31,767.80	3	12.50%
471	Asialoglycoprotein receptor 1 GN=ASGR1	P07306	33,167.40	3	10.30%
472	Ras-related protein Rab-1A GN=RAB1A	P62820	22,660.40	3	19.00%
473	Formimidoyltransferase-cyclodeaminase GN=FTCD	O95954	58,909.00	3	10.40%
474	Epididymal secretory protein E1 GN=NPC2	P61916	16,552.00	3	31.80%
475	Inositol monophosphatase 1 GN=IMPA1	P29218	30,170.50	3	17.00%
476	Lysosomal alpha-glucosidase GN=GAA	P10253	105,306.40	3	3.78%
477	Apolipoprotein A-I-binding protein GN=APOA1BP	Q8NCW5	31,657.40	3	13.20%
478	Pyridoxine-5'-phosphate oxidase GN=PNPO	Q9NVS9	29,970.20	3	18.40%
479	Out at first protein homolog GN=OAF	Q86UD1	30,670.40	3	20.10%
480	Nucleophosmin GN=NPM1	P06748	32,557.40	3	18.00%
481	Gamma-interferon-inducible lysosomal thiol reductase GN=IFI30	P13284	29,131.20	3	11.90%
482	S-adenosylmethionine synthase isoform type-1 GN=MAT1A	Q00266	43,629.50	3	9.87%
483	Poliovirus receptor GN=PVR	P15151	45,283.50	3	11.30%
484	Cysteine and glycine-rich protein 1 GN=CSRP1	P21291	20,549.10	3	21.80%
485	Phosphatidylinositol transfer protein beta isoform GN=PITPNB	P48739	31,522.30	3	17.30%
486	26S proteasome non-ATPase regulatory subunit 2 GN=PSMD2	Q13200	100,184.20	3	5.07%
487	Endoplasmic reticulum aminopeptidase 1 GN=ERAP1	Q9NZ08	107,219.90	3	4.14%
488	Cell adhesion molecule 1 GN=CADM1	Q9BY67	48,491.30	3	10.90%
489	Sulfhydryl oxidase 1 GN=QSOX1	O00391	82,560.70	3	5.76%
490	Aldo-keto reductase family 1 member C2 GN=AKR1C2	P52895	36,717.90	3	63.20%
491	Serum amyloid A protein GN=SAA1	P02735	13,514.50	3	35.20%
492	3'(2'),5'-bisphosphate nucleotidase 1 GN=BPNT1	O95861	33,374.70	3	10.70%
493	ADP-sugar pyrophosphatase GN=NUDT5	Q9UKK9	24,309.80	3	24.70%
494	DNA-(apurinic or apyrimidinic site) lyase GN=APEX1	P27695	35,537.70	3	15.40%
495	Phosphoserine phosphatase GN=PSPH	P78330	24,990.10	3	16.90%

496	Proline synthase co-transcribed bacterial homolog protein GN=PROSC	O94903	30,325.80	3	12.70%
497	Complement factor H-related protein 1 GN=CFHR1	Q03591	37,632.40	3	24.50%
498	Ubiquitin-fold modifier-conjugating enzyme 1 GN=UFC1	Q9Y3C8	19,441.00	3	16.20%
499	Tripeptidyl-peptidase 1 GN=TPP1	O14773	61,229.60	3	10.50%
500	26S proteasome non-ATPase regulatory subunit 13 GN=PSMD13	Q9UNM6	42,927.90	3	10.60%
501	Hepatocyte growth factor activator GN=HGFAC	Q04756	70,663.50	3	5.19%
502	Cathepsin H GN=CTSH	P09668	37,375.80	2	3.28%
503	Biliverdin reductase A GN=BLVRA	P53004	33,411.00	2	9.46%
504	Thyroxine-binding globulin GN=SERPINA7	P05543	46,307.60	2	5.78%
505	Cell surface glycoprotein MUC18 GN=MCAM	P43121	71,588.50	2	4.80%
506	Putative hydrolase RBBP9 GN=RBBP9	O75884	20,982.00	2	11.30%
507	Pantetheinase GN=VNN1	O95497	56,994.30	2	4.68%
508	Haloacid dehalogenase-like hydrolase domain-containing protein 3 GN=HDHD3	Q9BSH5	27,982.10	2	15.10%
509	Apolipoprotein M GN=APOM	O95445	21,235.90	2	11.20%
510	F-box only protein 2 GN=FBXO2	Q9UK22	33,308.70	2	9.12%
511	Diablo homolog, mitochondrial GN=DIABLO	Q9NR28	27,112.70	2	8.79%
512	Nicotinate phosphoribosyltransferase GN=NAPRT1	Q6XQN6	57,560.50	2	6.13%
513	Lysophospholipase-like protein 1 GN=LYPLAL1	Q5VWZ2	26,299.00	2	15.20%
514	Inhibin beta E chain GN=INHBE	P58166	38,543.60	2	5.71%
515	Protein CREG1 GN=CREG1	O75629	24,057.00	2	14.10%
516	Macrophage-capping protein GN=CAPG	P40121	38,480.80	2	7.47%
517	Elongation factor 1-beta GN=EEF1B2	P24534	24,746.20	2	12.40%
518	Coatomer subunit alpha GN=COPA	P53621	138,331.30	2	2.86%
519	Echinoderm microtubule-associated protein-like 4 GN=EML4	Q9HC35	108,899.50	2	2.55%
520	Acidic leucine-rich nuclear phosphoprotein 32 family member B GN=ANP32B	Q92688	28,770.60	2	23.50%
521	Junctional adhesion molecule A GN=F11R	Q9Y624	32,565.10	2	6.35%
522	Dipeptidyl peptidase 1 GN=CTSC	P53634	51,836.30	2	4.54%
523	Hydroxymethylglutaryl-CoA synthase, mitochondrial GN=HMGCS2	P54868	56,619.00	2	6.50%
524	Amyloid-like protein 2 GN=APLP2	Q06481	86,937.00	2	3.93%
525	40S ribosomal protein S5 GN=RPS5	P46782	22,859.00	2	10.30%
526	Ras-related protein Rab-7a GN=RAB7A	P51149	23,472.00	2	11.60%
527	Hypoxanthine-guanine phosphoribosyltransferase GN=HPRT1	P00492	24,562.20	2	9.17%
528	Citrate lyase subunit beta-like protein, mitochondrial GN=CLYBL	Q8N0X4	37,342.70	2	6.18%
529	26S proteasome non-ATPase regulatory subunit 8 GN=PSMD8	P48556	39,595.90	2	4.86%
530	Vitamin K-dependent protein C GN=PROC	P04070	52,053.10	2	5.86%
531	Beta-hexosaminidase subunit alpha GN=HEXA	P06865	60,686.00	2	5.67%
532	Tetratricopeptide repeat protein 38 GN=TTC38	Q5R3I4	52,770.40	2	4.26%
533	Scavenger receptor cysteine-rich type 1 protein M130 GN=CD163	Q86VB7	125,429.40	2	1.73%
534	Myosin-binding protein C, cardiac-type GN=MYBPC3	Q14896	140,588.50	2	1.26%
535	Phosphoacetylglucosamine mutase GN=PGM3	O95394	59,834.40	2	4.24%
536	Proteasome subunit beta type-10 GN=PSMB10	P40306	28,918.00	2	11.00%
537	Calpain small subunit 1 GN=CAPNS1	P04632	28,298.60	2	13.40%
538	Cathepsin L1 GN=CTSL1	P07711	37,546.10	2	10.50%
539	Xanthine dehydrogenase/oxidase GN=XDH	P47989	146,408.10	2	2.78%
540	Hydroxymethylglutaryl-CoA lyase, mitochondrial GN=HMGCL	P35914	34,342.30	2	11.10%
541	Phospholipid transfer protein GN=PLTP	P55058	54,723.10	2	5.88%
542	Carboxypeptidase N catalytic chain GN=CPN1	P15169	52,268.30	2	5.02%
543	Serine/threonine-protein phosphatase 2A activator GN=PPP2R4	Q15257	40,649.70	2	6.42%
544	Vacuolar protein sorting-associated protein 35 GN=VPS35	Q96QK1	91,692.00	2	3.02%
545	UPF0568 protein C14orf166 GN=C14orf166	Q9Y224	28,051.30	2	13.90%
546	Semaphorin-4B GN=SEMA4B	Q9NPR2	92,176.00	2	2.76%
547	Beta-2-microglobulin GN=B2M	P61769	13,696.90	2	26.90%
548	Complement C1r subcomponent-like protein GN=C1RL	Q9NZP8	53,479.50	2	8.83%
549	Complement factor D GN=CFD	P00746	27,014.40	2	15.00%
550	Coagulation factor IX GN=F9	P00740	51,759.60	2	4.34%
551	Dihydropyrimidinase GN=DPYS	Q14117	56,611.90	2	6.17%
552	Afamin GN=AFM	P43652	69,052.10	2	4.51%
553	Glutathione S-transferase A1 GN=GSTA1	P08263	25,615.00	2	48.60%
554	Myosin-9 GN=MYH9	P35579	226,519.50	2	1.12%
555	Succinate dehydrogenase [ubiquinone] flavoprotein subunit, mitochondrial GN=SDHA	P31040	72,673.70	2	3.77%
556	HLA class I histocompatibility antigen, A-69 alpha chain GN=HLA-A	P10316	40,958.20	2	25.80%
557	Clathrin heavy chain 1 GN=CLTC	Q00610	191,600.90	2	1.25%
558	Carboxypeptidase M GN=CPM	P14384	50,497.20	2	7.67%

559	Stress-induced-phosphoprotein 1 GN=STIP1	P31948	62,624.10	2	4.60%
560	Alcohol dehydrogenase 1A GN=ADH1A	P07327	39,840.70	2	49.60%
561	Cystathionine beta-synthase GN=CBS	P35520	60,569.30	2	3.45%
562	Isoamyl acetate-hydrolyzing esterase 1 homolog GN=IAH1	Q2TAA2	27,581.70	2	10.90%
563	Ubiquitin thioesterase OTUB1 GN=OTUB1	Q96FW1	31,266.60	2	12.50%
564	Importin-5 GN=IPO5	O00410	123,614.20	2	2.10%
565	Serine protease HTRA1 GN=HTRA1	Q92743	51,269.30	2	6.67%
566	Carboxylesterase 2 GN=CES2	O00748	61,789.30	2	3.40%
567	Phosphoglucomutase-2 GN=PGM2	Q96G03	68,267.70	2	4.08%
568	Aminopeptidase B GN=RNPEP	Q9H4A4	72,579.40	2	3.69%
569	Ribonuclease pancreatic GN=RNASE1	P07998	17,625.80	2	17.90%
570	Ephrin-A1 GN=EFNA1	P20827	23,769.20	2	13.20%
571	Propionyl-CoA carboxylase alpha chain, mitochondrial GN=PCCA	P05165	80,041.20	2	3.16%
572	Angiopoietin-related protein 4 GN=ANGPTL4	Q9BY76	45,196.00	2	5.67%
573	Thioredoxin reductase 1, cytoplasmic GN=TXNRD1	Q16881	70,888.90	2	4.93%
574	Elongation factor 1-delta GN=EEF1D	P29692	31,103.90	2	12.80%
575	Polypeptide N-acetylgalactosaminyltransferase 2 GN=GALNT2	Q10471	64,715.10	2	3.68%
576	26S proteasome non-ATPase regulatory subunit 14 GN=PSMD14	O00487	34,558.60	2	8.71%
577	Mammalian ependymin-related protein 1 GN=EPDR1	Q9UM22	25,419.50	2	8.48%
578	Gelsolin GN=GSN	P06396	85,679.80	2	2.94%
579	Bile acid-CoA:amino acid N-acyltransferase GN=BAAT	Q14032	46,282.00	2	6.94%
580	Ras-related protein Rab-11A GN=RAB11A	P62491	24,375.90	2	11.10%
581	Ephrin-B1 GN=EFNB1	P98172	37,989.40	2	8.38%
582	Hsc70-interacting protein GN=ST13	P50502	41,314.40	2	5.15%
583	Quinone oxidoreductase PIG3 GN=TP53I3	Q53FA7	35,519.30	2	10.80%
584	Very low-density lipoprotein receptor GN=VLDLR	P98155	96,080.00	2	2.63%
585	Receptor-type tyrosine-protein phosphatase kappa GN=PTPRK	Q15262	162,085.20	2	2.71%
586	N(G),N(G)-dimethylarginine dimethylaminohydrolase 2 GN=DDAH2	O95865	29,626.30	2	11.20%
587	Phosphopantothenate--cysteine ligase GN=PPCS	Q9HAB8	33,988.00	2	5.47%
588	Histone H2A type 1-B/E GN=HIST1H2AB	P04908	14,118.00	2	21.50%
589	Acyl-protein thioesterase 1 GN=LYPLA1	O75608	24,652.20	2	11.70%
590	Apoptosis-inducing factor 1, mitochondrial GN=AIFM1	O95831	66,883.50	2	3.75%
591	Leucine-rich repeat-containing protein 59 GN=LRRC59	Q96AG4	34,913.40	2	7.49%
592	Complement factor H-related protein 2 GN=CFHR2	P36980	30,632.60	2	20.70%
593	Ribosome-binding protein 1 GN=RRBP1	Q9P2E9	152,452.50	2	2.20%
594	26S proteasome non-ATPase regulatory subunit 3 GN=PSMD3	O43242	60,961.60	2	4.31%
595	Glutathione S-transferase Mu 3 GN=GSTM3	P21266	26,543.10	2	15.60%
596	Ubiquitin carboxyl-terminal hydrolase 5 GN=USP5	P45974	95,770.10	2	3.26%
597	Protein CYR61 GN=CYR61	O00622	42,008.00	2	7.09%
598	Lysosome-associated membrane glycoprotein 2 GN=LAMP2	P13473	44,942.90	2	4.88%
599	Deoxyribonucleoside 5'-monophosphate N-glycosidase GN=RCL	O43598	19,090.30	2	19.50%
600	Rab GDP dissociation inhibitor alpha GN=GDI1	P31150	50,566.10	1	22.10%
601	Na(+)/H(+) exchange regulatory cofactor NHE-RF1 GN=SLC9A3R1	O14745	38,850.30	1	7.26%
602	Interleukin-1 receptor antagonist protein GN=IL1RN	P18510	20,037.40	1	10.70%
603	Actin, alpha cardiac muscle 1 GN=ACTC1	P68032	42,002.10	1	31.80%
604	Tubulin beta-2A chain GN=TUBB2A	Q13885	49,889.10	1	46.50%
605	Tubulin alpha-1A chain GN=TUBA1A	Q71U36	50,117.70	1	39.20%
606	L-lactate dehydrogenase B chain GN=LDHB	P07195	36,620.60	1	9.88%
607	Legumain GN=LGMN	Q99538	49,393.00	1	3.93%
608	HLA class I histocompatibility antigen, A-3 alpha chain GN=HLA-A	P04439	40,822.60	1	17.80%
609	DCN1-like protein 1 GN=DCUN1D1	Q96GG9	30,107.90	1	6.56%
610	Interferon-induced guanylate-binding protein 2 GN=GBP2	P32456	67,193.10	1	3.89%
611	Betaine--homocysteine S-methyltransferase 2 GN=BHMT2	Q9H2M3	40,336.40	1	13.50%
612	Calsyntenin-3 GN=CLSTN3	Q9BQT9	106,080.20	1	1.78%
613	Arylsulfatase A GN=ARSA	P15289	53,571.20	1	3.35%
614	Putative tropomyosin alpha-3 chain-like protein PE=5	A6NL28	26,252.00	1	14.30%
615	Ganglioside GM2 activator GN=GM2A	P17900	20,821.20	1	5.18%
616	Multiple inositol polyphosphate phosphatase 1 GN=MINPP1	Q9UNW1	55,034.90	1	2.26%
617	Vasorin GN=VASN	Q6EMK4	71,696.10	1	2.38%
618	N-acetylglucosamine-1-phosphotransferase subunit gamma GN=GNPTG	Q9UJJ9	33,956.00	1	6.56%
619	Keratin, type II cytoskeletal 6B GN=KRT6B	P04259	60,050.60	1	12.10%
620	Trypsin-1 GN=PRSS1	P07477	26,540.00	1	8.10%
621	Alpha-soluble NSF attachment protein GN=NAPA	P54920	33,216.10	1	3.73%

622	Disintegrin and metalloproteinase domain-containing protein 9 GN=ADAM9	Q13443	90,538.10	1	2.20%
623	Enoyl-CoA hydratase domain-containing protein 1 GN=ECHDC1	Q9NTX5	33,681.30	1	4.23%
624	Ras-related protein Rab-10 GN=RAB10	P61026	22,524.10	1	11.00%
625	Arginyl-tRNA synthetase, cytoplasmic GN=RARS	P54136	75,364.00	1	1.97%
626	Xylulose kinase GN=XYLB	O75191	58,364.00	1	2.61%
627	Xaa-Pro dipeptidase GN=PEPD	P12955	54,529.70	1	2.03%
628	Ras-related protein Rap-1b-like protein	A6NIZ1	20,906.90	1	6.52%
629	Heat shock protein 75 kDa, mitochondrial GN=TRAP1	Q12931	80,094.90	1	3.41%
630	3-ketoacyl-CoA thiolase, peroxisomal GN=ACAA1	P09110	44,274.10	1	3.07%
631	Mu-crystallin homolog GN=CRYM	Q14894	33,757.10	1	4.78%
632	Aldose reductase GN=AKR1B1	P15121	35,835.90	1	6.65%
633	Phenylalanine-4-hydroxylase GN=PAH	P00439	51,846.40	1	1.99%
634	Eukaryotic initiation factor 4A-II GN=EIF4A2	Q14240	46,385.60	1	18.70%
635	NADH dehydrogenase [ubiquinone] flavoprotein 2, mitochondrial GN=NDUFV2	P19404	27,373.80	1	5.22%
636	Complement component 1 Q subcomponent-binding protein, mitochondrial GN=C1QBP	Q07021	31,344.60	1	4.96%
637	Glucosamine--fructose-6-phosphate aminotransferase [isomerizing] 1 GN=GFPT1	Q06210	78,789.70	1	2.29%
638	Isocitrate dehydrogenase [NAD] subunit alpha, mitochondrial GN=IDH3A	P50213	39,574.50	1	2.73%
639	Follistatin-related protein 1 GN=FSTL1	Q12841	34,967.30	1	3.25%
640	Calcium-regulated heat stable protein 1 GN=CARHSP1	Q9Y2V2	15,873.60	1	10.90%
641	D-3-phosphoglycerate dehydrogenase GN=PHGDH	O43175	56,632.60	1	1.50%
642	Nuclear pore complex protein Nup153 GN=NUP153	P49790	153,921.20	1	0.61%
643	Coatomer subunit epsilon GN=COPE	O14579	34,464.90	1	6.49%
644	Cadherin-1 GN=CDH1	P12830	97,439.60	1	2.04%
645	Plastin-1 GN=PLS1	Q14651	70,239.20	1	8.59%
646	Beta-galactoside alpha-2,6-sialyltransferase 1 GN=ST6GAL1	P15907	46,588.20	1	5.67%
647	THUMP domain-containing protein 1 GN=THUMPD1	Q9NXG2	39,297.50	1	2.27%
648	Heterogeneous nuclear ribonucleoprotein D0 GN=HNRNPD	Q14103	38,416.50	1	3.94%
649	F-actin-capping protein subunit alpha-2 GN=CAPZA2	P47755	32,931.20	1	8.74%
650	Tropomyosin alpha-3 chain GN=TPM3	P06753	32,802.20	1	23.60%
651	Glutamate--cysteine ligase regulatory subunit GN=GCLM	P48507	30,709.30	1	4.74%
652	Putative gamma-glutamyltranspeptidase 3 GN=GGT3P PE=5	A6NGU5	61,484.00	1	2.29%
653	Cadherin-2 GN=CDH2	P19022	99,793.80	1	1.55%
654	Uncharacterized protein C21orf96 GN=C21orf96	Q9H7H1	14,655.50	1	10.10%
655	Thiosulfate sulfurtransferase GN=TST	Q16762	33,410.80	1	6.06%
656	Aflatoxin B1 aldehyde reductase member 2 GN=AKR7A2	O43488	39,571.00	1	6.13%
657	T-complex protein 1 subunit alpha GN=TCP1	P17987	60,327.20	1	2.16%
658	Nck-associated protein 1-like GN=NCKAP1L	P55160	128,140.30	1	0.71%
659	Coatomer subunit gamma-2 GN=COPG2	Q9UBF2	97,606.50	1	1.38%
660	Adenosine kinase GN=ADK	P55263	40,528.60	1	4.42%
661	Beta-glucuronidase GN=GUSB	P08236	74,714.70	1	1.38%
662	Serpin B6 GN=SERPINB6	P35237	42,604.80	1	3.99%
663	Calpain-15 GN=SOLH	O75808	117,293.90	1	0.55%
664	Complement C1q subcomponent subunit C GN=C1QC	P02747	25,756.00	1	5.31%
665	Bleomycin hydrolase GN=BLMH	Q13867	52,544.50	1	2.42%
666	Bifunctional purine biosynthesis protein PURH GN=ATIC	P31939	64,598.50	1	1.18%
667	T-complex protein 1 subunit theta GN=CCT8	P50990	59,603.00	1	2.19%
668	Dual specificity protein kinase TTK GN=TTK	P33981	97,057.20	1	0.70%
669	Importin-7 GN=IPO7	O95373	119,501.50	1	1.45%
670	Myomesin-1 GN=MYOM1	P52179	187,608.50	1	0.53%
671	GDP-L-fucose synthase GN=TSTA3	Q13630	35,874.60	1	3.43%
672	Hydroxyacylglutathione hydrolase, mitochondrial GN=HAGH	Q16775	33,787.50	1	5.19%
673	Glutathione S-transferase kappa 1 GN=GSTK1	Q9Y2Q3	25,480.10	1	6.19%
674	Osteoclast-stimulating factor 1 GN=OSTF1	Q92882	23,769.70	1	5.61%
675	CASP8-associated protein 2 GN=CASP8AP2	Q9UKL3	222,641.80	1	0.45%
676	Tissue factor pathway inhibitor 2 GN=TFPI2	P48307	26,916.90	1	3.40%
677	Sialate O-acetylesterase GN=SIAE	Q9HAT2	58,297.30	1	2.87%
678	Beta-mannosidase GN=MANBA	O00462	100,878.70	1	1.48%
679	Endothelial cell-specific molecule 1 GN=ESM1	Q9NQ30	20,076.30	1	6.52%
680	Enolase-phosphatase E1 GN=ENOPH1	Q9UHY7	28,914.40	1	4.60%
681	Integral membrane protein 2B GN=ITM2B	Q9Y287	30,321.10	1	3.76%